TECHNICAL UNIVERSITY OF MOLDOVA

JOURNAL OF ENGINEERING SCIENCE

Technical and applied scientific publication founded on 9 February 1995
Alternative title: Meridian ingineresc

2022
Vol. XXIX (1)

ISSN 2587-3474
eISSN 2587-3482

TECHNICAL UNIVERSITY OF MOLDOVA (PUBLISHING HOUSE)
„TEHNICA UTM" (PRINTING HOUSE)

According to the Decision of the NAQAER No. 19 from 06.12.2019, JES is classified as B+ journal

Main subjects areas of the Journal of Engineering Science:

A. Industrial Engineering

- Mechanical Engineering and Technologies
- Applied Engineering Sciences and Management
- Materials Science and New Technologies
- Electrical Engineering and Power Electronics
- Energy systems
- Light Industry, New Technologies and Design
- Industrial and Applied Mathematics
- Vehicle and Transport Engineering

B. Electronics and Computer Science

- Electronics and Communication
- Microelectronics and Nanotechnologies
- Biomedical Engineering
- Computers and Information Technology
- Automation

C. Architecture, Civil and Environmental Engineering

- Architecture, Urbanism and Cadaster
- Civil Engineering and Management
- Energy Efficiency and New Building Materials
- Environmental Engineering

D. Food Engineering

- Food Technologies and Food Processes
- Food Industry and Management
- Biotechnologies, Food Chemistry and Food Safety
- Equipment for Food Industries

The structure of the journal corresponds to the classification of scientific publications: ***Engineering, Multidisciplinary*.**

How to publish a paper:

1. Send the manuscript and information about the author to the **Editorial Board address:** jes@meridian.utm.md
2. Manuscripts are accepted only in English, by e-mail, in template file (www.jes.utm.md)
3. After a review, you will be notified of the editorial board's decision.
4. After the Journal has been published, we will send it to you immediately by mail.

Editor-in-Chief
Dr. hab. prof. univ. Viorel BOSTAN
Technical University of Moldova
viorel.bostan@adm.utm.md

Editorial Board

Responsible Editor:
Dr. hab. Rodica STURZA
Technical University of Moldova
rodica.sturza@chim.utm.md

Editorial Production:
Dr. Nicolae Trifan
Dr. Svetlana Caterenciuc Dr.
Rodica Cujba
Dr.hab. Aliona Ghendov-Moșanu

CONTENT

A. Industrial Engineering

Eduard Monaico	*Engineering of semiconductor compounds via electrochemical technologies for nano-microelectronic applications*	*8*
Silvia Andronic, Eugeniu Grigoriev, Vasile Tronciu	*Generation of high amplitudes pulses with excitable DFB lasers and an integrated dispersive reflector*	*17*
Ion Bostan, Petru Stoicev, Alexandru Buga, Gheorghe Poştaru, Nicolae Trifan, Andrei Platon	*Theoretical contributions on the selection of possible tribological couples of materials for the manufacture of precessional transmissions*	*23*
Vasile Plămădeală, Sergiu Dîntu	*Driver or autopilot – who is the future*	*48*
Titu-Marius I. Băjenescu	*The transition to a hydrogen energy*	*62*

B. Electronics and Computer Science

Veaceslav Perju	*Systems for invariant target recognition based on central image chord transformation*	*71*
Serghei Peancovschii	*Elaboration and application of graphical models to optimize the response time to emergency situations*	*86*
Vaidas Giedrimas	*Proof-of-stake consensus algorithms for the software components blockchain*	*97*
Adekunle I. Musa-Olokuta, Collins Nwaokocha, Adeola S. Shote, Samson A. Aasa	*Ergonomic investigation and assessment of motorcyclists musculoskeletal disorders*	*105*

C. Architecture, Civil and Environmental Engineering

Vladimir Polcanov, Alina Polcanova, Alexandru Cîrlan	*Landslide protection of roadway network during the construction and reconstruction*	*112*
Octavian Mangos, Vasile Rachier, Ion Sobor, Vadim Cazac	*Regarding the characteristics of the wind in northern region districts of the Republic of Moldova*	*121*
Toyese Oyegoke, Geoffrey T. Tongshuwar, John E. Oguche	*Biomass pretreatment as a key process in bioethanol productions: a review*	*130*

D. Food Engineering

Liliana Popescu, Aliona Ghendov-Moșanu, Alexei Baerle, Alexandra Savcenco, Pavel Tatarov	*Color stability of yogurt with yellow food dye from safflower (Carthamus Tinctorius L)*	142
Vladislav Reşitca, Anatol Balanută, Iurie Scutaru, Ecaterina Covaci, Aliona Sclifos, Antoanela Patraș, Ana-Maria Borta	*Possibility and necessity of tartaric acid production in the Republic of Moldova*	151
Elisaveta Sandulachi, Artur Macari, Daniela Cojocari, Greta Balan, Sergiu Popa, Nadejda Turculet, Aliona Ghendov-Mosanu, Rodica Sturza	*Antimicrobial properties of sea buckthorn grown in the Republic of Moldova*	164

CONȚINUT

A. Industrial Engineering

Eduard Monaico	*Ingineria compusilor semiconductori prin tehnologii electrochimice pentru aplicații nano-microelectronice*	8
Silvia Andronic, Eugeniu Grigoriev, Vasile Tronciu	*Generarea impulsurilor de amplitudine mare cu laser DFB excitabil și reflector dispersiv integrat*	17
Ion Bostan, Petru Stoicev, Alexandru Buga, Gheorghe Poştaru, Nicolae Trifan, Andrei Platon	*Contribuții teoretice privind selecția posibilelor cupluri tribologice de materiale pentru fabricarea transmisiilor precesionale*	23
Vasile Plămădeală, Sergiu Dîntu	*Conducătorul auto sau autopilotul – al cui este viitorul*	48
Titu-Marius I. Băjenescu	*Tranziția la o energie de hidrogen*	62

B. Electronics and Computer Science

Veaceslav Perju	*Sisteme pentru recunoaștere invariantă a țintelor bazate pe transformarea imaginii coordului central*	*71*
Serghei Peancovschii	*Elaborarea și aplicarea modelelor grafice pentru optimizarea timpului de răspuns la situații de urgență*	*86*
Vaidas Giedrimas	*Algoritmi de consens proof-of-stake pentru componentele software blockchain*	*97*
Adekunle I. Musa-Olokuta, Collins Nwaokocha, Adeola S. Shote, Samson A. Aasa	*Investigarea și evaluarea ergonomică a tulburărilor musculo-scheletale la motocicliști*	*105*

C. Architecture, Civil and Environmental Engineering

Vladimir Polcanov, Alina Polcanova, Alexandru Cîrlan	*Protecția rețelei de șosele la alunecări de teren în timpul construcției și reconstrucției*	*112*
Octavian Mangos, Vasile Rachier, Ion Sobor, Vadim Cazac	*Cu privire la caracteristicile vântului în regiunea de nord a Republicii Moldova*	*121*
Toyese Oyegoke, Geoffrey T. Tongshuwar, John E. Oguche	*Pretratarea biomasei ca proces cheie în producția de bioetanol: o revizie*	*130*

D. Food Engineering

Liliana Popescu, Aliona Ghendov-Moșanu, Alexei Baerle, Alexandra Savcenco, Pavel Tatarov	*Stabilitatea culorii iaurtului cu colorant alimentar galben din șofrănel (Carthamus Tinctorius L)*	*142*
Vladislav Reşitca, Anatol Balanută, Iurie Scutaru, Ecaterina Covaci, Aliona Sclifos, Antoanela Patraș, Ana-Maria Borta	*Posibilitatea și necesitatea producției de acid tartric în Republica Moldova*	*151*
Elisaveta Sandulachi, Artur Macari, Daniela Cojocari, Greta Balan, Sergiu Popa, Nadejda Turculet, Aliona Ghendov-Mosanu, Rodica Sturza	*Proprietăți antimicrobiene ale catinei albe cultivate în Republica Moldova*	*164*

Journal of Engineering Science *Vol. XXIX, no. 1 (2022), pp. 8 - 16*
Fascicle *Industrial Engineering* *ISSN 2587-3474*
Topic *Materials Science and New Technologies* *eISSN 2587-3482*

https://doi.org/10.52326/jes.utm.2022.29(1).01
CZU 621.382:546:621.3.049.77

ENGINEERING OF SEMICONDUCTOR COMPOUNDS VIA ELECTROCHEMICAL TECHNOLOGIES FOR NANO-MICROELECTRONIC APPLICATIONS

Eduard Monaico, ORCID: 0000-0003-3293-8645

National Center for Materials Study and Testing, Technical University of Moldova, 168 Stefan cel Mare Blvd., Chisinau, MD-2004, Republic of Moldova
*Corresponding author: Eduard Monaico, *eduard.monaico@cnstm.utm.md*

Received: 11. 25. 2021
Accepted: 01. 28. 2022

Abstract. The paper is focused on electrochemical approaches for nanostructuring of semiconductor compounds with further applications in nano - microelectronic devices. A cost-effective technology for nanowires and nanotubes obtaining by pulsed electrochemical deposition is presented. Functionalization of elaborated nanostructures with gold or platinum via electroplating improves the properties of the nanostructures. An optimization of the varicap design to increase the capacitance is proposed and discussed as well as the optimization of pulsed electrochemical deposition of several hundred micrometer long Pt nanotubes is performed. Herein, the elaboration of contacts to GaAs nanowires via different approaches for photoelectrical investigations is reported.

Keywords: *electrochemistry, nanostructures, nanowires, photodetector, contacts, varicap device.*

Rezumat. Lucrarea se concentrează pe abordări electrochimice pentru nanostructurarea compușilor semiconductori cu aplicații ulterioare în dispozitive nano - microelectronice. Este prezentată o tehnologie cost-efectivă pentru obținerea de nanofire și nanotuburi prin depunere electrochimică în impulsuri. Funcționalizarea nanostructurilor elaborate cu aur sau platină prin galvanizare îmbunătățește proprietățile nanostructurilor. Este propusă și discutată o metodologie de optimizare a designului varicap pentru a crește capacitatea și optimizarea depunerii electrochimice pulsate a Pt pe nanotuburi de câteva sute de micrometri. Este raportată elaborarea contactelor cu nanofire de GaAs prin diferite abordări pentru investigații fotoelectrice.

Cuvinte cheie: *electrochimie, nanostructuri, nanofire, fotodetector, contacte, dispozitiv varicap.*

Introduction

Nowadays, a lot of applications e.g. in electronics, photonics, sensors, communications, etc implies the synthesis of functional low-dimensional materials and devices. Nanotechnology is a developing field in which researchers elaborate technological approaches to manipulate with materials at the atomic and molecular scale to obtain nanomaterials with improved or even completely new properties. It is worth to mention that the properties of material at dimensions of a few nanometers often differ significantly from the characteristics of the same bulk material. It can be explained by the enhancement of properties of low-dimensional materials and devices caused by high surface aria to volume ratio [1, 2].

Usually, semiconductor nanowires are fabricated by means of well-known techniques like electrochemical deposition in porous templates, chemical transport, chemical vapor deposition using Au catalytic seed, etc. [3 - 5] representing bottom-up technologies. During the last two decades it was demonstrated that electrochemical etching of massive semiconductor crystals can be used as a cost-effective approach for nanostructuring [6 - 8]. Moreover, optimization of electrochemical parameters leads to fabrication of a huge amount of semiconductor nanowires aligned perpendicular to the crystal surface. The preparation of nanowires by anodization has some advantages: short time of etching; anodization is performed at room temperature; no costly equipment is required; small amount of electrolyte; etc. Moreover, the possibility of cost-effective fabrication of InP nanowires via "fast electrochemical etching" of InP semiconductor compound was demonstrated [9]. Using this approach, the authors fabricated semiconductor nanowires with a length of 2 μm during 3 seconds of electrochemical etching, reaching an etching rate about 40 μm/min.

In comparison to Si, nanostructures based on III-V or II-VI semiconductor compounds offer larger possibilities for engineered nanofabrication due to the chemical composition, larger band-gap which give the possibilities to use these nanostructures even in visible spectral range, diversity of produced pores, and novel characteristics resulting in broad application possibilities. Furthermore, semiconductor nanotemplates, have a lot of advantages compared with dielectric nanotemplates based on porous anodic aluminum oxide or etched ion-track membranes. First of all, the properties of semiconductor nanotemplates can be adjusted by application of external electric field, illumination, etc, lead to more opportunities of application in nanofabrication. The second major advantage consist in the issue that the walls of the porous semiconductor skeleton, which have a higher electrical conductivity compared to the walls of dielectric nanotemplates, provide favorable conditions for metal nucleation and uniform deposition on the pores walls [6, 10, 11]. In other words, using a combination of two approaches and namely: anodization and electroplating of metal give the possibilities of cost-effective fabrication of metallic nanowires or nanotubes with well-defined diameters and shapes. The elaborated metal nanostructures possessing unique properties can find applications in nanoelectronics and optoelectronics as flexible electrodes, interconnectors with well-designed direction of propagation, electrodes, magnetic devices and sensors [6, 11].

An important issue to be solved for device fabrication and characterization is related to the contacting of elaborated nanostructures. In this work we will focus on the realization of the electrical contacts via different approaches to the single GaAs nanowire for photoelectrical investigations. At the same time, an optimized design of varicap device with the aim to increase the capacitance is proposed and technological realization is demonstrated.

The technological process and materials

Pt nanotubes deposition in porous GaP

The n-GaP with a free electron concentration of 1.2×10^{17} cm^{-3} with crystallographic orientation (100) and substrate thickness of 500 μm were subjected to electrochemical anodization in 5% H_2SO_4 aqueous electrolyte for porous matrix obtaining. To obtain the desired deepness of the porous layer, the duration of anodization was changed from 30 min up to 2 h. Platinum electrodeposition was performed at 40°C temperature of electrolyte during 6 hours in fabricated porous GaP templates characterized by several important

parameters as follows: (i) thickness of porous layer about 70 μm; (i) pore diameter 200 nm; and (iii) pore wall thickness about 150-200 nm. The configuration of cell with two electrodes was used. The porous GaP sample served as working electrode and as counter electrode a mesh from Pt wire with the total surface 6 cm^2 was used. To assure the uniform deposition inside the porous matrix, the pulsed electrochemical deposition was used at applied negative cathodic potential of 20 V with the pulse length of 200 μs and duration between the pulses as long as 1 s. During this delay, a refreshment of the electrolyte inside of the pores is realized.

GaAs nanowires obtaining. For GaAs nanowires obtaining, the n-type GaAs semiconductor crystals with crystallographic orientation (111) and free carriers concentration of $2x10^{18}$ cm^{-3} were used. More detailed description of GaAs nanowires obtaining and optimization of the electrochemical parameters, sample surface, etc can be found in early published paper [7]. Briefly, prior the anodization, to remove the native oxide, the samples were etched for 2 min in $HCl:H_2O$ solution with ratio (1:3). The electrical contact to the back side of the sample was realized with the silver paste. The anodization was carried out on the (111)B surface of GaAs through a 0.2 cm^2 surface area in 1M HNO_3 electrolyte at applied anodic potential of 3 V. For anodization, the configuration of cell with three electrodes was used. A piece of GaAs sample, with a surface of 1 cm^2 served as working electrode while a mesh from Pt wire with the total surface 6 cm^2 was used as counter electrode. The third one is a saturated Ag/AgCl electrode. A Scanning Electron Microscope (SEM) TESCAN Vega TS 5130 MM in configuration with an INCA Energy EDX system from Oxford Instruments operated at 20 kV was used for morphology and chemical composition analysis of obtained GaAs nanowires.

Contacts manufacturing to GaAs nanowires

Focused Ion Beam (FIB) contacting: The FIB instrument used in this work was a FEI Helios Nanolab 600. At the beginning, the sample with GaAs nanowires was placed in a small amount of deionized water and sonicated for 5 seconds in order to detach the nanowires from the substrate. 1 ml of obtained solution with GaAs nanowires was dropped on a Si substrate and let dry until the water was completely evaporated. For investigation of electrical and sensing properties of a single nanowire, a special chip was fabricated on a Quartz substrate with the distance between the contacts varying from 5 to 20 μm. A single nanowire was transferred from Si substrate to the prefabricated chip with contacts inside the FIB chamber using an Omniprobe micromanipulator. The contacts to the nanowires were performed with Pt using $(CH_3)_3Pt(CpCH_3)$ as the precursor gas under the Ion Beam.

Laser Beam Lithography contacting: The contacts to the produced GaAs nanowires via electrochemical etching in one step were performed by means of Laser Beam Lithography μPG 101 from Heidelberg Instruments. To detach the nanowires from the GaAs substrate, the samples were subjected to sonication for 15 s in an ultrasound bath containing ethanol. In the second step, a suspension containing dispersed GaAs nanowires in ethanol were deposited on the glass substrate with the dimensions of 1 cm^2. The glass substrate with the GaAs nanowires was covered with the photorezist (LOR 3B and ma-P 1205) and a designed contact pads were transferred by illumination using Laser writer μPG 101 from Heidelberg. Prior to the metal deposition by magnetron sputtering for contacts consisting from thin layers of Cr and Au with thickness of 50 nm and 250 nm respectively, the contacts pads were

developed in photorezist remover. A final step was lift-off with Microposit remover 1165 at 50°C. To mention that on the same glass substrate it is possible to fabricate several contacted nanowires.

Photoelectrical study

The photoconductivity of the fabricated photodetectors based on single GaAs nanowire was exited with a Xenon lamp DKSS-150. Due to the band-gap of GaAs, the infrared region is expected to give perspective results. However, also UV spectral region has been investigated. Optical filters were used to select the desired spectral range (ultraviolet, near infrared (IR) and visible). The optical power in IR region after optical filter was 100 mW. The current in the dark and under illumination was recorded at 300 K by means of Keithley 2400 Source Measure Unit connected to the computer via IEEE 488 interface.

Results and discussions

As it was mentioned in Introduction section, porous nanotemplate-based nanomaterials are promising for a lot of applications, especially in micro-nanoelectronics. A good example is a fabricated device consisting from deposited metal in porous semiconductor matrix resulting in high contact area at the metal/semiconductor interface [12]. In comparison with the case of 2D contact of metal and semiconductor, the approach with use of porous template, representing 3D structure leads to an enormous capacitance which has been used for realization of the variable capacitance device. The device was obtained via pulsed electroplating of Pt on the whole GaP pores walls resulting in formation of Pt nanotubes [13]. The formation of Schottky contact is clearly seen from SEM images of investigated metallo-semiconductor networks. As a rule, the metal is not charging during the scanning because have a higher conductivity than semiconductor matrix. In our case, the deposited nanotubes look bright, indicating the charge accumulation in metal due to the high Schottky contact. The height of the formed Schottky contact depends from the used metal. For GaP, some metal like Zn and Mg give an ohmic contact, while Pt possesses the highest value of difference between work function of the metal and electron affinity of the used semiconductor (ϕ_m - χ_s) which is 1.68 eV.

The schematic representation of the fabricated variable capacitance device is presented in Figure 1a, as well as the SEM image of the deposited Pt nanotubes in porous GaP template presented in the inset of Figure 1a. The GaP porous layer (2 from Figure 1a) was created in a bulk GaP substrate (1) with a 500-μm thickness at depth of 70 μm. The In metal, giving ohmic contact (1), was deposited on the back side of the GaP substrate. The Schottky contact was formed on the top and internal surfaces of the GaP pores via successive pulsed electrochemical deposition of Pt. Successive pulsed electrochemical deposition means that after formation of Pt nanotubes on internal surface of pores, the duration (length) of pulses was increased to force the deposition of more quantity of metal ions, also the duration between pulses was reduced with the aim to not allow the penetration of metal ions deeply inside of porous layer. In this pulsed electrochemical deposition regime, we provide the deposition at interface of porous layer and electrolyte, thereby, growing up, each Pt nanotube are interconnected with the deposited thin film on the surface.

The measured I-V characteristics demonstrated the existence of the Schottky contact reaching a rectifying ratio of 10^5 at applied potential of 12 V (see Figure 1b). The relationship between device capacitance and voltage is presented in Figure 1c.

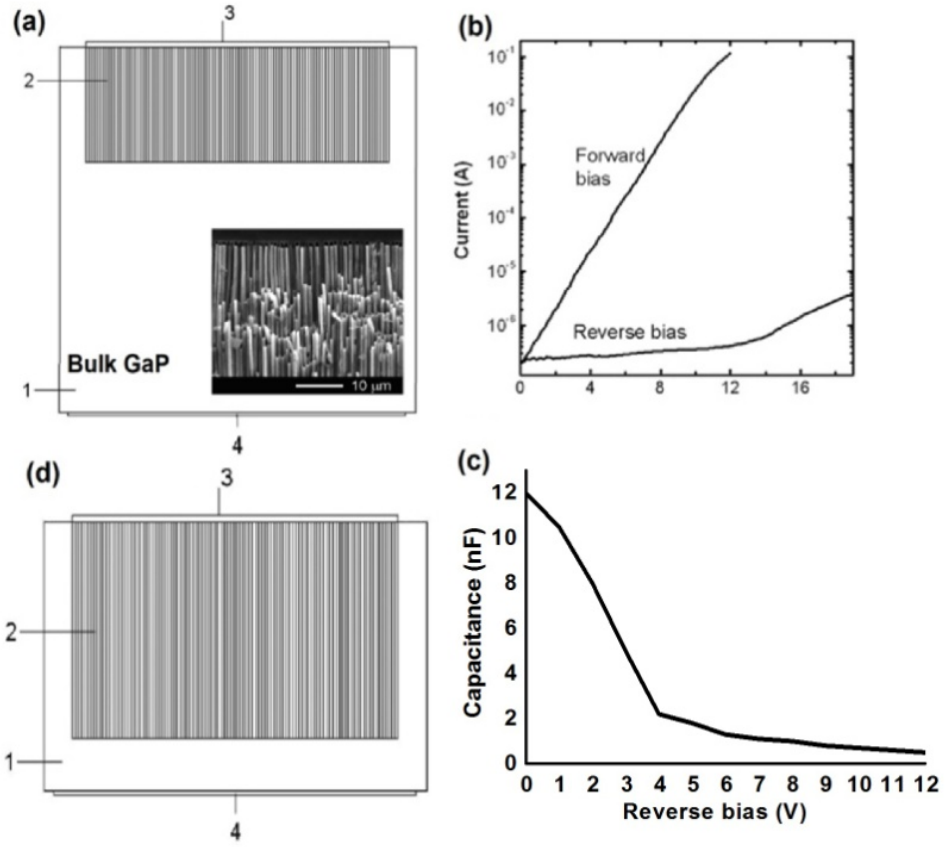

Figure 1. (a) The variable capacitance device schematics with deepness of 70 μm are as follows: 1 - GaP substrate; 2 - Pt nanotube-filled porous GaP template; 3 - Pt Schottky contact interconnecting deposited Pt nanotubes in pores and thin Pt film on the top surface; 4 - Ohmic contact. (b) Characteristics of current and voltage. (c) Capacitance-voltage characteristics of the varicap device elaborated in (a). (d) Proposed design with improved capacitance-voltage characteristics by 5 times due to use of 300 μm thick porous layer. The inset in (a) represent SEM image of Pt/GaP nanocomposite used for device fabrication.

It is worth to mention that the capacitance of varicap device, usually named barrier capacitance, is measured at reverse polarization. It can be seen, that in the range of 0.5 to 4 V of applied voltage, the capacitance value drops sharply from 12 to 2 nF, indicating that the device reaches a capacitance density variation of about $6x10^{-3}$ pF/V for 1 μm^2 of surface. This obtained value is much higher in comparison with other 2D variable capacitance device consisting from flat p-n junction or deposited two-dimensional thin film on the semiconductor surface.

In this paper, based on our calculations and preliminary results, there have been established that taking into account that the deposited Pt nanotubes were on depth of 70 μm, the capacitance value can be increased using porous layers with deepness of several hundred of micrometers (see Figure 1d). For this purpose, an optimization of pulsed electrochemical deposition of Pt is required. The optimization of parameters of pulsed electrochemical deposition showed that uniform deposition of Pt nanotubes inside pores along 300 μm thickness occurs at pulse duration of 100 μs and duration between the pulses of 3 sec. The total time of electrodeposition is 15 hours. Beside this, a mechanical steering of the electrolyte is performed.

Via electrochemical etching not only porous structures can be obtained but also due to optimization of electrochemical parameters during the anodization leads to the formation of arrays of nanowires [7 - 9, 14]. Recently, the fabrication of photodetector based on single GaAs nanowire was reported [7]. As was discussed in the introduction section, nanowires obtaining via anodization is a cost-effective technology, while the contacts fabrication to single nanowire is a challenge and require more investigations. In continuation, the formation of contacts via three different methods is investigated. The first one is fabrication using the FIB. The SEM image of contacted GaAs nanowire is presented in Figure 2a. In this case, the measured I-V characteristic demonstrated formation of Schottky contacts requiring an applied voltage with amplitude about 8 V for fabricated device. It is worth to mention that the fabrication of contacts with FIB it is very expensive while require a lot of work-hours in clean room and expensive equipment. The second approach is based on contacts fabrication via Laser Beam Lithography. Used equipment in this case is not so expensive. The optical image of contacted GaAs nanowire is presented in Figure 2b. The possibilities to choose the deposited material in magnetron sputtering (e.g. Cr/Au) give the advantage to obtain ohmic contact resulting in linear dependence of photodetectivity.

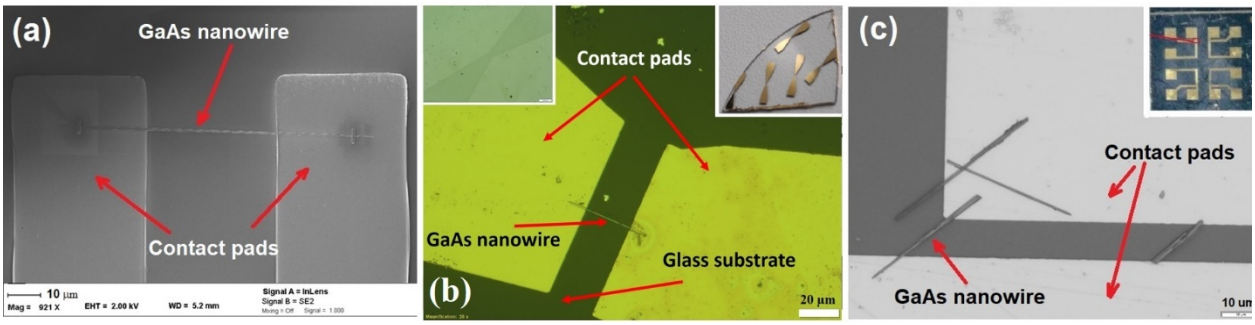

Figure 2. (a) SEM image of contacted GaAs nanowire with FIB technique. Photos at optical microscope of contacted GaAs nanowires via Laser Beam Lithography in (b) and prefabricated Si chip with contacts in (c). The inset in (b) represents design of contacts (left) and photo of 4 fabricated photodetectors (right) while inset in (c) shows the Si chip (1×1 cm) with contacted nanowire.

The third approach, representing a low-cost fabrication, could serve the use of Si/SiO_2 chips with prefabricated contacts (see inset in Figure 2c). The technological route implies the following steps: nanowires fabrication via anodization, sonication to assure the release of nanowires from the substrate to ethanol; a drop of ethanol suspension with nanowires is deposited on the surface of the chip with prefabricated contacts; evaporation of the ethanol; the chip is subjected to investigation, until the condition that at least one nanowire is caught between contacts is met. Otherwise, the procedure is repeated until electrical contact with a nanowire is created. Despite the accessibility and the low cost of this method, it should be mentioned that the photodetector manufactured by this approach demonstrated a degradation over the time (after 3 months). We assume that the cause is the formation of unstable contact, the nanowire is just placed on the contact and any mechanical action, electrical stress, and temperature gradient can affect the integrity of the contact between the nanowire and the contact pad. So, this method could be recommended just for rapid investigation of electrical properties of fabricated nanowires with further deposition of contacts by Laser Beam Lithography or FIB.

Schematic of photodetector realization on the basis of single GaAs nanowire is presented in Figure 3a. The measured photoresponse demonstrated the increase of the current in the case of illumination about 4 times (see Figure 3c).

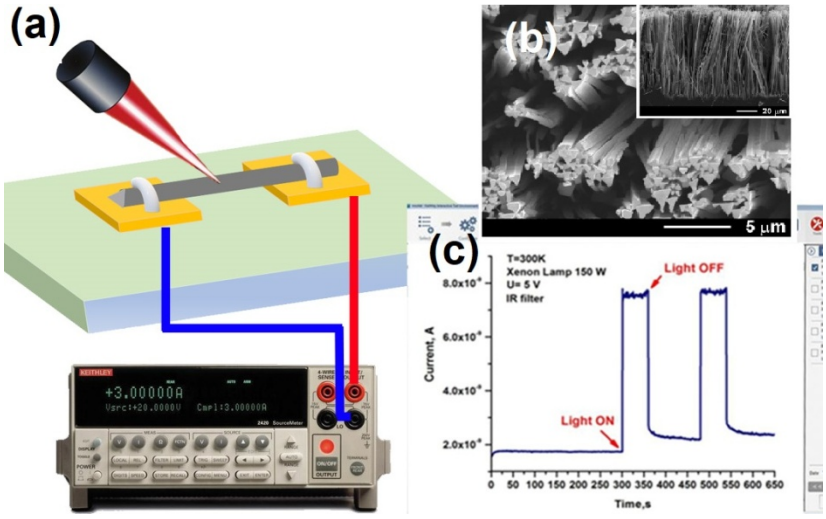

Figure 3. (a) Schematic representation of realization of IR photodetector based on single GaAs nanowire. (b) SEM image from top view and inset cross-section view of obtained GaAs nanowires via electrochemical etching. (c) Photoresponse as a function of time measured at infrared radiation with the excitation density of 800 mW/cm^2 of elaborated photodetectors on the basis of single GaAs nanowire.

The responsivity of the photodetector R is calculated according to the formula [15]:

$$R = \frac{I_{photo} - I_{dark}}{P_{ill}} \quad (1)$$

where I_{photo} and I_{dark} represent the measured current of the elaborated photodetector at illumination and in the dark respectively, while P_{ill} is the illumination power. As was mentioned above, the value of the band-gap of GaAs define the use of IR radiation.

The calculation of the right illumination power is a very important issue. In our case, beam power (P_{beam}) was 100 mW and beam diameter (d) 9 mm. Taking into account that the active area of the photodetector was (S_{phd}) 20 × 0.4 µm^2 (length and diameter of the nanowire respectively).

The excitation density per square centimeter is calculated in equation 2:

$$P_{exc} = \frac{P_{beam}}{S_{beam}} = \frac{100 \times 10^{-3}}{0.1} = 100 \text{ mW/cm}^2 \quad (2)$$

To calculate how much light drops on photodetector, the obtained excitation density needs to be multiplied with the area of the photodetector giving a power of illumination P_{ill}=800 mW/cm^2. Accordingly, to the results presented in Figure 3c, the calculated responsivity of the elaborated photodetector based on single GaAs nanowire is equals to 100 mA/W at the applied potential of 5 V.

Another important parameter for the detection capability of the photoelectric device is the detectivity which can be calculated from equation 3 [15].

$$D^* = \frac{R\sqrt{A}}{\sqrt{2eI_{dark}}} \quad (3)$$

where *A* - represent the active area of the nanowire exposed to the illumination, *e* is the elementary charge. Introducing the calculated responsivity in the equation 3 we get the value ≈1.2x10^9 cm Hz$^{1/2}$/W.

Thus, the elaborated photodetector based on single GaAs nanowire is characterized by good sensitivity and dynamic characteristics in the IR region of the spectrum.

As was mentioned above, the band-gap of GaAs define the use of this material in IR region of the spectrum. Notwithstanding this, the elaborated photodetectors were studied also in the UV region of the spectrum with *cut*-off *filters*. In this case, a small enhancement in the photocurrent was registered at polarization voltage of 10 V for UV region of the spectrum, as can be seen in Figure 4.

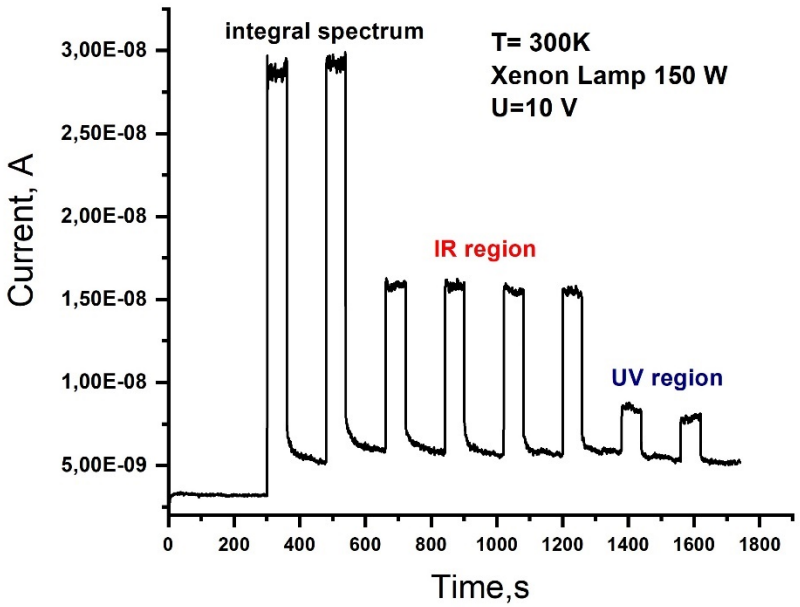

Figure 4. Photoresponse as a function of time measured at integral spectral range, infrared and ultraviolet radiation of elaborated photodetectors on the basis of single GaAs nanowire biased at applied voltage 10 V. The integral spectrum means that no optical filters were used.

Conclusions

Nowadays, anodization of semiconductor compounds represents a cost-effective top-down approach in nanofabrication. Cost-effective technology means that it not requires sophisticated equipment, high temperatures and long durations of nanostructuring in comparison with bottom-up approach. To extend the area of applications it is proposed to combine these two approaches for micro-nanodevice manufacturing. This route was used to fabricate varicap device based on Pt/porous GaP with increased capacitance. At the beginning, the porous templates were fabricated by anodization and then, Pt nanotubes were electroplated via pulsed electrochemical deposition. An optimized design of varicap device with the aim to increase the capacitance was proposed and technological conditions of pulsed electrochemical deposition for realization of metal/semiconductor with deepness of 300 μm were elaborated.

The influence and formation of contacts to the single GaAs nanowire via three different methods was investigated. It was demonstrated that, contacting with means of laser beam lithography represent an efficient and cost-effective approach for photodetector elaboration. The elaborated photodetector based on single GaAs nanowire is characterized by good sensitivity and dynamic characteristics in the IR region of the spectrum. Moreover, the developed photodetector shoved photosensivity in the UV region of the spectrum at applied potential of 10 V.

Acknowledgements. This work received partial funding from National Agency for Research and Development from Moldova under the PostDoc Grant no. 21.00208.5007.15/PD *"Micro- and nano-engineering of semiconductor compounds based on electrochemical technologies for electronic and photonic applications"*.

References

1. Jeevanandam J., Barhoum A., Chan Y.S., Dufresne A., Danquah M.K. Review on nanoparticles and nanostructured materials: history, sources, toxicity and regulations. In: *Beilstein journal of nanotechnology,* 2048, 9, pp. 1050-1074. DOI: https://doi.org/10.3762/bjnano.9.98
2. Berger M. *Nanotechnology: The Future is Tiny. The Future is Flat—Two-Dimensional Nanomaterials*. Chapter 4, RSC Publishing, Cambridge, 2016, pp. 85-115. DOI: https://doi.org/10.1039/9781782628873
3. Morales A.M., Lieber C.M. A laser ablation method for the synthesis of crystalline semiconductor nanowires. In: *Science*, 1998, 279 (5348), pp. 208-211. DOI: https://doi.org/10.1126/science.279.5348.208
4. Wang J., Li Z., Gu Z. A comprehensive review of template-synthesized multi-component nanowires: From interfacial design to sensing and actuation applications. In: *Sensors and Actuators Reports*, 2021, 3, 100029. DOI: https://doi.org/10.1016/j.snr.2021.100029
5. Chen Y. Y., Yang S. M., Lu K. C. Synthesis of High-Density Indium Oxide Nanowires with Low Electrical Resistivity. In: *Nanomaterials*, 2020, 10, 2100. DOI: https://doi.org/10.3390/nano10112100
6. Monaico E., Tiginyanu I., Ursaki V. Porous semiconductor compounds. In: *Semiconductor Science and Technology*, 2020, 35, 103001. DOI: https://doi.org/10.1088/1361-6641/ab9477
7. Monaico E.I., Monaico E.V., Ursaki V.V., et al. Electrochemical nanostructuring of (111) oriented GaAs crystals: from porous structures to nanowires. In: *Beilstein journal of nanotechnology*, 2020, 11, pp. 966–975. DOI: https://doi.org/10.3762/bjnano.11.81
8. Asoh H., Kotaka S., Ono S. High-aspect-ratio vertically aligned GaAs nanowires fabricated by anodic etching. In: *Materials Research Express*, 2014, 1, 045002. DOI: https://doi.org/10.1016/j.electacta.2013.06.025
9. Monaico E., Tiginyanu I., Volciuc O., Mehrtens T., Rosenauer A., Gutowski J., Nielsch K. Formation of InP nanomembranes and nanowires under fast anodic etching of bulk substrates. In: *Electrochemistry Communications*, 2014, 47, pp. 29-32. DOI: https://doi.org/10.1016/j.elecom.2014.07.015
10. Tiginyanu I., Monaico El., Monaico Ed. Ordered arrays of metal nanotubes in semiconductor envelope. In: *Electrochemistry Communications,* 2008, 10, pp. 731-734. DOI: https://doi.org/10.1016/j.elecom.2008.02.029
11. Tiginyanu I., Monaico E., Ursaki V. Two-Dimensional Metallo-Semiconductor Networks for Electronic and Photonic Applications. In: *ECS Transactions*, 2012, 41, pp. 67-74. DOI: https://doi.org/10.1149/2.0011503jss
12. Vanmaekelbergh D., Koster A., Marin F.I. A schottky barrier junction based on nanometer-scale interpenetrating GaP/Gold networks. In: *Advanced Materials*, 1997, 9, pp. 575 - 579. DOI: https://doi.org/10.1002/adma.19970090713
13. Tiginyanu I., Monaico E., Sergentu V., Tiron A., Ursaki V. Metallized Porous GaP Templates for Electronic and Photonic Applications. In: *ECS Journal of Solid State Science and Technology*, 2015, 4, pp. 57 - 62. DOI: https://doi.org/10.1149/2.0011503jss
14. Monaico Ed., Moise C., Mihai G., Ursaki V.V., Leistner K., Tiginyanu I.M., Enachescu M., Nielsch K. Towards Uniform Electrochemical Porosification of Bulk HVPE-Grown GaN. In: *Journal of The Electrochemical Society*, 2019, 166, pp. H3159 - 3166. DOI: https://doi.org/10.1149/2.0251905jes
15. Sirkeli V.P., Yilmazoglu O., Hajo A.S., Nedeoglo N.D., Nedeoglo D.D., Preu S., Kuppers F., Hartnagel H.L. Enhanced Responsivity of ZnSe-Based Metal–Semiconductor–Metal Near-Ultraviolet Photodetector via Impact Ionization. In: *Physica Status Solidi RRL*, 2018, 12, 1700418. DOI: https://doi.org/10.1002/pssr.201700418

Journal of Engineering Science *Vol. XXIX, no. 1 (2022), pp. 17 - 22*
Fascicle *Industrial Engineering* *ISSN 2587-3474*
Topic *Materials Science and New Technologies* *eISSN 2587-3482*

https://doi.org/10.52326/jes.utm.2022.29(1).02
CZU 621.375.826

GENERATION OF HIGH AMPLITUDES PULSES WITH EXCITABLE DFB LASERS AND AN INTEGRATED DISPERSIVE REFLECTOR

Silvia Andronic*, ORCID: 0000-0002-7092-6867,
Eugeniu Grigoriev, ORCID: 0000-0002-0665-7500,
Vasile Tronciu, ORCID: 0000-0002-9164-2249

Department of Physics, Technical University of Moldova
*Corresponding author: Silvia Andronic, *silvia.andronic@mt.utm.md*

Received: 12. 20. 2021
Accepted: 02. 11. 2022

Abstract. This paper is devoted to investigation of pulse generation by a distributed feedback (DFB) laser with an integrated passive dispersive reflector. This configuration is treated in the framework of the simple rate equation model for dimensionless carrier and photon numbers. The two functions describe the influence of reflector on the laser dynamics. The theoretical results show that under certain condition the laser is operating in excitable regime suitable for pulse generation. We have identified the appropriate values of parameters for pulse generation. We apply small perturbation to the system in order to generate periodic pulses. Finally, the influence of these parameters on shape of pulses is investigated.

Keywords: *DFB laser, passive dispersive reflector, excitability, pulse generation.*

Rezumat. Această lucrare este dedicată investigării generării impulsurilor de către un laser cu feedback distribuit (DFB) cu un reflector dispersiv pasiv integrat. Această configurație este tratată în cadrul unui model de ecuații simple pentru purtători adimensionali și numărul de fotoni. Cele două funcții descriu influența reflectorului asupra dinamicii laserului. Rezultatele teoretice arată că, în anumite condiții, laserul funcționează în regim excitabil adecvat pentru generarea de impulsuri. Am identificat valorile adecvate ale parametrilor pentru generarea impulsurilor. Aplicăm mici perturbări sistemului pentru a genera impulsuri periodice. În final, este investigată influența acestor parametri asupra formei impulsurilor.

Cuvinte cheie: *laser DFB; reflector dispersiv pasiv; excitabilitate; generarea impulsului.*

Introduction

Over the last years it was observed an increased interest in excitable optoelectronic devices and in particular for excitable semiconductor lasers [1]. Excitability has been investigated both theoretically and experimentally. This can be defined as a dynamic property of the system underlying the responses. When a system is in rest state, it can admit two different responses to a perturbation. These two responses will depend on the size of the perturbations compared to a given threshold. In the first case, the perturbation is smaller than a given threshold. In this situation the system generates a linear response that is proportional to the perturbation and is of small amplitude. For an external perturbation greater than that of threshold, the system's answer will be an excitable spike. The amplitude

of response (spike) is independent of any other attributes of the perturbation. We mention that after the response, in both cases, the system returns to its initial rest state.

The interest in excitable systems comes to photonics from chemistry and biology, with a variety of applications such as reaction-diffusion systems, cardiac tissue, and neural modeling [2]. Excitability is also of interest for optical systems. Some specific laser systems were shown to be excitable: a semiconductor laser with optical feedback [3 - 6], with injected signals [7 - 9]. In [5], the authors reported experimental evidence of coherence resonance in an optical system. It was shown that when the noise is adding in a laser diode with optical feedback the regularity of the excitable pulses increases up to an optimal value of the noise strength. One can observe that both phase and amplitude fluctuations of the pulses are very important for the dynamics of the system. For generalize the indicator of coherence it was introduced the common entropy of the two variables mentioned above and it was shown the mechanism of destruction of the excitable orbit after the resonance.

In [8] the dynamics of a quantum dot semiconductor laser operating under optical injection was experimentally analyze. Following the experiment, the appearance of single- and double-pulse excitability at one boundary of the locking region it was observed. In [9] the authors analyzed the response of an injection-locked semiconductor laser to different external perturbations. They demonstrated the existence of a perturbation threshold beyond which the response of the system is independent of the strength of the stimulation and, thus, demonstrated its excitable character. It was shown that optically perturbing such an excitable system via the control of the phase of the injection beam can be useful for optical pulse generation. Also, excitability was demonstrated in a Q-switched fiber ring laser with graphene as a saturable absorber [10]. In [11] with the aim to show the system's response to external perturbation, the authors presented excitability in an all-fiber laser with a saturable absorber section. They perturbed the laser system with a secondary pump diode that generates pulses of varying amplitude and fixed pulse width. In this way, the presence or absence of a system response was shown to verify the excitability. It was observed a monotonous increase of the response rate from 0 to 1 over a well-defined range of perturbation amplitudes which is caused by the presence of the noise in the experience.
Furthermore, the authors showed a characteristic decrease in the delay of the response of the fiber laser as a function of the amplitude of the triggering perturbation pulse.

This paper is concerned with investigations of generation of pulses in an excitable DFB lasers with passive dispersive reflector. In Section II Laser structure and equations, we introduce the setup, and an appropriate model to describe it. Section III Results and discussions presents a study of pulse generation. Finally, conclusions are given at the end.

Laser structure and equations

A sketch of the investigated structure of DFB lasers and an additional passive dispersive reflector is shown in Figure 1. The pump current is applied to the active region. The small phase current is just for the control of phase. The active and passive sections are integrated together in a compound chip. The reflection between sections is considered to be very small. It is well known that similar devices are used for generation of high frequency single mode self-pulsations [12]. A single mode approximation was proposed in [13 - 16], and used to discuss the self-pulsating behavior and excitability. Here we concentrate our attention to generation of pulses when laser is operating in excitable mode.
We start our analysis based on the rate equations [14].

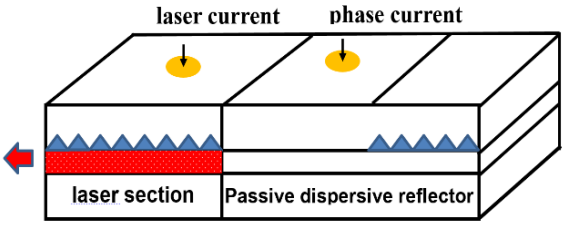

Figure 1. The DFB laser with additional passive dispersive reflector. The main injected current is applied to the laser section. The control current is applied to phase section for variation of detuning n_0.

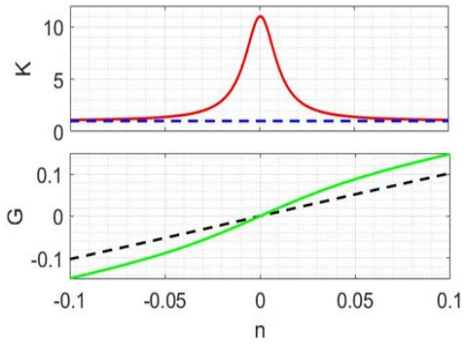

Figure 2. The dependences K and G on n from equations (3) and (4) for the following parameters: A = 10, W = 0.02, n_0 = 0.0005, α = 0.05 and Δn =0.05.

$$\frac{dn}{dt} = J - n - (1+n)K(n)p + n_{perturb}, \tag{1}$$

$$\frac{dp}{dt} = TG(n)p, \tag{2}$$

where n and p are the dimensionless carrier and photon numbers, respectively. τ is the dimensionless time. The parameter J is the relative excess injection rate (1 < J < 10). The ratio between the carrier and photon lifetimes is denoted by T. The functions $K(n)$ and $G(n)$ in equations (1)-(2) describe the influence of reflector on the laser dynamics approximated by [14].

$$K(n) = K_0 + \frac{AW^2}{4(n-n_0)^2 + W^2}, \tag{3}$$

$$G(n) = n + \alpha \cdot \Delta n \cdot \tanh\left(\frac{n}{\Delta n}\right), \tag{4}$$

where A, W, K_0, n_0 are constants. n_0 is the detuning between the resonance peak of $K(n)$ and the threshold density n = 0. This detuning can be controlled in the real devices by tuning the phase current (see Figure 1).

The rate equations (1)-(4) have two stationary solutions, corresponding to laser "off" and "on". We are not interested in laser state "off" but in the laser "on".

$$n = 0 \quad \text{and} \quad p = \frac{J}{K(0)}. \tag{5}$$

This state has sense only for J > 0. Thus, we consider J = 2. When varying the detuning n_0, while keeping all other parameters fixed, the resonance structure of K causes a dip of the photon number p. However, within a certain range on the low n_0 side of this dip, the phenomena of excitability can be observed [12]. The unstable i.e. self-pulsating region that appears in the system is described into details in [14]. We mention that for fixed set of parameters A = 10, W = 0.02, n_0 = 0.0005, α = 0.05 and Δn =0.05 the lasers is operating in the excitable regime.

Results and discussions

The generation of pulses in our case is related to excitable properties of laser shown in Figure 1. In this section, we discuss the behavior of laser when a perturbation is applied to the system. The applied perturbation is done as follows. At time t = 0 we allow to the system to reach the steady state.

Subsequently, over time, i.e. delay time 0.5 ns, we act with a small pulse on the system. The duration of the action is 0.05 ns. After this time the amplitude of the injected pulse returns to zero. We analyze the evolution of the system over time (for example see red line in Figure 3a). We notice that the amplitude of the system rises suddenly and then it decreases. For some values of parameter *T* the amplitude decreases with the presence of a delay time, named refractory time, and for other values of the parameter *T* we notice that the decrease is similar to the increase.

Let us analyze the influence of parameter *T* (ratio between the carrier and photon lifetimes) on the generation of pulses by PDRL. The parameter *T* determine the slow –fast nature of our model. Figure 3a shows the evolution in time of photon number for different values of *T* and set of parameters as in Figure 2. The perturbation amplitude is above threshold 0.5. From this figure we distinguish the slow-fast nature of the system for small *T*. Thus, for *T* = 100 the output photon number *P* increases and then forming a long (slow) excursion in the phase space return back to the stationary state (see Figure 3b-black line). For large *T* the long excursion in the phase plane disappears. The amplitude of output photon number is smaller and the pulse are practically symmetric. Thus one can conclude that for a ratio between the carrier and photon lifetimes of 500 the shape of generated pulses will be symmetric and the amplitude sufficient large to be use in different applications. In what follows, we vary the perturbation of injected pulse and look for the laser output. Figure 4 shows maximum of output number *P* in dependence of amplitude of perturbation.

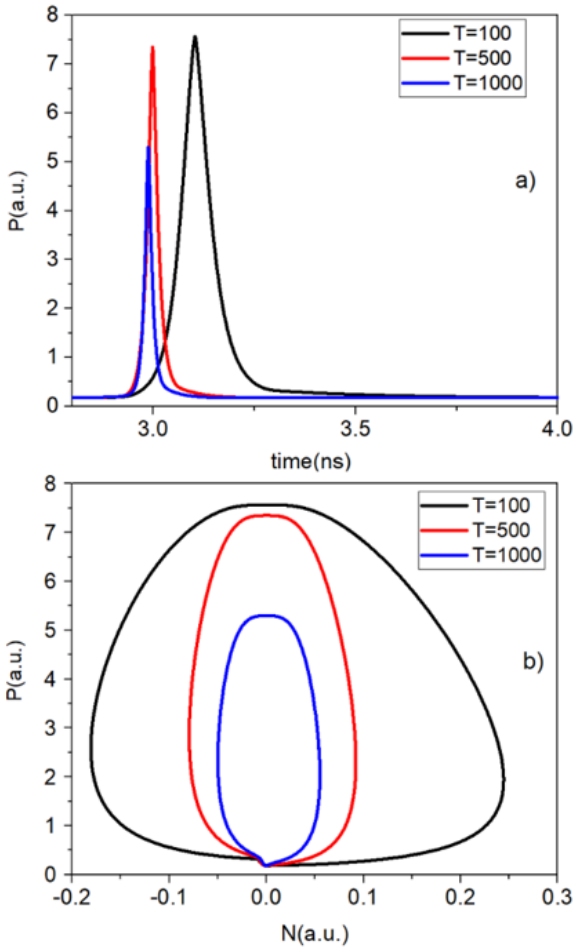

Figure 3. a) The evolution in time of photon number *P* for different values of parameter *T*. b) The phase portraits in the plane *(P-n)*. The parameters are the same as in Figure 2.

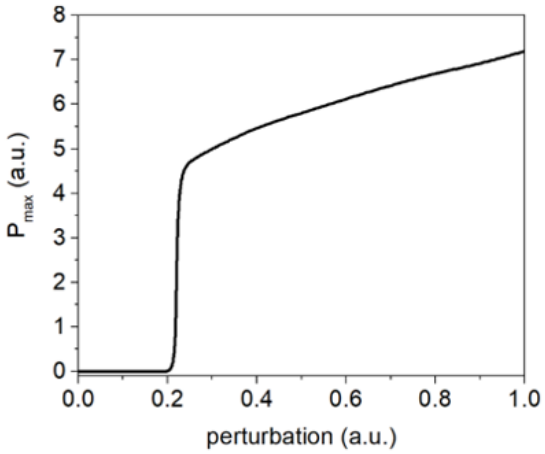

Figure 4. The dependence of maximum of output photon number on the applied perturbation. The parameter *T* = 500. Other parameters are as in Figure 2.

As long as the amplitude is small, the response of the laser system is negligible. For amplitude of 0.21 a jump of the response of

the system is observed. This is a requirement of phenomena of excitability, where the threshold has to be present. When the amplitude is increased the P_{max} is slightly increased.

Figure 5 shows the generation of pulses by PDRL under the influence of train of perturbation with different amplitudes. The supplied current pulses with 0.05 ps pulse width have the 0.05 delay time between them. For low amplitude of perturbation the response of laser is very small and close to the stationary state (red line in Figure 5).

On the other hand, for an increase of perturbation amplitude to 0.5 the train of pulses is generated by system (see Figure 5b). The output is almost periodic.

Figure 6 shows the evolution of photon number on the influence of sequences of pulses for different delay time between pulses. The response for in Figure 6a is seldom and more complicated for Figure 6b.

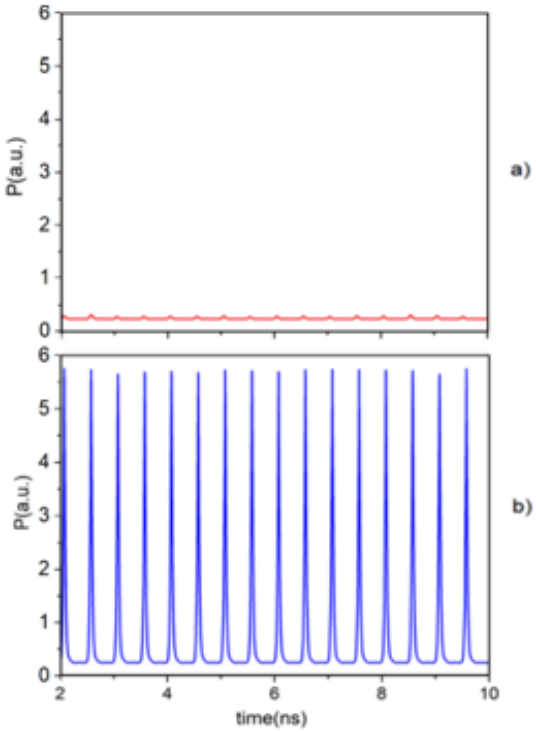

Figure 5. The dependence of photon number on time for different applied perturbation. Amplitude = 0.2, Width = 0.05, Delay = 0.5 ns, red line, b) Amplitude = 0.5, Width = 0.05, Delay = 0.5 ns, blue line.

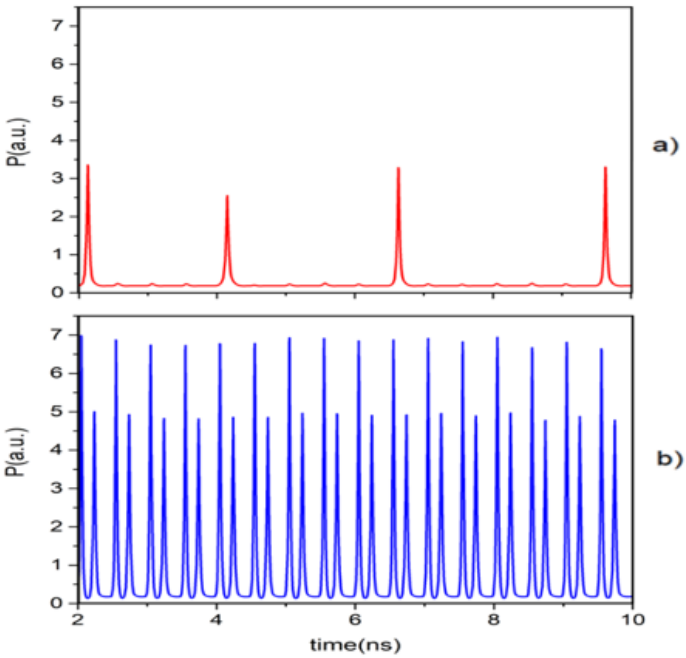

Figure 6. The same as in Figure 5 for: a) Amplitude = 0.22, Width = 0.05, Delay = 0.5 ns, red line, b) Amplitudine = 1, Width = 0.05, Delay = 0.25 ns, blue line.

Thus, for small delay between perturbations the output pulses are deformed and not suitable for applications.

Conclusions

We have carried out investigations on pulse generation by an excitable DFB laser with incorporated passive dispersive reflector. In the fremework of rare equation model, first we looked for set of parameters when the system is operating in excitable regime. Under the excitable regime we injected into the system a small perturbation and analyze the response. In particular, we got the symmetric pulse generated. The increase of ratio between the carrier and photon lifetimes reduces the amplitude of pulses. We also injected into system the sequence of perturbations and look for the response. We found that under small perturbations

no response was observed. On the other hand, when perturbation is increased the periodic response was observed. The delay time between perturbations influences the response of system by losing the periodicity. We believe that the results presented in this paper suggest that the proposed design is promising for the pulse generation.

Acknowledgments. This work was supported by project no. 20.80009.5007.08 *"Study of optoelectronic structures and thermoelectric devices with high efficiency"*.

References

1. Prucnal P. R., Shastri B. J., Ferreira De Lima T., Nahmias M. A., N, and Tait A. N. Recent progress in semiconductor excitable lasers for photonic spike processing. In: *Advances in Optics and Photonics*, 2016, 8 (2), pp. 228 - 299.
2. Taylor D., Holmes P., and Cohen A. H. Excitable Oscillators as Models for Central Pattern Generators, Series on Stability, Vibration and Control of Systems. In: *Series B, World Scientific*, Singapore, 1997.
3. Giudici M., Green C., Giacomelli G., Nespolo U., and Tredicce J. R. Andronov bifurcation and excitability in semiconductor lasers with optical feedback. In: *Phys. Rev. E*, 1997, 55 (6), pp. 6414.
4. Giacomelli G., Giudici M., Balle S., and Tredicce J. R. Experimental evidence of coherence resonance in an optical system. In: *Phys. Rev. Lett.*, 2000, 84 (15), pp. 3298-3301.
5. Tredicce J. R. Excitability in laser systems: the experimental side. In: *AIP Conf. Proc.*, 2000, 548, pp. 238–259.
6. Wieczorek S., Krauskopf B., and Lenstra D. Multipulse excitability in a semiconductor laser with optical injection. In: *Phys. Rev. Lett.*, 2002, 88, pp. 063901.
7. Gouldin D., Hegarty S. P., Rasskazov O., Melnik S., Hartnett M., Greene G., Mcinerney J. G., Rachinskii D., and Huyet G. Excitability in a quantum dot semiconductor laser with optical injection. In: *Phys. Rev. Lett.*, 2007, 98, pp. 153903.
8. Turconi M., Garbin B., Feyereisen M., Giudici M., and Barland S. Control of excitable pulses in an injection-locked semiconductor laser. In: *Phys. Rev. E*, 2013, 88, pp. 022923.
9. Plaza F., Velarde M. G., Arecchi F. T., Boccaletti S., Ciofini M., and Meucci R. Excitability following an avalanche-collapse process. In: *Europhys. Lett.*, 1997, 38 (2), pp. 91.
10. Shastri B. J., Tait A. N., Ferreira De Lima T., Nahmias M. A., Peng H.-T., and Prucnal P. R. Principles of neuromorphic photonics. In: *Unconventional Computing*: A Volume in the Encyclopedia of Complexity and Systems Science, 2018, 2nd ed., pp. 83 – 118.
11. Otupiri R., Garbim B., Broderick Neil G. R., and Krauskopf B. Excitability in an all-fiber laser with a saturable absorber section. In: *Journal of the Optical Society of America B*, 2021, 38 (5), pp. 1695 - 1701.
12. Tronciu V. Z., Wuensche H.-J., Schneider K., and Radziunas M. Excitability of laser with integrated dispersive reflector. In: *SPIE Proceedings, Physics and Simulation of Optoelectronic Devices IX*, 2001, 4283, ed. by Arakawa Y., Osinski M. and Blood P.
13. Radziunas M., and Wuensche H.-J. Multisection Lasers: Longitudinal Modes and their Dynamics. In: *Optoelectronic Devices - Advanced Simulation and Analysis*, 2004, ed. J. Piprek, Springer, New York, 452, pp. 121-150.
14. Tronciu V. Z., Wuensche H.-J., Sieber J., Schneider K., and Henneberger F. Dynamics of single mode semiconductor lasers with passive dispersive reflectors. In: *Optics Communications*, 2000, 182 (1-3), pp. 221-228.
15. Adziunas M., Wuensche H.-J., Sartorius B., Brox O., Hoffmann D., Schneider K., and Marcenac D. Modeling self-pulsating DFB lasers with an integrated phase tuning section IEEE. In: *Journal of Quantum Electronics*, 2000, 36, pp. 1026 - 1035.
16. Bandelow U., Radziunas M., Tronciu V. Z., Wuensche H.-J., and Henneberger F. Tailoring the dynamics of diode lasers by passive dispersive reflectors. In: *Proc. SPIE 3944, Physics and Simulation of Optoelectronic Devices VIII*, 2000. https://doi.org/10.1117/12.391461.

Journal of Engineering Science *Vol. XXIX, no. 1 (2022), pp. 23 - 47*
Fascicle *Industrial Engineering* *ISSN 2587-3474*
Topic *Mechanical Engineering and Technologies* *eISSN 2587-3482*

https://doi.org/10.52326/jes.utm.2022.29(1).03
CZU 621.83:678.073

THEORETICAL CONTRIBUTIONS ON THE SELECTION OF POSSIBLE TRIBOLOGICAL COUPLES OF MATERIALS FOR THE MANUFACTURE OF PRECESSIONAL TRANSMISSIONS

Ion Bostan, ORCID: 0000-0001-9217-999x,
Petru Stoicev, ORCID: 0000-0003-0405-1879,
Alexandru Buga*, ORCID: 0000-0002-4342-0502,
Gheorghe Postaru, ORCID: 0000-0003-2019-0975,
Nicolae Trifan, ORCID: 0000-0002-5772-1349,
Andrei Platon 0000-0001-8326-0147

Technical University of Moldova, 168 Ștefan cel Mare Blvd., MD-2004, Chișinău, Republic of Moldova
*Corresponding author: Alexandru Buga, *alexandru.buga@precesia.utm.md*

Received: 01. 12. 2022
Accepted: 02. 21. 2022

Abstract. Selecting gear materials is a great challenge for engineers. Gear teeth are subject to difficult and severe loading conditions. Simultaneous action of alternating normal and tangential dynamic stresses occurs, contact deformations accompanied by sliding friction. Gears are subject to increased requirements in terms of strength, geometric accuracy, dimensional stability, and durability. For the manufacture of gears, especially from thermoplastic materials, a theoretical argumentation of the materials is needed. An extensive study of thermoplastic materials, around the world needs to be done and the most efficient tribological couples to be chosen in terms of heat transfer from the gear zone, operation with or without lubrication, and gear life. In this paper, a theoretical synthesis of the Steel / Plastic, Plastic / Plastic, Plastic/Steel tribological couples is made, which were used in conformist and non-conformist experiments. Therefore, selected tribological couples are supposed to be used in the Precessional Transmissions applications.

Keywords: *gear materials, sliding friction, manufacture of gears, thermoplastic materials, heat transfer, tribological couples, gear life, theoretical synthesis.*

Rezumat. Selectarea materialelor pentru angrenaje este o mare provocare pentru ingineri. Dinții angrenajului sunt supuși unor condiții de încărcare dificile și severe. Are loc acțiunea simultană a tensiunilor dinamice normale și tangențiale alternative, deformații de contact însoțite de frecare de alunecare. Angrenajele sunt supuse unor cerințe sporite în ceea ce privește rezistența, precizia geometrică, stabilitatea dimensională și durabilitatea. Pentru fabricarea angrenajelor, în special din materiale termoplastice, este necesară o argumentare teoretică a materialelor. Trebuie făcut un studiu amplu al materialelor termoplastice în întreaga lume și să fie alese cele mai eficiente cupluri tribologice în ceea ce privește transferul de căldură din zona angrenajului, funcționarea cu sau fără lubrifiere și durata de viață a angrenajului. În această lucrare se realizează o sinteză teoretică a cuplurilor

tribologice Oțel / Plastic, Plastic / Plastic, Plastic / Oțel, care au fost utilizate în experimente conformiste și nonconformiste. Prin urmare, cuplurile tribologice selectate ar trebui să fie utilizate în aplicațiile de transmisii precesionale.

Cuvinte cheie: *materiale de angrenaj, frecare de alunecare, fabricare angrenaje, materiale termoplastice, transfer de căldură, cupluri tribologice, sinteză teoretică.*

Introduction

The choice of materials is an important and difficult stage in the design of solar wheels and satellites in the gears with Precessional Transmissions (PT), [1, 2]. Although in this field and not only the cost of the material is generally low compared to the cost of labor either by mechanical processing or injection into the die. The choice of materials must take into account some criteria related to the use and manufacture of the elements in the gear. From a functional point of view, for good operational behavior, resistant parts with low specific weight are required. As a result, the ratios between the allowable resistance σ_a or τ_a and the specific gravity ϒ must be as high as possible, [3]

$$\frac{\sigma_a}{\gamma} \; and \; \frac{\tau_a}{\gamma} \tag{1}$$

Reports of the type $$k_\sigma = \frac{\sigma_a}{\gamma} \tag{2}$$

called material strength characteristics (k_σ) and are influenced by stress.
Weight ratio G_1 and G_2 will be:

$$\frac{G_1}{G_2} = \frac{\gamma_1 A_1}{\gamma_2 A_2} = \frac{\gamma_1}{\gamma_2} : \frac{\sigma_{r_2}}{\sigma_{r_1}} \tag{3}$$

Where: A_1 and A_2 are the areas of the sections; σ_{r_1} and σ_{r_2} breaking limits, [3].

For bending stress (the situation is similar for torsional stresses) on parts with the same sections can write, [3]: $$\frac{W_1}{W_2} = \frac{\sigma_{i_2}}{\sigma_{i_1}} = \left(\frac{A_1}{A_2}\right)^{3/2} \tag{4}$$

Where: W_1 and W_2 bending strength modulus of the sections A_1 and A_2, σ_{i_1} σ_{i_2} bending stresses. It follows:

$$\frac{G_1}{G_2} = \frac{\gamma_1}{\gamma_2} . \frac{A_1}{A_2} = \frac{\gamma_1}{\gamma_2} \left(\frac{\sigma_{i_2}}{\sigma_{i_1}}\right)^{2/3} = \frac{\sigma_{i_2}{}^{2/3}}{\gamma_2} : \frac{\sigma_{i_1}{}^{2/3}}{\gamma_1} \tag{5}$$

It follows that the strength of the elements influences to a greater extent the specific weight of the materials at the stress of stretching-compression than at the stress of bending. Also to get rigid parts with low specific weight need, [3] $$\frac{E}{\gamma} \; si \; \frac{G}{\gamma} \tag{6}$$ the ratio between the modulus of elasticity of materials E or G and the specific gravity γ should be as high as possible, [3].

Reports of the type $$k_r = \frac{E}{\gamma} \tag{7}$$

they are called stiffness characteristics and are also related to the masses of the elements and the stress [3]. In Figure 1 are presented the strength of generic materials.
From a technological point of view, the choice of materials must take into account the possibilities of their processing, as appropriate, by casting, pressing, rolling, stamping, cutting, and the ability of the material to form, by chemical and galvanic coatings resistant layers corrosion to other environmental agents [3].

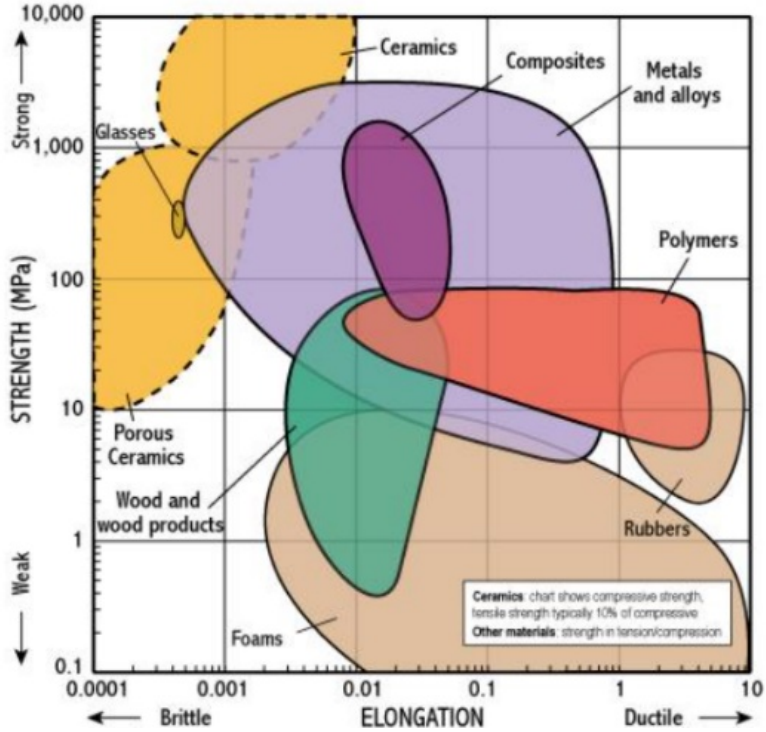

Figure 1. Strength of materials, [4].

In all the design stages, when choosing the material, the economic criterion must also be taken into account, following their cost and the fact whether or not it is deficient. Depending on the character of the production (mass, in large or small series), the ratio between the cost of the material and that of processing varies, [3]. Thus, in mass production due to the automation and mechanization of production processes, the cost of processing becomes lower than that of the material. However, it is not advisable to try to reduce production costs by using cheaper, lower-quality materials, because the results of mechanization and automation of production are conditioned by the use of homogeneous materials, both dimensionally and in terms of technological properties. On the other hand, in small series production, the share of the material in the cost of the part is small in relation to the cost of processing, the latter encompassing the work of the highest qualification. Under these conditions, it is found that it is cost-effective to use more expensive but higher quality materials when necessary (for ex. PEEK or PBI). All materials with industrial value are used in the manufacture of gears. Thus, ferrous materials, non-ferrous metals, and their alloys, thermoplastic materials, are used. Higher quality carbon steels are used in the manufacture of gears that require high strength even without the use of heat or thermochemical treatments. Such alloys are *OL 70, OLC 55,* [3], if precise processing and resistance of the teeth are pursued without a heat treatment, which could cause their deformation. However, it should be remembered that these steels are not easy to process, the tools are worn faster than those used for low carbon steel, [3].

Alloy steels and higher alloy steels for machine building are often used for the manufacture of gears, especially those with chromium as an alloying element *(40 Cr10),* [2]. Consequently, alloy steels are much less deformed by heat treatment than carbon steels, this conclusion being of great importance for small and precise parts whose further hardening processing is difficult and sometimes impossible due to their small size.

It should be noted that steel is in itself an ideal solid matter or in other words a Euclidean rigid with linear Hooke's behavior. Compared to thermoplastics which are real fluid

bodies with Maxwellian behavior, [5]. Thermoplastics are viscoelastic bodies that, under the action of force, the viscoelastic body "flows" but also deforms elastically. Some of the (*Wr)* energy accumulates in the form of reversible deformation. The other part of the (*Wc)* energy is consumed to achieve the irreversible deformation in the flow process, it dissipates in the form of heat. The total energy(*Wa*), transferred to the viscoelastic body is consumed to achieve its deformation and flow, [5].

$$W_a = W_r + W_c \quad (8)$$

A fluid can be considered perfectly viscous if the effects of its elasticity properties are negligible, *Wr* tends to 0. A real solid can be considered perfectly elastic if the effects of its viscosity properties are negligible, *Wc* tends to 0. The deviation from the perfectly elastic behavior of elastoviscous solids is due to the viscous effect *Wc* and the deviation from the perfectly viscous behavior of viscoelastic fluids is the result of the elastic effect *Wr*, [5]. A similar explanation of the rheological behavior of thermoplastic only in terms of the ratio between the relaxation time and the time of the material called the Deborah number is made by Poole R.J. [6].

When designing a thermoplastic gear wheel it is necessary to know the rheological deformations, thus a solid or liquid body, henceforth thermoplastics, unlike steels, depending on the mechanical stresses can have the following states of aggregation: elastic solid, viscoelastic fluid, viscous fluid, [5].

The application of an external force on a polymer triggers a structural reaction, which is located at the molecular or supramolecular level depending on the intensity of the stress and the presence of defects that focus the elastic energy. The way in which the polymer responds to mechanical stress is determined by its physical state and materializes in the deformation processes. The deformation of complex structures, of the nature of polymers, is composed of a succession of specific phenomena, from the elastic behavior to the viscous one, [5].

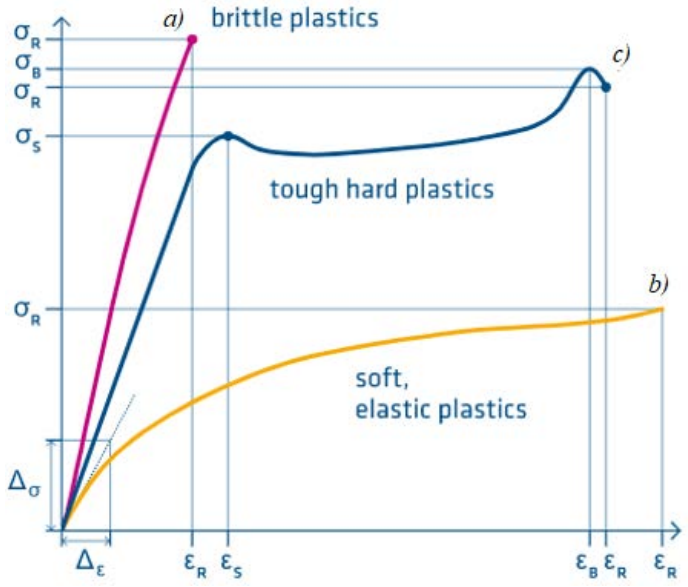

σ_B Ultra-high tension

ε_B Elongation under ultra-high tension

σ_R Tensile strength at break

ε_R Elongation at break

Figure 2. The behavior of thermoplastic polymers, during the quasi-static uniaxial deformation: a) Brittle (eg. PS at room temperature); b) Soft (PTFE at 100°C); c) Tough hard plastic (PA.6 at room temperature), [7].

In Figure 2 shows examples of the behavior of thermoplastic polymers, during the quasi-static uniaxial deformation, in the temperature region corresponding to the vitreous state. The stress-strain curve (a) is characteristic for brittle polymer (eg. polystyrene at a temperature that is characterized by a very limited elongation and a rapid monotonous increase in strain stress). Curve (b) represents the behavior of a soft elastic polymer (eg. PTFE at 100 0C), it is characteristic of polymers with low (soft) hardness, those at a temperature close to glass transition (Tg), or for plasticized ones, which have not yet become highly elastic. Curve (c) describes the behavior of a hard rigid plastic polymer. The initial monotonous increase of stress is generally slower than of a brittle polymer, the secant modulus is smaller, [5].

1. Polymers as substitute materials in the steel gears

Polymers are used as substitute materials in steel gears due to their technical and economic advantages. Compared to the metal ones [9], the advantages of polymer gears are: low specific gravity [10], no maintenance is required [11], high wear resistance in a dry condition (auto lubrication) [12], low noise, [13]; vibration damping, [14]; corrosion resistance; resistant to chemical solvents [15]; moment of inertia and low mass [16]; low cost production figure 3, [17], possibility of recycling. And the disadvantages are presented in the form of: requires increased attention to operating temperature [18], lower mechanical and thermal properties compared to ferrous and non-ferrous materials, [19], low manufacturing tolerances, [20].

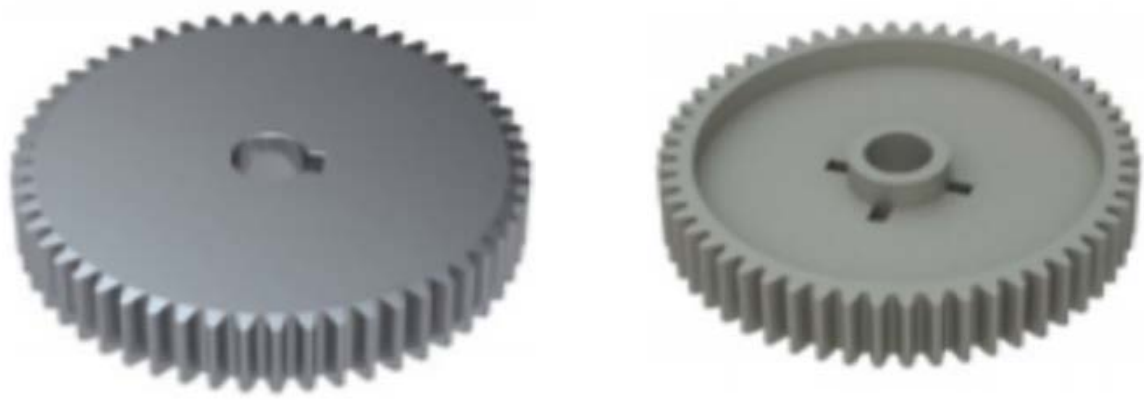

Metal gear: 22.10 cm^3
When SG is 7.8, weight is 172.4 g

Plastic gear: 9.26 cm^3
When SG is 1.3, weight is 12.04 g

Figure 3. Advantages of manufacturing die-cast gears compared to other manufacturing technologies, [17].

Figure 4 shows an example of calculating the manufacturing costs of a steel gear wheel and a plastic one. Sintered metal gear cost $2.33 = powder metal $1.10 + sintering $1.00 + secondary $0.23, or machined metal gear $2.80 = metal blank $0.60 + machining $2.20 vs. plastic gear $0.73 = resin $0.48 + injection molding $0.25, [17].

Therefore it can be said that thermoplastics are ideal to replace metal gears. It offers flexibility in design and increased performance throughout the exploitation.

Fillers, fibers, and additives, Figure 4 - are substances added in low concentrations in polymers to improve (from 30% to 40%) physical, chemical, electrical properties, to facilitate production or to change these properties, [21, 22, 23]. Due to the great diversity of polymers, fields of use, it is difficult to classify the polymers used in the manufacture of gears. A simplified classification of polymers is shown in Figure 5.

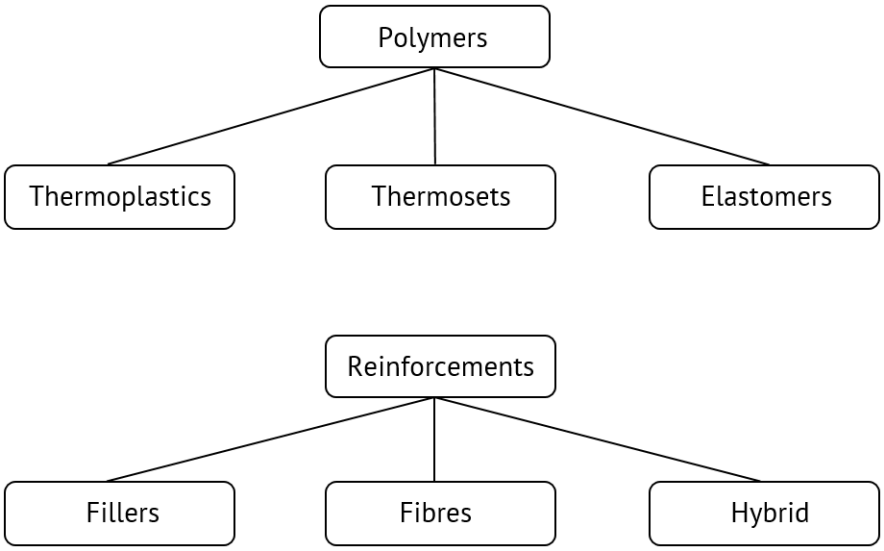

Figure 4. Simplified classification of polymers and their reinforcements, [24, 34].

Based on experimental research conducted by scientists around the world, the most commonly used basic resins with a pure crystalline structure used in the manufacture of gears are highlighted: unsaturated polyester resins (PA6 și PA66), polyacetals (POM), polyphenylene sulfide (PPS), polyether ether ketone (PEEK) and polybenzimidazole (PBI), materials which are used in the pure and composite states (reinforced with fibers, fillers, lubricants, etc.), [21-84].

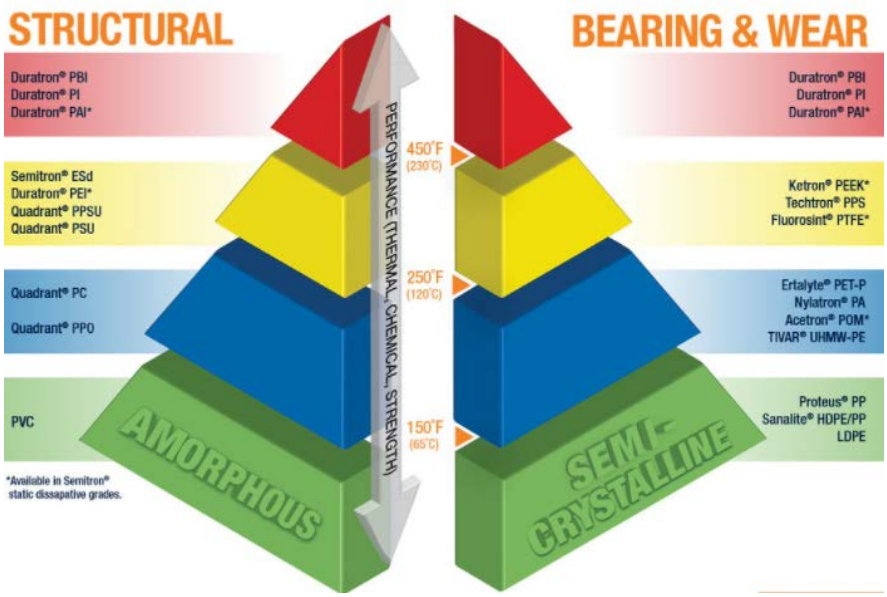

Figure 5. Mitsubishi chemical advanced materials, [24]

It is not possible to make a universal gear for all possible types of applications, the purposes of the gear must be identified:

- Moment, impact, rigidity;
-Thermal (temperature field and maximum use temperature);
-Environment of use (water, cosmic space, humidity and ambient air temperature, etc.);
-Identification of the chemical environment - defining chemical requirements, temperature, contact time;
-Identification of specific requests – the action of ultraviolet waves, opaque or transparent, resistance to fatigue and deformation under the continuous application of forces;

-Defining of the manufacturing processes – injection molding, mechanical processing, etc.;
-Assembly, plating, gluing, welding, etc.; [25].
- Availability and accessibility of thermoplastic material.

2. Theoretical argumentation of materials and tribological couples for classical gears: Plastic/Plastic, Steel/Plastic, Plastic/Steel

In order to replace steel gears with plastic gears, the operating environment, stiffness, weight, material properties, and cost must be considered [25].

Standards for the design of plastic gears are known: AGMA, British Standard, and German Standard VDI 2736, [26]. Compared to steel, defects in polymeric gears are different due to the properties of thermoplastics, for example, the defect often encountered in polymeric gears is tooth melting (thermal damage).

2.1 Theoretical argumentation of Plastic/Plastic tribological couples

K. Mao et al. [27] found that the wear of the POM / POM gears is different from the NYLON gears (PA6 / PA6). The POM gear is damaged in a high torque field for thermoplastics (10-16.1 N*m). But for the NYLON (PA6 / PA6) gear, the damage occurred at the maximum 10 N*m moment, (Figure 6).

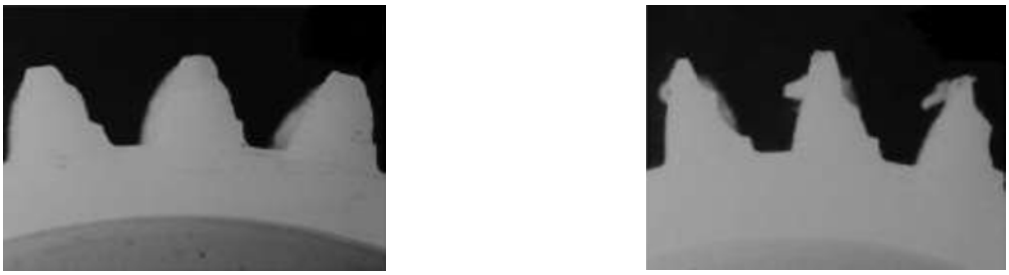

a) b)

Figure 6. Wear of gear wheels made from: a) Nylon (PA6), b) Acetal (POM), module 3 mm, 30 teeth, [27].

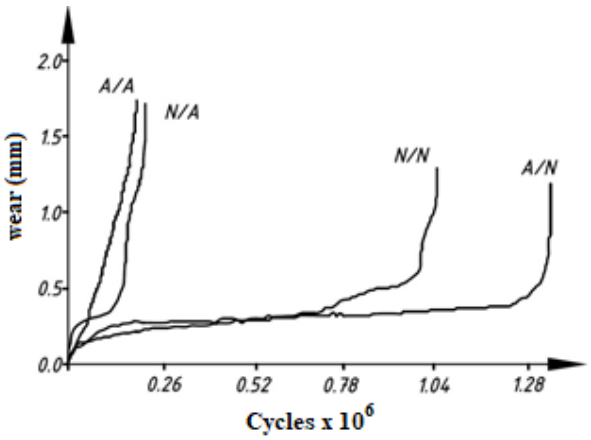

Figure 7. Graph results of the wear rate: PA6 / POM (N/A), POM / PA6 (A/N), POM/POM (A/A), PA6/PA6 (N/N), [28].

Marcel Suciu [29] and K. Mao [30] found that the primary influence on the wear of the teeth of the gears made from POM has the manufacturing process, mold die or by cutting. In [29] mentioned that the tripling of the pressure holding time, respectively from 7 to 20 sec. and at the same time doubling the piston pressure, from 200 to about 400 kg/cm^2, reduces from 7% to 3% the content of low molecular weight fractions and creates the possibility of

raising the accuracy of the parts with a class. Mao et al. [27] noted that the gear wear influenced by temperature and service life. The appearance of the temperature is due to the friction, that occurs while sliding/rolling effect of the gear teeth. The results of the tests were introduced in two-dimensional graphs, Figure 8 and Figure 9, [27].

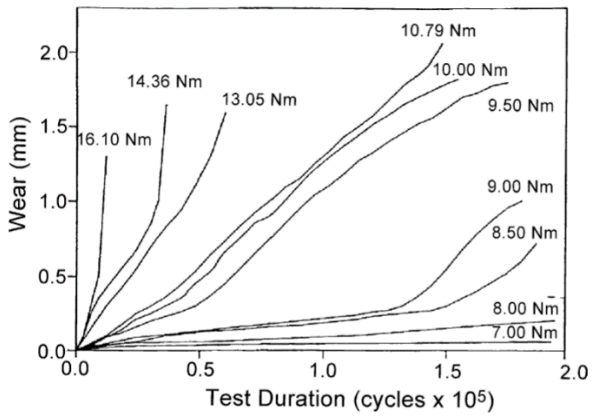

Figure 8. POM / POM gear wear and service 15PTFE life at various moments.

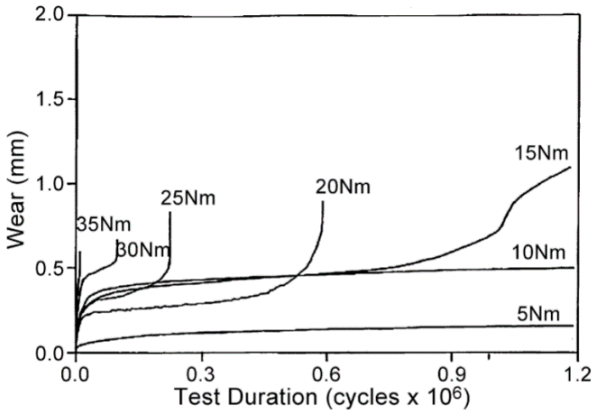

Figure 9. PA66 30GF 15PTFE/ PA66 30GF gear wear and service life at various moments.

From Figure 8 it is observed that for the proper functioning of the POM gear pairs the maximum moment of 8 N*m is recommended. For the *PA66 30GF 15PTFE/ PA66 30GF 15PTFE*pairs, the wear is higher but can be transmitted moments up to 10 Nm, (Figure 9).

Other research carried out on plastic/plastic gears was performed by Jože TAVCAR and others [31], on PA6, PA66, POM, and PPS materials, reinforced and unreinforced ones, (Table 1).

Table 1

Tested polymer materials, [31]

Polymer abbreviation	Polymer description
PA6	PA6 Polyamid; Ultramid® B3S, BASF
PA6+30GF	PA6 + 30% Glass Fiber; Zytel 73G30L NC010, DuPont
PA66+20PTFE	PA66 + 20% PTFE + SI; LNP C, RP004 (RL-4540), Sabic
PA66+30GF/15/2	PA66 + 30% Glass Fiber + 15% PTFE + 2% SI; LUVOCOM, Lehmann&Voss
POM	POM Polyacetal; Delrin® 500P, DuPont
POM+10GF	POM + 10% Glass Fiber; Delrin® 510GR NC000, DuPont
POM+20PTFE	POM + 20% PTFE; Delrin® 520MP NC010, DuPont
PPS+30CF/15	PPS + 30% Carbon Fiber + 15% PTFE; LNP LUBRICOMP C, OCL36A, Sabic

They used an original testing procedure consisting of the following steps: preliminary design of gears, (choice of material and preliminary calculation of the gear), testing (increasing the moment step by step), life cycle testing, detailed design of gear (accurate calculation of the gear based on the test results), gear testing in the final application and product validation. The life cycle results of the gear pairs of different materials are shown in Figures 10 and 11, [31]. PA66 30GF 15PTFE2Si / POM 20PTFE the longest-lived pair of gears made from, figure 11, [31]. In Table 2 are presented the friction coefficients calculated depending on the temperature in the gear, [31].

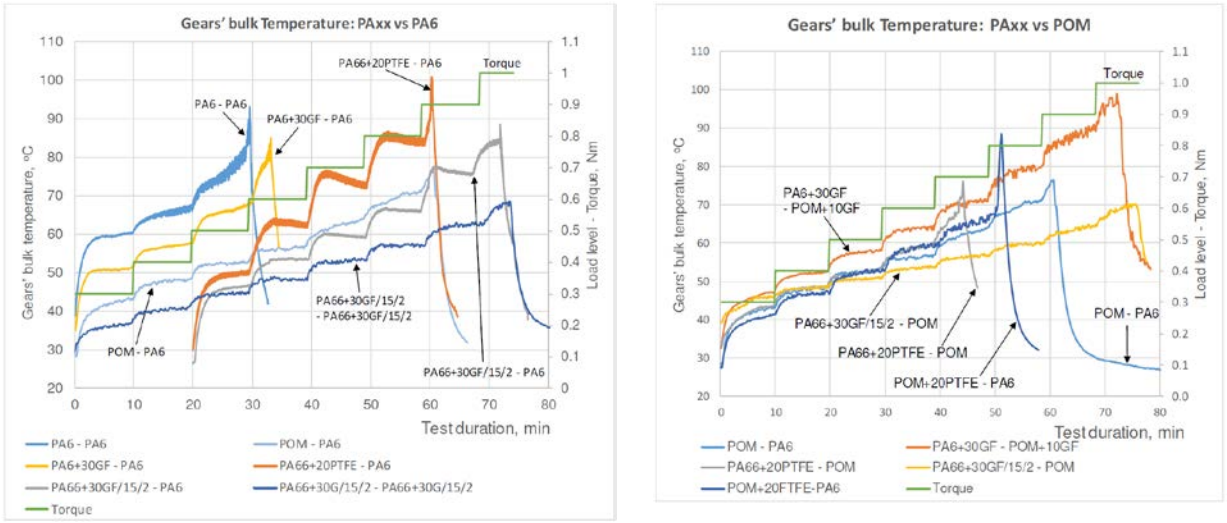

a) b)

Figure 10. a) The PA gears (with different fillers) bulk temperature during the step test. b) The PA6 and PA66 / POM gear pairs temperatures.

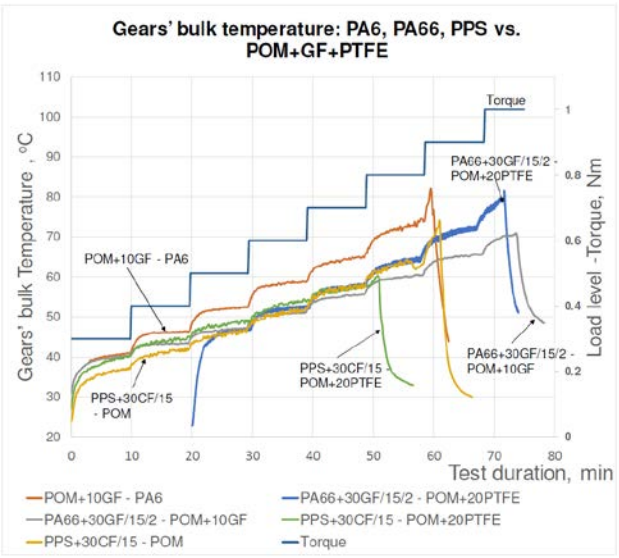

Figure 11. The PA and PPS in pair with POM gears (with different fillers) temperature profiles during the step test. Note that one test was carried out from the 0.5 Nm of torque onwards.

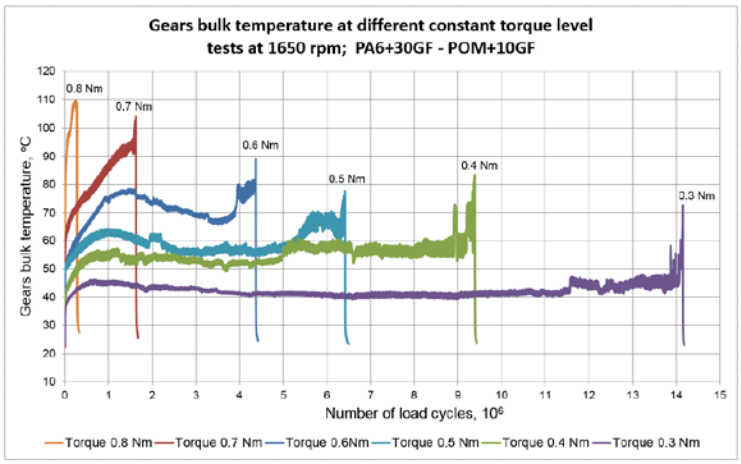

Figure 12. Gears bulk temperature profiles during several life span tests of PA6+30GF – POM+10GF material pair.

Table 2

Polymer material pairs and calculated indicator of CoF on the basis of gear bulk temperature measurements

Material pair	μ - Indicator of CoF
PA6 – PA6	0.53
PA6+30GF – PA6	0.45
PA6+30GF – POM + 10GF	0.34
POM + 20PTFE – PA6	0.29
POM – PA6	0.29
PA66 + 20PTFE – POM	0.29
POM +10GF – PA6	0.29
PA66 + 20PTFE – PA6	0.27
PA66 + 30GF/15/2 – POM	0.27
PPS + 30CF/15 – POM + 20PTFE	0.25
PA66 + 30GF/15/2 – PA6	0.23
PA66 + 30GF/15/2 – POM + 20PTFE	0.22
PPS + 30CF/15 – POM	0.22
PA66 + 30GF/15/2 – POM +10GF	0.22
PA66+30GF/15/2 – PA66 + 30GF/15/2	0.21

Figure 12 are shown the primary influence of temperature on the life cycle of the polymer gear. All pairs were tested until the complete damage. The defects in the gears were analyzed optically (Figures 13 – 16) [31].

Figure 13. Sudden tooth fracture failure of POM gear is caused by fatigue and lunker created in the injection molding.

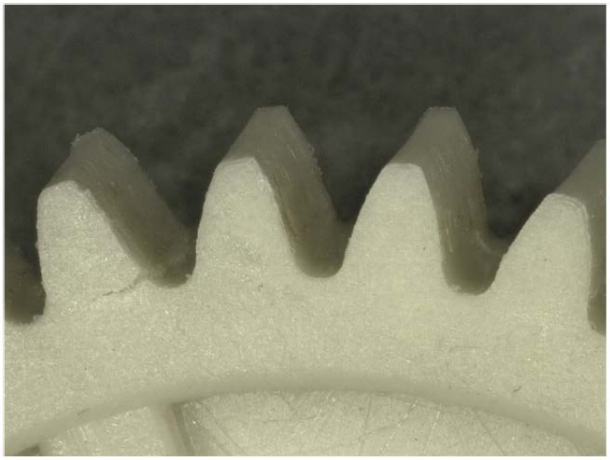

Figure 14. Crack in the tooth root of reinforced PA6+30GF gear is caused by fatigue, 15 million load cycles at 1650 rpm and 0.3 Nm load level.

The applications of PTFE lubricant in the pure PA polyamide matrix reflect a low coefficient of friction. As a result, the gear operates at lower temperatures. The use of the combination PTFE-POM does not significantly improve the tribological performance of the gear. The coefficient of friction is determined on the basis of temperature measurements. The exact determination of the temperature in the gear optimizes the design of the gears.

Fiberglass-reinforced polymers significantly increase durability at high moments (Figure 10a, b and Figure 11).

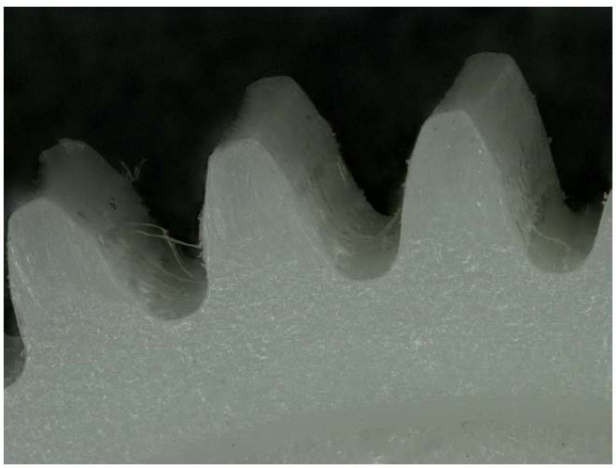

Figure 15. Wear damage on reinforced POM+ 10GF gear in pair with PA6+30GF after step test.

Figure 16. Fatigue failure mode of reinforced PPS+ 30CF/15 in pair with POM after 0.77 million load cycles at 1650 rpm and 0.5 Nm load level.

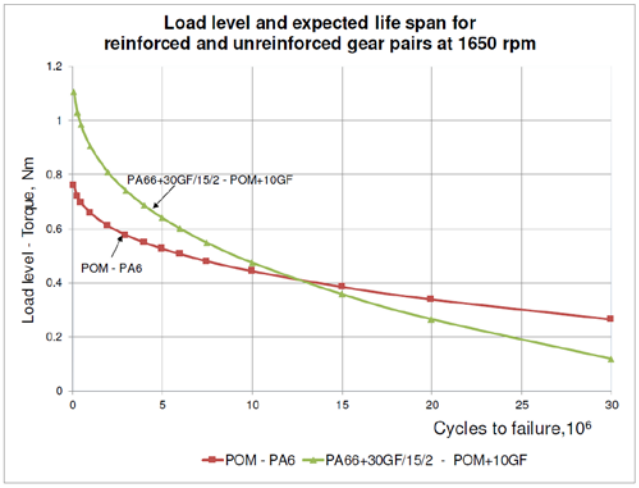

Figure 17. The PA6+30GF/POM and PA6+30GF/ POM+10GF gear pairs load level in relation to the cycles to failure.

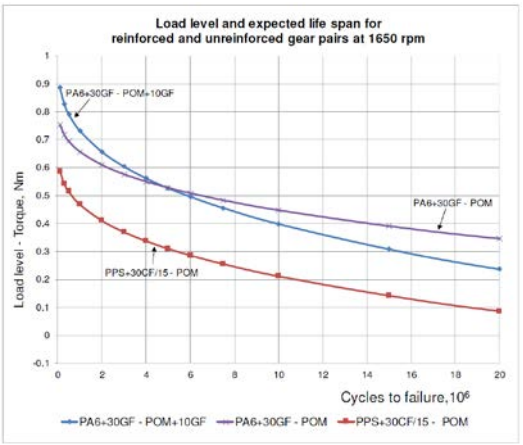

Figure 18. The PA6+30GF/POM and PA6+30GF/POM+10GF gear pairs load level in relation to the cycles to failure.

The transmission torque decreases more slowly in the unreinforced pairs than the reinforced ones. At the higher number of cycles (10^7) it is necessary to check whether it is not better to apply unreinforced materials, [31].

Hoskins et al. analyzed the tribological performance of two PEEK 450G disks (position 7 in Figure 19), [32].

They analyzed temperature-dependent time of pure PEEK disks, (Figure 20). Concluded that the wear of PEEK pairs is much lower than for other polymers. At high loads, the surfaces of the discs are deformed and melted, observable with the naked eye, [32].

Nonconformist tribological research was also done by D.H. Gordon and S.N. Kukureka [33] with discs from PA46 (Figure 21) unreinforced and reinforced with aramid fibers 6,%, 12%, 15%.

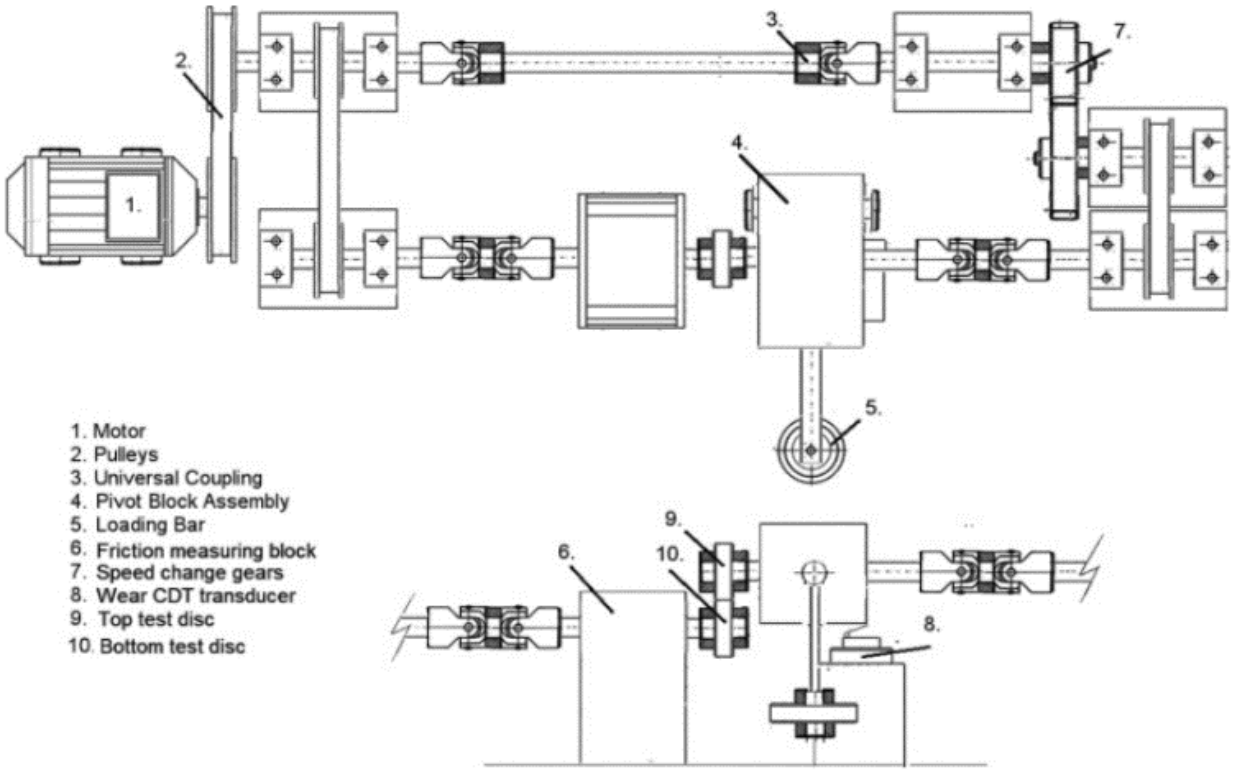

Figure 19. Schematic presentation of the experiment on establishing the tribological performance of two PEEK 450G disks.

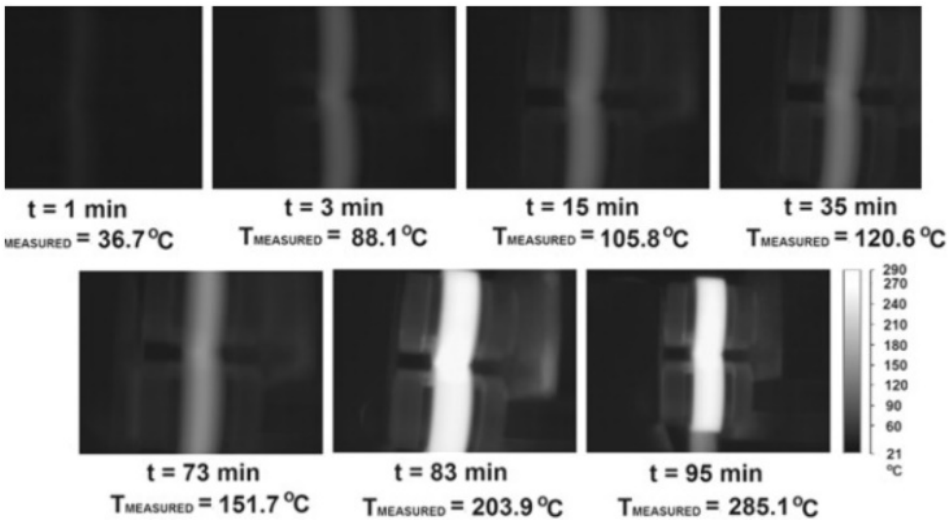

Figure 20. Temperature-dependent time of pure PEEK disks.

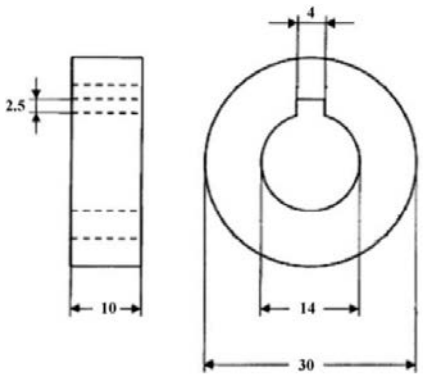

Figure 21. The shape and dimensions of the tested discs from PA46.

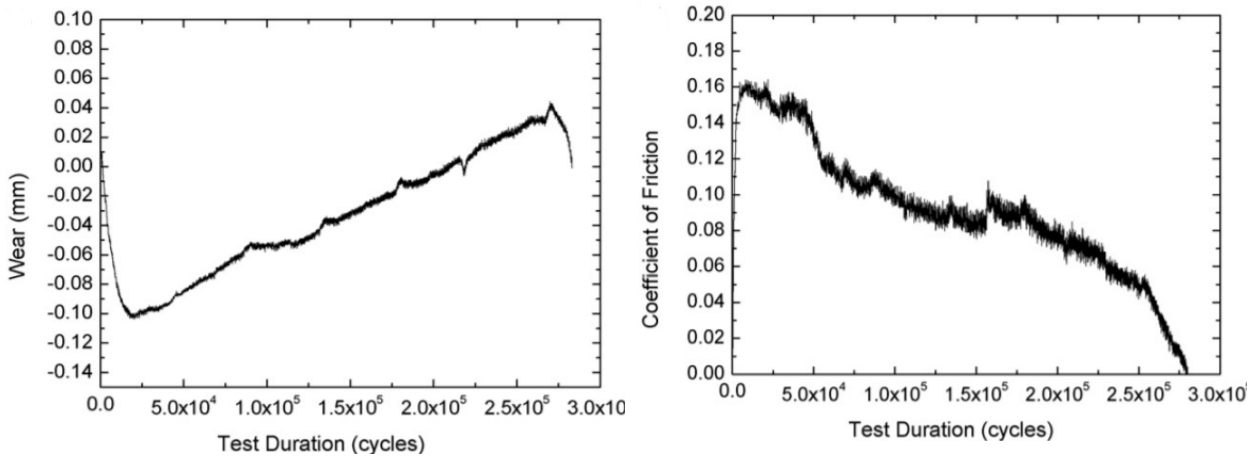

a) b)

Figure 22. a) Wear of PA46+15% aramid fibers at 1500rpm; slip ratio 2%; load 400 N
b) Friction coefficient of PA46 + 15% aramid fibers (1500 rpm; 2% slip ratio; 400 N load).

The research results showed that PA46 reinforced with 15% aramid fibers has higher wear than PA46 reinforced with a lower percentage of aramid fibers. Instead, PA46 reinforced with 15% aramid fibers has the lowest coefficient of friction. Weight loss through wear is generally the same for all tested materials. They found that weight loss and wear are a linear relationship for all types of PA46 materials reinforced with aramid fibers. Finally, PA 46 reinforced with aramid fibers in different proportions can be used in toothed transmissions with low moments, speeds, and pressures, [33].

2.2 Theoretical argumentation of Steel/Plastic tribological couples

Most thermoplastic polymers generate a film transfer on the metal surface, which helps to reduce the wear and the coefficient of friction of the materials, (Figure 23a). However, at a high-level interface temperature plastic deformation occurs which damages the soft surface leading to large damage. Reinforcement of thermoplastic materials will help reduce the wear rate, and to obtain good friction for applications with gears, (Figure 23b).

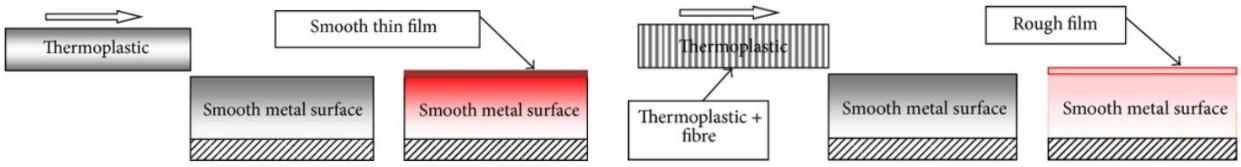

a) b)

Figure 23. Possibility of film transfer on the metal counter face:
a) pure thermoplastics b) composite thermoplastics reinforced with fiber, [34].

An extensive damage study was conducted by Senthilevan and R. Gnanamoorthy [35] on PA66-driven wheel reinforced by glass fibers or carbon fibers and unreinforced, paired by steel pinion (SS316). They performed research at speeds of 1000 RPM and moments from 1.5 to 3 Nm. They established differences of wear between the PA66 reinforced glass fiber and PA66 unreinforced. In the unreinforced ones, the wear is uneven due to the fact that the glass fibers have better adhesion in the matrix. After reducing the thickness of the teeth by 33%, the gear gripped. Wheel wear of PA 66 is due to scraping of the teeth of the opposite steel pinion, (Figure 24). Wear also occurs due to the low thermal resistance of the base material (PA66). In the case of the (PA66) gear wheel reinforced with carbon fibers, no such large

deformations of the teeth are observed due to the high rigidity and good thermal resistance of the material.

S. Senthilvelan in [36] mentioned that (PA6) reinforced with glass fibers shows high performances related to mechanical rigidity and thermal deformation. The performance of PA6 gears is only influenced by speed and high torque. Cracks of the teeth root appeared at a pressure of 8 MPa.

Figure 24. Reduction of the thickness of the polymeric tooth due to scraping of the opposite steel wheel, [35].

Tribological research on the SS316/ PA66 gear wear reinforced with 20% fiberglass or 20% carbon fiber were made by S. Senthilvelan and R. Gnanamoorthy [37]. In these experiments they used: constant rotation speed of 1000 rpm, 1,5 till 3 Nm moments, and the pressure on the tooth calculated according to the LEWIS equation [38] from 15 till 30 MPa. Several methods have been undertaken to determine wear on plastic wheel: weight measurement before and after the running cycle, temperature monitoring during running, use of the electron microscope to analyze rolling damage. The tests were performed until the complete deterioration of the wheel from PA66 approx. up to 5 mln. rotations. The test results were integrated in the two-dimensional graphs in Figures 25, 26, 27.

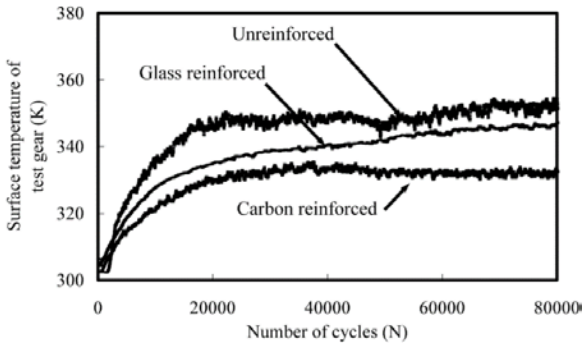

Figure 25. Gear temperature measured during running, pressure on the tooth 25 MPa, [37].

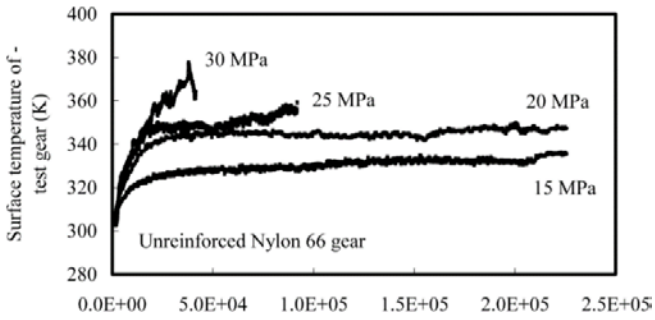

Figure 26. Temperatures in the steel gear / PA66 unreinforced with different pressures on the tooth, [37]

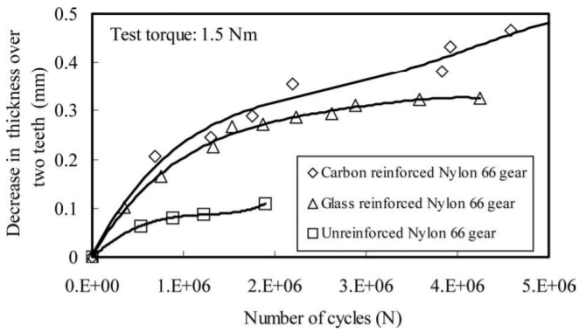

a)

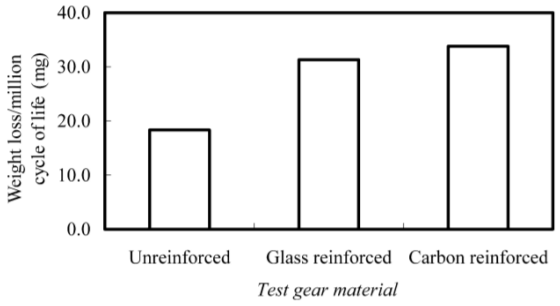

b)

Figure 27. Wear resistance of gears subjected to a bending stress of 15 MPa on tooth: a) Decrease in tooth thickness; b) The weight loss of PA66 reinforced wheel and unreinforced / million cycles, [31].

In the conclusions they mentioned that the wear depends on the type of reinforcement of the basic resine and on the orientation of the fibers, in the running direction the wheel wears less and the placement of the fibers perpendicular to the running direction the wheel wears more. Reinforced wheels have much less wear than unreinforced ones.

2.2 Theoretical argumentation of Plastic/Steel tribological couples

H. Duzcukoglu [39] did experiments on plastic/steel gear tribological couples. The main scope was to reduce the running temperature and improving heat transfer. He observed that this aim can be obtain by drilling holes in the body of the plastic teeth. The pinion made by PA6 (lubricated with oil during running) and the driven wheel from AISI 8620 (equivalent EN 20NiCrMo2) hardened and cooled in oil to a hardness of 56 HRC, Table 3. Active zones of teeth was polishing at Ra=0,6...0,8μm surface roughness. The PA6 pinion was made by 2 modes: solid one Figure 28, and drilling holes in the body of the plastic teeth (Figures 29, 30), [39].

Table 3

Properties of materials used in the tests, [39]

	Polyamide 6	**AISI 8620**
Density (gr/cm^3)	1.135	7.85
Tensile modulus of elasticity (N/mm^2)	3000	205.000
Thermal conductivity (W/Km)	0.28	46.6
Poisson`s ratio	0.41	0.3
Hardness	M80	56 HRC
Tensile strength, yield (N/mm^2)	70	560

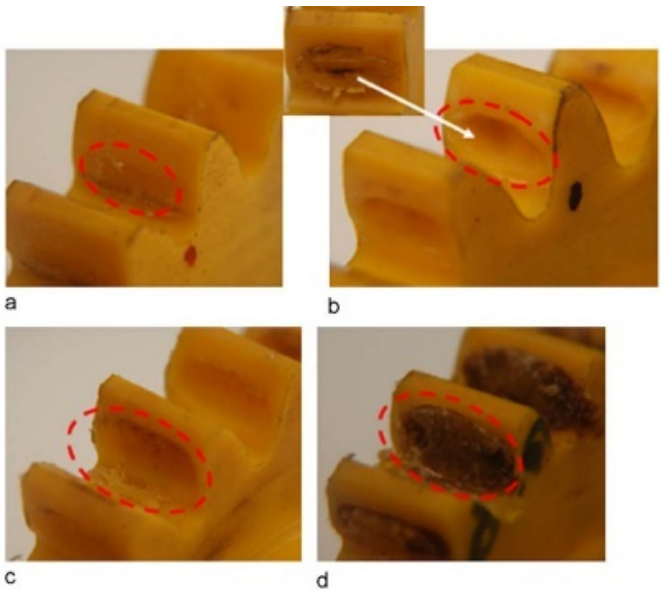

Figure 28. Damage of the gear wheel teeth (without holes) at moments:
a) 6,12 Nm, b) 10,32 Nm, c) 16,53 Nm, d) 23,3 Nm.

Considerable performance of the drilled gear was observed. This can be explained by the fact that the holes in the tooth have absorbed the deformation of the material, hysterical heat loss was did by the orifices in the teeth. Cooling holes on the tooth body absorb deformation energy, lowering running temperatures. As the torque increased by 23.3 Nm, the temperature at the gear surface increased for a certain period of time to 100^{0}C and then reached a thermal equilibrium of 84^{0}C.

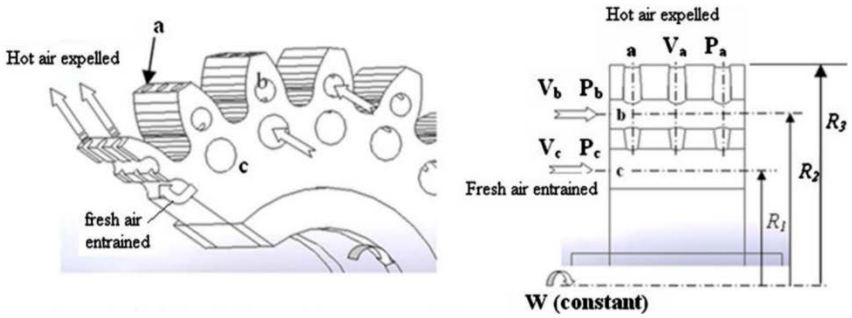

Figure 29. View of the gear provided with cooling holes.

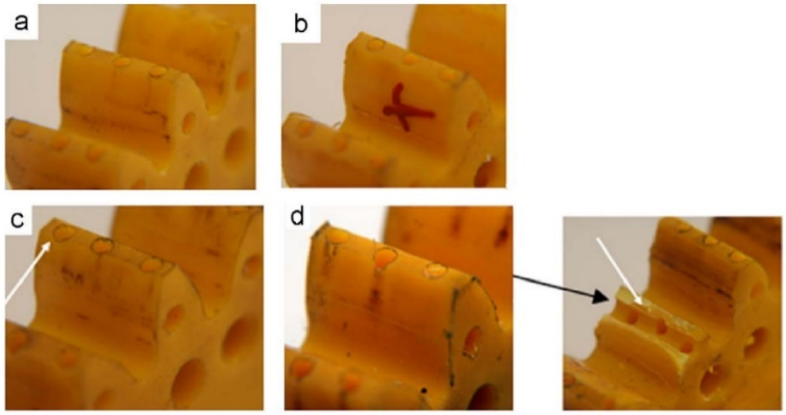

Figure 30. Damage of the gear wheel teeth provided with holes at moments:
a) 6,12 Nm, b) 10,32 Nm, c) 16,53 Nm, d) 23,3 Nm.

Teeth breakage was observed on two of the eight gears used in the experiment, due to the larger diameters of the cooling holes, which decreased the strength of the tooth and led to its breakage due to the bending stress, (Figure 30 d).

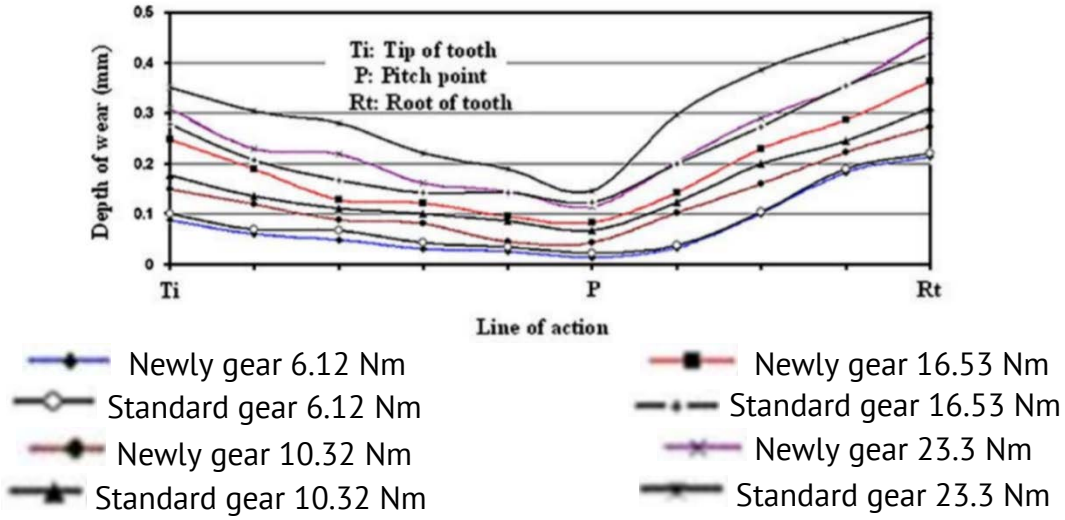

Figure 31. Wear of solid and perforated PA6 gears.

Figure 31, [39], shows the wear profiles of the teeth of solid and perforated wheels made from PA6 geared with steel wheel in the oil bath at different moments. The authors obtained following conclusions:

- was observed more wear on the root of teeth (Rt).
- low thermal conductivity of solid PA6 polyamide
- at torques greater than 9 Nm - melting and detachment of large particles from the active flank of the tooth occurs

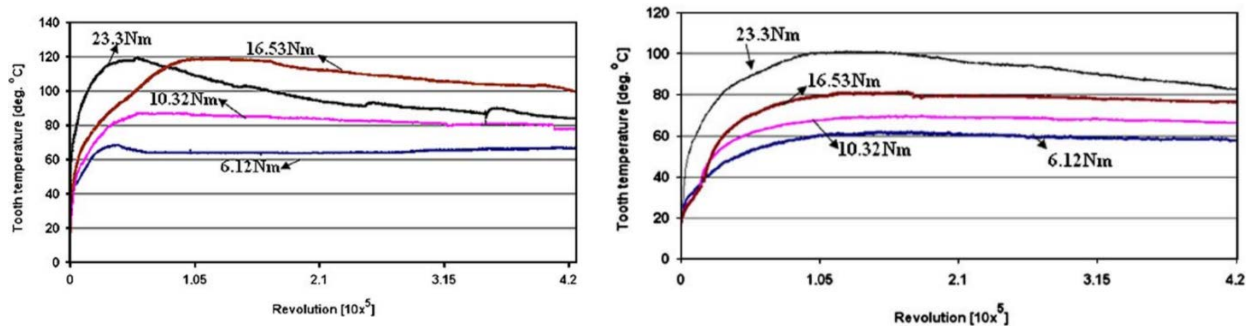

a) b)

Figure 32. a) Running temperature of solid PA6 /Steel gear
b) Running temperature of perforated PA6/Steel gear.

- the highest temperature in the active zone of teeth from PA6,
- loss of mechanical properties due to high temperature, extensive tooth wear.
- When the temperature suddenly rises, the sprocket teeth break.
- Cooling holes in the body of the tooth delayed damage by increasing heat transfer, the teeth were broken on the wheels with cooling holes at loads higher than 23 Nm, this failure did not occur due to melting at the flank of the tooth but occurred due to the concentration of stresses around the cooling holes.

One of the most important problems of polyamide gears are high loads and sliding speeds that generate heat and damage the running surfaces of the teeth.

Similar research was done by Choong Hyun Kim [40]. The pinion from POM and PA66 were designed in 3 ways: the solid tooth, the perforated tooth, the hole provided with a steel pin, (Figure 33).

Figure 33. Wear at different pinions, [40].

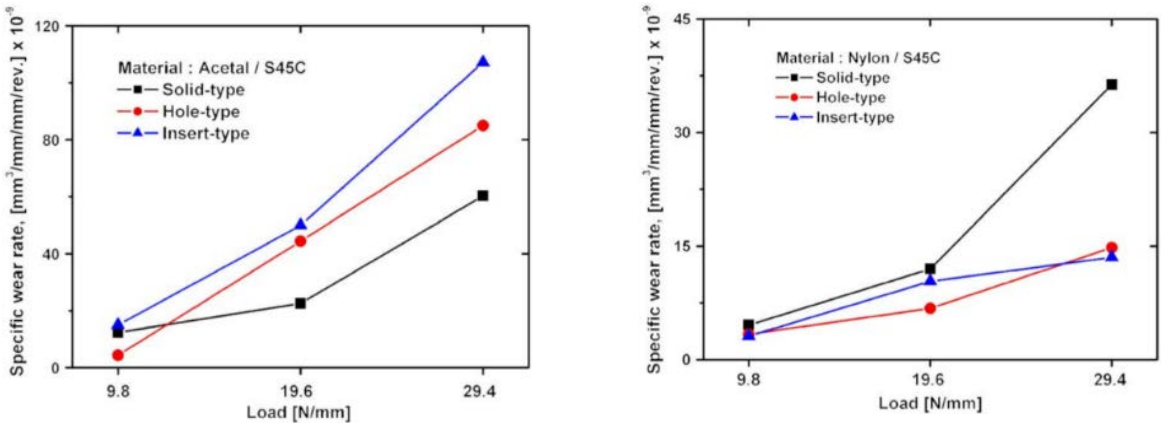

a) b)

Figure 34. a) Specific wear of POM / S45C gears at different moments;
b) Specific wear of PA6 / S45C gears at different moments, [40].

Choong Hyun Kim's results have been controversial:
-The running temperature has decreased in the gear with the pinion from PA66 provided with steel pins with 3–10^{0}C. Was reduced the wear rate by more than 30% and increased the service life to 415%.

Choong Hyun Kim's recommended to completely avoid pairing the POM sprocket and the steel driven wheel.

H. Imrek [41] conducted research on reducing the wear of gears from PA6 by changing the shape of the teeth. The shape of the tooth was modified (Figure 35b) by increasing the area of the functional flank of the tooth, [41].

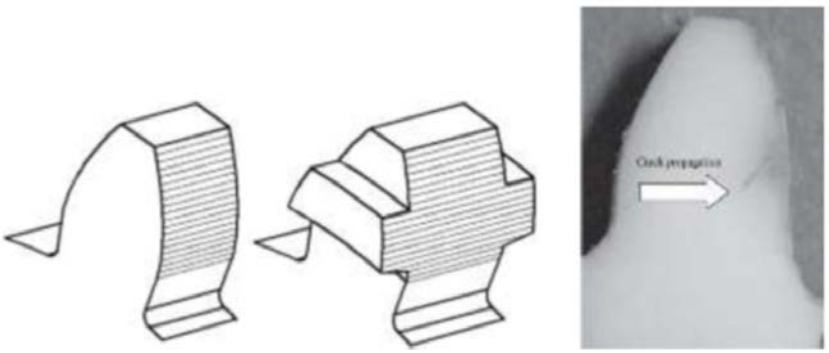

a) b) c)

Figure 35. The tooth profiles. The arrow indicates the propagation of the crack:
a) Unmodified; b) Modified; c) Crack on the flank of the tooth.

By increasing the area of the functional flank of the tooth the wear ratio decreased and the operating temperature increased. Cracks appeared on the active side of the unmodified teeth (Figure 34c), but on the modified ones the wear highlighted by the displacement of the material following the increase of the temperature appeared at the root of the teeth. H. Imrek concluded that gears with modified teeth, (Figure 35b) from PA6 have a much longer life cycle than unmodified ones (Figure 35 a) due to the lower wear coefficient, figure 36. Modified PA6 gear wheels can be used successfully in both Steel / PA6 and PA6 / Steel tribological couples.

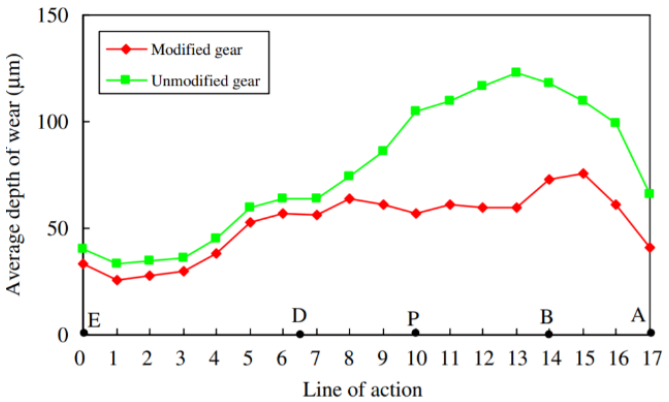

Figure 36. PA6 gear wheel wear with solid shape and modified at the moment of 8.82 Nm.

N. A. Wright and S. N. Kukureka, [42] studied experimentally and developed the technique of measuring tooth wear using the calculation of the weight of the gear wheel before the rolling cycle and after, thus determining the degree of wear. The changes in tooth shape after running experiments was observed under a microscope.

They used in their conformist experiments, real gears, made from the different materials, table 4, and non-conformist, polymer pin on steel rotating disc and simulation on rolling / sliding device with two discs, made from materials in Table 5. In all experiments they used the tribological couples Steel / Plastic and vice versa Plastic / Steel.

Table 4

Materials used in the conformist experiments

Materials used for test gears[a]			
Material designation	**Matrix**	**Reinforcement**	**Lubricant**
RF1006	PA66	30% Short glass fibres	
RFL4036	PA66	30% Short glass fibres	15 % PTFE
RC1006	PA66	30% Short carbon fibres	
RCL4036	PA66	30% Short carbon fibres	15 % PTFE
Verton	PA66	30% Long glass fibres	

Table 5

Wear material by non-conformist method, [42]

Wear factor values as supplied by LNP Plastics (1995b)	
Material	**Wear factor (K)**
2 K PA66 (skin material)	200
RF1006	75
RFL4036	16
RC1006	18
RCL4036	10
2 K PA + PTFE[a] (skin material)	12
Verton[b]	75
[a]Values for RL4040 (PA66 + 20% PTFE)	
[b]Values for RF1006.	

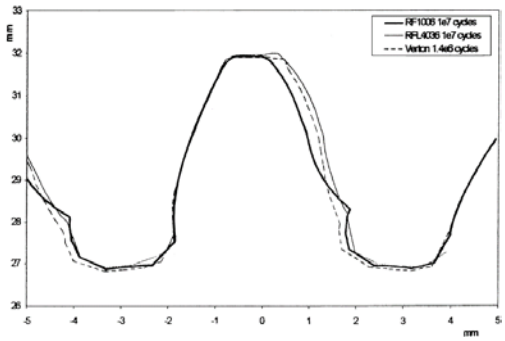

Figure 37. PA66 30 GF / SFG (RF 1006) gear tooth wear, PA 66 30 GF 15PTFE / SFG (RFL 4036), PA66 30 GF-LFG (VERTON) in gear with steel pinion.

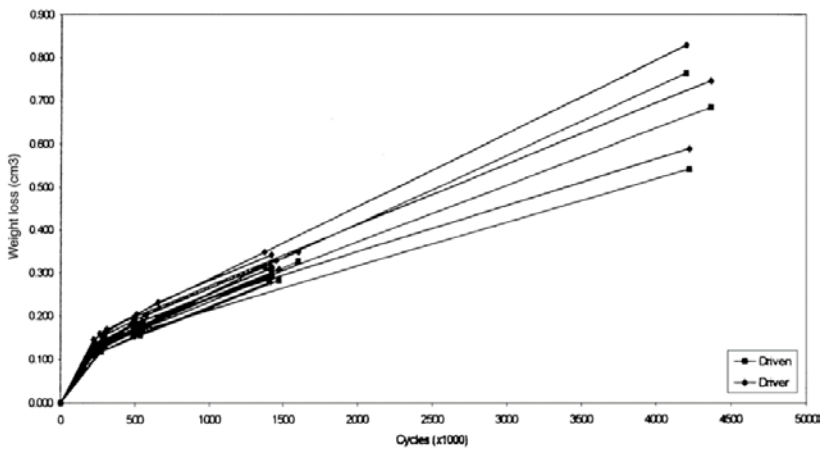

Figure 38. The PA66 30 GF gear wheel wear, [42].

N. A. Wright and S. N. Kukureka [42] mentioned that (PA 66) absorbs a significant amount of water so it is recommended to place this gear in a sealed box. By the non-conformist method they found out that PA66 30GF 15 PTFE (with short glass fibers) and PA66 20 PTFE have the lowest wear coefficient, (Table 5). The minimal and uniform wear of the tooth flank has gear wheel made from PA66 30GF 15 PTFE (with short glass fibers), (Figure 37). It is also recommended to use PA66 30 GF gears as driven wheels to achieve a lower wear coefficient. Obtained wear ratio by conformist and nonconformist tests they introduced in Figure 38.

They concluded that PA66 30GF 15 PTFE gear wheel can be used brilliantly in pair with steel gear wheel because of the lower wear compared to other materials used in their tests.

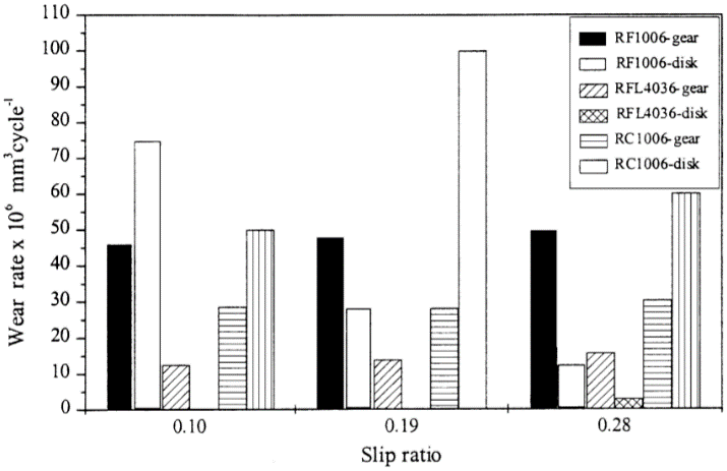

Figure 39. Comparison of wear rates, [42].

Many defects occur due to material erosion, high moments and insufficient heat transfer. In order to optimize the wear of the plastic gear, the following parameters must be taken into account; moment, ambient temperature, tooth contact temperature, running speed, running medium (acids, bases, space, petrochemistry).

Conclusions

In this article was studied the tribological pairs Plastic / Plastic, Steel / Plastic, Plastic / Steel for classic gears. The main goal is to find the best compatible tribological pairs for precessional transmission, where more than two pairs of teeth can be in contact. Compared to the classical gears in precessional transmissions the torque is distributed on several teeth at the same time. Thus, from a theoretical point of view in the precessional transmission it is possible to use the same tribological couplings as for classical gears.

Following the study, it was established:

1.The steel gear wheel can be produced from ***40Cr10, X5CrNiMo17, 20NiCrMo2, C45E*** because are much less deformed by heat treatment than carbon steels, this conclusion being of great importance for small and precise parts whose further hardening processing is difficult and sometimes impossible due to their small size.

2. Based on experimental research conducted by scientists around the world, the most commonly used basic resins with pure crystalline structure used in the manufacture of gears are highlighted: unsaturated polyester resins ***(PA6 și PA66),*** polyacetals *(POM),* polyphenylene sulfide ***(PPS)***, polyether ether ketone ***(PEEK)*** and polybenzimidazole ***(PBI)*** materials which are used in the pure and composite states (reinforced with fibers, fillers, lubricants, etc.). Fillers, fibers, and additives are substances added in low concentrations in polymers to improve (from 30% to 40%) physical, chemical, electrical properties, to facilitate production or to change these properties.

3. Compared to metal gears, the thermoplastic pinion and driven gear wheel can be made from same material ***PA6/PA6, POM/POM*** with transmission torques around 10 Nm.

4. For the ***PA66 30GF 15PTFE/ PA66 30GF 15PTFE*** pairs, the wear is higher but can be transmitted torques up to 10 Nm short period of time.

5. The longest-lived pair with lowers friction coefficient (μ=0.22) is ***PA66 30GF 15PTFE2Si / POM 20PTFE.***

6. The applications of ***PTFE*** lubricant in the pure polyamide matrix (***PA)*** reflect a low coefficient of friction. As a result, the gear operates at lower temperatures.

7. The use of the combination ***PTFE-POM*** does not significantly improve the tribological performance of the gear.

8. The coefficient of friction is determined on the basis of temperature measurements. The exact determination of the temperature in the gear optimizes the design of the gears.

9. Fiberglass-reinforced polymers significantly increase durability at high torques.

10. The transmission torque decreases more slowly in the unreinforced pairs than the reinforced ones.

11. At the higher number of cycles (10^7) it is necessary to check whether it is not better to apply unreinforced materials.

11. In ***SS316/ PA66*** (reinforced by glass fibers or carbon fibers and pure state) was highlighted that in the unreinforced ones, the wear is uneven due to the fact that the glass fibers have better adhesion in the matrix.

12. In the case of the ***(PA66)*** gear wheel reinforced with carbon fibers, no such large deformations of the teeth are observed due to the high rigidity and good thermal resistance of the material.

13. Thermal conductivity is better to fiberglass-reinforced gears.

14. The wear depends on the type of reinforcement of the basic resin and on the orientation of the fibers, in the running direction the wheel wears less and the orientation of the fibers perpendicular to the running direction the wheel wears more.

15. Reinforced gear wheels have much less wear than unreinforced ones.

16. To reduce the running temperature and improving heat transfer can be drill the teeth of the PA6 gear wheel, (as shown in Figure 29). The „cooling holes" on the tooth body absorb deformation energy and lowering running temperatures. More attention should be paid to the position and size of the cooling holes.

17. To reduce the running temperature and improving heat transfer the cooling holes can be provided with steel pins. By this way was obtained significantly improvements: running temperature has decreased in the gear with the pinion from PA66 provided with steel pins with 3...10^0C. Was reduced the wear rate by more than 30% and increased the service life to 415%.

18. By increasing the area of the functional flank of the tooth the wear ratio decreased and the running temperature increased, (Figure 35 b). Modified PA6 gear wheels can be used successfully in both Steel / PA6 and PA6 / Steel tribological couples.

19. N. A. Wright and S. N. Kukureka mentioned that (PA 66) absorbs a significant amount of water, so it is recommended to place it in sealed box.

20. The minimal and uniform wear of the tooth flank has gear wheel made from ***PA66 30GF 15 PTFE*** (with short glass fibers), (Figure 37). It is also recommended to use ***PA66 30 GF*** gears as driven wheel to achieve a lower wear coefficient.

Many defects occur due to material erosion, high moments and insufficient heat transfer. In order to optimize the wear of the plastic gear, the following parameters must be

taken into account; torque, ambient temperature, tooth contact temperature, running speed, running medium (acids, bases, space, petrochemistry).

The results of the studies made have major differences but virtually all researchers mention that the primary influence on polymer gears has temperature and time of use, two factors that contribute to wear. One the other hand the most important problems of polyamide gears are high loads and sliding speeds that generate heat and damage the running surfaces of the teeth.

There is a wide range of plastics, but they have limited information on mechanical and tribological properties, so it is necessary to test the gear pairs to find out the tribological performance of the gear. It is recommended to do a comprehensive study for such materials It is important to research the wear of thermoplastics and their thermal resistance. The addition of thermoplastic reinforcing materials helps to harden the surface, which will improve the tribological behavior of the polymer. This reduces wear and decreases the coefficient of friction in dry conditions. And in conditions of lubrication, contradictory work takes place and further investigations are needed.

Therefore, it is not possible to make a universal gear for all possible types of applications, it is necessary to identify the purposes of the gear:

- Identifying the purpose of the gear (torque, impact, rigidity);
- Thermal (temperature range and maximum operating temperature, etc.);
- Ambient (cosmos, water, humidity and air temperature, etc.);
- Identifying the chemical environment
- Defining the demands of the chemicals,
- Temperature,
- Contact time;
- Identification of specific requirements
- UV actuation, opaque or transparent, resistance to fatigue and deformation under the continuous application of forces;
- Definition of manufacturing processes: injection molding, hot / cold pressing, extrusion.
- Assembly, plating, adhesion, welding, etc.
- Availability and accessibility of thermoplastic material.

Acknowledgements. The article was elaborated within the state project *"Increasing the competitiveness of precessional transmissions by developing of the teeth gear with „conformist" contact and expanding their area of application*". Approved no. 160 PS from 31.01.2020.

References

1. Bostan I. *Precessional Transmissions. Synthesis, Kinematics and Calculation Elements*. Volume I. Chişinău: Bons Offices, 2019, 477 p. ISBN 978-9975-87-495-3. (in romanian)
2. Bostan I. *Precessional Transissions. Contact Geometry, Surface Generation and Applications*. Volume II. Chişinău: Bons Offices, 2019, 593 p. ISBN 978-9975-87-525-7. (in romanian)
3. Traian D. *Fine mechanical construction elements*. Didactic and pedagogical publishing house, Bucharest 1980, pp. 73 – 82. (in romanian)
4. David R. T. Roberts, Simon James Holder. Mechanochromic systems for the detection of stress, strain and deformation in polymeric materials. In: *Journal of Materials Chemistry* , 2011, 21(23):8256-8268; DOI:10.1039/C0JM04237D
5. Valeriu V. Jinescu. *Physical properties and thermomechanics of plastics*. Volume II. Bucharest: Technical Publishing House, 1979, pp. 13 - 34.

6. Poole R. J. The Deborah and Weissenberg numbers. In: *Rheology Bulletin,* 2012, 53 (2) pp. 32 – 39.
7. https://www.ensingerplastics.com/en/shapes/engineering-solutions/mechanical-properties
8. Yunhua L. Isotropized Voigt-Reuss model for prediction of elastic properties of particulate composites. In: *Mechanics of Advanced Materials and Structures*, 2021, pp. 1 – 13. https://doi.org/10.1080/15376494.2021.1913772
9. Mort L. *Machine Elements in Mechanical Design*: Pearson Education South Asia Pte Ltd, (2006).
10. Milani A.S., Shanian A., Lynam C., Scarinci T. An application of the analytic network process in multiple criteria material selection. In: *Material and Design*, 2013, 44 pp. 622 – 632, doi:10.1016 /j.mat-des.2012.07.057.
11. Verein Deutscher Ingenieure, VDI 2736: Part 2, Thermoplastic gear wheels, Cylindrical gears, Calculation of the load-carrying capacity, VDI-RICHTLINIEN (2014).
12. Pogačnik A. Effect of physical parameters on tribological properties of polymers for gears (in Slovenian language), phD thesis, 2013.
13. Hoskins T.J., Dearn K.D., Kukureka S.N., Walton D. Acoustic noise from polymer gears –A tribological investigation. In: *Material and Design*, 2011, 32, pp. 3509–3515, doi: 10.1016/j.matdes. 2011 02.041.
14. ISO 1328-1:2013, Cylindrical gears - ISO system of flank tolerance classification - Part 1: Definitions and allowable values of deviations relevant to flanks of gear teeth, 2013 .
15. Victrex PEEK 650 G material datasheet. https://www.victrex.com/en/datasheets (accessed 27 May 2019).
16. Thermoplastics and Thermoplastic Composites 3rd Edition-Michel Biron, ISBN: 978-0081-02-501-7 Published Date: 8th June 2018 Page Count: 1164.
17. https://www.sabic.com/assets/en/Images/Advanced%20Gear%20Solutions_tcm1010-5058.pdf;
18. Fernandes C.M.C.G., Rocha D.M.P., Martins R.C., Magalhães L., Seabra J.H.O. Finite element method model to predict bulk and flash temperatures on polymer gears, Tribol. Int. 120 (2018) 255–268, doi: 10.1016/j.triboint.2017.12.027.
19. https://www.slideshare.net/manishrdtata/1-plastic-materials
20. Hakimian E., Sulong A.B. Analysis of warpage and shrinkage properties of injection-molded micro gears polymer composites using numerical simulations assisted by the Taguchi method, Mater. Des. 42 (2012) 62–71, doi: 10.1016/j.matdes. 2012.04.058.
21. Kurokawa M., Uchiyama Y., Nagai S. Performance of plastic gear made of carbon fiber reinforced poly-ether-ether-ketone, Tribol. Int. 32 (1999) 491–497,: 10.1016/S0301- 679X(99)0 0 078-X. PEEK
22. Kurokawa M., Uchiyama Y., Nagai S. Performance of plastic gear made of carbon fiber reinforced poly-ether-ethe-ketone: part 2, Tribol. Int. 33 (20 0 0) 715–721, doi 10.1016/S0 301-679X(0 0)0 0111-0.
23. M. Kalin, M. Zalaznik, S. Novak, Wear and friction behaviour of poly-ether-ether-ketone (PEEK) filled with graphene, WS 2 and CNT nanoparticles, Wear 332–333 (2015) 855–862, doi: 10.1016/j.wear.2014.12.036.
24. https://www.mcam.com/en/products
25. Elmquist J. L. Deciding When to Go Plastic. *Gear Technology*. 46 - 47 (2014).
26. VDI 2736: 2013-2, Thermoplastische Zahnräder, Stirnradgetriebe, Tragfähigkeits-Berechnung, VDI Riehtlinien, VDI-Verlag GmbH, Duesseldorf (2014).
27. Mao K., Li W., Hooke C. J., and Walton D. "Friction and wear behaviour of acetal and nylon gears," *Wear,* 267, pp. 639-645, 6/15/ (2009).]
28. Li W., Wood A., Weidig R., and Mao K. An investigation on the wear behaviour of dissimilar polymer gear engagements, *Wear,* 271, pp. 2176 - 2183, Jul 29 (2011)
29. Suciu V., Suciu M. V. Study of Materials" Bucharest, Fair Partners, 2007- 251 pages; ISBN 978-973-1877-01-3
30. Mao K., Langlois P., Hu Z., Alharbi K., Xu X., Milson M., et al. "The wear and thermal mechanical contact behaviour of machine cut polymer gears," *Wear,* 332–333, pp. 822-826, 5// (2015).
31. Jože TAVCAR, Gašper GRKMAN and Jože DUHOVNIK [Accelerated lifetime testing of reinforced polymer gears, 19 December 2017
32. Hoskins T.J., Dearn K.D., Chen Y.K., and Kukureka S.N., The wear of PEEK in rolling-sliding contact – simulation of polymer gear applications, Wear, Vol. 309, No. 1–2 (2014), pp. 35–42.
33. Gordon and Kukureka ,,The wear and friction of polyamide 46 and polyamide 46/aramid-fibre composites in sliding–rolling contact," Wear, 267 (2009), pp. 669-678
34. Aldousiri B., Shalwan A., and Chin C. W. A Review on Tribological Behaviour of Polymeric Composites and Future Reinforcements, 01 Jul 2013
35. Senthilvelan S., and Gnanamoorthy R. "Damage Mechanisms in Injection Molded Unreinforced, Glass and Carbon Reinforced Nylon 66 Spur Gears," *Applied Composite Materials,* 11, pp. 377-397, (2004)]

36. Senthilvelan S., R. Gnanamoorthy R. Effect of rotational speed on the performance of unreinforced and glass fiber reinforced Nylon 6 spur gears, In: *Materials and Design,* 2007, 28 (3), pp. 765 - 772.
37. Gnanamoorthy R. Damage Mechanisms in Injection Molded Unreinforced, Glass and Carbon Reinforced Nylon 66 Spur Gears, In: *Applied Composite Materials*, 2004, 11 (6), pp. 377 – 397.
38. Maitra G. M. *Handbook of Gear Design*, New Delhi: Tata McGraw-Hill, 1994, p. 534.
39. Duzcukoğlu H. Study on development of polyamide gears for improvement of loadcarrying capacity, In: *Tribology International,* 2009, 42 (8), pp. 1146 – 1153.
40. Kim C. H. Durability improvement method for plastic spur gears, In: *Tribology International*, 2006, 39 (11), pp. 1454 - 1461.
41. Imrek H. Performance improvement method for Nylon 6 spur gears, In: *Tribology International*, 2009, 42 (3), pp. 503 – 510.
42. Wright N. A., and Kukureka S. N. Wear testing and measurement techniques for polymer composite gears, In: *Wear*, 2001, 251, pp. 1567 - 1578.
43. Linke H., Börner J., Heß R., Röhle E., Römhild I., Senf M. (Eds.), Cylindrical gears: calculation-materials-manufacturing, Hanser, München, 2016.
44. Hasl C., Illenberger C., Oster P., Tobie T., Stahl K. Potential of oil-lubricated cylindrical plastic gears, J. Adv. Mech. Des. Syst. Manuf. 12 (2018) JAMDSM0016 –JAMDSM0016, doi: 10.1299/jamdsm.2018jamdsm0016.
45. https://www.scribd.com/document/384413954/5816067-MATERIALE-PLASTICE-doc
46. Letzelter E., Guingand M., J.-P. de Vaujany, Schlosser P. A new experimental approach for measuring thermal behaviour in the case of nylon 6/6 cylindrical gears, Polym. Test. 29
47. H. Linke, J. Börner, R. Heß, E. Röhle, I. Römhild, M. Senf (Eds.), Cylindrical gears: calculation-materials-manufacturing, Hanser, München, 2016.
48. http://web.rtpcompany.com/info/data/index.htm
49. Singh A.K., Siddhartha, P.K. Singh, Polymer spur gears behaviors under different loading conditions: a review, Proc. Inst. Mech. Eng. Part J J. Eng. Tribol. 232 (2017) 210–228, doi:10.1177/1350650117711595
50. Roda-Casanova V., Sanchez-Marin F. A. 2D finite element based approach to predict the temperature field in polymer spur gear transmissions, Mech. Mach. Theory 133 (2019) 195 - 210, doi: 10.1016/j.mechmachtheory.2018.11.019 .
51. https://matmatch.com/materials/arke0008-kepstan
52. Li G., Qi H., Zhang G., Zhao F., Wang T., Wang Q. Significant friction and wear reduction by assembling two individual PEEK composites with specific functionalities, Mater. Des. 116 (2017) 152–159, doi: 10.1016/j.matdes.2016.11.100.
53. Ramachandra S., Ovaert T. The effect of controlled surface topographical features on the unlubricated transfer and wear of PEEK, Wear 206 (1997) 94–99, doi: 10.1016/S0043- 1648(96)07354-1.
54. T.F. de Andrade, Wiebeck H., Sinatora A. Effect of surface finishing on friction and wear of Poly-Ether-Ether-Ketone (PEEK) under oil lubrication, Polímeros 26 (2016) 336–342, doi:10.1590/0104-1428.2183
55. Zhang L., Qi H., Li G., Wang D., Wang T., Wang Q., Zhang G. Significantly enhanced wear resistance of PEEK by simply filling with modified graphitic carbon nitride, Mater. Des. 129 (2017) 192–200, doi: 10.1016/j.matdes.2017.05.041.
56. Davim J.P., Cardoso R. Tribological behaviour of the composite PEEK-CF30 at dry sliding against steel using statistical techniques, Mater. Des. 27 (2006) 338–342, doi:10.1016/j.
57. https://www.aeroexpo.online/prod/mitsubishi-chemical-advanced-materials/product-170365- 20271.html
58. http://www.pbi-am.com/en/molding-technology.
59. https://pbipolymer.com/wp-content/uploads/2016/06/High-Performance-PBI-Peek-Polymer-is-Revolutionizing-Industry.pdf
60. http://qepp.matweb.com/search/DataSheet.aspx?Bassnum=P1SM02&ckck=1
61. https://www.ensingerplastics.com/en/shapes/high-performance-plastics/pps
62. Milani A .S., Shanian A., Lynam C., Scarinci T. An application of the analytic network process in multiple criteria material selection, Mater. Des. 44 (2013) 622–632, doi: 10.1016/j.mat-des.2012.07.057.
63. Miler D., Žeželj D., Loncar A., Vuckovic K., Multi-objective spur gear pair optimization focused on volume and efficiency, Mech. Mach. Theory 125 (2018) 185–195, doi: 10.1016/j.mechmachtheory.2018.03.012.
64. https://gearsolutions.com/features/a-plastic-gear-design-update/
65. https://www.scribd.com/document/384413954/5816067-MATERIALE-PLASTICE-doc
66. Jabbour T., Asmar G. Stress calculation for plastic helical gears under a real transverse contact ratio, Mech. Mach. Theory 44 (2009) 2236–2247, doi 10.1016/j.mechmachtheory.2009.07.0 03.

67. Mao K., Langlois P., Hu Z., Alharbi K., Xu X., Milson M., Li W., Hooke C.J., Chetwynd D. The wear and thermal mechanical contact behaviour of machine cut polymer gears, Wear 332–333 (2015) 822–826, doi: 10.1016/j.wear.2015.01.084.
68. Xianqiang Pei and Klaus Friedrich, Sliding wear properties of PEEK, PBI and PPP, wear 274, January 2011, DOI:10.1016/j.wear.2011.09.009
69. Kukureka S. N., Hooke C. J., Rao M., Liao P. and Chen Y. K.'The Effect of Fiber Reinforcement on the Friction and Wear of Polyamide 66 under Dry Rolling–Sliding Contact', Tribology International 32, 1999, 107–116
70. Greco A.C., Erck R., Ajayi O., Fenske G. Effect of reinforcement morphology on high-speed sliding friction and wear of PEEK polymers, 18th Int. Conf. Wear Mater. 271 (2011) 2222–2229, doi: 10.1016/j.wear.2011.01.065
71. Damijan Zorko, Simon Kulovec, Jože Duhovnik, Jože Tavcar, Durability and design parameters of a Steel/PEEK gear pair, Mechanism and Machine Theory 140 (2019) pp. 825–846
72. Berer M., Tscharnuter D., Pinter G. Dynamic mechanical response of polyetheretherketone (PEEK) exposed to cyclic loads in the high stress tensile regime, Int. J. Fatigue 80 (2015) 397–405, doi: 10.1016/j.ijfatigue.2015.06.026.
73.Abbasnezhad N., Khavandi A., Fitoussi J., Arabi H., Shirinbayan M., Tcharkhtchi A. Influence of loading conditions on the overall mechanical behavior of polyether-ether-ketone (PEEK), Int. J. Fatigue 109 (2018) 83–92, doi: 10.1016/j.ijfatigue.2017.12.010.
74. Avanzini A., Petrogalli C., Battini D., Donzella G. Influence of micro-notches on the fatigue strength and crack propagation of unfilled and short carbon fiber reinforced PEEK, Mater. Des. 139 (2018) 447–456, doi: 10.1016/j.matdes.2017.11.039.
75. Greco A.C., R. Erck, O. Ajayi, G. Fenske, Effect of reinforcement morphology on high-speed sliding friction and wear of PEEK polymers, 18th Int. Conf. Wear Mater. 271 (2011) 2222–2229, doi: 10.1016/j.wear.2011.01.065.
76. Regis M., Lanzutti A., Bracco P., Fedrizzi L. Wear behavior of medical grade PEEK and CFR PEEK under dry and bovine serum conditions, Wear 408–409 (2018) 86–95, doi: 10.1016/j.wear.2018.05.005.
77. Schroeder R., Torres F.W., Binder C., Klein A.N., J.D.B. de Mello, Failure mode in sliding wear of PEEK based composites, Wear Mater 301 (2013) 717–726, doi: 10.1016/j.wear.2012.11.055.
78. Mohammed A.S., M.I. Fareed, Improving the friction and wear of poly-ether-etherketone (PEEK) by using thin nano-composite coatings, Wear 364–365 (2016) 154–162, doi: 10.1016/j.wear.2016.07.012.
79. Pei X.-Q., Bennewitz R., Busse M., Schlarb A.K. Effects of single asperity geometry on friction and wear of PEEK, Wear 304 (2013) 109–117, doi: 10. 1016/j.wear.2013.04.032.
80. Rodriguez V, Sukumaran J., Schlarb A.K., De Baets P. Reciprocating sliding wear behaviour of PEEK-based hybrid composites, Wear 362–363 (2016) 161–169, doi: 10.1016/j.wear.2016.05.024. [10] V. Rodriguez, J. Sukumaran A.K. Schlarb P. De Baets, Influence of solid lubricants on tribological properties of polyetheretherketone (PEEK), Tribol. Int. 103 (2016) 45–57, doi: 10.1016/j.triboint.2016.06.037.
81.Shrestha R., Simsiriwong J., Shamsaei N. Mean strain effects on cyclic deformation and fatigue behavior of polyether ether ketone (PEEK), Polym. Test. 55 (2016) 69–77, doi: 10.1016/j.polymertesting.2016.08.002.
82. Shrestha R., Simsiriwong J., Shamsaei N., Moser R.D. Cyclic deformation and fatigue behavior of polyether ether ketone (PEEK), Int. J. Fatigue 82 (2016) pp. 411–427, doi: 10.1016/j.ijfatigue.2015.08.022.
83.Kurokawa M., Uchiyama Y., S. Nagai, Performance of plastic gear made of carbon fiber reinforced poly-ether-ether-ketone, In: *Tribology International,* 1999, 32 pp. 491 – 497, doi: 10.1016/S0301- 679X(99)0 0 078-X.
84. Kurokawa M., Uchiyama Y., Nagai S. Performance of plastic gear made of carbon fiber reinforced poly-ether-ether-ketone: part 2, In: *Tribology International,* 2000, 33 (10) pp. 715 – 721, doi: 10.1016/S0301-679X(0 0)0 0111-0.

Journal of Engineering Science *Vol. XXIX, no. 1 (2022), pp. 48 - 61*
Fascicle *Industrial Engineering* *ISSN 2587-3474*
Topic *Applied Engineering Sciences and Management* *eISSN 2587-3482*

https://doi.org/10.52326/jes.utm.2022.29(1).04
CZU 656.13.08

DRIVER OR AUTOPILOT – WHO IS THE FUTURE

Vasile Plămădeală*, ORCID ID: 0000-0003-1722-2649,
Sergiu Dîntu, ORCID ID: 0000-0003-3482-9039

Technical University of Moldova, 168 Stefan cel Mare Blvd., Chisinau, Republic of Moldova
*Corresponding author: Vasile Plămădeală, *vasile.plamadeala@fimit.utm.md*

Received: 01 12. 2022
Accepted: 02. 25. 2022

Abstract. The human factor is the main element in the production of road events, not only in terms of percentage, but also in absolute importance, because, ultimately, road and technical issues are involved in road accidents only in strict accordance with the behavior and the direct action of the driver, who, within the road traffic system, is more variable and unpredictable than the vehicle, road and environmental factors. The driver is guilty of 70-90% of the total number of road accidents. More than a third of people killed and injured in road accidents worldwide are drivers. The article describes the role of the driver in the DVRE system, the risk factors and the causes contributing to the occurrence of road accidents. A brief analysis of road accident statistics due to drivers in the Republic of Moldova and around the world is performed. It also describes the evolution of the unmanned car and other innovative technologies and ideas for automating car driving.

Keywords: *driver, autopilot, road accidents, traffic accidents, traffic safety.*

Rezumat. Factorul uman constituie elementul principal în producerea evenimentelor rutiere, nu numai din punct de vedere procentual, dar şi ca importanţă absolută, pentru că, în ultima instanţă, aspectele rutiere ca şi cele tehnice sunt implicate în accidentul rutier numai în strictă concordanţă cu comportamentul și acțiunea nemijlocită a conducătorului de vehicul, care, din sistemul de trafic rutier este mai variabil şi imprevizibil, decât factorii vehicul, drum și mediu. Conducătorul auto este vinovat în 70 - 90% din numărul total de accidente rutiere. Peste o treime din cei decedați și traumatizați în accidentele rutiere în întreaga lume sunt conducători de vehicule. În articol este descris rolul conducătorului auto în sistemul CVDM, factorii de risc și cauzele contribuitoare la producerea accidentelor rutiere. Este efectuată o analiză succintă a statisticii accidentelor rutiere din vina conducătorilor auto în Republica Moldova și în întreaga lume. De asemenea, este descrisă evoluția automobilului fără pilot și altor tehnologii și idei inovative privind automatizarea conducerii automobilului.

Cuvinte cheie: *conducător auto, autopilot, accidente rutiere, accidente de circulație, siguranța circulației.*

Road safety depends on the safe operation of all components of the „*Driver – Vehicle – Road – Environment*" system. The reliability of this complex system must be ensured by the

technical perfection of the road and the reliability of the car, as well as by the safety of the driver's actions in different traffic situations. The main element of this system is the driver, whose reliability means the ability to choose correctly and in a timely manner the most optimal traffic regime and to assess the road situation.

According to the *Road Traffic Regulations*, the driver is the person who drives a vehicle on public roads, an organized group of people, accompanies isolated animals, burdens, riding or herds, herds etc., as well as the person who conducts training in driving [1, 2].

The driver is the factor that most influences the traffic conditions. In heavy traffic, the driver performs the function of a traffic controller, following the legal speed and correct distance from the vehicle in front, correctly assessing the distance and speed of overtaken vehicles and those coming from the opposite direction, as well as distances and intervals in relation to the overall dimensions of the driven vehicle.

In addition to knowing and respecting the rules of road traffic, the driver must have a good command of the driving technique, which requires a long practice, so that the driver is able to solve without difficulty the difficult situations of increasing crowded road traffic. Traffic safety depends directly on the driver's attention and vigilance, on his ability to anticipate all possible situations, which could lead to an unwanted road accident, as well as to sense measures to prevent it. The driver must also know how to act in situations when, for fortuitous reasons, the road accident could occur in order to minimize its consequences.

It turns out that the main role in road traffic is played by the human factor, first by the driver, beginner or experienced, amateur or professional, being important the way in which he participates, actively engaged in traffic, in the mechanical tumult of the street. Therefore, anticipating situations that may lead to accidents, avoiding the accident that is about to occur or engage in a traffic event, as well as choosing the best option for getting out of an accident that cannot be avoided with a minimum of consequences, represents the basic norms of traffic and preventive conduct.

Experience shows that drivers could avoid many road accidents if [3, 4]:

- would anticipate the actions taken in the next seconds by pedestrians engaged in crossing without insurance or those who suddenly appear from the sidewalks on the road;
- would take into account the behavior of children and the elderly near the road;
- would take into account the behavior of some drunk pedestrians stopped on the road or crossing it;
- would take into account the unexpected maneuvers of cyclists and other road users;
- would take into account the dangers that may occur when driving near parked cars;
- would drive at adequate speeds in all places with limited field of vision;
- would anticipate the dangers that may arise in the process of driving a car with an advanced degree of wear;
- would keep the tracking distance while walking in the column depending on the speed, the condition of the road surface, visibility etc.

Anticipation is thus of great importance in driving the car, the human factor having at its disposal this „*tool*" to help achieve a safe and smooth flow.

The rapid increase in the number of cars, which currently amounts to about 1,2 billion worldwide [5 - 7] and 1,2 million in the *Republic of Moldova* [8], requires a proportionate development of the driver training system, which takes place in various educational institutions, many of them without the necessary material and technical basis, as well as, highly qualified teaching staff. In this sense, in the process of road traffic takes place self-

education, learning and retraining of an important part of drivers. Naturally, as the density and intensity of road traffic increase, this phenomenon complicates in particular the task of ensuring road safety.

Given the current traffic conditions, the driver must respond quickly and promptly to a wide range of external stimuli, assimilate and continuously process a large amount of information, which sometimes exceeds its physiological possibilities, and then make appropriate decisions. to perform command actuation movements.

In countries with heavy road traffic, it has been found, that the average frequency of various information, processes, situations and events to which a driver's attention is subjected has high values. Thus, he receives an average of 125 information and makes 12 - 15 decisions per kilometer traveled, at 3,2 *km* he makes a mistake and is put in a position to avoid a collision at 800 *km*. The statistics also show that a collision is possible at every 100000 *km*, an accident with injuries at every 700000 *km* and a fatal accident at every 25 million kilometers. A survey of 100 drivers in *Hanover* showed that in urban traffic conditions, the driver receives an average of 62 pieces of information per minute (external stimuli) and has to make 35 - 40 decisions in this short period of time [3].

The ability of a person to carry out the professional activity of a driver is generally determined by the following qualities such as [9]:

- agility, endurance, physical development and good coordination of movements;
- ease in education and change of motor skills;
- high level of development of the functions of the sensory organs, especially of hearing, muscular sensation and sight;
- speed and accuracy of sensorimotor reactions;
- the accuracy and speed of determining the spatial relations and the speed of circulation;
- wide distribution, speed of switching and stability of attention;
- sufficiently good visual memory, as well as the high level of memory preparation;
- courage, determination and perseverance;
- inclination towards technical thinking, technology, interest in the professional activity of the leader;
- discipline, emotional stability and self-control;
- ingenuity and initiative;
- developed imagination, the ability to reflect and anticipate the actions of other traffic participants etc.

An analysis of accident statistics, including road accidents, in over 45 countries in the last 10 - 15 years shows that 75 - 80% of accidents in transport, production and daily life occur for three reasons: from the cause of „*unwillingness*", „*ignorance*" and „*incapacity*". The remaining 20 - 25% of accidents, including traffic accidents, occur due to adverse climatic and operating conditions, as well as reasons related to the technical condition of vehicles and mechanisms. The maximum number of accidents and casualties is due to car transport. It is the most dangerous type of transport – 12 times more dangerous than sea and river transport, 8 times more dangerous than rail transport and 4 times more dangerous than air transport [10].

According to estimates by the *World Health Organization* (*WHO*), approximately 1,4 million people die in traffic accidents each year, 30 to 50 million are injured with bodily injuries, of which about 17 million lose their ability to work or remain with disabilities. people [10 - 16]. More than a third of road accident victims worldwide are drivers (Figure 1). 29% of

those who died in road accidents belong to drivers and passengers of cars, 28% to motorcyclists, 23% to pedestrians, and the remaining 20% – to other road users [12 - 16]. The situation varies significantly between regions of the world. In most low- and middle-income countries, the percentage of road accident victims, such as pedestrians, cyclists, drivers and passengers of two - and three-wheeled motor vehicles, is significantly higher than in high-income countries. For example, in the *WHO African Region*, 40% of all road accident deaths are due to pedestrians, and in the *WHO West Pacific Region* 36% are to motorcyclists, ie drivers and passengers of 2 - or 3-wheel motor vehicles (Figure 1). Drivers and passengers represent between 16% of those killed in road accidents in the *South-East Asia Region* to 48% in the *European Region*.

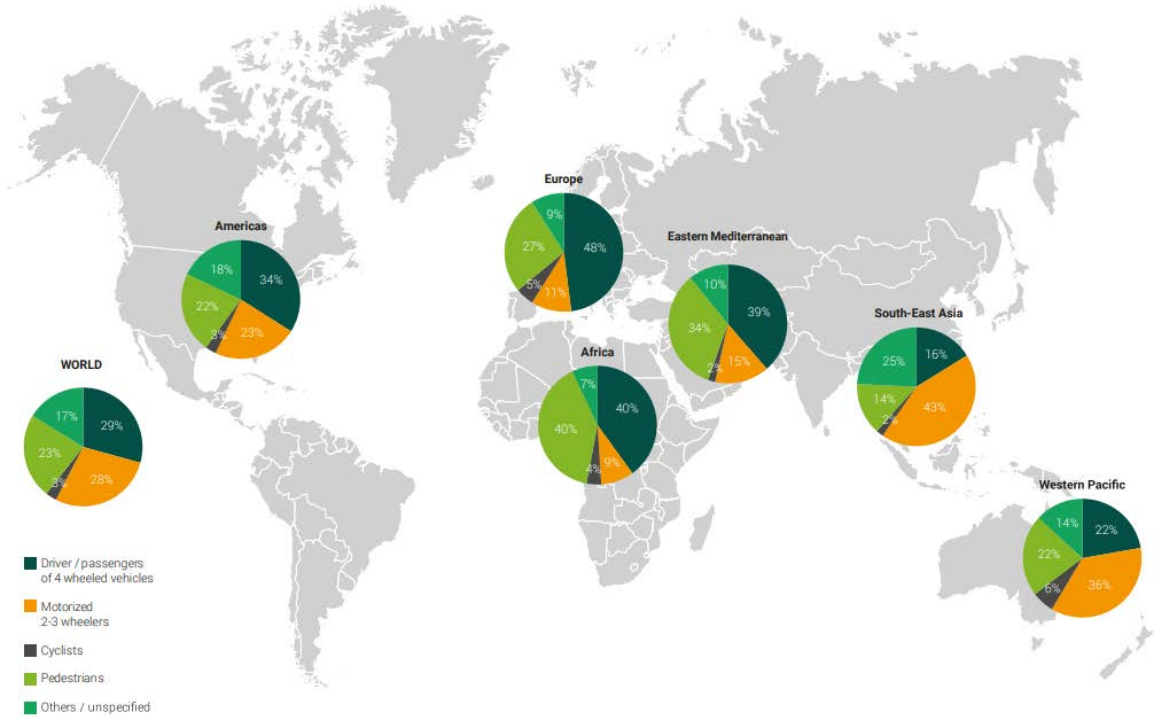

Figure 1. Distribution of deaths by categories of road users by *WHO* regions [10].

Worldwide 70 - 90% of the total number of road accidents occur due to drivers [3, 4, 10, 12 - 17]. From 35 to 40% of road accidents occur as a result of exceeding the vehicle speed above the set limit, 23-28% – due to carelessness of drivers and 15 - 20% – due to fatigue of drivers. From 45 to 50% of road accidents are committed by drivers, who have consumed alcohol and drugs [10].

Numerous special studies show that, depending on the degree of predisposition to danger, drivers can be divided into three categories: extremely reliable (safe) – 15-20%; potentially dangerous or prone to accidents – 7 - 12% and so-called indifferent drivers – 55-65%, which in some cases can lead safely, and in other circumstances can cause an accident [10]. However, such a classification does not allow the development of preventive measures at the individual level, as the driver's ability to ensure safe driving depends on individual characteristics, requiring a more detailed classification and analysis.

Based on complex studies [10], a parabolic dependence of road accidents has been established according to the age of drivers, according to which drivers are classified into: potentially dangerous – under the age of 25, dangerous – over 65, with medium danger – of at 25 to 30 years and from 55 to 65 years, less dangerous – from 30 to 35 years and from 45

to 55 years and relatively reliable (safe) – from 35 to 45 years. Also, as a result of the processing of statistical data, a curve was built, which shows the degree of danger of drivers depending on driving experience. According to these data, drivers can be divided into three categories depending on management experience: I – drivers with 10 - 25 years of work experience; II – with an experience of over 25 years; III – with less than 5 years experience. According to studies conducted in *England*, driving experience is more important than age. Drivers under the age of 30 with less than 4 years of work experience have 4 times more road accidents than drivers aged 60 - 65 with more than 14 years of experience.

The analysis of the road accident statistics during the years 2000 – 2019 in the *Republic of Moldova* (Table 1) indicates that on the territory of the country were registered 52383 (on average 2619 per year) serious road accidents, as a result of which 7702 died (385 per year) people, and another 63560 (3178 per year) were traumatized. The severity index of road accidents (the number of deaths per 100 victims) in the country as a whole in the reference period is 10,81 [2, 3, 6, 18 - 23].

According to statistics, most of the number of road accidents occurred through the fault of drivers: 44886 (on average 2244 per year, which is 85,69% of all road accidents in the country during the reference period).

Table 1

Frequency of road accidents (years 2000–2019)

Year	Road accident	Road accidents involving drivers	% of the total number of road accidents	Deceased	Traumatized	Coefficient of severity of road accident consequences
2000	2580	2128	82,48	406	3147	11,43
2001	2666	2219	83,23	410	3277	11,12
2002	2899	2327	80,27	412	3505	10,52
2003	2670	2166	81,12	424	3215	11,65
2004	2447	2170	88,68	405	2888	12,30
2005	2289	1975	86,28	391	2770	12,37
2006	2298	1989	86,55	382	2807	11,98
2007	2437	1976	81,08	464	2984	13,46
2008	2875	2215	77,04	508	3511	12,64
2009	2755	2324	84,36	487	3297	12,87
2010	2930	2604	88,87	452	3747	10,76
2011	2826	2480	87,76	443	3535	11,14
2012	2712	2435	89,79	441	3510	11,16
2013	2603	2281	87,63	295	3221	8,39
2014	2564	2209	86,15	324	3080	9,52
2015	2527	2278	90,15	297	3021	8,95
2016	2479	2267	91,45	311	2928	9,60
2017	2640	2322	87,95	302	2993	9,17
2018	2614	2265	86,65	274	3123	8,03
2019	2572	2256	87,71	274	3001	8,37
Total	**52383**	**44886**	**85,69**	**7702**	**63560**	**10,81**

Analyzing the violation of traffic rules committed by drivers, which lead to road accidents, it was found that the highest number of road accidents occurred because of the

following causes:

- exceeding the set speed and speed unsuitable for road conditions [24];
- non-compliance with handling rules;
- not giving priority to pedestrians;
- driving the vehicle while intoxicated [19].

In the near future we could witness a real technological revolution, in which man-made cars will become part of history, and unmanned vehicles will come to replace them. *An unmanned vehicle* is called a robotic vehicle, capable of perceiving the environment and moving between the points of destination without the intervention of man (driver) [7, 25]. The fact that artificial intelligence will remove the man from driving is spoken about a lot and loudly. Currently, unmanned cars are recognized as the safest way to travel, and tomorrow may be the only choice for humanity. It could take 10-20 years for their dominance to become total.

The past of unmanned cars is no less interesting than their future. Today, the issue of the dominance of unmanned vehicles on the roads is no longer discussed – it has been solved long time ago. Now, some 40 - 50 years ago, there could be no question of passing control of the vehicle to a robot. These ideas seemed utopian to all, but the pioneers of the unmanned automotive industry.

It all started back in the 1930s, when *General Motors* engineers came up with two brilliant ideas from that period. The first idea was to drive the car with radio signals, and the second and more interesting was to build special tracks in the form of skateboard ramps [26]. Although the ideas were skeptical, they gave a strong impetus to the development of technology in the right direction.

The year 1961 went down in the history of unmanned vehicles, when *Stanford* student *James Adams* created and tested the first autonomous vehicle. It was directed by an ordinary signal through a cable. But already the second prototype was driven by radio signals.

This experiment did not go unnoticed and in the 70's of the last century, the famous scientist *J. McCarthy* introduced his corrections in the construction of the vehicle and modernized it with the help of a technological vision system. The vehicle could move independently and orient itself along the white line. The prototype was also equipped with a rangefinder, video cameras and 4 channels for data collection.

Following *McCarthy's* success, the engineers' efforts were directed towards creating a 100% autonomous vehicle with no remote control. Scientists in the *US* and *Japan* have had significant success, but real progress has been made by German researchers led by *Ernst Dieckmans*, where calculation mechanisms and a system for simulating eye movement have been applied for the first time. These innovations have led to the formation of a car preparation model, which independently assesses the situation and makes decisions.

Other notable moments in the history of the evolution of unmanned cars are listed below [26]:

- ✓ In 2004, the first car competition in history took place with the participation of *DARPA* robots, where unmanned cars appeared.
- ✓ In 2010, the world saw the first *Google* autopilot, developed based on the *Toyota* model. Equipped with radars, camcorders and the *Lidar* system, this *Google-mobile* could navigate in space, recognize road signs and interact with other road flow participants.
- ✓ In 2012, *Audi* tested its unmanned car. The autopilot car reached a speed of 193 *km/h*, perfectly entered corners and accelerated on the track.

- ✓ In 2013, *Nissan* and *Honda* demonstrated the efficiency of their patented autopilot systems. The companies plan to start mass production of robotic cars in 2020.
- ✓ In 2014, the Swedish company *Volvo* tested the first unmanned car with the unique *Drive Me* system.
- ✓ In 2015, the first unmanned mass production cars appeared – *Tesla Model S*, which travels on roads 100% independently. Together with *Google-mobile*, they are considered a standard of unmanned technology.
- ✓ 2016 - 2017 is the period in which all major car companies announced the development of their own prototyping and series production plans.

The construction of an unmanned vehicle includes the following main components [7, 25]:

- different sensors (optical, infrared, radar, ultrasound, laser);
- navigation, which combines *GPS* and electronic maps;
- the server with the installed program and power supplies;
- automated steering elements of the car (steering system, braking system, engine control system);
- automatic transmission;
- wireless network for communication between vehicles, access to program updates, electronic maps, road condition information, emergencies etc.

Many car manufacturers are currently working to create the unmanned car: *Audi*, *BMW*, *General Motors*, *Ford*, *Mercedes-Benz*, *Nissan*, *Tesla*, *Toyota*, *Volkswagen*, *Volvo*. *Apple*, *Autoliv*, *Bosch*, *Continental*, *Delphi*, *Google*, *Mobileye*, *Vislab* and others help them actively.

The potential advantages of unmanned cars are [7, 25, 27]:

- the reduction of the number of road accidents, caused by the driver's errors, and the practically total exclusion of the victims among the passengers, thus resulting in the decrease of the insurance, medicine, legal expenses etc.;
- reduction of freight and passenger transport costs, due to the economy of drivers' pay and rest, as well as the fuel economy;
- increasing the mobility of certain categories of the population (minors, young people, the elderly, people with disabilities, people with low incomes, without a driving license, etc.);
- raising the efficiency of traffic organization and therefore the ability to cross the road;
- reducing the need for personal cars and parking spaces;
- saving time spent driving, allows you to do more important things directly during the trip or rest;
- transport of goods in dangerous areas, during natural and technical disasters or military operations;
- in future, the reduction of the global ecological burden, both due to the quantitative optimization of the car fleet, and due to the wider use for their movement of alternative types of energy etc.

The disadvantages of autonomous vehicles, which prevent their rapid and widespread implementation, can be attributed [7, 25, 27]:

- software reliability, limited artificial intelligence capabilities and high system sensitivity to weather conditions (rain, snow, fog);
- liability for damages caused;
- loss of the ability to drive a car and the driver job. It is possible for lovers to drive the car to provide special roads, with additional safety measures, similar to the current ones, thus separating both the road network and the transport flows between them;

- loss of privacy;
- their use for criminal purposes;
- the ethical question faced by the car computer, in case of an inevitable collision, about the most acceptable number of victims, similar to the situation of choosing from two dangers the smallest.

In 2014, the professional association *SAE International* proposed a classification of unmanned vehicles according to the degree of automation. The classification includes six levels – from zero to complete automation 7, 25, 28].

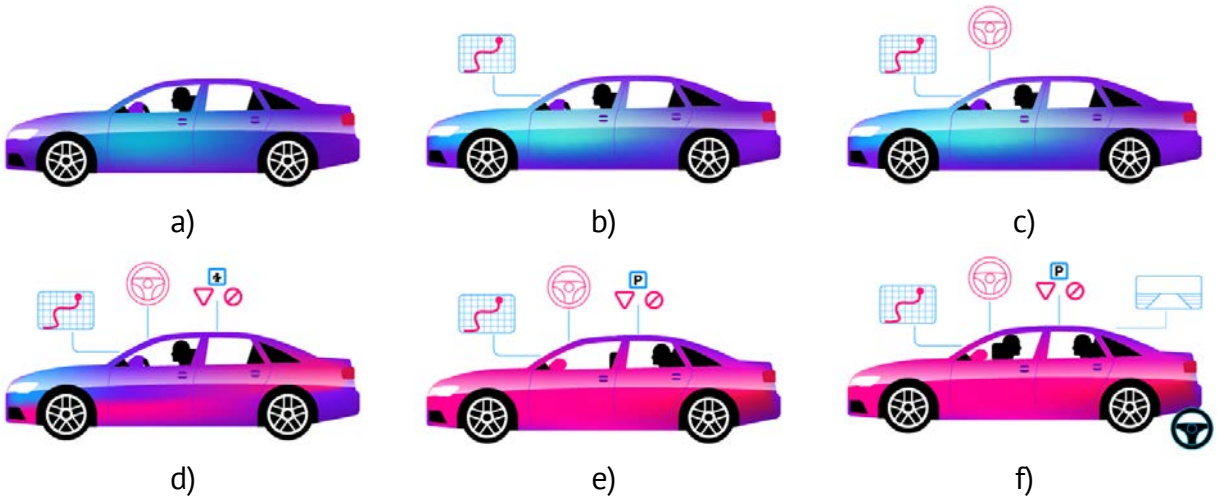

Figure 2. Automation levels of unmanned cars [26].

Zero level systems (Figure 2a), called *without automation*, do not perform driving functions, only warn the driver about the dangerous situation. Examples of systems with zero level of automation are:

- night vision system;
- band preselection assistance system;
- parking system.

In *level one* systems (Figure 2b), called *driver assistance*, some of the car's driving functions (steering system, acceleration and braking) are performed by the automation system. The driver permanently controls the traffic with the intention of taking complete control over the car. Examples of level one automation systems are:

- adaptive cruise control system (driver – steering system, automated system – speed);
- active lane departure assistance system (driver – speed, automated system – steering system);
- automatic parking system (driver – speed, automated system – steering system).

Level two automated systems (Figure 2c), called *partial automation*, are fully driven by the car. The hands can be taken from the steering wheel, the foot from the accelerator pedal. The driver follows the traffic with the intention of taking control. If the system does not handle the assigned functions, it can be disabled. Examples of level two automation systems are:

- *Tesla* autopilot;
- automatic traffic system in traffic jams (*Traffic Jam Assistant*);
- *Temporary Auto Pilot.*

Level three systems (Figure 2d), called *conventional automation*, allow the driver to completely distract from the movement of the car. During this time, the leader can read, write, watch a video. The driver intervenes in driving the car only at the request of the system. The following systems depend on level three automation systems:

- *Super Cruise* system;
- *SARTRE* system.

Level four systems (Figure 2e), called *high automation*, do not generally require the driver's attention. He can fall asleep, leave the driver's seat. When a dangerous situation arises, the system parks the car in a safe place and informs the driver about it. Systems, which can be attributed to level four automation are still few:

- the *Google* unmanned car;
- autonomous parking system.

In *level five* systems (Figure 2f), called *total automation*, human presence is generally not required. Therefore, the steering elements (steering wheel, pedals) can be removed from the passenger compartment of the car. The passenger activates (indicates the destination) and deactivates the system. There are currently no tier five automation systems.

The rapid development of electronic car systems makes the idea of the unmanned car a reality. Many car manufacturers and car component manufacturers are actively working to create the automatic driving system [29].

The problem is solved in two directions:

- complex automation of the car;
- automation of special vehicle traffic regimes (*parking, traffic in traffic jams, driving on the highway*).

A complex approach to creating an unmanned vehicle is taken by *Google*. Currently, the *Google* automatic control system is implemented on six experimental cars *Toyota Prius*, *Lexus RX 450h* and *Audi TT*, which have traveled in unmanned mode over 2,5 million kilometers. To perform the automatic control functions, the system includes the following input devices: lidar, radar, video camera, position appreciation sensor, inertial motion sensor, *GPS* receiver (Figure 3).

The *leader* scans the area around the car at a distance of more than 60 *m* and creates an exact three-dimensional image of his entourage. The leader has a rotating sensor on the roof of the car.

Radars help determine the exact position of distant objects. Four radars are installed on the car, three of which are located at the front and one radar at the rear. The *camcorder* sets traffic light signals and allows the control unit to recognize moving objects, including pedestrians and cyclists. The camcorder is located on the windshield behind the rearview mirror.

The *position sensor fixes* the movement of the car and helps determine the exact location on the map. The position sensor is mounted on the left rear wheel.

The *inertial motion sensor* measures the direction of acceleration or deceleration, the longitudinal and transverse inclination of the car body while driving. The directional stability system sensor is used.

The signals from the input devices are transmitted to the electronic control unit, where they are processed according to the established program and the control actions on the actuators are formed. The construction elements of the steering system, the braking system, the steering stability system, the engine control system are used as execution devices.

Unmanned cars do not fit simple maps and simple *GPS* accuracy (3 - 10 *m* error), the car must understand where it is with the accuracy of one centimeter. Despite the fact that the unmanned car has a lot of sensors, it must have accurate information about the environment (geometry of road markings, road boundaries, nearby traffic lights, etc.). All this information can be found in the so-called *HD*-maps. In order to keep cartography in its current state, special cartographic cars (special cars with cameras and lidars) have to travel the streets and „*digitize*" them. Thus, with the advent of the unmanned car race, the cartographic race between companies such as *Here*, *TomTom*, *DeepMap*, *lvl5*, *Carmera*, *Google* and others began [30].

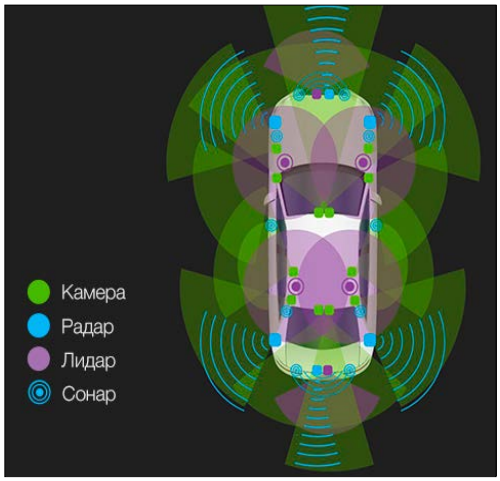

Figure 3. Car devices without a pilot.

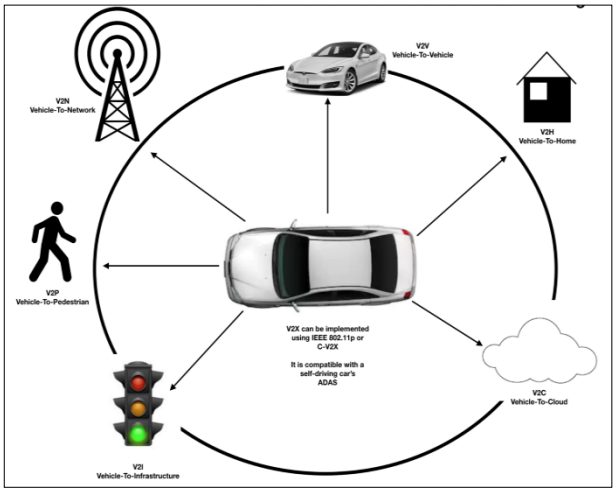

Figure 4. *Car-to-X* system [7, 30].

Unmanned cars require a new road infrastructure. And not only an infrastructure, but an intelligent infrastructure, in which cars could communicate not only with the infrastructure (indicators, traffic lights etc.), but also with other cars, pedestrians, etc. The communication system between cars has several names (Figure 4), in *Europe* it is *Car-to-Car* (*Car2Car*, *C2C*), in the *USA* – *Vehicle-to-Vehicle* (*V2V*). Car communication with infrastructure objects is called *Car-to-Infrastructure* (*C2I* or *V2I*), *Vehicle-to-Road* (*V2R*), and with pedestrians, *Car-to-Pedestrian* (*C2P* or *V2P*) – cars exchange information with pedestrians (for exemple, the car sees the pedestrian's smartphone and understands that there is a person there). The car also communicates with the buildings (houses), *Car-to-Home* (*C2H* or *V2H*), the connection network, *Car-to-Network* (*C2N* or *V2N*), and the information storage space, *Car-to-Cloud* (*C2C* or *V2C*). But all these names do not reveal the essence of the communication system, so more recently another name is circulating – *Car-to-X* (*C2X* or *V2X*). „*X*" means vehicles and infrastructure objects [7, 31].

The car communication system provides security in the following directions:

- assistance in crossing the intersection;
- left turn assistance;
- passing safely in opposite directions with the car in the opposite direction;
- warning when exiting the highway;
- detecting obstacles on the road;
- information about a traffic accident;
- emergency braking warning;
- rear collision warning (electronic brake lamp);
- warning about changing lanes;
- warning about adverse weather conditions;

- information about road signs;
- information about the approaching motorcyclist etc.

For example, a car travels on the highway, and the road sign 300 *m* ahead announces: „I'm a road sign and my name is..., I'm there...". The unmanned car will be able to understand in advance what is to come and plan its actions according to this information.

Within the *HAVit* project (*Highly Automated Vehicles for Intelligent Transport*), in 2011 he presented the *Temporary Auto Pilot* semi-automatic system, *TAP* (*Temporary Autopilot*). The system allows the driver, under certain conditions, to hand over the control of the car under automatic control. In essence, the system is an intermediate step towards a robotic car [29].

The *TAP* system integrates into a common whole the already known elaborations of *Volkswagen*: the adaptive cruise control system, the lane traffic assistance system, the road sign recognition system. In its activity, the *temporary autopilot* system uses standard input devices of the listed active safety systems: lidar, radar, video camera, ultrasonic sensors. The system ensures the optimal degree of automation depending on the road situation and the driver's condition, thus contributing to accident-free driving. The system operates at speeds of up to 130 *km/h*. The *TAP* system is fully prepared for implementation on series cars.

Audi's Traffic Jam Assistant system is the first autopilot system for traffic congestion. The system automatically maintains the distance to the car in front, brakes, accelerates, turns, bypasses the obstacle and even gives way to emergency vehicles. Constructively, the traffic jam autopilot is based on adaptive cruise control and operates at speeds between 0 and 60 *km/h*. The system combines a number of input devices: two radars, a wide-angle video camera and eight ultrasonic sensors. Radar scans certain areas at a distance of 250 *m*. The video camera determines road markings and various obstacles. Ultrasonic sensors monitor the space in the front, rear and sides of the car. At any time, the driver can take control of the car.

Ford has prepared the automatic traffic system in traffic jams and has been using it in mass-produced cars since 2017. The *Traffic Jam Assist* system includes a radar and a camera, which monitors the movement of neighboring vehicles. The electronic control unit selects the desired speed and ensures the car's flow.

BMW is working on the *ConnectedDrive Connect* (*CDC*) system, designed for highway travel. The *CDC* system includes an ultrasound sensor, a video camera, a radar and a lidar, the signals from which are processed in an electronic control unit. As a result of the action on the execution mechanisms of the different systems of the car, the speed and the trajectory of circulation change. In addition, the system does not exceed the speed limit on the road sector, does not exceed on the right and returns the car to its lane after overtaking. In general, in the autopilot the algorithm of an ideal driver is realized. According to the company, the system is not yet ready for mass use.

Cadillac's Super Cruise automatic control system ensures the car's movement on the highway. It allows maneuvering, braking, driving on the belt without the participation of the driver. The system is based on a series of existing company solutions: adaptive cruise control system, automatic emergency braking systems, collision warning, lane departure assistance, lane preselection assistance, active light etc.

An interesting solution for automating car traffic is offered by *Volvo*. The *Safe Road Trains for the Environment* (*SARTRE*) system allows the movement of several cars on the road in an organized column. The cars move after the leading car, as a truck with a professional driver. The cars line up at a distance of 6 *m* from each other and completely repeat the

movement of the leading truck, which allows the driver to rest, eat and talk on the phone. If desired, each car can leave the group at any time.

If road accidents involving people are a common phenomenon, then road accidents with unmanned vehicles become a real sensation. The press publishes hundreds of articles, paying attention to the smallest details, so that the news of a car accident with an unmanned vehicle cannot go unnoticed. At the same time, these smart vehicles are declared the safest: they have nothing to do with negligence and fatigue, poor visibility or irresponsibility, do not consume alcohol, drugs, do not talk on the phone, do not sleep etc. However, the development of artificial intelligence has not yet reached the point where errors are reduced to zero. Therefore, in road accident reports, the presence of unmanned vehicles is extremely rare. In average traffic conditions, traveling with an unmanned vehicle is almost 9 times safer than with human-driven cars [32]. Road accident statistics are also in favor of unmanned vehicles: other road users [33] cause 98% of accidents.

The only fatal road accident with an unmanned vehicle took place in 2016, in the American state of *Florida*. The *Tesla Model S* Robocar, driven by an autopilot, which bumped into a truck with a trailer at the intersection [33].

Conclusion. The 21st century has already become for the whole of humanity an era of innovative technologies, interesting ideas, automation of machines and the creation of „*intelligent*" robots. This is only a small part of what scientists and inventors can surprise us with. Some technologies have begun to modernize since the last century, referring to unmanned vehicles.

Innovation is a key vector of development; it is also a benefit, which makes life better, more comfortable, safer, cheaper, etc. It is understandable that today, with the old approaches, you do not get far. If we stop at this level, we have no chance of survival. The world is very conservative about innovation. If we get used to something, it is very difficult to move on to something new, even if it is better.

The profession of driver will disappear, like other obsolete professions, and this does not hurt anyone, in the end everyone could win. This is exactly what happens with constant technological progress – there are fears, is it a real benefit. Thousands of people die on the roads every day around the world because of the mistakes of others. If safety, comfort, economy and ecology are to be weighted, then it becomes obvious that the benefits for society as a whole are enormous.

References

1. Government Decision No. 357 of 13.05.2009 regarding the approval of the Road Traffic Regulation. In: *Official Monitor of the Republic of Moldova*, 15.05.2009, no. 92-93, art. 409. Date of entry into force: 15.07.2009 (in Romanian).
2. Ududovici D., Plămădeală V. *Regulation and safety of road traffic*. Driver's manual. 3rd edition, revised and completed. Chisinau, 2010, 288 p. ISBN 978-9975-109-22-2 (in Romanian).
3. Plămădeală V. *Road accidents and traffic safety*, Master's thesis, Chisinau TUM 2006, 159 p. (in Romanian).
4. Plămădeală V. Road traffic safety. In: *The second practical-scientific conference „Management strategies, engineering and technologies in transport"*. Chisinau, October 27, 2006, TUM, p. 67-72. ISBN 978-9975-45-009-6 (in Romanian).
5. *How many cars are there in the world and how many will be in 2050* [online]. Copyright 2020 Ringier Romania [quote 03.02.2020]. Available: https://www.auto-bild.ro/stiri/cate-masini-sunt-in-lume-si-cate-vor-fi-in-2050-72426.html.
6. Goian V., Plămădeală V., Beiu I. *Organization and safety of road traffic. Volume 1. Normative acts, safety elements and characteristics of road traffic*. University course. „Tehnica-UTM" Publishing House. Chisinau 2021, 341 p. ISBN 978-9975-45-721-7, ISBN 978-9975-45-722-4 (PDF) (in Romanian).

7. Plămădeală V., Goian V., Beiu I. *Organization and safety of road traffic. Volume 2. Car safety: active, passive, post-crash and environmentally friendly*. University course. „Tehnica-UTM" Publishing House. Chisinau 2021, 435 p. ISBN 978-9975-45-721-7, ISBN 978-9975-45-723-1 (PDF) (in Romanian).
8. *Statistical data on the composition of the State Register of Transports in profile of the type of means of transport (status as of January 1, 2022)* [online]. Copyright © Public Services Agency, 2022 [quote 23.01.2022]. Available: http://www.asp.gov.md/node/1662.
9. Penshin N., Ivlev V. Physiology of the driver and its impact on road safety. In: *International Research Journal*. No. 1 (43), Part 2, Yekaterinburg, January 2016, 125 p., ISSN 2303-9868 PRINT, ISSN 2227-6017 ONLINE (in Russian).
10. Ambarczumyan V. *Road safety. Volume 1. Safety of drivers and road users*. Moscow, 2008, 350 p. ISBN 5-217-02871-8 (in Russian).
11. Plămădeală V., Pădure O. Analysis of road accidents. In: *The second practical-scientific conference „Management strategies, engineering and technologies in transport"*. Chisinau, October 27, 2006, TUM, p. 62-66. ISBN 978-9975-45-009-6 (in Romanian).
12. Shherbakova E. M. *Global trends in road traffic deaths according to WHO estimates 2018* [online]. Demoskop Weekly. 2019. № 819-820 [quote 05.02.2020]. Available: http://demoscope.ru/weekly/2019/0819/barom01.php.
13. *Global status report on road safety 2018*, World Health Organization, 2018, 419 p. ISBN 978-92-4-156568-4.
14. *Report on the state of road safety in the world 2015. Executive Summary*, World Health Organization, 2015, 12 p. ISBN: 978 92 4 456384 7 (in Russian).
15. *Report on the state of road safety in the world. Time to act*, World Health Organization, 2009, 297 p. ISBN: 978 92 4 456384 7 (in Russian).
16. *Safety of pedestrians. Guide to road safety for managers and professionals*. World Health Organization 2013, 130 p. ISBN 978-92-4-450535-9 (in Russian).
17. Onceanu V., Bulgac A. *The basics of driving behavior and road safety*. Chisinau, 2008, 237 p. ISBN 978-9975-4012-0-3 (in Romanian).
18. Plămădeală V. Analysis of road accidents in the Republic of Moldova during the years 2000–2014. In: *Materials of the national scientific-practical conference „Transport: engineering, economics and management"*. Chisinau, May 22-23, 2015, TUM, p. 198 – 208. ISBN 978-9975-45-380-6 (in Romanian).
19. Plămădeală V. Alcohol and driving – a dangerous combination. In: *Materials of the national scientific-practical conference „Transport: engineering, economics and management"*. Chisinau, November 17-18, 2017, TUM, p. 103 – 117. ISBN 978-9975-45-511-4 (in Romanian).
20. Plămădeală V., Plamadeala A. The roads of the future. In: *Journal of Engineering Science*. 2019, no. 2, pp. 22 – 35. ISSN 2587-3474, eISSN 2587-3482.
21. *Information note on the accident situation for the period 01.01.2019 – 31.12.2019* [online]. National Patrol Inspectorate [quote 08.02.2020]. Available: http://politia.md/sites/default/files/situatia_accidentara_12_luni_2019.pdf.
22. *Information note on the accident situation for the period 01.01.2018 – 31.12.2018* [online]. National Patrol Inspectorate [quote 08.02.2020]. Available: http:// politia.md/sites/default/files/accidenta_inp_in_rm_pentru_12_luni_a_anului_2018.pdf.
23. *Information note on the accident situation for the period 01.01.20178 – 31.12.2017* [online]. National Patrol Inspectorate [quote 08.02.2020]. Available: http://politia.md/sites/default/files/nota_informativa_privind_situatia_accidentara_pentru_perioada_a_12_luni_2017.pdf.
24. Plămădeală V., Corpocean A. Speed and safety of road traffic. In: *Materials of the national scientific-practical conference „Transport: engineering, economics and management"*. Chisinau, November 17-18, 2017, TUM, pp. 127 – 133. ISBN 978-9975-45-511-4 (in Romanian).
25. *Unmanned vehicle* [online]. Modern car systems © Suslinnicov Alexandr, 2009-2017 [quote 05.01.2020]. Available: http://systemsauto.ru/another/driverless-car.html.
26. *History of unmanned vehicles* [online]. Unmanned vehicles. News and sale of unmanned vehicles [quote 05.01.2020]. Available: https://bespilot.com/info/istoriya.
27. *Unmanned vehicle* [online]. Wikipedia® [quote 20.01.2020]. Available: https://ru.wikipedia.org/wiki/Беспилотный_автомобиль.
28. *How an unmanned vehicle works* [online]. Yandeks Dzen [quote 20.01.2020]. Available: https://zen.yandex.ru/media/id/5aa68a0d9e29a29a15012d13/kak-rabotaet-bespilotnyi-avtomobil-5d58ad73027a1500ae2d2d5c.

29. *Automatic vehicle control system* [online]. Modern car systems © Suslinnicov Alexandr, 2009-2017 [quote 05.01.2020]. Available: http://systemsauto.ru/another/ automatic_driving.html.
30. *Unmanned cars for beginners* [online]. © 2006 – 2020 «TM» [quote 05.01.2020]. Available: https://habr.com/ru/post/431758/.
31. *Communication system between vehicles* [online]. Modern car systems © Suslinnicov Alexandr, 2009-2017 [quote 05.01.2020]. Available: http://systemsauto.ru/active/car-to-car.html.
32. *Autopilot VS Driver? Who is safer?* [online]. © 2006-2019 ELMOB company – electric vehicles [quote 05.01.2020]. Available: https://elmob.ua/news/avtopilot-vs-voditel-s-kem-bezopasnee/.
33. *Have there been accidents with unmanned vehicles* [online]. Unmanned vehicles. News and sale of unmanned vehicles [quote 05.01.2020]. Available: https://bespilot.com/chastye-voprosy/byli-li-avarii-ba.

Journal of Engineering Science *Vol. XXIX, no. 1 (2022), pp. 62 - 70*
Fascicle *Industrial Engineering* *ISSN 2587-3474*
Topic *Electrical Engineering and Power Electronics* *eISSN 2587-3482*

https://doi.org/10.52326/jes.utm.2022.29(1).05
CZU 662.769.2:620.9

THE TRANSITION TO A HYDROGEN ECONOMY

Titu-Marius I. Băjenescu*, ORCID ID: 0000-0002-9371-6766

Swiss Technology Association, Electronics Group Switzerland
*Corresponding author: Titu-Marius I. Băjenescu, *tmbajenesco@gmail.com*

Received: 12.19.2021
Accepted: 01.28.2022

Abstract. The article examines the problem of the hydrogen market - from production to how to use it, as well as the prospects for the development of these energy sources. To combat climate change, more and more countries are investing in low-carbon energy, which is produced from renewable sources and is therefore neutral throughout the chain. Thus, the global hydrogen market is growing. Hydrogen can help decarbonise industrial sectors and combat climate change, either as an environmentally friendly fuel in the transport sector or as a means of reducing emissions in steel production and many other industries. Hydrogen can also play a vital role in energy transport. But even though hydrogen does not pollute itself, because its combustion releases only water vapour, it emits CO_2 when fossil fuels are used for its production ("Grey" hydrogen). "Green" hydrogen is still in its infancy: less than 1% of global hydrogen production, which is itself only 2% of global energy consumption. "Green" hydrogen is very expensive to produce, considerably more than "Grey" hydrogen.

Keywords: *Hydrogen energy, "Green hydrogen",* "Grey" *hydrogen, present challenge, Hydrogen economy, CO_2-free hydrogen, Use of hydrogen.*

Rezumat. Articolul analizează problema pieței de hidrogen - de la producere si pana la modul de utilizare, precum si perspectivele dezvoltării acestei surse de energie. Pentru a combate schimbările climatice, tot mai multe țări investesc în energie cu emisii scăzute de carbon, care este produsă din surse regenerabile și, prin urmare, este neutră pe tot parcursul lanțului. Astfel, piața globală a hidrogenului este în creștere. Hidrogenul poate ajuta la decarbonizarea sectoarelor industriale și la combaterea schimbărilor climatice, fie drept combustibil prietenos cu mediul în sectorul transporturilor, fie ca mijloc de reducere a emisiilor în producția de oțel și în multe alte industrii. Hidrogenul poate juca, de asemenea, un rol vital în transportul de energie. Dar, deși hidrogenul nu poluează în sine, arderea sa eliberând doar vapori de apă, acesta emite CO_2 atunci când se folosesc combustibili fosili pentru producerea sa (hidrogenul „gri"). Hidrogenul „verde" este încă la început: mai puțin de 1% din producția globală de hidrogen, care reprezintă ea însăși doar 2% din consumul global de energie. Hidrogenul „verde" este foarte scump de produs, considerabil mai mult decât hidrogenul "gri".

Cuvinte cheie: *Energia hidrogenului, Hidrogenul "verde", hidrogenul"gri", Provocare actuală, Economia hidrogenului, hidrogenul fără CO_2, utilizarea hidrogenului.*

Introduction

Etymologically, the word hydrogen is a combination of two Greek words, meaning 'to produce water'.

Elemental hydrogen is the main component of the Universe, accounting for 75% of its mass. In the plasma state, it is found as the majority element in the composition of stars. Elemental hydrogen is very rare on Earth. In the 16th century, the Swiss physician Paracelsus investigated the properties of the 'air' that is released when vitriol reacts with iron. A century later, the Irish scientist Robert Boyle isolated a smoking liquor from this 'air'.

To implement the energy and climate plans and achieve the targets, the EU is allocating substantial funds to all Member States between 2021 and 2027 through the following programmes: Horizon Europe, InvestEU, Connecting Europe Facility, Recovery and Resilience Facility, Technical Support Instrument, LIFE programme, European Agricultural Fund for Rural Development and Innovation Fund.

Without minimising the importance of the others, I believe that Horizon Europe launched in January 2021, worth over €100 billion, is of strategic importance because it was created exclusively to stimulate European research and innovation [1]. The programme is aimed at companies of all sizes, aims to encourage collaboration between the public and private sectors and in the coming months, more detailed information is expected about it and its strategic planning process, work programmes, funding calls and other relevant activities.

Although the EU is allocating the largest R&D budget in its history through this programme, competition for funding can be fierce and I think it would be good to pay a bit more attention to it! An agreed direction at EU level for achieving CO_2 neutrality - meaning achieving a balance between emissions and reductions in the atmosphere - would be towards the widespread use of hydrogen, and it is more than likely that a significant proportion of Horizon Europe funding will be spent on research and development of technologies for its production, storage, transport and conversion to electricity [2, 3].

The use of hydrogen as an efficient form of renewable energy storage relies on its ability to be converted back into electricity [4 - 6]. The most likely focus will be on very low-carbon hydrogen - green hydrogen - that is, hydrogen produced exclusively from cheap green energy sources such as solar panels, wind and hydro, which can be easily converted to hydrogen in nearby electrolyser stations [7, 8]. Unlike electricity, hydrogen can be stored and then transported long distances without loss through existing methane gas pipelines [9].

The properties of hydrogen

The advantages of hydrogen are numerous [10 - 12]:

- it is a very abundant atom on earth (in the form of water),
- it is the most energetic molecule (120 MJ/kg), i.e. 2.2 times natural gas,
- it is neither polluting nor toxic,
- its combustion in the air generates only water,
- It is the lightest gas, which is a positive factor with regard to safety (high speed of diffusion in the air).

The disadvantages of this gas include [13 - 15]

● its lightness implies an energy density by volume that is less favourable for transport and storage in gaseous form than for natural gas (a factor of 4 at 200 bar, for example)

● its flammability and detonation limits with air are wider than for natural gas (by a factor of about 5), but in fact only the lower limit counts: 4% by volume in air instead of 5.3% for the lower flammability limit and 13% instead of 6.3% for the lower detonation limit

● the minimum energy required to ignite it is 10 times less than that required for conventional hydrocarbons (20 μJ for hydrogen, compared to 260 for propane),

● its flame is almost invisible, and its combustion (not electrochemical) in the presence of air generates NOx.

● Its image in the public is not good (it is considered a dangerous gas) and its acceptability is therefore not yet acquired.

The "green" hydrogen

The battle for "green" hydrogen is in full swing. To combat climate change, more and more countries are investing in this low-carbon energy, which is produced from renewable energy sources and is therefore neutral throughout the chain. Although hydrogen does not pollute in itself, since its combustion only releases water vapour, it emits CO_2 when fossil fuels are used for its production. This is known as "grey" hydrogen, which emits as much CO_2 each year as the United Kingdom and Indonesia combined (830 million tonnes according to the IEA, the international energy agency) [16, 17]. Green hydrogen is still in its infancy. Its importance is extremely low today: less than 1% of global hydrogen production, which itself represents only 2% of global energy consumption. Certain problems have so far hindered the democratisation of hydrogen, notably its difficult storage and dangerous transport [18, 19]. And green hydrogen has an additional subtlety: it is very expensive to produce, even more so than grey hydrogen. Its production by electrolysis of water costs about four times as much as grey hydrogen by steam reformation of methane.

While Emmanuel Macron has just announced an additional envelope of 2 billion Euros (in addition to the 7 billion unveiled in September 2020), to boost the development of green hydrogen in France and integrate it into its national energy strategy, one country is making it the core of its energy policy, to the point of wanting to export it: Iceland [20].

A symposium on green hydrogen brought together French and Icelandic institutions and companies at the Senate, which examined the opportunities and challenges of this energy source. Iceland's President Guðni Jóhannesson took the opportunity to declare that he wanted to make green hydrogen "the key pillar of his national energy strategy". This rhetoric was immediately echoed by Iceland's private sector players, such as IDUNNH2, which declared its desire to "make Iceland the leader in green hydrogen", notably by focusing on transport and the export of e-fuels [21, 22].

Hydrogen storage

Hydrogen can only play its role as an energy carrier if it can be stored efficiently, at low cost and under acceptable safety conditions. At room temperature and atmospheric pressure, hydrogen is a highly volatile gas due to the small size of its molecule. The challenge is to create compact, low-cost tanks. When there is no need to reduce the storage volume (for example, for stationary applications), it can be stored in gaseous form at a relatively low pressure (75 bar). This means of storage is inexpensive and perfectly controlled. Storage in liquid form at low pressure is currently mainly reserved for certain very high technology applications such as space propulsion. It allows large quantities of hydrogen to be stored in a small volume. Current tanks condition the hydrogen to -253°C at 10 bars [23]. But it is impossible to avoid leaks: even very well insulated tanks absorb heat which slowly vaporises the liquid. In order to achieve satisfactory compactness while avoiding the disadvantages associated with the very low temperatures of storage in the liquid state, efforts are being made to develop storage in the gaseous state under high pressure (700 bar) [24]. The aim is

to reconcile impermeability, resistance to high pressure and resistance to shocks by working on an architecture and materials adapted to the reservoir. Lastly, a more recent line of research concerns the use of materials called hydrides which have the capacity to absorb and desorb hydrogen in a reversible manner, under temperature conditions ('solid' storage). Storage in hydrides is the most efficient way to achieve high energy density.

However, this is at the expense of weight, since the weight of the material in which the hydrogen is embedded must be added to the balance. Depending on the intended use of the hydrogen, the criteria of cost, performance, compactness or weight of these different technologies are arbitrated [25, 26].

Use of hydrogen

Worldwide hydrogen consumption is estimated at more than 500 billion cubic metres per year for various purposes and in various fields, the variety and need for which is increasing as fossil fuel resources dwindle and as climate change increases due to rising CO_2 emissions into the atmosphere [27]. In order to ensure access to hydrogen sources for different consumers, an appropriate infrastructure needs to be developed [28].

Figure 1 shows the percentages of hydrogen use in various industrial sectors. Figure 2 gives a schematic representation of steam reforming of methane. Figure 3 shows the hydrogen fuel cell. Figure 4 shows a hydrogen atom and Figure 5 shows the operation of a fuel cell.

In the air, on land or at sea: who will be driving on hydrogen tomorrow?

Cars, vans, trucks, trains, buses, boats and even aeroplanes could all use hydrogen. Hydrogen is seen as an alternative to batteries at the start of the 2020s, replacing everything that runs, flies or sails on fossil fuels.

The public authorities are not the last to believe in it. France and Germany are backing their H_2 (hydrogen) industries with billions. Japan and South Korea are making it a national priority. If we refer to the many announcements (nearly two hundred initiatives in France!), everyone should be driving on hydrogen in ten years' time... Except that in reality, nothing is less certain [26, 28].

But what exactly are we talking about? Hydrogen is the simplest of materials, very present in nature but almost never in its pure state. Producing - or rather isolating - hydrogen (H_2 molecule) - for example from water (H_2O molecule) - requires energy. The operation known as hydrolising allows this energy to be stored and then released in the form of electricity using a fuel cell. The hydrogen-powered vehicle then emits nothing more than a little water vapour [29].

These vehicles are far from being science fiction. To get an idea of what they are like, we headed for the foot of the Eiffel Tower, where at the end of May a hydrogen "village" was set up at the initiative of Toyota and the H_2 Energy Observer ship project. Several prototypes and solutions based on the Japanese manufacturer's fuel cell were on display. It was a good opportunity to review the modes of hydrogen mobility and their development potential [30].

Passenger cars

Some manufacturers (Toyota, but also Honda, Hyundai and Mercedes) market hydrogen-powered cars. These vehicles combine the advantages of a battery-powered electric car (zero emissions when in use) without the disadvantages (hydrogen refills in three minutes). However, the solution remains confidential for private individuals and will probably remain so for a long time [31].

The first problem is that the manufacture of H_2 gas is still very expensive when it is green hydrogen produced by hydrolisis from a wind turbine or solar panels. Currently, the only affordable way to produce hydrogen is to "crack" methane (known as steam reforming), which not only burns a lot of carbon energy but also releases the CO_2 contained in the methane. The climate balance is catastrophic [32].

Second problem: the large-scale deployment of hydrogen stations is very expensive (around 1 million Euros per station) and complex. H_2 is super-explosive, difficult to store and transport in large quantities. Without a vast supply network, it is not conceivable that motorists will adopt this technology. Oil-based fuels are running out, polluting and contributing to global warming. Now it's time for hydrogen, the most common element in the universe [33].

Annette and Ron simply rented a car, a Honda. So far, nothing extraordinary. Except that they have become the first people to use a vehicle that runs on hydrogen and spits out ... only water! It's nothing to do with a billionaire's eco-fad: they only pay 600 dollars (about 400 Euros) a month. Nor is it a gadget for shopping around the corner [34]. The Honda FCX Clarity can travel 430 km before it has to go back to the hydrogen pump. And the little Japanese car, which reaches 16.0 km/h, does not emit a single gram of CO_2!

Since 16 June 2008, the Clarity has been the first hydrogen-powered car to go into series production. Japanese manufacturers are ahead of the game. Most of them already have their prototypes. They will be presented at the Paris Motor Show, which starts on 4 October (in 2008). In France, Peugeot has its Partner H_2Origin and Renault, its Scenic ZEVH2. And this is just the beginning. At European level, a six-year, €470 million research programme will be launched in mid-October, and companies in the sector will be asked to invest at least as much [35 - 36]. This means that almost a billion Euros will be spent to achieve the European objective of starting to market hydrogen cars between 2015 and 2020. That's right! You'll be driving one before long.

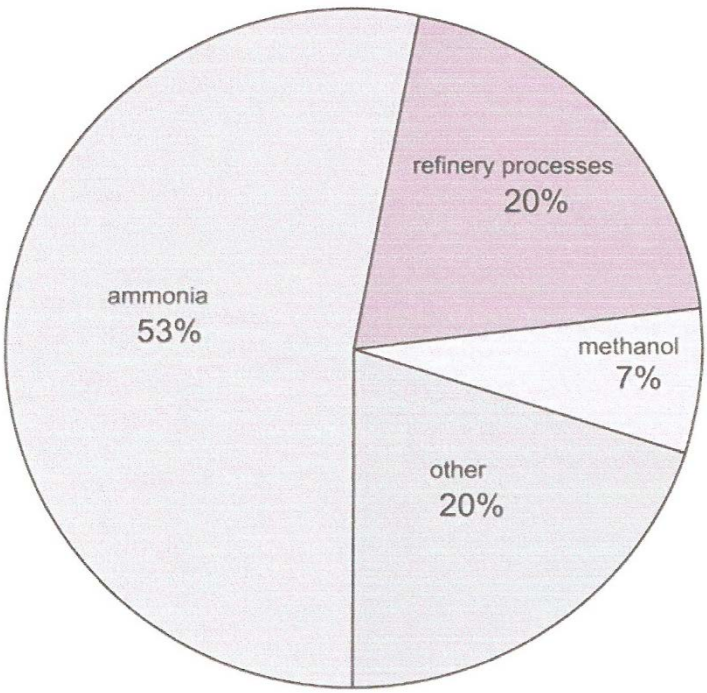

Figure 1. Use of hydrogen.

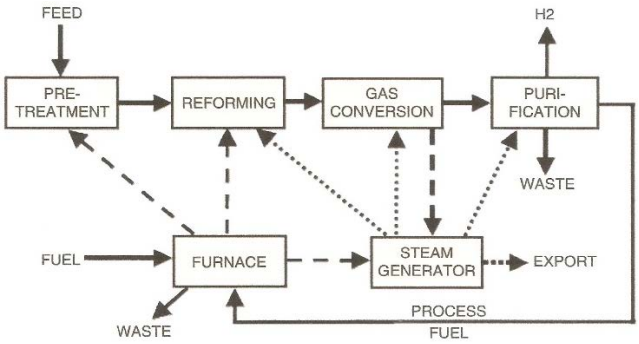

Figure 2. Schematic representation of steam methane reforming.

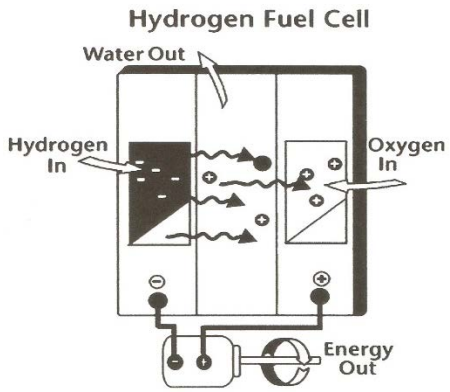

Figure 3. Hydrogen fuel cell (after [1]).

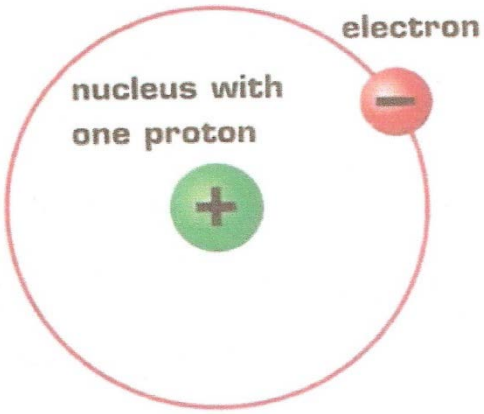

Figure 4. A hydrogen atom.

And not run out of fuel, since it's everywhere (see box His Majesty the Hydrogen). It's infuriating! The most common element in the universe does not exist in its pure state on Earth, but only in combination with more complex molecules.

The hydrogen we put in our tanks will have to be found by tearing hydrogen atoms from the molecules that contain it.

Entrepreneurial perspective

To seize the opportunities in this field, companies need to take strategic risks. They should strive to build ecosystems, continuously develop further insights and proactively interact with policy makers. On the demand side, much of the attention will be focused on the big brands of the world. They are looking at renewable alternatives for their non-electrifiable energy needs so that they can fulfil their sustainability ambitions [32, 33]. This could lead to a hydrogen-based equivalent to the current Power Purchase Agreements (PPAs) that have emerged in the electricity market.

On the supply side, consortia of leading global energy companies will focus on expanding the hydrogen market. Due to their size - and thus their ability to manage such large-scale projects at all - they are just as predestined for this as they are due to their very own interest in using the hydrogen business to secure their relevance in a decarbonised world of the future. They will therefore increase the pressure on governments to enable an appropriately sized hydrogen market [37].

We have an order of merit that fundamentally closes on the price of CO_2. As long as fossil fuels close the merit order, one of the fundamentals we have to consider is the CO_2 price. According to information from *European Commission* documents, the tonne of CO_2 could reach between 55 and 90 Euros in 2030, and the evolution of the CO_2 price from 2021

(doubling the price compared to 2020, to around 50 EUR/t CO_2) makes the worst case scenario impossible to ignore. In any fossil fuel energy production, at a price of 90 EUR/tonne/CO_2, the energy price would transfer somewhere in the range of at least 45 EUR/MWh even with the most modern technology (and around 80 EUR/tonne for coal).

Hydrogen has been tested for alternative use in vehicles equipped with internal combustion engines [38]. Its main advantage is that it is environmentally friendly, as water vapour is produced when it is burnt. The disadvantages are the high explosion hazard, the difficulty of storing it in vehicles and the lack of a hydrogen refuelling station infrastructure. It can be used for direct electricity generation via fuel cells.

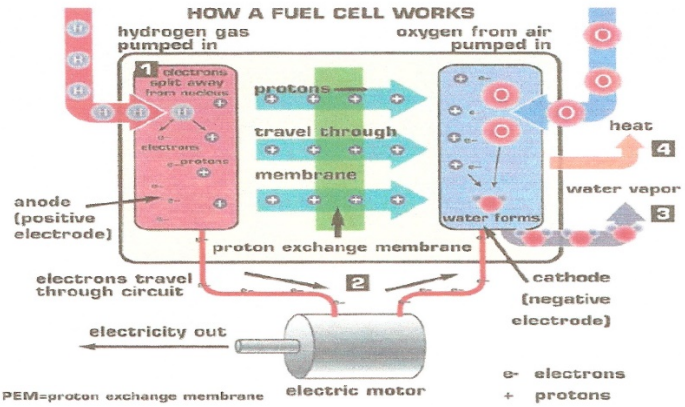

Figure 5. Operation of a fuel cell (after [1]): 1. Electron splits; 2. Electrons travel through the circuit to make electricity, then the protons travel to the cathode. At this stage, hydrogen reforms and unites with oxygen; 3. Water vaporizes and 4. Heat is produced.

Hydrogen – a good fuel

Hydrogen accounts for about 2% of the EU's energy mix, 95% of which is produced by burning fossil fuels, which releases 70 - 100 million tonnes of CO_2 every year [39]. According to research, renewable energies could provide a substantial part of the European energy mix by 2050, with hydrogen accounting for up to 20% of this mix, or between 20 - 50% of energy needs in transport and 5 - 20% in industry [40, 41]. It is mainly used as a raw material in industrial processes, but also as a fuel for space rockets. Hydrogen can be considered a good fuel because of its properties: Its use as an energy source does not produce greenhouse gases (water is the only by-product) It can be used to produce other gases, such as liquid fuels Existing infrastructure for transporting and storing gas can be reused for hydrogen It has a higher energy density than batteries, so can be used for long-distance, or large tonnage transport.

Conclusion

The current context of globalization of market innovation is helping to understand the hydrogen learning processes inside and outside companies, how they acquire new knowledge, how they organize their resources and capabilities to sustain the business strategy.

References

1. European Union, *A Hydrogen Strategy for a Climate-Neutral Europe*, juillet 2020, https://eur-lex.europa.eu/legal-content/FR/TXT/PDF/?uri=CELEX:52020DC0301&from=EN
2. Zohuri B. *Hydrogen Energy - Challenges and Solutions for a Cleaner Future,* Springer, 2019.

3. Global Shift Institute, *Bulletins d'août 2019, d'août 2020 et de décembre 2020*, https://www.globalshift.ca/bulletins/
4. *Hard-to-electrify sectors*: Secteurs difficiles à électrifier; *Hard-to-abate sectors*: secteurs dans lesquels la réduction des émissions est difficile
5. Word Energy Council, *New Hydrogen Économy – Hope or Hype,* https://www.worldenergy.org/assets/downloads/WEInnovation-Insights-Brief-New-Hydrogen-Economy-Hype-or-Hope.pdf
6. IRENA. *Green Hydrogen, A Guide to Policy Making*, https://www.irena.org/publications/2020/Nov/Green-hydrogen
7. IRENA. *Hydrogen Cost Reduction, Scaling up Electrolysers to meet the 1,5° Climate Goal*, https://irena.org/-/media/Files/IRENA/Agency/Publication/2020/Dec/IRENA_Green_hydrogen_cost_2020.pdf
8. Hydrogen Council, Path to Hydrogen Competiveness, A Cost Perspective, Janvier 2020,
9. https://hydrogencouncil.com/wp-content/uploads/2020/01/Path-to-Hydrogen-Competitiveness_Full-Study-1.pdf
10. Gilles L. Bourque et col, IREC, *L'hydrogène, un vecteur énergétique pour la transition*, janvier 2020, https://irec.quebec/ressources/publications/Hydrogene-Vecteur-energetique-pour-la-transition-IREC2020.pdf
11. IRENA, *As global economies strive for carbon neutrality, cost-competitive renewable hydrogen is possible within the decade,* Quaterly janvier 2021, https://www.irena.org/-/media/Files/IRENA/Agency/ Quarterly/ IRENA_Quarterly_2021_Q1.pdf
12. BDI 2018: Klimapfade für Deutschland. Boston Consulting Group und Prognos im Auftrag des BDI.
13. Beckers T., Gizzi F., Schäfer-Stradowsky S., Wilms S. u.a. (2018): Rechtliche Rahmenbedingungen für ein integriertes Energiekonzept 2050 und die Einbindung von EE-Kraftstoffen. Forschungsbericht von BBH (Becker Büttner Held), LBST (Ludwig Bölkow Systemtechnik), ISE (Fraunhofer Institut für Solare Energiesysteme) und IKEM (Institut für Klimaschutz, Energie und Mobilität) im Auftrag des Bundesministeriums für Verkehr und digitale Infrastruktur.
14. BMWi (Bundesministerium für Wirtschaft und Energie) (2019): Dialogprozess Gas 2030 – Erste Bilanz – Oktober 2019. Berlin
15. Dena 2018: Leitstudie integrierte Energiewende. Gutachterbericht von ewi Energy Research & Scenarios GmbH im Auftrag der Dena. Berlin
16. IEA 2019: The Future of Hydrogen - Report prepared by the IEA for the G20, Japan, June 2019, Paris
17. IW Köln und frontier economics, (2018): Synthetische Energieträger – Perspektiven für die deutsche Wirtschaft und den internationalen Handel. Eine Untersuchung der Marktpotenziale, Investitions- und Beschäftigungseffekte. Studie im Auftrag von IWO, MEW und UNITI.
18. LBST (Ludwig Bölkow Systemtechnik) (2019): Wasserstoffstudie Nordrhein-Westfalen. Eine Expertise für das Ministerium für Wirtschaft, Innovation, Digitalisierung und Energie des Landes Nordrhein-Westfalen
19. Nymoen H., Sendler S. C., Steffen R., und Pfeiffe R. (2019): Kurzstudie "Quote erneuerbare und dekarbonisierte Gase". Kurzstudie im Auftrag der Vereinigung der Fernleitungsnetzbetreiber Gas e.V. (FNB Gas) Nymoen Strategieberatung GmbH, Berlin.
20. POWER TO X ALLIANZ (2019): Ein Markteinführungsprogramm für Power to X-Technologien.
21. Smolinka T., Wiebe N., Sterchele P., Palzer A. u. a. (2018): Studie IndWEDe. Industrialisierung der Wasserelektrolyse in Deutschland. Chancen und Herausforderungen für nachhaltigen Wasserstoff für Verkehr, Strom und Wärme
22. UBA 2019: Ressourcenschonendes und treibhausgasneutrales Deutschland. Szenario GreenEe. UBA, Dessau-Roßlau
23. WWF 2019: Klimaschutz in der Industrie. Forderungen an die Bundesregierung für einen klimaneutralen Industriestandort Deutschland. WWF Deutschland, Berlin
24. The Oxford Institute for Energy Studies, "EU Hydrogen Strategy - A case for urgent action towards implementation" July 2020
25. Accompagner la transition vers l'hydrogène vert, https://group.bureauveritas.com/fr/magazine/accompagner-la-transition-vers-lhydrogene-vert, 12 mai 2021.
26. Bento N. "La transition vers une économie de l'hydrogène : infrastructures et changement technique" Thèse de doctorat, Université Pierre Mendès-France - Grenoble II,, 2010
27. OIES: Europe's energy transition trajectory: Is conventional wisdom at risk of becoming inconvenient truth? - June 2021

28. Dans les airs, sur terre ou sur mer : qui roulera à l'hydrogène demain ? *Le Monde,* 24/06/2021
29. Thomas Sandy C. E. *Solar Hydrogen,* ISBN-978-1-54-39742
30. Goltsov A. Victor and Veziroglu T. Nejat. *"A step to the road to hydrogen civilization", International Journal of Hydrogen Energy*, Vol. 27, Issues 7–8, July–August 2002, pp. 719-723
31. Ball M., Wietschel M. (2009), "The future of hydrogen - opportunities and challenges", International Journal of Hydrogen Energy 34: 615 – 627
32. Rifkin J. (2007), "Leading the way to the hydrogen economy and a Third Industrial Revolution: a New Energy Agenda for the European Union in the 21st Century", Présenté au Parlement UE en hiver 2007
33. Rifkin J. (2002). *L'Economie Hydrogène. Après la Fin du Pétrole, la Nouvelle Révolution Economique*, Ed. La découverte, Paris
34. Dunn S. (2002). "Hydrogen futures: towards a sustainable energy system", *International Journal of Hydrogen Energy* 27 (3): 235-264
35. Marchetti C. (1985). "Nuclear plants and nuclear niches", *Nuclear Science and Engineering* 90, 521– 526.
36. Sperling D., Gordon D. (2008). Advanced passenger transport technologies. Annual Review of Environment and Ressources 33, 63–84
37. Van Benthem A.A., Kramer G.J., Ramer R. (2006). An options approach to investment in a hydrogen infrastructure. Energy Policy 34, 2949–2963
38. International Energy Agency (IEA), (2009). Transport, Energy and CO_2: Moving Toward Sustainability. IEA/OECD, Paris
39. World Business Council for Sustainable Development (WBCSD), (2004). Mobility 2030: Meeting the Challenges to Sustainability, /http://www.wbcsd.chS
40. Conseil d'Analyse Stratégique (CAS), (2008). Perspectives concernant le véhicule "grand public" d'ici 2030. Coordination Jean Syrota, 18 septembre, /http:// www.strategie.gouv.frS
41. Bento N. "Is carbon lock-in blocking investments in the hydrogen economy? A survey of actors' strategies" Energy Policy 38(2010), 7189-7199.

Journal of Engineering Science *Vol. XXIX, no. 1 (2022), pp. 71 - 85*
Fascicle *Electronics and Computer Science* *ISSN 2587-3474*
Topic *Electronics and Communication* *eISSN 2587-3482*

https://doi.org/10.52326/jes.utm.2022.29(1).06
CZU 623.4.021:004.6

SYSTEMS FOR INVARIANT TARGET RECOGNITION BASED ON CENTRAL IMAGE CHORD TRANSFORMATION

Veaceslav Perju*, ORCID 0000-0002-7755-4277

Department of Strategical Studies in Defense and Security
Agency for Military Science and Memory
47 Tighina Str., Chisinau, MD-2001, Republic of Moldova
*Corresponding author: Veaceslav Perju, *vlperju@yahoo.com*

Received: 12.10.2021
Accepted: 02.06.2022

Abstract. Target recognition (TR) is widely used in different military and civil applications and permits enhanced intelligence and autonomously operating platforms design. The article describes existing systems for TR such as deep learning aided computer vision; target tracking architecture, based on the tracking-by-detection paradigm; a target detection dataset; deep neural networks; a system for the management of a plurality of sensors; a target recognition architecture, adaptive to operational conditions and a target detection system, based on the theory of multi-temporal recognition. Unfortunately, the existing systems do not orient for real-time processing or can be applied for synthetic aperture radar images only, or used for image processing of soft targets, etc. This article presents the data regarding proposed new systems for targets recognition and determination of their parameters, based on central image chord transformation. The systems' main processing units are described. The structures of the elaborated systems and the principles of their functioning are presented. The models of data processing flow in the systems are described. The determination of the processing time of the operations, realized in the systems was made and the estimation of the throughput of the systems was done. The optimization of the elaborated systems was made. The results regarding systems' characteristics are presented.

Kew words: *Target recognition, data processing flow, throughput, optimization.*

Rezumat. Recunoașterea țintei (RȚ) este utilizată pe scară largă în diferite aplicații militare și civile și permite proiectarea platformelor de operare autonomă inteligente îmbunătățite. Articolul descrie sisteme existente pentru RȚ, cum ar fi vizualizarea computerizată asistată de învățare profundă; arhitectura de urmărire a țintei, bazată pe paradigma detecției; utilizarea unui set de date de detectare a țintei; rețele neuronale profunde; un sistemul bazat utilizarea multitudinii de senzori; o arhitectură de recunoaștere a țintei, adaptabilă la condițiile operaționale și un sistem de detectare a țintei, bazat pe teoria recunoașterii multi-temporale. A fost stabilit, că sistemele existente nu permit procesarea datelor în timp real sau pot fi aplicate doar pentru imagini radar sintetice sau utilizate pentru procesarea imaginilor țintelor variabile etc. În acest articol se descriu noile sisteme propuse pentru recunoașterea țintelor și determinarea parametrilor lor, bazate pe transformarea centrală a

coardelor de imagine. Sunt descrise principalele unități de procesare ale sistemelor. A fost prezentate structurile sistemelor elaborate și principiile de funcționare a acestora. Se descriu modelele fluxului de procesare a datelor în sisteme. A fost estimat timpul de procesare a operațiilor, realizate în sisteme și s-a făcut analiza productivității sistemelor. S-a realizat optimizarea sistemelor elaborate. Sunt prezentate rezultatele privind caracteristicile sistemelor.

Cuvinte cheie: *Recunoașterea țintei, flux de procesare a datelor, productivitate, optimizare.*

Introduction

Target recognition is one of the core processes for enhancing intelligence and autonomously operating platforms. Deep learning-aided computer vision systems have yielded promised results on target recognition applications [1]. However, these approaches do not translate easily to engineered realizations. The article [2] presents a target tracking system aimed to be used in real-time conditions. The problems appear in the presents of specific challenges such as moving sensors, changing zoom levels, dynamic background, illumination changes, obscurations, and small objects.

The paper [3] presents a target detection dataset that depicts helicopters. Unfortunately, the targets are seen by the camera in real-world scenarios typically do not always appear large, focused, or in the center of the input image.

The perspective approach for target recognition consists using of deep neural networks [4]. However, within the real conditions appear necessary to define a large number and types of targets' classes. The paper [5] presents a system for the management of a set of sensors to improve the threat-detection capabilities of targets. The system architecture consists of three main components, such as 2D video tracking and re-identification, which allows the labeling and tracking of targets in a small area; 3D video tracking with a stereo camera, which gives a more accurate location measurement using recurrent neural networks for location prediction, and, finally, command and control unit. The data fusion combines the outputs of multiple sensors. Unfortunately, this system can be applied for image processing of the soft targets only.

In the paper [6] an automatic target recognition architecture is proposed, based on the current methodology trends. Unfortunately, the proposed architecture can be applied for synthetic aperture radar images only.

Based on the theory of multi-temporal recognition, an automatic target recognition system for the remote sensing image is proposed in the article [7], which includes four modules: remote sensing image segmentation; target extraction from an image; the processing of the target's image, and recognition of the target. Unfortunately, the elaborated system doesn't orient for real-time processing.

In this article, the systems for invariant target recognition and determination of their parameters – scale, angular rotation, and position in the plane are described, based on the methods of target recognition, proposed by the author in [8]. The elaborated systems are referred to as a specialized multiprocessor functional distributed class of systems, which represent a combination of the electronic and optical processing modules.

In section 1 the systems' main processing units are described. In sections 2 - 5 the structures of the elaborated systems are presented and the principles of their functioning are described. The data processing flow models in the proposed systems are presented in section 6. In section 7 the determination of the processing time of the operations, realized in the systems

was made and the estimation of the data processing time and throughput of the systems are presented. Based on the obtained results the optimization of the elaborated systems was made. The results regarding systems' characteristics are described.

1. The systems' main processing units

Suppose the target is describing as:

$$P'(x',y') = P'(x,y,e_1,e_2, e_3, e_4)=P'(x+e_3,y+e_4,e_1,e_2), \quad (1)$$

were e_1 is scale change, e_2 – rotation, and e_3, e_4 – shits of the target.

The systems described below consist of the next main units: laser (L) as a source of coherent light for data transmission and processing; preprocessing module (PPM) for target's image input and enhancement such as noise-reducing, contrast increasing, etc. [9]; optical multiplier (OM) for light beam dividing (multiplexing); a processor for determining the target's parameters e_3, e_4 (PTP) [10]; a processor for target's scale and rotation (PTSR) determination (parameters e_1, e_2) [11]; a processor for coordinate transformation (PCT) of the target's image [12]; processor for central image chord transformation (PICT) realization [13]; a processor for Fourier transformation (PFT) and determination the target's image complexity SL and maximum frequency f_m of the spectrum [14]; a processor for target's rotation (PTR) determination (parameter e_2) [15]; a processor for system's control, processing of the data and target classification (PCPC) [16].

2. Target recognition system TRS1

The system TRS1 realizes the method TRM1 of the target recognition, proposed by the author and described in [8], and is presented in Figure 1. The system works in the next mode. The target's image P'(x',y') is scanned into the processor PTIP where the operations are realized of the enhancement, noise extraction, etc.

$$P'(x',y') \longrightarrow P(x',y') = P(x,y,e_1,e_2,e_3,e_4). \quad (2)$$

The laser L light beam is modulated by the function P(x',y') in the processor PTIP and at the output is divided by multiplier OM1 into three light beams, which are introduced into the processors PTP, PCT1, and PFT, respectively. In the processor PTP the target's parameters e_3 and e_4 are calculated. In parallel, the Fourier spectrum of the function P(x',y') is formed in the processor PFT:

$$P(x',y') \longrightarrow |FT\{P(x',y')\}|^2=P(x'_1,y'_1) = P(x_1,y_1,e_1,e_2). \quad (3)$$

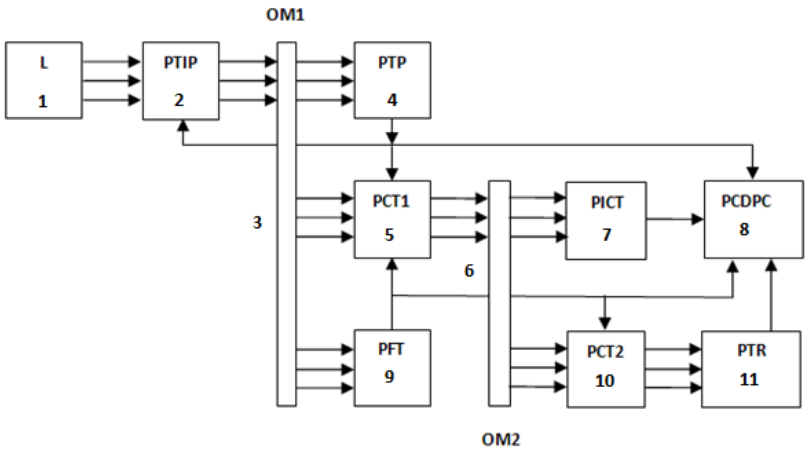

Figure 1. The structure of the system TRS1.

The maximum frequency f_m of the Fourier spectrum $P(x'_1,y'_1)$ and the complexity SL of image P(x',y') are calculated in this processor. The data regarding the target's shifts e_3 and e_4 from processor PTP, and the target's complexity SL from processor PFT are introduced into processors PCT1, about parameter SL – into processor PCT2, and regarding the parameters e_3, e_4, and f_m - into processor PCDPC. In the processor PCT1, the function P(x',y') is centered under parameters e_3, e_4, and SL:

$$P(x',y')=P(x+e_3,y+e_4,e_1,e_2)\rightarrow P(x'_2,y'_2)=P(x_2,y_2,e_1,e_2), \quad (4)$$

where $x_2=x-e_3$, $y_2=y-e_4$.

Then, the function $P(x_2',y_2')$ from the processor PCT1 is input via multiplier OM2 into processors PICT and PCT2. In the processor PICT the chords transformation of the function $P(x'_2,y'_2)$ is realized [13]:

$$P(x'_2,y'_2)\rightarrow P(x'_3,y'_3), \quad (5)$$

and the target's feature vector **v** is calculated. The information regarding vector **v is** sent to the processor PCDPC, where the target is classified [16]. The target's scale e_1 is calculated using the expression $e_1=f_{ms}/f_m$, where f_{ms} is the Fourier spectrum maximum frequency of the reference target.

In the processor PCT2, the function $P(x'_2,y'_2)$ is normalized on the parameter e_1 and is transformed to the polar coordinate system:

$$P(x'_2,y'_2)=P(x_2,y_2,e_1,e_2)\rightarrow P(x'_4,y'_4)=P[x_4+x_{40}(e_2),y_4], \quad (6)$$

where $x'_4=\text{arctg}(y_2/x_2)$, $y'_4=[(x^2_2+y^2_2)^{1/2}]/e_1$.

The function $P(x'_4,y'_4)$ is transmitted from the processor PCT2 to the processor PTR, where the target's scale e_2 is determined at the extraction and processing of the value $x_{40}(e_2)$.

3. Target recognition system TRS2

The system TRS2 realizes the target recognition method TRM2 [8], and the structure is the same as TRS1 (Figure 1). The difference consists in the computer processes organization. The system work in the next mode. The target's image P'(x',y') is introduced into the processor PTIP where the operations are realized of the image enhancement:

$$P'(x',y') \longrightarrow P(x',y')= P(x,y,e_1,e_2,e_3,e_4). \quad (7)$$

The laser L light beam in the processor PTIP scans the image P(x',y'), which is reflected in continuation by multiplier OM1 at the inputs of the processors PTP, PCT1, and PFT. In the processor PTP the target's coordinates e_3 and e_4 are calculated. Simultaneously, the function P(x',y') Fourier spectrum is calculated in the processor PFT:

$$P(x',y') \longrightarrow |FT\{P(x',y')\}|^2=P(x'_1,y'_1) = P(x_1,y_1,e_1,e_2). \quad (8)$$

Based on $P(x'_1,y'_1)$, the complexity SL of image P(x',y') is calculated. The information regarding coordinates e_3 and e_4 from processor PTP, and target's complexity SL from processor PFT is transmitted to processor PCT1, about SL – to processor PCT2, and about e_3 and e_4 - to processor PCDPC. In the processor PCT1, the function P(x',y') is centered following data e_3, e_4, and SL:

$$P(x',y')=P(x+e_3,y+e_4,e_1,e_2)\rightarrow P(x'_2,y'_2)=P(x_2,y_2,e_1,e_2), \quad (9)$$

where $x_2=x-e_3$, $y_2=y-e_4$.

After that, the image $P(x_2',y_2')$ is introduced, via multiplier OM2, into processors PICT and PCT2. In the processor PICT the operation of chord transformation is performed [13]:

$$P(x'_2,y'_2)\rightarrow P(x'_3,y'_3), \tag{10}$$

and a vector **v** of the target's features is calculated. The information from the processor PICT is transmitted to the processor PCDPC, where the operation of target classification is realized [16]. In processor PCT2, the function $P(x'_2,y'_2)$ is transformed to the log-polar coordinate system:

$$P(x'_2,y'_2) = P(x_2,y_2,e_1,e_2) \rightarrow P(x'_4,y'_4)= P[x_4+x_{40}(e_1), y_4+y_{40}(e_2)], \tag{11}$$

where $x_4=\text{arctg}(y_2/x_2)$, $y_4=(x_2^2+y_2^2)^{1/2}$, and $x_{40}(e_1)$, $y_{40}(e_2)$ are the parameters, depending on the values of e_1 and e_2 respectively. In this case, the effects of the target scaling on value e_1 and rotation on value e_2 will produce the shifts of the function $P(x'_4,y'_4)$ on the axis x_4 and y_4 respectively. The function $P(x'_4,y'_4)$ is transmitted from processor PCT2 to processor PTSR, where the parameters value e_1 and e_2 are determined based on the correlation function, calculated between this function and reference target's function $P_s(x_4,y_4)$ determined on the stage of classification:

$$U(x,y) = \max\{\iint P(x'_4,y'_4)P_s(x_4,y_4)\, dx_4dy_4. \tag{12}$$

4. Target recognition system TRS3

The system TRS3 realizes the method TRM3 of the target recognition [8] and is presented in Figure 2.

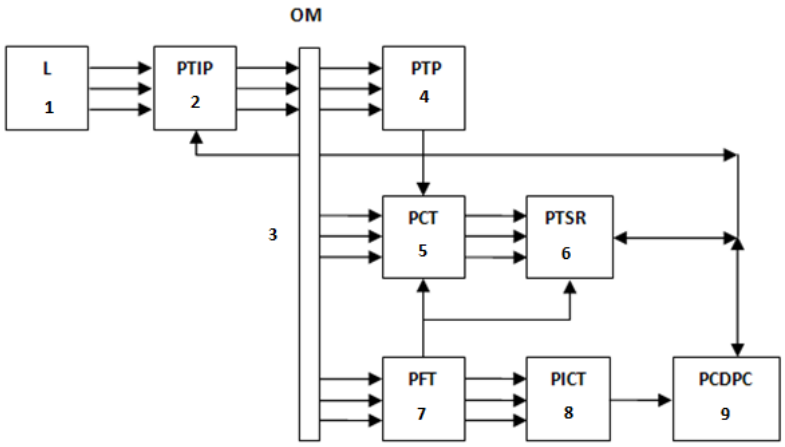

Figure 2. The structure of the system TRS3.

The system operates in the following way. The target's image P'(x',y') is scanned into processor PTIP were are realized the operations of enhancement:

$$P'(x',y') \rightarrow P(x',y') = P(x,y,e_1,e_2,e_3,e_4). \tag{13}$$

The light beam generated by laser L going via processor PTIP is modulated by image P(x',y') after which is introduced via multiplier OM in the processors PTP, PCT, and PFT. In the processor PTP, the target's coordinates e_3, e_4 in the plane are calculated. Contemporaneously, the Fourier spectrum of the input function is calculated in the unit PFT:

$$P(x',y') = P(x,y,e_1,e_2,e_3,e_4) \rightarrow |FT\{P(x',y')\}|^2=P(x'_1,y'_1) = P(x_1,y_1,e_1,e_2). \tag{14}$$

The parameter SL of the function P(x',y') also is determined in this unit. The image $P(x'_1,y'_1)$ is transmitted from processor PFT to the processor PICT, where the operation of chords transformation is performed [13]:

$$P(x'_1,y'_1) \rightarrow P(x'_2,y'_2), \tag{15}$$

Based on this the target's feature vector **v** is calculated. The information regarding vector **v** is transferred from processor PICT to processor PCDPC, where the target is classified [16]. The data about coordinates e_3 and e_4 from processor PTP, and complexity SL - from processor PFT have been introduced into processors PCT, where the function P(x',y') is centered on the parameters e_3, e_4 and is transformed to the log-polar coordinate system:

$$P(x',y')=P(x+e_3,y+e_4,e_1,e_2) \rightarrow P(x'_3,y'_3)=P[x_3+x_{30}(e_2),y_3+y_{30}(e_1)], \tag{16}$$

where $x'_3=\text{arctg}(y''/x'')$, $y'_3=\ln[(x'')^2+(y'')^2]/2$ and $x''=x'-e_3$, $y''=y'-e_4$.

Then, in the processor PTSR the parameters value e_1 and e_2 are determined based on the correlation function calculated between the function $P(x'_3,y'_3)$ and the standard target's function $P_s(x_3,y_3)$ determined on the stage of classification:

$$U(x_4,y_4) = \max\{\iint P(x'_3,y'_3)P_s(x_3,y_3)\, dx_3dy_3\}. \tag{17}$$

5. Target recognition system TRS4

The system TRS4 realizes the method TRM4 of the target recognition [8] and is presented in Figure 3.

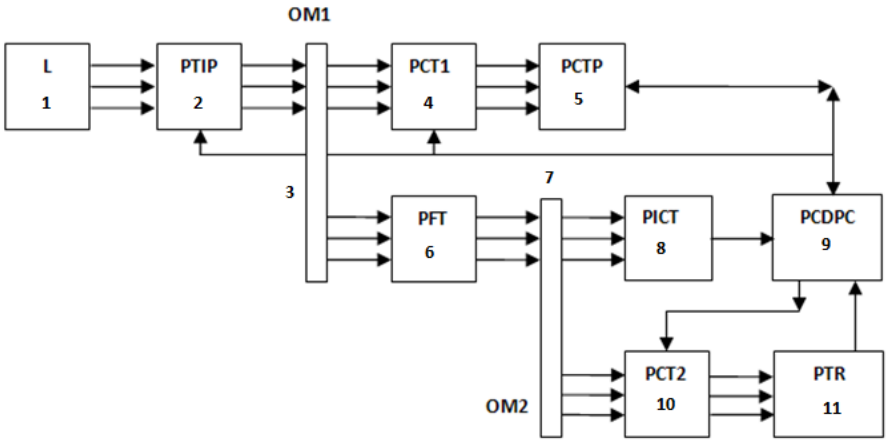

Figure 3. The structure of the system TRS4.

The system act in the next mode. 2-D image of the target P'(x',y') is input into the processor PTIP were are realized the operations of enhancement:

$$P'(x',y') \longrightarrow P(x',y') = P(x,y,e_1,e_2,e_3,e_4). \tag{18}$$

The optical beam formed by laser L going via processor PTIP is encrypted by the image P(x',y') after which is introduced via multiplier OM1 in the processors PCT1 and PFT. In the processor PFT, the Fourier spectrum of the target's image is formed:

$$P(x',y') = P(x,y,e_1,e_2,e_3,e_4) \longrightarrow |FT\{P(x',y')\}|^2=P(x'_1,y'_1) = P(x_1,y_1,e_1,e_2). \tag{19}$$

The P(x',y') image's parameters f_m and SL are determined in this unit. The function $P(x'_1,y'_1)$ is transmitted from processor PFT via multiplier OM2 to the processors PICT and PCT2. In the processor PICT, the chords transformation is calculated [13]:

$$P(x'_1,y'_1)\rightarrow P(x'_2,y'_2), \quad (20)$$

and the target's vector **v** of feature is calculated. The information regarding vector **v** is transferred from processor PICT to processor PCDPC, where the target is classified [16]. Also, in this processor, the target's scale e_1 is determined as $e_1=f_{ms}/f_m$, where f_{ms} is the Fourier spectrum's maximum frequency of the determined reference target. In the processor PCT2, the function $P(x'_1,y'_1)$ will be normalized on scale e_1 and converted to a polar coordinate system:

$$P(x'_1, y'_1)=P(x_1, y_1, e_1, e_2)\rightarrow P(x'_3,y'_3)=P[x_3 +x_{30}(e_2),y_3], \quad (21)$$

where $x_3=\text{arctg}(y''_1/x''_1)$, $y_3=[(x''_1)^2+(y''_1)^2]^{1/2}$ and $x''_1=x_1$, $y''_1=y_1/e_1$.

The function $P(x'_3,y'_3)$ is transferred from processor PCT2 to processor PTR, where the target's rotation e_2 is calculated based on the value $x_{30}(e_2)$ extracted. The data regarding parameters e_1 and e_2 are transmitted from unit PCDPC to unit PCT1, where the target's function P(x',y') is normalized on these parameters:

$$P(x',y') = P(x+e_3, y+e_4, e_1, e_2) \longrightarrow P(x'_4, y'_4) =P(x_4+e_3, y_4+e_4), \quad (22)$$

where $x'_4=[x'\cos(-e_2) - y\sin(-e_2)]/e_1$, $y'_4=[x'\sin(-e_2) + y\cos(-e_2)]/e_1$.

The function $P(x'_4, y'_4)$ is sent from processor PCT1 to processor PCTP, where the parameters e_3 and e_4 are determined based on the correlation function calculated between the function $P(x'_4,y'_4)$ and reference target's function $P_s(x_4,y_4)$ established on the stage of classification:

$$U(x_5,y_5) = \max\{\iint P(x'_4,y'_4)P_s(x_4,y_4)dx_4dy_4. \quad (23)$$

6. Models of data processing flow in the systems

The models of data processing flow in the systems which will be described in this section will permit the analysis of the efficiency of the computing processes organization in the systems and to optimize the systems' structures with the purpose of the increase their productivity.

6.1. Model of data processing flow in the system TRS1

Taking into account the system TRS1 operation presented in section 2, we will describe the stages of data processing in this system as follow. Stage S1/2 – target's image input and preprocessing in the processor 2; S2/4 – the target position in-plane (coordinates e_3, e_4) calculation in the processing unit 4; S2/9 - the Fourier spectrum of the target's image formation in processor 9, the maximum frequency f_m of the Fourier spectrum $P(x'_1,y'_1)$ and the complexity SL of image P(x',y') determination; S3/5 - the function P(x',y') centering in the processing unit 5 using the data regarding e_3, e_4, and SL; S4/7 - the operation of chord transformation performing in the processor 7 and the target's vector **v** of features calculation; S5/8 - the target classification in the processor 8; S6/8 - the target's scale e_1 determination in the processor 8; S7/10 - the target's image $P(x'_2,y'_2)$ normalization on e_1 and conversion to a polar coordinate system in the processor 10; S8/11 - the target's rotation (parameter e_2) calculation in the processing unit 11. The model MD1 of data processing flow is presented in Figure 4a.

6.2. Model of data processing flow in the system TRS2

Let's describe the stages of data processing in the system TRS2 in the next mode. Stage S1/2 – target's image input and preprocessing in the processor 2; S2/4 – the target position in-plane (coordinates e_3, e_4) calculation in the processing unit 4; S2/9 - the Fourier spectrum of the target's image formation in processor 9, the function P(x',y') complexity SL determination; S3/5 - the target's image centering (function P(x',y')) in the processing unit 5 using the data of e_3, e_4, and SL; S4/7 - the operation of chord transformation performing in the processor 7 and the target's vector **v** of features calculation; S5/8 - the target classification in the processor 8; S6/10 - the target's image (function $P(x'_2,y'_2)$) conversion to a log-polar coordinate system in the processor 10; S7/11 - the target's scale e_1 and rotation e_2 determination in the processor 11. The model MD2 of data processing flow in this system is presented in Figure 4b.

6.3. Model of data processing flow in the system TRS3

Let's determine the stages of data processing in the system TRS3, based on the system's description from section 4. Stage S1/2 – target's image input and preprocessing in processor 2; S2/4 – the target position in-plane (coordinates e_3, e_4) calculation in processor 4; S2/7 - the Fourier spectrum of the target's image formation in processor 7, the complexity

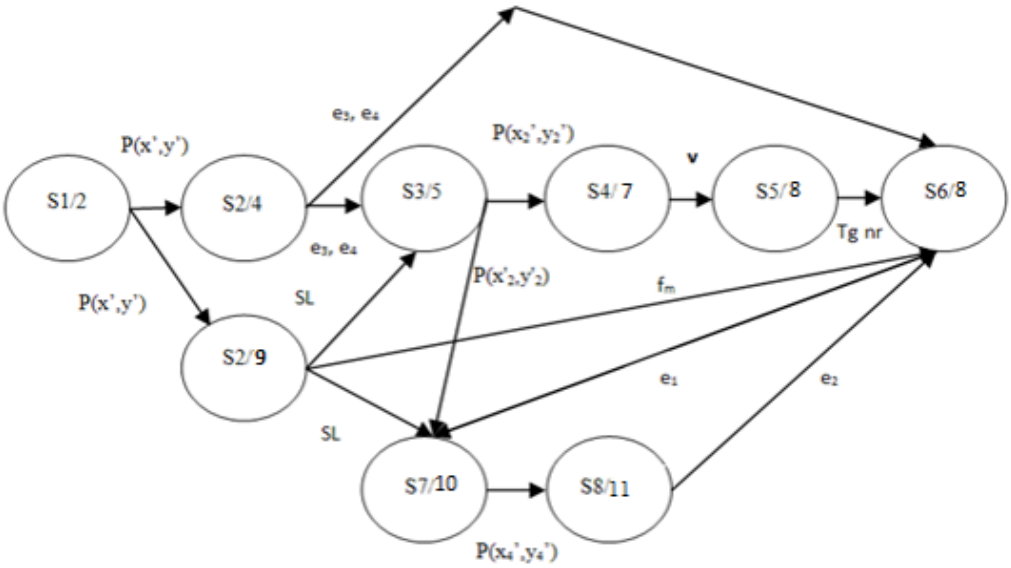

a)

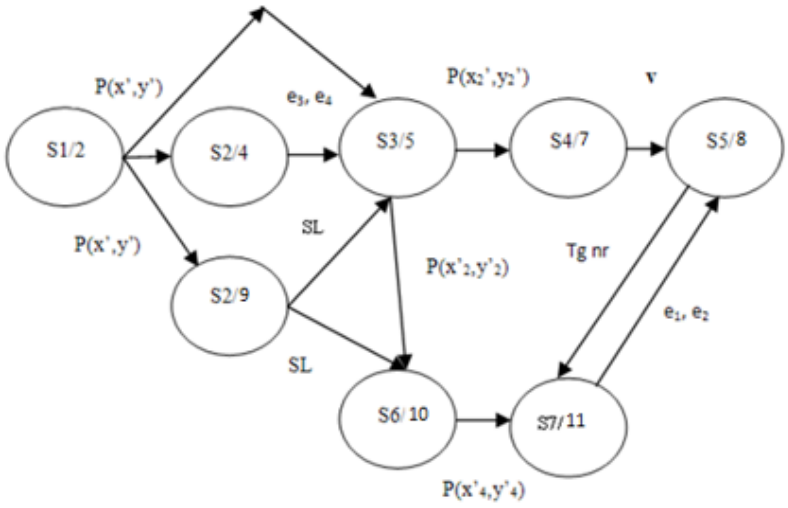

b)

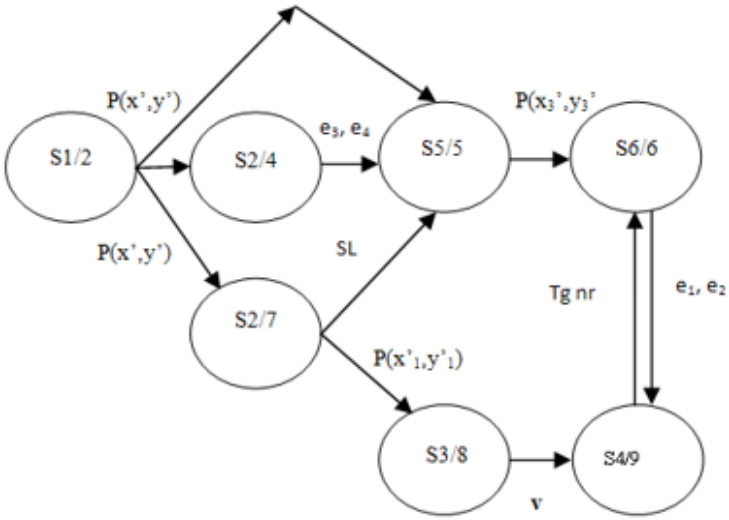

c)

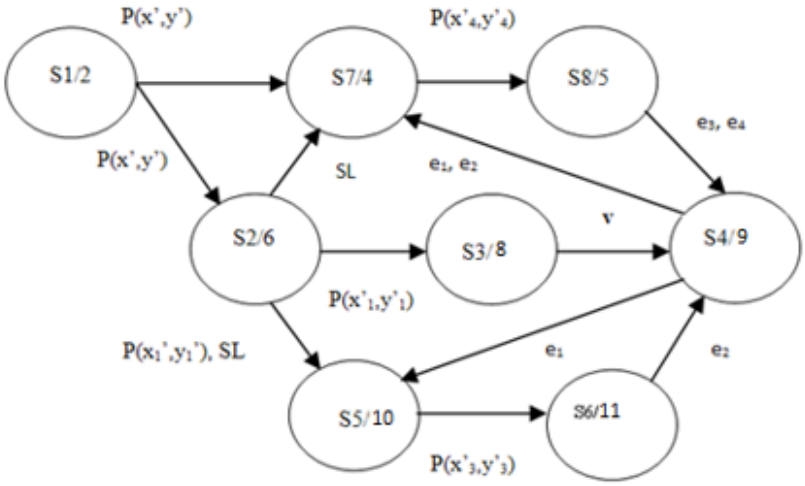

d)

Figure 4. The models of data processing flow in the systems: a) TRS1; b) TRS2; c) TRS3; d) TRS4.

SL of function P(x',y') calculation; S3/8 - the operation of chord transformation performing in the processor 8 and a feature vector **v** of the target calculation; S4/9 - the target classification in the processor 9; S5/5 - the target's image (function P(x',y')) normalization on parameters e_1 and e_2 in the processor 5 and conversion to a log-polar coordinate system; S6/6 - the target's scale e_1 and rotation e_2 determination in the processor 6. The model MD3 of data processing flow in the system is presented in Figure 4 c.

6.4. Model of data processing flow in the system TRS4

The stages of data processing in TRS4 can be formulated taking into account the respective functioning description (section 5), as follow. Stage S1/2 – target's image input and preprocessing in processor 2; S2/6 - the Fourier spectrum of the target's image formation in processor 6, the maximum frequency f_m and the complexity SL of image P(x',y') determination; S3/8 - the operation of chord transformation performing in the processor 8 and a vector **v** of the target's features calculation; S4/9 - the target classification in the processor 9 and determination of the target's scale e_1; S5/10 - the target's image spectrum (function $P(x'_1, y'_1)$) normalization on scale e_1 in the processor 10 and transformation to a polar coordinate system; S6/11 - the target's angular position e_2 calculation in the processing

unit 10; S7/4 – target's image normalization on parameters e_1 and e_2 in the processor 11; S8/5 – the target position in-plane (coordinates e_3, e_4) calculation in the processing unit 5. The model MD4 of data processing flow in this system is presented in Figure 4d.

7. Estimation of systems' data processing time and throughput

7.1. Determination of the processing time of the operations, realized in the systems

Let's determine the processing time of the operations, realized in the systems as follows. t_{PP} – the time of the target's image input and preprocessing, t_{PP} =6.6μs [9]; t_F – the total time of the operations: Fourier transform, and parameters f_m and SL calculation, t_F =4.24μs [14]; t_P - the time of the target's position in plane determination (parameters e_3, e_4), t_P =1.01μs [10]; t_{CT} – the time of the chord transformation of the centered target's image, t_{CT} =0.2μs [13]; t_{CT1} – the time of the chord transformation of the target's image Fourier spectrum, t_{CT}=t_{CT1}=0.2μs; t_S – the time of the target's scale e_1 calculation, t_S =0.04μs [11]; t_R – the time of the target's rotation e_2 calculation, t_R =53.7ms [15]; t_{SR} - the time of the target's scale e_1 and rotation e_2 determination in one step, t_{SR}=5.1+5.15N, μs [11]; t_C – the time of the target classification, t_C =(m_k -1)[DP(t_y+t_a)], where m_k is the number of the classes' targets; DP is the length of the target's image feature vector **v**; t_y, t_a - the multiplication and adding time, respectively [16]; t_{N0} – the time of the target's image normalization (centering) on values e_3, e_4; t_{N1} - the time of the target's image normalization on e_1 and transformation to a polar coordinate system; t_{N2} – the time of the target's image transformation to the log-polar coordinate system; t_{N3} – the time of the target's image normalization (centering) on parameters e_3, e_4 via Fourier spectrum calculation, t_{N3}=t_F=4.24μs; t_{N4} - the time of the target's image normalization (centering) on parameters e_3, e_4 and transformation to a log-polar coordinate system; t_{N5} - the time of the target's image spectrum normalization on e_1 and transformation to a polar coordinate system, t_{N5}=t_{N1}; t_{N6} - the time of the target's image normalization on data of e_1, e_2.

The values of parameters t_{N0} - t_{N6} can be determined as [12]: t_{Ni} = 14.2+α^2 N^2(t_{ep}+βt_{tpi}), where i=0÷6; the parameter α determine the complexity of the target's image; N – the total number of the target's image pixels in a row (colon); β – characterize the share of most informative pixels in the image; t_{ep} - time of the pixel's extracting from the target's image; t_{tpi} - time of the pixel's coordinates transformation. The data of parameters t_{tpi} will depend on the operation's kind realized, as follows: t_{tp0}=2t_a, t_{tp1}=t_{tp5}=t_a+4t_y+2t_f, t_{tp2}=t_a+3t_y+2t_f, t_{tp4}=3t_a+4t_y+2t_f, and t_{tp6}=2t_a+6t_y+2t_f, where t_a, t_y, and t_f are the times of adding, multiplication, and function calculation, respectively. The estimation of the data processing time and throughput of the systems was made for next values of the parameters: N=256, DP=180, m_k=10, α=0.5, β=0.1, G=NxN, t_{ep}=0.015μs, t_a=0.02μs, t_y=0.04μs, t_f=0.05μs. At these data, t_{SR}=1.3ms, t_C =97.2μs, t_{N0} =325.5μs, t_{N1}=718.7μs, t_{N2}=653.2μs, t_{N4}=784.2μs, t_{N6}=882.6μs

7.2. Estimation of the data processing time and throughput of the system TRS1

The system TRS1 data processing time will be determined in accordance with its functioning algorithm described in sections 2 and 6.1: T_{S1}=$t_{S1/2}$+max{$t_{S2/4}$,$t_{S2/9}$}+$t_{S3/5}$ +$t_{S4/7}$+$t_{S5/8}$+$t_{S6/8}$+$t_{S7/10}$+$t_{S8/11}$, were $t_{Si/j}$ is the time of the data processing on stage i in the processor j. The values of $t_{Si/j}$ will be determined as follows (section 7.1): $t_{S1/2}$=t_{PP}=6.6μs, $t_{S2/4}$=t_P=1.01μs, $t_{S2/9}$=t_F=4.24μs, $t_{S3/5}$=t_{N0}=325.5μs, $t_{S4/7}$=t_{CT}=0.2μs, $t_{S5/8}$=t_C=97.2μs, $t_{S6/8}$=t_S=0.04μs, $t_{S7/10}$= t_{N1}=718.7μs, $t_{S8/11}$=t_R=53.7ms. Taking into account that $t_{S2/8}$>$t_{S2/4}$,

$$T_{S1}=t_{S1/2}+t_{S2/9}+t_{S3/5}+t_{S4/7}+t_{S5/8}+t_{S6/8}+t_{S7/10}+t_{S8/11}=54.85\text{ms}. \quad (24)$$

The throughput of the system TRS1 will be $TP_{S1}=TIC/max\{t_{Si/j}\}$, where TIC is the target's image capacity. At TIC=256x256x8=524288 bits and $max\{t_{Si/j}\}=t_{S8/11}=53.7ms$, the processing time $TP_{S1}=9.7x10^6$ bits/sec. Figure 5 a. show, that the processing time on stage S8/11 is much bigger than on other stages, and the system is not optimal from the throughput point of view.

Obtaining an optimal system can be made by reducing the processing time on the stage S8/11 until the processing time on stages S7/10, at least, by changing the processors, implementing supplementary parallelism, etc. [17]. At the $t'_{S8/11}=t_{S7/10}$, the throughput of the modified system will increase up to $TP'_{S1}=729.5x10^6$ bits/sec, or, on $k_{S1}=TP'_{S1}/TP_{S1}=75$ times. The data processing time in the optimized system is estimated as:

$$T'_{S1}=t_{S1/2}+t_{S2/9}+t_{S3/5}+t_{S4/7}+t_{S5/8}+t_{S6/8}+2t_{S7/10}=1.87ms, \quad (25)$$

or, on $W_{S1}=T_{S1}/T'_{S1}=29.3$ times smaller than in the initial system.

7.3. Estimation of the data processing time and throughput of the system TRS2

The data processing time in the system TRS2 will be appreciated as: $T_{S2}=t_{S1/2}+max\{t_{S2/4},t_{S2/9}\}+t_{S3/5}+max\{\{t_{S4/7}+t_{S5/8}\},t_{S6/10}\}+t_{S7/11}$. The values of $t_{Si/j}$ will be estimated as (sections 6.2 and 7.1)): $t_{S1/2}=t_{PP}=6.6\mu s$, $t_{S2/4}=t_P=1.01\mu s$, $t_{S2/9}=t_F=4.24\mu s$, $t_{S3/5}=t_{N0}=325.5\mu s$, $t_{S4/7}=t_{CT}=0.2\mu s$, $t_{S5/8}=t_C=97.2\mu s$, $t_{S6/10}=t_{N2}=653.2\mu s$, $t_{S7/11}=t_{SR}=1.3ms$. Taking into account that $t_{S2/9}>t_{S2/4}$ and $t_{S6/10}>\{t_{S4/7}+t_{S5/8}\}$,

$$T_{S2}=t_{S1/2}+t_{S2/9}+t_{S3/5}+t_{S6/10}+t_{S7/11}=2.29ms. \quad (26)$$

The throughput of the system TRS2 will be evaluated as $TP_{S2}=TIC/max\{t_{Si/j}\}=403.3x10^6$ bits/sec. From Figure 5b is evident, that the processing time on stage S7/11 is much bigger than on other stages, and the system is not optimal.

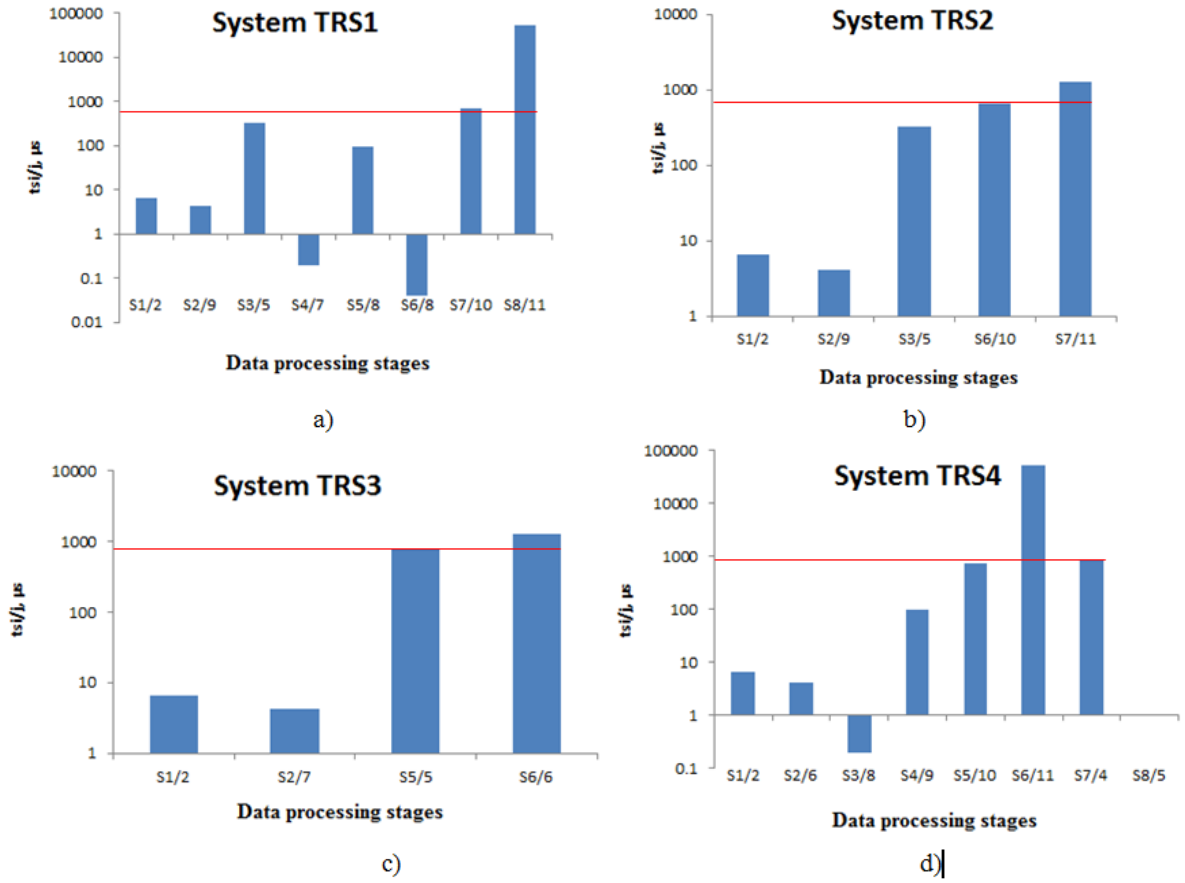

Figure 5. Processing time on different stages in the systems: a) TRS1; b) TRS2; c) TRS3; d) TRS4.

The enhancing of the system's characteristics is possible by reducing the processing time on stage S7/11 until the time on stage S6/10. At the $t'_{S7/11}=t_{S6/10}$, the throughput of the modified system will increase up to $TP'_{S2}=802.6x10^6$ bits/sec, or, on $k_{S2}=TP'_{S2}/TP_{S2}=2$ times. In this case, the data processing time will be:

$$T'_{S2}=t_{S1/2}+t_{S2/9}+t_{S3/5}+2t_{S6/10}=1.64ms, \quad (27)$$

or, on $W_{S2}=T_{S2}/T'_{S2}=1.4$ times less than in the initial system.

7.4. Estimation of the data processing time and throughput of the system TRS3

The data processing time in the system TRS3 can be determined as: $T_{S3}=t_{S1/2}+\max\{t_{S2/4},t_{S2/7}\}+\max\{\{t_{S3/8}+t_{S4/9}\}, t_{S5/5}\}+t_{S6/6}$.

The values of $t_{Si/j}$ will be estimated in the next mode: $t_{S1/2}=t_{PP}=6.6\mu s$, $t_{S2/4}=t_P=1.01\mu s$, $t_{S2/7}=t_F=4.24\mu s$, $t_{S3/8}=t_{CT}=0.2\mu s$, $t_{S4/9}=t_C=97.2\mu s$, $t_{S5/5}=t_{N4}=784.2\mu s$, $t_{S6/6}=t_{SR}=1.3ms$. Taking into account that $t_{S2/7}> t_{S2/4}$, and $t_{S5/5}>\{t_{S3/8}+t_{S4/9}\}$,

$$T_{S3}=t_{S1/2}+t_{S2/7}+ t_{S5/5}+t_{S6/6}=2.09ms. \quad (28)$$

The throughput of the system TRS3 will be evaluated as $TP_{S3}=TIC/\max\{t_{Si/j}\}=403.3x10^6$ bits/sec. From Figure 5c is evident, that the highest processing time in the system is on stage S6/6.

The optimization of the system is possible by reducing the processing time in this stage until stage S5/5. At the $t'_{S6/6}=t_{S5/5}$, the throughput of the modified system will increase up to $TP'_{S3}=668.5x10^6$bits/sec, or, on $k_{S3}=TP'_{S3}/TP_{S3}=1.66$ times. In this case, the processing time in the system will be:

$$T'_{S3}=t_{S1/2}+t_{S2/7}+2t_{S5/5}=1.58ms, \quad (29)$$

or, on $W_{S3}=T_{S3}/T'_{S3}=1.3$ times smaller than in the initial system.

7.5. Estimation of the data processing time and throughput of the system TRS4

The data processing time in the system TRS4 can be estimated as: $T_{S4}=t_{S1/2}+t_{S2/6}+t_{S3/8}+t_{S4/9}+t_{S5/10}+t_{S6/11}+t_{S7/4}+t_{S8/5}$.

The values of $t_{Si/j}$ will be determined as: $t_{S1/2}=t_{PP}=6.6\mu s$, $t_{S2/6}=t_F=4.24\mu s$, $t_{S3/8}=t_{CT}=0.2\mu s$, $t_{S4/9}=t_C=97.2\mu s$, $t_{S5/10}=t_{N5}=718.7\mu s$, $t_{S6/11}=t_R=53.7ms$, $t_{S7/4}= t_{N6}=882.6\mu s$, $t_{S8/5}=t_P=1.01\mu s$. For these data,

$$T_{S4}=t_{S1/2}+t_{S2/6}+t_{S3/8}+t_{S4/9}+t_{S5/10}+t_{S6/11}+ t_{S7/4}+t_{S8/5}=55.41ms. \quad (30)$$

The throughput of the system TRS4 will be estimated as $TP_{S4}=TIC/\max\{t_{Si/j}\}=9.7x10^6$ bits/sec. From Figure 5d is possible to conclude that the bigger processing time is on stage S6/11. The system throughput increasing is possible by reducing the processing time on this stage until stage S7/4.

At the $t'_{S6/11}=t_{S7/4}$, the throughput of the modified system will increase up to $TP'_{S4}=594x10^6$ bits/sec, or, on $k_{S4}=TP'_{S4}/TP_{S4}=61.2$ times. The data processing time in the optimized system will be:

$$T'_{S4}=t_{S1/2}+t_{S2/6}+t_{S3/8}+t_{S4/9}+t_{S5/10}+2t_{S7/4}+t_{S8/5}=2.59ms, \quad (31)$$

or, on $W_{S4}=T_{S4}/T'_{S4}=21.4$ times smaller than in the initial system.

7.6. Comparative analysis of the data processing time and throughput of the systems

The data regarding processing time and throughput of the elaborated initial and optimized systems are presented in Table 1 and Figures 6a, 6c and show the following.

The initial system TRS3 is characterized by a minimal processing time, T_{S3}=2.09ms. The processing time in the system TRS2 is small bigger, T_{S2}=2.29ms, or, in 1.1 times (Figure 6b). This time is much bigger in the system TRS1, T_{S1}=54,9ms (26.3 times), and in the system TRS4, T_{S4}=55.4ms (26.5 times).

Respectively, the throughput of the systems TRS2 and TRS3 is higher 41.5 times than that of the systems TRS1 and TRS4 (Figure 6d).

Table 1

The data of the initial and optimized systems

	TRS1	TRS2	TRS3	TRS4	TRS1´	TRS2´	TRS3´	TRS4´
Processing Time T_s, ms	54,9	2,29	2,09	55,41	1,87	1,64	1,58	2,59
Throughput TP_s, Mbs	9,7	403,3	403,3	9,7	729,5	802,6	668,5	594,0
$W_s=T_s/T'_s$	29,3	1,4	1,3	21,4				
$K_s=TP'_s/TP_S$					75,0	2,0	1,7	61,2

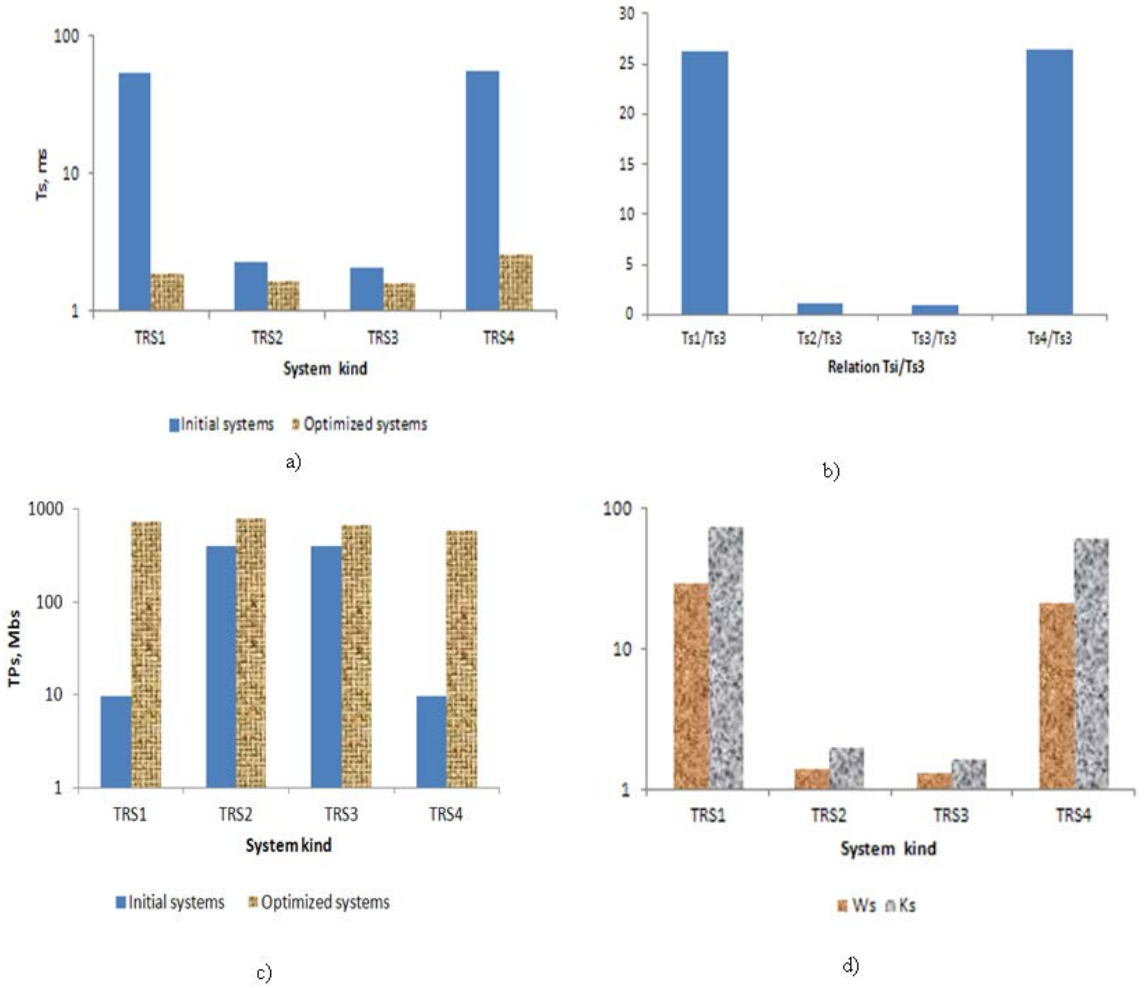

Figure 6. The data of the initial and optimized systems: a) – processing time; b) - relation T_{Si}/T_{S3}; c) – throughput; d) - effectiveness of the optimized systems in time – W_s, and productivity - K_s in comparison with initial systems.

Optimization permitted to decrease the processing time in the systems from 1.3 (system TRS3') until 29.3 times (system TRS1') and to increase the throughput of the systems from 1.7 (system TRS3') to 75 times (system TRS1').

The biggest optimization effect is referred to in the systems TRS3' and TRS4'. These systems are characterized by the very close processing time and throughput and can be effectively used in target recognition.

Conclusions

There were elaborated the structures of the four new specialized multiprocessor functional distributed systems, destinated for targets recognition and calculation of their position, scale, and rotation. The systems represent a combination of electronic and optical processing modules. The principles of their functioning are described.

The graphical models of data processing flow in the proposed systems are designed. The calculation of the processing time of the different operations, realized in the systems was made. The estimation of the data processing time and throughput of the systems' was done, based on the results of which the optimization of the proposed systems was made.

A comparative analysis of the data processing time and throughput of the systems was made which shows the following. The system TRS3 is characterized by a minimal processing time, T_{S3}=2.09ms. The processing time in the system TRS2 is small bigger, T_{S2}=2.29ms, or, 1.1 times. This time is much bigger in the system TRS1, T_{S1}=54,9ms (26.3 times), and in the system TRS4, T_{S4}=55.4ms (26.5 times). Respectively, the throughput of the systems TRS2 and TRS3 is higher 41.5 times than that of the systems TRS1 and TRS4.

Optimization permitted to decrease the processing time in the systems from 1.3 (TRS3') to 29.3 times (TRS1') and to increase the throughput of the systems from 1.7 (TRS3') to 75 times (TRS1'). The biggest optimization effect is obtained in the systems TRS3' and TRS4'. These systems are characterized by the very close processing time and throughput and can be effectively used in target recognition.

References

1. Haley J., Tucker J., Kessler B., Fish T. Bridging the gap from academia to application: rapid algorithm design and deployment for artificial intelligence (RADD-AI). Proc. SPIE 11870, Artificial Intelligence and Machine Learning in Defense Applications III, 118700A, 2021. DOI: 10.1117/12.2601858
2. Xie W., Ide J., Izadi D. at all. Multi-object tracking with deep learning ensemble for unmanned aerial system applications. Proc. SPIE 11870, Artificial Intelligence and Machine Learning in Defense Applications III, 118700I, 2021. DOI: 10.1117/12.2600209
3. Mediavilla C., Nans L., Marez D., Parameswaran S. Detecting aerial objects: drones, birds, and helicopters. Proc. SPIE 11870, Artificial Intelligence and Machine Learning in Defense Applications III, 118700J, 2021. DOI: 10.1117/12.2600068
4. Hollander R., Rooij S., Broek S. et all. Vessel classification for naval operations. Proc. SPIE 11870, Artificial Intelligence and Machine Learning in Defense Applications III, 118700N, 2021. DOI: 10.1117/12.2599513
5. Dominicis L., Bouma H., Toivonen S. et all. Video-based fusion of multiple detectors to counter-terrorism. Proc. SPIE 11869, Counterterrorism, Crime Fighting, Forensics, and Surveillance Technologies V, 118690J, 2021. DOI: 10.1117/12.2598147.
6. Kechagias-Stamatis O., Aouf N. Automatic Target Recognition on Synthetic Aperture Radar Imagery: A Survey. Computer Vision and Pattern Recognition, Dec 2020, pp.1-21. https://arxiv.org/abs/2007.02106.
7. Shu C., Sun L. Automatic target recognition method for multi-temporal remote sensing image. Open Physics, 2020, Volume 18 Issue 1, pp.170-181. https://doi.org/10.1515/phys-2020-0015.
8. Perju V. Methods of target recognition based on central image chord transformation. Journal of Engineering Science Vol. XXVIII, no. 4 (2021), pp. 52 - 62. ISSN 2587-3474/ eISSN 2587-3482. . https://doi.org/10.52326/jes.utm.2021.28(4).05.

9. Perju V., Casasent D. Optical-electronic multiprocessors computer systems controlled by input images parameters. In Optical Pattern Recognition XVI. David P. Casasent, Tien-Hsin Chao, Editors. Proc. SPIE 5816, pp. 306-314 (2005).
10. Perju V., Saranciuc D. et all. The operative analysis of the correlation fields in the optical processors. //Proc. of International Conference on Microelectronics and Computer Science ICMCS-97, 1997, Vol.2, pp.192-196, Chisinau, Republic of Moldova.
11. Perju V., Casasent D. Optical multichannel correlators for high-speed targets detection, recognition, and localization. In: Proc. SPIE 8398, 2012.
12. Perju V. The method of adaptive image coordinate transformation. In: Proc. SPIE 1978, pp. 280-288, 1993.
13. Perju V., Cojuhari V. Central and logarithmic central image chord transformations for invariant object recognition. In: Journal of Engineering Science. 2021, Vol. XXVIII, no. 1 (2021), pp. 38 - 46 ISSN 2587-3474/E-ISSN 2587-3482. https://doi.org/10.52326/jes.utm.2021.28(1).03.
14. Perju V., Casasent D. The investigation of the Fourier spectrum-based image complexity metrics for recognition applications. In: Proc. SPIE 8398, 2012. [21, JES]
15. Katys G., Perju V., Rotary S. *Methods and computer means of image processing*. Shtiintsa, Kishinev, 1991.
16. Perju V. Target recognition based on central and logarithmic central image chord transformations. Journal of Engineering Science. 2021, Vol. XXVIII, no. 2 (2021), pp. 44 – 52. ISSN 2587-3474/E-ISSN 2587-3482. https://doi.org/10.52326/jes.utm.2021.28(2).03
17. Perju V. Adaptive high-speed targets recognition systems controlled by the image's parameters. Proc. SPIE 11400, Pattern Recognition and Tracking XXXI, 114000S; 2020, DOI: 10.1117/12.2559616.

Journal of Engineering Science *Vol. XXIX, no. 1 (2022), pp. 86 - 96*
Fascicle *Electronics and Computer Science* *ISSN 2587-3474*
Topic *Electronics and Communication* *eISSN 2587-3482*

https://doi.org/10.52326/jes.utm.2022.29(1).07
CZU 614.8.084

ELABORATION AND APPLICATION OF GRAPHICAL MODELS TO OPTIMIZE THE RESPONSE TIME TO EMERGENCY SITUATIONS

Serghei Peancovschii*, ORCID: 0000-0002-7414-1127

Free International University of Moldova, 52 Vlaicu Pârcălab Str., Chisinau, Republic of Moldova
General Inspectorate of Emergency Situations of the Republic of Moldova,
*Corresponding author: Serghei Peancovschii, *an_stern@hotmail.com*

Received: 01. 21. 2022
Accepted: 02. 22. 2022

Abstract. This article presents methods for timing the key milestones and timing of the emergency response. A graphic model is proposed that allows you to determine the stage and time of the response process, regardless of the nature of the ongoing processes manifestation. The model allows a detailed analysis the process effectiveness of responding to various emergencies. And it also allows to determine the boundaries of responsibility areas to optimize management decisions of the response process, increasing its quantitative and qualitative values. The presented mathematical models exclude errors in assessing the effectiveness of the response. The developed mathematical apparatus can be used for effective management of emergency response units.

Keywords: *decision making, safety, timing, emergency situations, areas of responsibility, emergency response.*

Rezumat Articolul prezintă metode de cronometrare a reperelor cheie și de sincronizare a răspunsului în caz de urgență. Este propus un model grafic care permite determinarea stadiului și timpului procesului de răspuns, indiferent de natura manifestării proceselor în derulare. Modelul permite o analiză detaliată a eficacității procesului de răspuns la diverse situații de urgență. Și, de asemenea, să determine limitele domeniilor de responsabilitate pentru a optimiza deciziile de management ale procesului de răspuns, sporind valorile cantitative și calitative ale acestuia. Modelele matematice prezentate exclud erorile în evaluarea eficacității răspunsului. Aparatul matematic dezvoltat poate fi utilizat pentru gestionarea eficientă a unităților de răspuns la urgențe.

Cuvinte cheie: *luarea deciziilor, siguranță, sincronizare, situații de urgență, domenii de responsabilitate, răspuns în caz de urgență.*

Introduction

The statistics of recent years indicate an increase in natural and man-made phenomena and disasters (Figure 1). As a result, there is a steady dynamics of an increase in the number of human victims and material losses. All this leads to the economic weakening

of the affected territories, thereby significantly reducing the values of the economic indicators of the development of certain states.

At the initial stage of occurrence, each emergency situation proceeds purely individually, in view of many internal characteristics and external factors, in conditions of complete uncertainty [1, 2]. To conduct successful missions, it is necessary to define a set of qualitative and quantitative indicators, to develop a set of monitored and measurable indicators, with the help of which it is possible to standardize and optimize the processes of responding to emergency incidents.

This article proposes to consider the key points of response to determine effective time intervals that allow to assess qualitatively the actions of each participant in the process. The formation of the content of the material presented is based on the works [3 – 7]. Various stages of the response process of specialized emergency teams, focused on individual emergency situations, are described in detail.

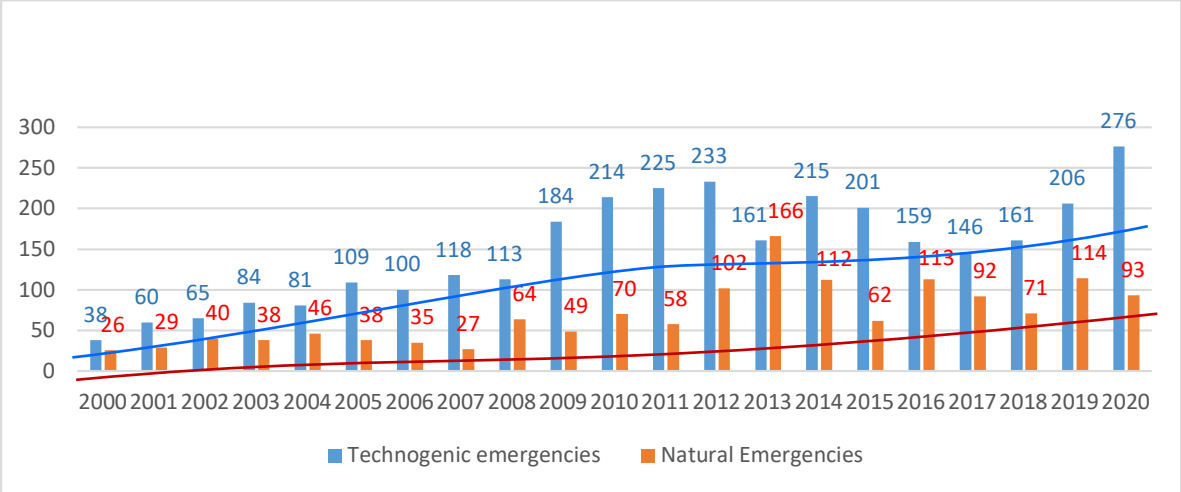

Figure 1. Graphical model of statistics of data on the growth of man-made and natural emergencies in quantitative terms that occurred in the Republic of Moldova.

It is also necessary to bear in mind that structural units, endowed with various functions, interact in the time interval. To improve the quality of management decisions, it is necessary to determine the exact boundary of the areas of responsibility of these services [8, 9]. The model proposed in this article will improve the efficiency and quality of the decision made and, as a result, reduce the response time to sudden processes.

1. The essence and content of the emergency response process.

As a rule, the response process begins with the receipt of information in a specialized subdivision, which includes dispatching subdivisions of enterprises and specialized services. At the state level, such a unit is the Unified National Emergency Call Service 112. The process ends when the last rescue team departs.

The size of the duration of the time period of the process is set based on the difference between the start time and the end time of the response.

$$T_r = t_f - t_s \tag{1}$$

where:

T_r – response time

T_s – response start time

T_f – response end time

The usage of only the given two time parameters does not allow to fully assess the level of effectiveness of actions taking place within the response stage.

The effected analysis of the ongoing events made it possible to divide the responders into the following four groups, as well as to highlight the main functions they are responsible for.

1) A group of participants that generates information provision. These include victims, witnesses of emergencies or specialized devices that record physical deviations of the ongoing processes.

2) Personnel responsible for receiving, validating and registering incoming information with subsequent transfer to a specialized dispatch service. This group includes operators of the Unified National Emergency Call Service 112.

3) Personnel for dispatching the response forces and means, organizing the arrival to the scene of the incident, with the subsequent technical and informational support of these forces. The group consists of dispatchers of various emergency response services.

4) Forces of emergency response, which include - any resources with their own individual response means and specialized capabilities subordinate to their dispatching services.

This division was carried out on the basis of the need for a clear delineation of areas of functional responsibility. Figure 2 visually reflects the sequence of linear interactions of the above four groups involved in the emergency response process. The vertical lines delineate the limits of the areas of responsibility. The participants of the third and fourth groups are in constant interaction until the completion of the response mission (Figure 2).

It should be noted that in the Republic of Moldova three main groups are constantly involved in the response process: 1) 112 service operators; 2) dispatchers of three emergency services (rescuers and firefighters, police officers, ambulance); 3) response forces related to emergency response services.

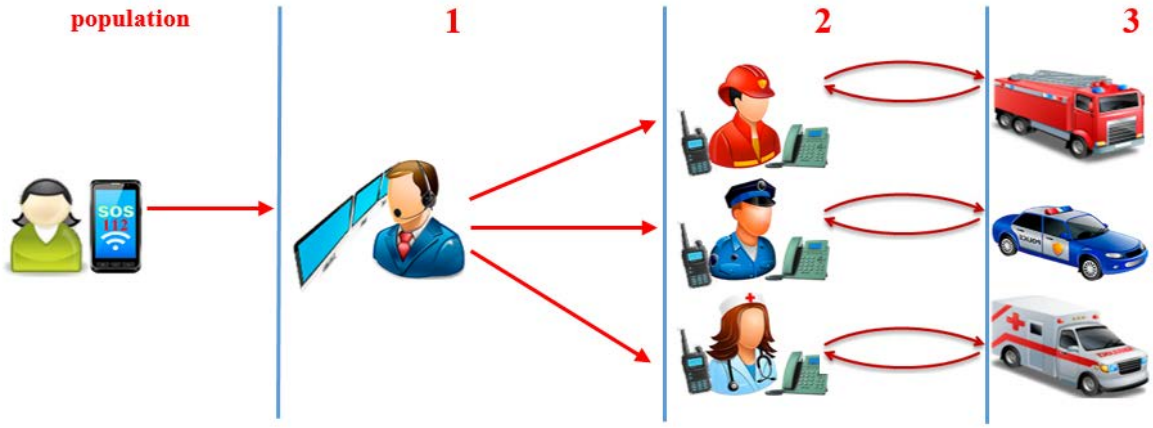

Figure 2. A graphical model of the sequence of interaction of participants in a unified emergency response process.

In the presented model, the beginning of each significant event is considered to be a time value determined by a spatial point in time with which a specific trigger is associated. The beginning of the next action is the moment of completion of the previous one. The interval between two spatial time points allows you to determine the period of time spent performing a particular action.

Any response to emergencies or their consequences begins with dialing the emergency call number, after which the operator 112 receives the call, then there is a dialogue between the operator and the caller. At this stage, the operator performs the function of validating the incoming information, on the basis of which the area of responsibility between the named participants is delineated. If the validation is successful, the operator interviewing the caller creates and fills out an incident card, then the latter provides it to the appropriate emergency response service.

As soon as the dispatcher of the emergency response service received the card about the incident from the operator 112, at this time moment the zone of responsibility for the ongoing processes is delineated between the latter. Based on the information received, the dispatcher decides what forces and means to send for the successful completion of the mission.

The stage of transferring the mission begins, which includes actions, dialing (dialing a phone number in order to establish communication) to the selected forces and transferring the response mission. At this stage, the area of responsibility is transferred to the emergency response forces at the moment the dispatcher receives confirmation of receipt of the transmitted information from the latter.

It is important to emphasize that at this stage the value of the time period directly depends on the following factors: a) the stability (reliability) of communication systems, b) the promptness (speed) of the response of the emergency response forces to the incoming call, c) the brevity and accuracy of the presentation of the content of the transmitted information by the dispatcher, as well as its perception and understanding by the emergency response team.

At the initial stage of the transfer of the mission, it is enough to transfer only two basic triggers:

1) where to go, that is, the address of the object or geographic territorial coordinates;

2) what kind of emergency or incident needs to be responded to.

This bundle of triggers allows you to instantly activate the next stage - collecting on alarm, and additional information can be received at the stage of moving to the scene.

It should be borne in mind that outside the emergency mode, members of the emergency response team are not in the same room at the same time, but perform various tasks (training, chores, personal hygiene, etc.).

Therefore, this time period is necessary to analyze the actions of the persons involved in the response, in order to determine how quickly they will go to the scene of the incident. The moment the rescue team gets into the vehicle and starts moving towards the scene of the incident, it is necessary to record this event of the control time point.

In the future, the same emergency response team is obliged to report to its control center the time points indicating the evolution of events such as arrival at the scene of an emergency, localization (this factor applies only to fires and situations of chemical leakage), completion of rescue operations, leaving the place of work, readiness to fulfill new missions.

These indicators of temporary control points allow the dispatcher or decision-maker to ensure an appropriate level of response safety, timely provide technical support to the emergency response leader, and also understand at what time stage the response process is.

The accumulated experience of the Republic of Moldova, as well as the results of the analysis of foreign activities, indicate that for a more detailed mastery of the current situation, it is necessary to divide the stage of the response process into 11 intermediate time stages, which are part of the twelve temporary control points of the response.

The stages, in turn, are combined into the following three time phases.

1) The phase of the reaction time of specialized services to emergency calls from citizens. This includes the reaction period between the time the first call is received by the emergency operator and the time the first emergency response crew arrives at the scene of the emergency. In this interval, all time characteristics are subject to mandatory fixation and standardization.

2) The phase of the time of the rescue operations. For this period of time, the values are fixed, but not standardized, in view of the pronounced specificity of the ongoing processes.

3) The phase of the time of returning to the base or determining the moment of readiness to continue serving. The data from this phase allows the dispatcher to determine which emergency response forces are available for the following missions.

For optimal tracking of the ongoing emergency response processes, a universal timeline of control points has been developed and used, shown in Figure 3.

2. Development and application of a scale of control points at the stages of a unified emergency response process.

The named scale provides the following composition, content and sequence of the control points of the stages of response to emergency situations.

Point 1 - dialing the emergency call number. It represents the so-called zerotime point when the subscriber starts calling the emergency service. The unique emergency call number in the Republic of Moldova is 112. From this point, the operator's response time begins, which ends at the moment of fixing the second checkpoint. At this stage, the response time of the operator of the 112 service is recorded, which determines the speed of the call addressed to emergency services, while simultaneously controlling the quality of the reliability of the communication equipment and the promptness of the operator's response to the call. Indicated as the $t_{\text{operator's answer}}$

Point 2 - Receiving a call from the operator of the service 112. Between points 2 and 3, the parameter $t_{\text{interview}}$ is entered - fixing the working time of the operator of the service 112 to collect information about the incident, filling out an emergency response card and transferring the latter to a specialized dispatch service.

Point 3 - Sending an emergency card to the dispatcher's room. This time point is given a special attention, since it contains the moment of transition of zones of responsibility and the zone of responsibility of service 112 ends, and the process goes to the emergency response **dispatcher's** room. Between points 3 and 4, the parameter $t_{\text{dispatcher response}}$ is entered. It comes down to recording the time spent on opening an emergency card, monitoring the quality and reliability of the software, network equipment and the actions of the dispatcher.

Point 4 - Opening of the emergency card by the dispatcher. Between points 4 and 5, a $t_{decision\text{-}making}$ parameter is introduced, which boils down to identifying the time of the dispatcher's true understanding of which emergency it is necessary to respond to and which unit will be sent to perform the assigned task.

Point 5 - Selection of reaction forces (S). Between points 5 and 6, the parameter $t_{transfer\text{-}mission}$ is entered, on the basis of which the time spent by the dispatcher to make a call to the emergency response unit, activate the alarm, transmit a message about the type of emergency and the address is calculated.

Point 6 - Confirmation (C). It is activated from the moment the dispatcher receives confirmation of the upcoming mission from the response team. This temporary point also has an important role, as it provides for the transfer of the area of responsibility from the dispatch service and the emergency response forces.

Between points 6 and 7, the $t_{collection}$ parameter is entered, which consists of calculating the collection time for an emergency response unit, the time for putting on specialized uniforms, and the time for the rescue team to get into the car.

Point 7 - Departure (D). The time of departure is fixed, i.e. the beginning of the movement of the vehicle with the crew to carry out an emergency response mission.

Between points 7 and 8, the parameter $t_{en\ road}$ is introduced, which is reduced to calculating the time stage of finding the combat response units on the way to the scene of the incident.

Point 8 - Arrival at the scene (A). At this time point, the standardization of time indicators ends. The stage of immediate response to an emergency begins.

Between points 8 and 9, the $t_{localization}$ parameter is introduced, which consists of calculating the time stage spent on localization. As a rule, this parameter is used mainly in response to a fire, in other cases of response is not used.

Point 9 - Localization of fire (LZ). The point fixes the moment of termination of the further spread of combustion and the creation of conditions for its elimination with the available forces and means.

Between points 8 and 10, the $t_{liquidation}$ parameter is introduced, which consists of calculating the time stage spent on carrying out all the necessary work to eliminate the emergency at the response stage.

Point 10 - Liquidation (L). It records the end time of all rescue operations.

Between points 10 and 11, the parameter $t_{of\ equipment\ collection}$ is introduced, which consists of calculating the time step spent on collecting all the equipment used, the time for the rescue team to get into the car.

Point 11 - Return (R). The starting point for the return of the emergency response forces to the place of deployment.

Between steps 11 and 12, the parameter is entered to $t_{return\ to\ base}$ for calculating the time spent on the way back to the place of deployment, refueling, if necessary, with fuel, water, and completing the missing equipment. As practice shows, the maximum time of this stage is equal to twice the travel time to the scene.

$\text{Max } t_{return\ to\ base} = 2 * t_{\ on\ the\ way}$

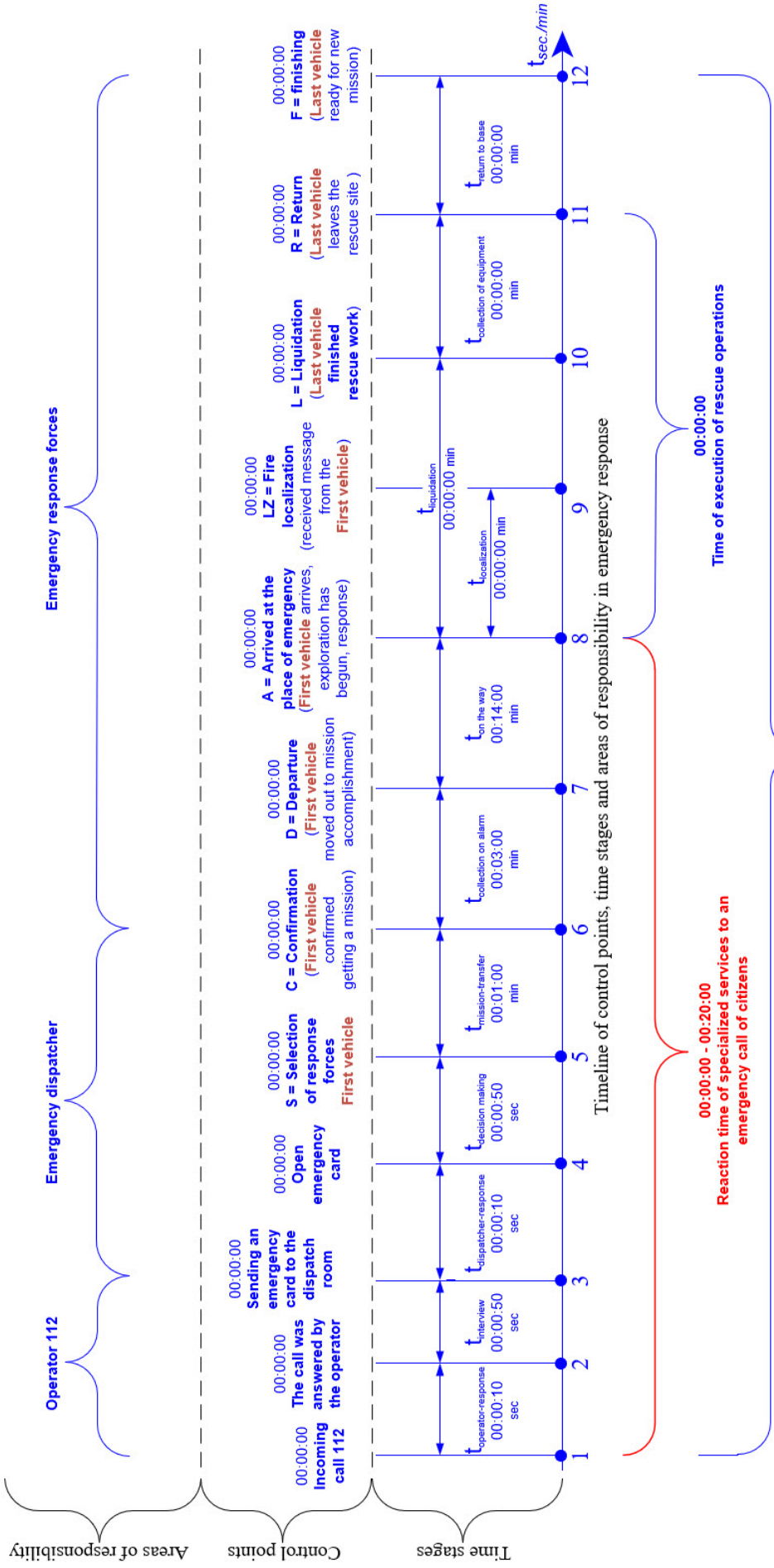

Figure 3. Graphical model of the response time to emergency calls.

Point 12 - Finishing (F). It is activated when the dispatcher receives a corresponding message from the response team. This message completes the process of splitting the response phases in time, assuming that the vehicle is complete, fueled and the rescue team is ready for new response missions.

Based on the developed composition of response time points and the sequence of their implementation, the volume of the total response time is determined by the following formula:

$$T_r = (t_2 - t_1) + (t_3 - t_2) + (t_4 - t_3) + (t_5 - t_4) + (t_6 - t_5) + (t_7 - t_6) + (t_8 - t_7) + (t_9 - t_8) + (t_{10} - t_9) + (t_{11} - t_{10}) + (t_{12} - t_{11}) \quad (2)$$

or

$$T_r = \sum_{n=1}^{12}(t_n - t_{n-1}) \quad (3)$$

where **n** - is the number of response checkpoints.

Below there are given the calculation formulas for all intermediate stages of the response time.

$$t_{operator's\ answer}\ (t_o) = (t_2\text{-}t_1) \quad (4)$$

$$t_{interview}\ (t_i) = (t_3\text{-}t_2) \quad (5)$$

$$t_{dispatcher\ response}\ (t_d) = (t_4\text{-}t_3) \quad (6)$$

$$t_{decision\text{-}making}\ (t_{dm}) = (t_5\text{-}t_4) \quad (7)$$

$$t_{transfer\text{-}mission}\ (t_{tm}) = (t_6\text{-}t_5) \quad (8)$$

$$t_{collectoin\ on\ alarm}\ (t_a) = (t_7\text{-}t_6) \quad (9)$$

$$t_{on\ the\ way}\ (t_w) = (t_8\text{-}t_7) \quad (10)$$

$$t_{localization}\ (t_{lz}) = (t_9\text{-}t_8) \quad (11)$$

if $t_{lz} \neq 0$, then the liquidation stage is calculated as $t_{liquidation}\ (t_l) = (t_{10}\text{-}t_9)$ (12)

if $t_{lz} = 0$, then the liquidation stage is calculated as $t_{liquidation}\ (t_l) = (t_{10}\text{-}t_8)$ (13)

$$t_{collecton\ of\ eqipment}\ (t_c) = (t_{11}\text{-}t_{10}) \quad (14)$$

$$t_{return\ to\ base}\ (t_{rt}) = (t_{12}\text{-}t_{11}) \quad (15)$$

$$T_r = t_o + t_i + t_d + t_{dm} + t_{mt} + t_a + t_w + t_{lz} + t_l + t_c + t_r \quad (16)$$

where:

T_r - is the total time of a single response process,

t_o - the time stage of the response of the operator of the service 112,

t_i - the time stage of the collection of information by the operator of the 112 service,

t_d - the time step of the response of the emergency response dispatcher,

t_{dm} - the time stage of decision making by the dispatcher,

t_{tm} - the time stage of information transfer to the dispatcher's emergency response units,

t_a - the time stage of the collection on the alarm of the emergency response forces,

t_w - time stage of travel on the way to the scene of the incident,

t_{lz} - the time stage during which the spread of fire was stopped,

t_l – the time stage, fixing the end of rescue operations,

t_c - the time stage of the collection of the applied response means,

t_{rt} - is the stage of time spent returning to the base.

The available experience and the results of the research conducted indicate that the developed formula is applicable for all cases of response to any type of emergency situation in which one unit is involved on one specialized vehicle. If two or more vehicles from two or more units take part in the reaction, the formula takes the following form:

$$T_r = t_o + t_i + t_d + t_{dm} + \sum_{i=1}^{n} t_{tm} + \sum_{j=1}^{m} t_a + \sum_{j=1}^{m} t_w + \sum_{j=1}^{m} t_{lz} + \sum_{j=1}^{m} t_l + \sum_{j=1}^{m} t_c + \sum_{j=1}^{m} t_{rt} \quad (17)$$

where:

T_r - is the total response time,

t_o - the time stage of the response of the operator of 112 service,

t_i - the time stage of the collection of information by the operator of 112 service,

t_d - the time step of the response of the emergency response dispatcher,

t_{dm} - the time stage of decision making by the dispatcher,

t_{tm} - the time stage of information transfer to the dispatcher's emergency response units,

t_a - the time stage of the collection on the alarm of the emergency response forces,

t_w - time stage of travel on the way to the scene of the incident,

t_{lz} - the time stage during which the spread of fire was stopped,

t_l - time stage, fixing the end of rescue operations,

t_c - the time stage of the collection of the applied response means,

t_{rt} - time step spent on returning to base.

n - department,

m - vehicle,

This formula leads to distorted, incorrect results when calculating the response time to emergency calls within the range between dialing the emergency number before the arrival of the first emergency response crew at the scene of missions separately for each unit, since there is a summation of the intermediate time t_{mt} spent by the dispatcher to transmit information about the mission separately for each unit. There is also a summation of the *alarm collection time* t_a and the t_{id} *time on the way* spent by each individual response team.

In this case, the following conditions (factors), indicators and formulas for their calculations are taken into account to calculate the response time to an emergency situation in which more than one unit is involved using more than one vehicle:

Response Force Selection (S) - First Unit Alert Control Point;

Acknowledgment (C) - control point of time of acknowledgment of receipt of information in the first subdivision;

Departure (D) - checkpoint for the departure time of the first emergency response team;

Arrival at the scene (A) - the checkpoint of the arrival time of the first team;

Fire localization (LZ) - time of the checkpoint of the first localization report. In some cases, the head of extinguishing the fire announces the same time for all teams;

Liquidation (L) - time of the checkpoint of the end of the work by the last team;

Return (R) - time of the checkpoint of the last group that left the place of rescue operations;

Finalization (F) - The checkpoint time of the last rescue team's report on readiness for new response tasks.

$$T_r=t_o + t_i + t_d + t_{dm}+n_1*t_{tm}+m_1*t_a+m_1*t_w+m_1*t_{lz}+m_x*t_l+m_x*t_c+m_x*t_{rt} \quad (18)$$

where:

T_r - is the total response time,

t_o - the time stage of the response of the operator of the service 112,

t_i - the time stage of the collection of information by the operator of the service 112,

t_d - the time step of the response of the emergency response dispatcher,

t_{dm} - the time stage of decision making by the dispatcher,

t_{tm} - the time stage of information transfer to the dispatcher's emergency response units,

t_a - the time stage of the collection on the alarm of the emergency response forces,

t_w - time stage of travel on the way to the scene of the incident,

t_{lz} - the time stage during which the spread of fire was stopped,

t_l – the time stage, fixing the end of rescue operations,

t_c - the time stage of the collection of the applied response means,

t_{rt} - time step spent on returning to base.

n - department,

m - vehicle,

x - is the maximum quantity,

Analysis of the calculation of the response time to an emergency call, in which all stages of the response time are subject to mandatory standardization, demonstrates that only one stage has a variable value - this is t_{id} = the time spent on the way, the values of the remaining indicators are determined by the maximum values of time indicators approved by the internal documents of the services response. These include validity periods in the operator's and dispatcher's area of responsibility, where the reaction time is recorded in seconds:

$t_o = 10_{sec}$, $t_i = 50_{sec}$, $t_d = 10_{sec}$, $t_{dm} = 50_{sec}$ and $t_{tm} = 60_{sec}$.

The value of the time interval ($t_{collection\ on\ alarm} = t_a$) is equal to two minutes and is constant and it is determined by an internal order. It consists of the time of collection on alarm, putting on specialized equipment, and getting the rescue team into the vehicle.

$$T_{rc} = 10_{sec} + 50_{sec} + 10_{sec} + 50_{sec} + 60_{sec} + 2*60_{sec} + 15*60_{sec} = 1200_{sec} \text{ or } 20_{min}, \quad (19)$$

By summing the maximum values of the initial indicators, the value of the result obtained is optimized

$$T_{rc} = 300_{sec} + 15*60_{sec} = 1200_{sec} (20) \quad (20)$$

or

$$T_{rc} = 5_{min} + 15_{min} = 20_{min} \quad (21)$$

where: T_{rc} – emergency reaction time

The accumulated experience indicates that in order to reduce the reaction time and increase the response zone, it is necessary to keep in mind the revision of the processes taking place on the way to the scene of the incident. According to international standards, the reaction time should not exceed 20 minutes, if, according to calculations, the route is no longer than 15 km [10].

The proposed approach of timing can be applied and adapted to any type of response, regardless of the nature of the manifestation of the ongoing processes. It also allows for a detailed analysis of the efficiency in terms of the time taken to complete the actions of all participants in the response process, identify weaknesses, which, in turn, will lead to optimization and systematization of the response process, improving its quantitative and qualitative values of indicators.

Conclusions

From a science-based perspective, effective emergency response requires an initial detailed analysis

For this purpose, graphic models of algorithms for timing the main reaction processes have been developed, which allow a detailed analysis of the ongoing processes.

On their basis, algorithms for determining the size of the execution time of a single response process and its stages have been compiled.

Each time point is also described in detail, as well as the sequence of calculating the sizes of the response time stages. At the same time, calculations were made both for one unit and one response team, and for two or more units and emergency response teams.

As a result of the implementation of this approach, all participants in a single process are guided by the same standards, which made it possible to establish a clear boundary between their areas of responsibility.

Implementation and management in real conditions of the concept of a unified information system for emergency management based on the developed graphical models and algorithms, with a high probability, allows you to determine at what stage of time is the implementation of the response process to any specific type of emergency.

References

1. Peancovschii S.P. Classifiers for decision support system in emergency situations. // Actual problems of natural and human sciences among senior young scientists "Rodzinka-2019" / XXI All-Ukrainian Scientific Conference of Young Scientists. Cherkasy: ChNU im. B. Khmelnitsky, 2019, -556 p., p. 241 - 243 [in Russian].
2. Yamalov I. U. Modeling of management and decision-making processes in emergency situations [Electronic resource] / I. U. Yamalov. - 2nd ed. (electronic). - Moscow: BINOM. Lab. knowledge, 2012. - 288 p.
3. Plotnikov V.A. Abstract. Modeling of the system of operational management of the liquidation of emergency situations. St. Petersburg: 2013 [in Russian].
4. Vishnyakov Ya. D. et al., Life safety. Protection of the population and territories in emergency situations: textbook. allowance for students. higher textbook institutions / - M .: Publishing Center "Academy", 2007. - 304 p.
5. Brushlinsky N.N., Modeling the operational activities of the fire service. – M.: Stroyizdat, 1981. – 96 p. [in Russian].
6. Brushlinsky N.N., Sokolov S.V. Mathematical Methods and Management Models in the State Fire Service: Textbook. M.: Academy of GPS EMERCOM of Russia, 2011. 173 p.
7. Brushlinsky N.N., Kolomiets Yu.I., Sokolov, S.V., Wagner, P.M. Security of cities: simulation of urban processes and systems: Proc. allowance /. M.: FAZIS, 2004. 172 p.
8. Sokolov S.V., Solodov A.N. Rationing the arrival time of the units of the State Border Service of St. Petersburg by urban development zones // Proceedings of the XIV All-Russian Scientific and Practical Conference. M., 1997. S. 67-69.
9. Pryanichnikov V.A. The concept of the model for ensuring the standard time of arrival of emergency services in a metropolis. Fires and emergencies: prevention, liquidation. - 2015. - No. 3 (15). pp. 37 - 39.
10. Government Decree Nr. 908 of 05.11.2014 on regulating the organization of forces and means of the civil protection and emergency service, subordinate to the Ministry of Internal Affairs. Published: 07.11.2014 in Monitorul Oficial al Republicii Moldova Nr. 333 - 338. Available: https://www.legis.md/cautare/getResults?doc_id=18647&lang=ru http://lex.justice.md/viewdoc.php?action=view&view=doc&id=355328&lang=2

Journal of Engineering Science *Vol. XXIX, no. 1 (2022), pp. 97 - 104*
Fascicle *Electronics and Computer Science* *ISSN 2587-3474*
Topic *Computers and Information Technology* *eISSN 2587-3482*

https://doi.org/10.52326/jes.utm.2022.29(1).08
CZU 004

PROOF-OF-STAKE CONSENSUS ALGORITHMS FOR THE SOFTWARE COMPONENTS BLOCKCHAIN

Vaidas Giedrimas*, ORCID: 0000-0003-1979-9978

Vilnius University, Siauliai Academy, 84 Vytauto St., LT-76352 Siauliai, Lithuania
*Corresponding author: Vaidas Giedrimas, *vaidas.giedrimas@sa.vu.lt*

Received: 11. 05. 2021
Accepted: 01. 19. 2022

Abstract. In the blockchain context, the information system (IS) is considered a part of its infrastructure. However, blockchain itself can be used for IS development using software components and services. As the trust for binary components or services is still a problem, we propose to use the blockchain of components to solve this problem. In this paper, the part of such solution, namely consensus algorithms, is discussed. We focus on Proof-of-Stake algorithms and present their feasibility to be used in the blockchain of software components. It was found that the use of probabilistic algorithms (RRR, CloudPoS, WV, DDPoS, Panda) allow the partial solution of the problem in the blockchain of reliable software components.

Keywords: *software component, CBSE, consensus algorithm, blockchain.*

Abstract. În contextul blockchain, sistemul informational (SI) este considerat o parte a infrastructurii sale. Cu toate acestea, blockchain-ul în sine poate fi folosit pentru dezvoltarea SI folosind componente și servicii software. Deoarece încrederea pentru componentele sau serviciile binare este încă o problemă, ne propunem să folosim blockchain-ul de componente pentru a rezolva această problemă. În această lucrare este discutată o astfel de soluție, și anume algoritmii de consens. Ne concentrăm pe algoritmii Proof-of-Stake și prezentăm fezabilitatea acestora pentru a fi utilizați în blockchain-ul componentelor software. S-a constat, că utilizarea algoritmilor cu finalitate probabilistică (RRR, CloudPoS, WV, DDPoS, Panda) permite rezolvarea parțială a problemei în blockchain-ul componentelor software de încredere.

Cuvinte cheie: *componentă software, CBSE, algoritm de consens, blockchain.*

Introduction

Distributed software in most cases consist of various distributed components or is made using a few orchestrated software services. As the software components are binary, they can be the objects of the commerce (selling and buying) and the objects of third-part composition. It is possible to reuse the functionality of some component without any idea what exactly its implementation is. In the other hand, system integrators cannot to evaluate component in other ways than the black box approaches. In result they cannot be sure that the component is not harmful. The problem of the lack of trust on software components is

already discussed in various sources [4, 11, 13, 22, 24, 25, 30]. There are few possible solutions to increase trust on the component:

- Trusted computer security evaluation criteria (TCSEC) by NSA and NIST, USA;
- Trusted Components Initiative (TCI);
- The use of various formal methods for ensuring *a-priori* correctness of the components (e.g., type theories, category theories, mathematical frameworks) [15, 31];
- Prediction-oriented component-based technologies, for the analysis of the relationship between structural restrictions and assumptions of the domain models, which helps to predict properties of the systems [13].

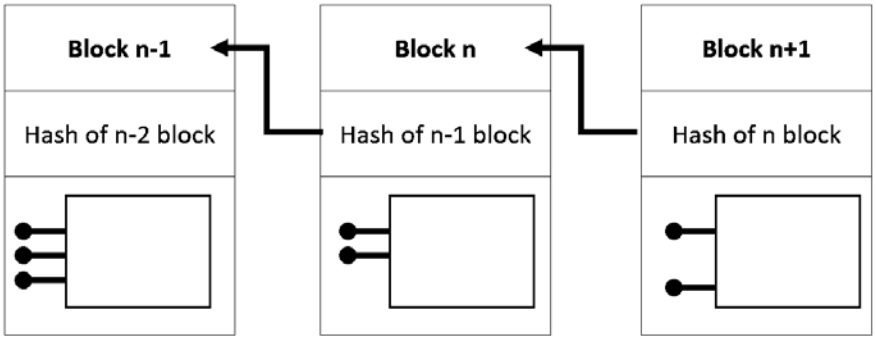

Figure 1. Blockchain of the components.

The methods can be divided to two categories: invasive methods and non-invasive ones. Invasive methods are used for such purposes as component stress testing, prediction of component inner properties or to make simulation of real-time use of the component. If invasive methods are used, then the component is considered as a "gray-box", or "glass-box". Sometimes even reverse engineering methods are used to reveal an internal structure of the component, or the algorithms used in its implementation.

Non-invasive methods are based on hash codes, formal certificates and so on. The component is considered as "safe" and "trustful" in the case well-known manufacturer, or some another authority approve it. From some point of view the situation is comparable to the banking system. E.g., if the Government of some state claims that its coins and banknotes are trustful, we consider this currency as reliable. Consequently, non-invasive trust of software components have the same disadvantages as the banking system have:

- The power is not in the user-side. Well-known manufacturer of the components or an open-source community can cancel the support as easy as the governments can devalue its currency. The user/developer is only informed in the best case, but no negotiations are made before.
- The threat to be hijacked. Some hackers can try to hijack well-known component or made fake signatures of the components (on behalf of real manufacturer) as the criminals are trying to make fake banknotes or goods.

Nowadays the banking system is started to move towards big "promise" of FinTech age, i.e., towards decentralization [20]. Trustful, DLT-based systems are among the contemporary hype cycle [17]. DLT or blockchain is considered as a storage point for the descriptors of software components in this paper. Here and below, we will call it as the "blockchain of the components". This blockchain consists of the records, with the comprehensive information about the component interface, functionality, manufacturer, and rating (see. Figure 1). For the security reasons binary component (or trustful link to it),

described in the blockchain node, is stored in the same record as well. The goal of the blockchain is to increase the trust in software components. As pointed in [16], such secure structure has a promising side effect – distributed component repository.

Every blockchain is based on some Consensus algorithm, which provides the rule which exactly node should be able to produce a record and how the changes must be made. Most of the algorithms is tuned to work in potentially dangerous conditions. It is known that some nodes in the distributed system can be malicious/unfair. But the algorithm must ensure that the right decision would be made event in that case. The goal of this paper is to select blockchain consensus protocols, which could be used in the blockchain of trustful software components (or services). The rest of the paper is organized as follows: Section 2 shortly introduces related work in this area, Section 3 presents the consensus algorithms and their selection criteria. Section 4 outlines the consensus achieving algorithms of Blockchain of components (or services). Finally, the conclusions are made, and some consecutive questions are exposed.

Related work

It is several references about the use of the blockchain for different purposes: academic affairs in the university [18], e-voting [5], medical image sharing, supply chain management, software engineering [10, 12, 14, 21, 27] etc. Despite it, we almost not found the papers covering the use of the blockchain for component-based software engineering nor about the component trust solutions using DLT.

The paper [33] is dedicated to the support of operations, but not to ensure the trust on software assets. The topic is introduced in [16], where the overall possibility for using blockchain as a helper for CBSE is discussed. According to [16], Proof-of-work (PoW) and Proof-of-authority (PoA) consensus algorithms are not suitable to use in component-based software context. The former is not applicable, because is nothing to "burn" in this context. The usage of the later (PoA) is not desirable as it would led back to centralization [16].

Selection criteria

There is a high number of blockchain consensus algorithms having different names and (partially) different aspects [7]. However, for simplicity reasons, we will focus on a very comprehensive study [8], which claims that most of the existing blockchain consensus algorithms by their nature (or origin) can be divided into 3 groups: Proof-of-Stake (PoS), Proof-of-Work (PoW), and Practical Byzantine Fault Tolerance (PBFT).

In PoW, the right to write the block is assigned to the node, which just solved dedicated crypto problem. It is a basis on most of cryptocurrencies. In PoS, the block can be created by the node selected in random order. However in the set of "lottery"-participants could be only the nodes, which can put at "stake" (i.e. to use some part of the goods/cryptocurrency/time/etc.). The block is approved if the confirmations from at least 51% nodes are got. In PBFT [8, 9] three phases are used for decision: initial, prepare and commit. In initial phase candidate node send the block to backup nodes (via primary node). If the conditions for the validity of the block is met, then the backups pre-accept this block. Then, in preparation phase the block is considered by all the nodes (not only the backups).

We continue the work of [16], in which 10 possible consensus algorithms were considered: PoW, PoS, DPos/LPos, Proof of Burn (PoB), Proof of Authority (PoA), Ripple Protocol Consensus Algorithm (RPCA), Stellar Consensus Protocol (SCP), Register-Deposit-Vote (RDV) [26], and Hashgraph [1, 2, 28]. As pointed in [16], PoW, PoB, and few other

algorithms are not suitable for the blockchain of components, so we will focus only on the PoS algorithm class in this paper.

Next, we will examine each algorithm from the PoS class, using the classification framework, described in [8]. The framework consists of 4 categories: origin, design, performance, and security. The assessment will be made having in mind two contexts: a) the blockchain of the components and b) blockchain of the services.

The evaluation of POS consensus algorithms

From the list consisting of almost 30 algorithms [8] by the criteria of origin, we selected 7 consensus algorithms based on PoS:

- Medical image sharing (MIS) algorithm is proposed for the healthcare domain. Using this algorithm, the probability of a node producing the next block is driven by the number of Define Study transactions designating that node's public key as the image source. However, the procedure of block validation is not explained in more detail.
- Robust RR (RRR). Round Robin theory-based algorithm is specific by using deterministic round-robin selection with a lightweight leader endorsement mechanism. Every time the set of oldest identities are chosen as leading candidates. Endorsers are selected randomly form the set of active identities. A candidate proposes a block and the endorsers confirm the block from the oldest candidate they observe. The leader candidate (who receives the required number of confirmations from the endorsers), is chosen as the leader to add a new block. The authors of RRR [3] claim that the algorithm guarantees the highest possible probability, that only one block from one leader is produced on each round and that re-writing cannot be made.
- Fantomette. This protocol uses BlockDAG theory and is based on Caucus [6, 8]. It is a secure leader election protocol, providing game-theoretic guarantees. The participants (nodes) commit its states to a public list and then the nodes are considered eligible to be elected leader after some fixed number of rounds. In the first round, when some number of participants is reached, participants run a secure coin-tossing protocol to obtain a random value. If each next round, every participant verifies their eligibility. The eligible participant (if any) creates a transaction with its data and broadcasts it to their peers.
- CloudPoS. In this algorithm, the concept of epoch is used. For each epoch, the need to stake resources once again to be electable as the leader (for this epoch). After the bets, the leader is selected randomly based on the individual stakes. Only the leader can create a block, however, this must be approved by most participants [8, 29].
- Trust-CP. The Trust Consensus Protocol [23] introduces the concept of trust score. Trust score is calculated for each participant. The scores must be committed using separate blockchain transactions (as the blocks are committed for the writing). When the block is committed, then the trust score of the "block producer" must be recorded in the same block as well. The goal of Trust-CP is a blockchain-based solution to ensure trust between peers (participants).
- Weighted Voting (WV). This is an extension of PoS, solving the problem of non-active validators [19]. If many validators would abstain from the voting, in classic PoS, the block would be not confirmed and written, even though the majority of

voted participants would approve it. In WV the validators have the weights of votes, so the problem would persist only in case if some "heavyweight" node does not vote. In another hand, this algorithm is more near to centralized solutions.

- BIFTS. The blockchain-IoT-based food traceability system [8] is a variation of the PoSCS consensus algorithm. The main contribution in BIFTS is an application area (supply chain management, as in Proof-of-Supply-Chain-Share (PoSCS) protocol), not the technical novelty.

And 2 more algorithms (partially) based on Delegated PoS (DPoS) were selected as well:

- DDPoS. Delegated Proof-of-Stake with Downgrade mechanism algorithm [34] is proposed as a solution for high centralization in other consensus algorithms, lack of security, and efficiency of generating blocks. In DDPoS, there are 101 nodes with the most votes that can be elected as witness nodes. This shortlists as in DPoS, is the subject of a regular update. During the update the nodes with the low rate of generating blocks and/or malicious behavior are removed, loses their credibility and witness identity. The consensus process of the DDPoS algorithm consists of three modules: selecting a certain number of consensus nodes, reaching a consensus on the verification of the block, and downgrading malicious nodes [34].
- Panda, or DPoS-BA-DAG consensus algorithm [35] is used in DLattice blockchain. The candidate secretly generates the consensus identity locally, and the consensus committee for this branch is also made at the same time. The algorithm is divided into two phases: voting and commit. Initially, the dedicated members of the voting committee select a TB to vote, and all consensus nodes get the vote results. In the second phase, the members of committees is starting to commit voting. The commit is done using previuosely collected vote results. IN result all the nodes get the commit voting results. The consensus is considered as done when the node counts commit voting results exceeds the threshold value.

By the Design category from Bouraga's classification framework [8], we evaluated RRR, Fantomette, CloudPoS, Trust-CP, WV, DDPoS, and Panda algorithms. RRR and CloudPoS use 3rd party tools for permission management, Trust-CP - for the trust evaluation. The other 4 approaches are self-contained. Most of the approaches use the reward as the main incentive for the nodes, while only DDPoS uses punishment. In the CBSE world, a punishment could be out-of-the-stock action, especially in the components-of-the-shield (COTS) case. The reward can be various, e.g., the higher rating in the software component list, increased level of trust, and so on. The concept of the stake itself is in the context of CBSE, can be defined as one of the follows:

- The number of already recorded component descriptions in the blockchain.
- The rate of recorded component descriptions. For example, if a new record about a new component in blockchain was rejected, that could mean that its quality is below the voters' expectations. If it happens in the second or n-th case, then the trust in existing products (software components) of the same manufacturer could be decreased.
- The (decreasing) number of possible submissions for recording in the future.

In the blockchain of software components, the concept of finality is controversial. If the finality is deterministic (i.e., it is impossible to add a node before already recorded one) the trust for the component. As pointed in [16], in component-based software engineering, the presence of different versions of the components is vital. However, in the blockchain of

components only some version (or some vendor) of the component will be marked as "trustful". All consecutive versions must to get new approval from all the nodes. In other hand, in the case of the adoption of a consensus algorithm with probabilistic finality, the problem of component versioning can be (partially) solved. Probabilistic finality is observed in RRR, CloudPoS, WV, DDPoS, and Panda algorithms.

Almost all the 7 algorithms have a formal background, except for the Trust-CP which formal development was not found in [23].

The Performance category (3rd in the Bouraga's classification framework [8]), is less relevant in the blockchain of the components unless we would talk about continuous development. Usually, the process of submission of a new component to the repository takes some time. e.g. the period of approving a new app for Android in GooglePlay repository can be done from few hours to 2 weeks (in the moment of this paper writing). By the number of successful transactions per second starting from the first transaction deployment time the best algorithms are [8] RRR (1500) and Panda (1200). Most of the algorithms do not have any latency between the completion time and the deployment time, however using CloudPoS the gap in time could be 10-15ms, while RRR - a minute. Unfortunately, the fault tolerance is not on the spot of the selected 7 algorithms. At least this wasn't considered in the referred literature. Only Trust-CP reports that in 84% cases the algorithm can recover from the failure of a node. Unfortunately, only RRR algorithm supports the scalability. Other algorithms should be improved according to these criteria. All seven algorithms are proved by its authors in some experimental evaluation.

The Security category [8], is very important as we focus on trust in components in the blockchain. They are reported thousands of cases of malware in information systems, which imply big organizational, performance, trust, and other problems. The problems would even bigger if the malware would be recorded to the Trusted component repository (in our case the blockchain of components). We consider 7 algorithms by their resilience to 4 most frequent threats [8, 32]: Sybil, DDoS, "51 percent", and Eclipse attacks. Unfortunately, no one algorithm from our research is ready for the Eclipse attack (when intruders influent the network that any communication must be performed with malicious nodes only). However other types of attacks are not so vulnerable for the selected consensus algorithms. Sybil attacks can be handled by Fantomette and Trust-CP algorithms, DDoS - by Fantomette, 51% attack - by RRR, CloudPoS. WV and DDPoS seams are the least secure variations of consensus algorithms. The best security level showed Panda, as it could resist Sybil, DDoS, and "51 percent" attacks.

Conclusions and future work

After the assessment of the Prove-of-the-Stake consensus algorithms and their possible implementation in distributed software components trust-ensurance system, we came to the conclusions:

1. Comprehensive classification frameworks for consensus algorithms exists, however the idea of using blockchain for component-based software engineering still have week coverage in scientific references.
2. The concept of the Stake using PoS algorithms in CBSE context could be defined as: a) the number of already recorded components, b) the rate of recorded components, c) the number of possible submissions for recording in the future. However, this concept should be discussed in more details in future.

3. The use of the algorithms with probabilistic finality (RRR, CloudPoS, WV, DDPoS, Panda) enable to (partially) solve the problem of component versioning in the blockchain of trusted software components.

Acknowledgements. This paper was presented at the *International Conference on Electronics, Communications, and Computing, IC ECCO*, 21-22 October, 2021, Chisinau, UTM.

References

1. Hashgraph consensus: Detailed examples. Tech. Rep. SWIRLDS-TR-2016-02, Swirlds, Inc. (2016), [online]. [accesat 10.04.2021]. Disponibil: http://leemon.com/papers/2016b2.pdf
2. The swirlds hashgraph consensus algorithm: fair, fast, byzantine fault tolerance. Tech. Rep. SWIRLDS-TR-2016-01, Swirlds, Inc. (2016), [online]. [accesat 10.04.2021]. Disponibil: http://leemon.com/papers/2016b.pdf
3. Ahmed-Rengers M., Kostiainen K. Don't mine, wait in line: Fair and efficient blockchain consensus with robust round robin, 2020.
4. Alvaro A., Land R., Crnkovic I. Software component evaluation: A theoretical study on component selection and certification. Tech. Rep. ISSN 1404-3041 ISRN MDH-MRTC-217/2007-1-SE, November 2007.
5. Awalu I.L., Kook P.H., Lim J.S. Development of a distributed blockchain evoting system. In: *Proceedings of the 2019 10th International Conference on e-Business, Management and Economics*. pp. 207–216. ICEME 2019, Association for Computing
6. Machinery, New York, NY, USA (2019). https://doi.org/10.1145/3345035.3345080
7. Azouvi S., Mccorry P., Meiklejohn S. Betting on blockchain consensus with fantomette (2018)
8. Bach L.M., Mihaljevic B., Zagar M. Comparative analysis of blockchain andnsus algorithms. In: *Proceedings of 41st International Convention on Information and Communication Technology, Electronics and Microelectronics (MIPRO)*. pp. 1545–1550, 2018. https://doi.org/10.23919/MIPRO.2018.8400278
9. Bouraga S. A taxonomy of blockchain consensus protocols: A survey and classification framework. *Expert Systems with Applications* 168, 114384, 2021. [online]. [accesat 01.03.2021]. Disponibil: https://doi.org/https://doi.org/10.1016/j.eswa.2020.114384,
10. Castro M., Liskov B. Practical byzantine fault tolerance and proactive recovery. *ACM Trans. Comput. Syst.* 20(4), pp. 398 – 461, 2002.
11. Chakraborty P., Shahriyar R., Iqbal A., Bosu A. Understanding the software development practices of blockchain projects: A survey. In: *Proceedings of the 12th ACM/IEEE International Symposium on Empirical Software Engineering and Measurement*. pp. 28:1–28:10. ESEM '18, ACM, New York, NY, USA, 2018.
12. Chaudhari D., Zulkernine M., Weldemariam K. Towards a ranking framework for software components. In: *Proceedings of the 28th Annual ACM Symposium on Applied Computing*. pp. 495 – 498. SAC '13, ACM, New York, NY, USA, 2013.
13. Chawla C. Trust in blockchains: Algorithmic and organizational. *Journal of Business Venturing Insights 14*, e00203, 2020, [online]. [accesat 05.01.2021]. Disponibil : https://doi.org/https://doi.org/10.1016/j.jbvi.2020.e00203.
14. Crnkovic I. *Building Reliable Component-Based Software Systems*. Artech House, Inc., Norwood, MA, USA, 2002.
15. Destefanis G., Marchesi M., Ortu M., Tonelli R., Bracciali A., Hierons R. Smart contracts vulnerabilities: a call for blockchain software engineering? In: *2018 International Workshop on Blockchain Oriented Software Engineering (IWBOSE)*. pp. 19 – 25, 2018.
16. Dimitriou T., Michalas A. Multi-party trust computation in decentralized environments. In: *2012 5th International Conference on New Technologies, Mobility and Security (NTMS)*. pp. 1 – 5, 2012. https://doi.org/10.1109/NTMS.2012.6208686
17. Giedrimas V. The role of blockchain for increase trust on software components and services. In: *2020 IEEE 14th International Conference on Application of Information and Communication Technologies (AICT)*. pp. 1–4, 2020. https://doi.org/10.1109/AICT50176.2020.9368582
18. Hawlitschek F., Notheisen B., Teubner T. The limits of trust-free systems: A literature review on blockchain technology and trust in the sharing economy. *Electronic Commerce Research and Applications 29*, pp. 50-63, 2018.
19. Ismail L., Hameed H., Alshamsi M., Alhammadi M., Aldhanhani N. Towards a blockchain deployment at uae university: Performance evaluation and blockchain taxonomy. In: *Proceedings of the 2019 International Conference on Blockchain Technology* (*ICBCT 2019)*. pp. 30 – 38., Association for Computing Machinery, New York, NY, USA, 2019.

20. Leonardos S., Reijsbergen D., Piliouras G. Weighted voting on the blockchain: Improving consensus in proof of stake protocols. In: *2019 IEEE International Conference on Blockchain and Cryptocurrency (ICBC)*. pp. 376 – 384, 2019.
21. Nicoletti B. *The Future of FinTech: Integrating Finance and Technology in Financial Services*. Palgrave Macmillan, 2017.
22. Porru S., Pinna A., Marchesi M., Tonelli R. Blockchain-oriented software engineering: Challenges and new directions. In: Proceedings of the 39th International Conference on Software Engineering Companion. pp. 169–171. ICSE-C '17, IEEE Press, Piscataway, NJ, USA, 2017.
23. Roshandel R. E. A. Estimating software component reliability by leveraging architectural models. In: *Proceedings of the 28th International Conference on Software andeering*. pp. 853–856. ICSE '06, ACM, New York, NY, USA, 2006.
24. Shala B., Trick U., Lehmann A., Ghita B., Shiaeles S. Novel trust consensus protocol and blockchain-based trust evaluation system for m2m application services. *Internet of Things 7*, 100058, 2019. [online]. [accesat 14.12.2020]. Disponibil: https://doi.org/https://doi.org/10.1016/j.iot.2019.100058.
25. Shaw M. Truth vs knowledge: The difference between what a component does and what we know it does. In: *Proceedings of the 8th International Workshop on Software Specification and Design*. pp. 181-186, IEEE Computer Society, Washington, DC, USA, 1996.
26. Singh L.K., Vinod G., Tripathi A.K. Impact of change in component reliabilities on system reliability estimation. *SIGSOFT Softw. Eng. Notes* 39(3), pp. 1–6, 2014.
27. Solat S. RDV: An alternative to proof-of-work and a real decentralized consensus for blockchain. In: *Proceedings of the 1st Workshop on Blockchain-enabled Networked Sensor Systems*. pp. 25–31. BlockSys'18, ACM, New York, NY, USA, 2018.
28. Tariq F., Colomo-Palacios R. Use of blockchain smart contracts in software engineering: A systematic mapping. In: Misra, S. Et al. (Eds.) *Computational Science and Its Applications – ICCSA 2019*. pp. 327–337. Springer International Publishing, Cham, 2019.
29. TELEKOM INNOVATION LABORATORIES Elements - An open source, sidechain-capable blockchain platform. [online] [accesat 03.01.2019]. Disponibil: https://bit.ly/2MT3SRE
30. Tosh D., Shetty S., Foytik P., Kamhoua C., Njilla L. CloudPOS: A proof-of-stake consensus design for blockchain integrated cloud. In: *2018 IEEE 11th International Conference on Cloud Computing (CLOUD)*. pp. 302–309, 2018.
31. Vale T., Crnkovic I., De Almeida E.S., Silveira Neto P.A.D.M., Cavalcanti Y.A.C., Meira S.R.D.L. Twenty-eight years of component-based software engineering. *J. Syst. Softw.* 111(C), pp. 128-148, 2016.
32. Voas J., Payne J. Dependability certification of software components. *Journal of Systems and Software* 52(2), pp. 165-172, 2000.
33. Wen Y., Lu F., Liu Y., Huang X. Attacks and countermeasures on blockchains: A survey from layering perspective. *Computer Networks* 191, 107978, 2021. [online] [accesat 12.03.2021]. Disponibil: https://doi.org/https://doi.org/10.1016/j.comnet.2021.107978
34. Wonjiga A.T., Peisert S., Rilling L., Morin C. Blockchain as a trusted component in cloud sla verification. In: Proceedings of the 12th IEEE/ACM International Conference on Utility and Cloud Computing Companion. pp. 93-100. UCC '19 Companion, Association for Computing Machinery, New York, NY, USA, 2019. https://doi.org/10.1145/3368235.3368872.
35. Yang F., Zhou W., Wu Q., Long R., Xiong N.N., Zhou M. Delegated proof of stake with downgrade: A secure and efficient blockchain consensus algorithm with downgrade mechanism. *IEEE Access* 7, pp. 118541-118555, 2019.
36. Zhou T., Li X., Zhao H. DLattice: A permission-less blockchain based on DPOSBA-DAG consensus for data tokenization. *IEEE Access* 7, pp. 39273 - 39287, 2019.

Journal of Engineering Science *Vol. XXIX, no. 1 (2022), pp. 105 - 111*
Fascicle *Electronics and Computer Science* *ISSN 2587-3474*
Topic *Biomedical Engineering* *eISSN 2587-3482*

https://doi.org/10.52326/jes.utm.2022.29(1).09
CZU 616.7:656.18.05: 331.101.1(669)

ERGONOMIC INVESTIGATION AND ASSESSMENT OF MOTORCYCLISTS MUSCULOSKELETAL DISORDERS

Adekunle I. Musa-Olokuta*, ORCID: 0000-0001-8787-0823,
Collins Nwaokocha, ORCID: 0000-0002-3566-8567,
Adeola S.Shote, ORCID: 0000-0002-6678-0009,
Samson A. Aasa, ORCID: 0000-0003-4380-4546

Olabisi Onabanjo University, Ago Iwoye, Ibogun Campus, Ogun State, Nigeria
*Corresponding author: Adekunle I. Musa-Olokuta, *musa-olokuta@oouagoiwoye.edu.ng*

Received: 01. 21. 2022
Accepted: 02. 20. 2022

Abstract. Motorcycles have become a mean of transportation in our rural and urban area in Nigeria. This cross sectional study was conducted in Abeokuta Ogun State to assess the work-related musculoskeletal disorders (WRMSDs) among the motorcyclist between October 2021 and January 2022 using snowball techniques. A structured modified Nordic Musculoskeletal disorder questionnaire (SNMQ) was administered to four hundred and fifty (450) motorcyclists. The result shows that 91.6% (412) of the motorcyclist participated. Furthermore, 76.1% of the cyclist experienced daily pains and 81.6% reported major pains in body parts. However, the results also show that major affected body regions were lower back (81.6%), leg (61.2%), upper back (82.0%), shoulder (55.1%), neck (82.5%), knee (73.3%), wrist/hand (98.8%), thigh (91.3%), ankle/feet (78.9%), ears (80.3%), eyes (59.0%), head (63.1%) respectively. The study concluded that high prevalence of WRMSDs existed among the commercial motorcyclists as a result of working hours, sitting posture, smoking and alcoholic drinking. Reduction of these symptoms could be achieved through the reduction of working hours.

Keywords: *WRMSDs, motorcyclist, smoking, alcohol, tiredness, break, shoulder, thigh.*

Rezumat. Motocicletele au devenit un mijloc de transport în zonele rurale și urbane din Nigeria. Acest studiu transversal a fost efectuat în statul Abeokuta Ogun pentru a evalua tulburările musculo-scheletale legate de muncă (WRMSD) în rândul motociclistului între octombrie 2021 și ianuarie 2022, folosind tehnici de bulgăre de zăpadă. Un chestionar modificat structurat pentru tulburări musculo-scheletale nordice (SNMQ) a fost administrat patru sute cincizeci (450) de motocicliști. Rezultatul arată că 91,6% (412) dintre motocicliști au participat. În plus, 76,1% dintre cicliști au avut dureri zilnice și 81,6% au raportat dureri majore în părți ale corpului. Cu toate acestea, rezultatele mai arată că regiunile majore ale corpului afectate au fost partea inferioară a spatelui (81,6%), picior (61,2%), partea superioară a spatelui (82,0%), umărul (55,1%), gâtul (82,5%), genunchi (73,3%), încheietura mâinii/mâna (98,8%), coapsă (91,3%), gleznă/picioare (78,9%), urechi (80,3%), ochi (59,0%), respectiv cap (63,1%). Studiul a concluzionat că există o prevalență ridicată a WRMSD în rândul

motocicliștilor comerciali ca urmare a orelor de lucru, a posturii pe scaun, a fumatului și a consumului de alcool. Reducerea acestor simptome ar putea fi realizată prin reducerea orelor de lucru.

Cuvinte cheie: *WRMSD, motociclist, fumat, alcool, oboseală, pauză, umăr, coapsă.*

Introduction

The application of ergonomics in all facet of our daily life cannot be overemphasized. Reference to this application, ergonomics is defined as the science of designing of workplace conditions, workstation and job demands to the capabilities of the working population, It is also involved the designing of fit-all approach. Ergonomics can be said to covers all facet of job being an aspect of industrial engineering discipline. Cumulative trauma disorders is defined as the excessive wear and tear on tendons, muscles and sensitive nerve tissue caused by continuous use over an extended period of time. The hazards of industries ranging from physical stress on joint, muscles, bone, tendons etc can be attributed to trauma injuries and disorders. This disorder could also be referred to as musculoskeletal disorders (MSDs). Similarly, environmental factors such as vision, hearing, health and comforts of individual cannot be jettison with a kick gloves but assessed as the risk factors.

Motorcycles in the recent days have become a mean of transportation in our rural and urban areas in Nigeria and some other developing countries. Research revealed that majority of individual in developing countries of low and middle level income ride motorcycle as a way of increasing their income couple with the vast unemployment [1].

Onawumi and Oyewale [1] reported further that poor road network with unpaved road linking rural area is glaring encouraged the increase in the use of motorcycle as well as increase unemployed youth venture into riding of motorcycle as a source of leaving. Riding of motorcycle is cheaper comparing to taxi or bus and most of the motorcycle operation area could not encourage taxi bus to ply due to the poor road couple with narrow nature of the road. The passengers of this motorcyclist also could not be spare of this discomfort. Riding motorcycle is risky and exposed the motorcyclist and passenger to hazards, environmental pollutions such as exhaust from other passer vehicle [1].

Karmegam et al., [2] reported that riding of motorcycle involves complex and risky maneuvers and processes. Though it could be cheap to procure, maintain and consume less fuel compare to taxi and buses but the risk of the man-machine, exposure to environmental dust etc still makes it very risky. The safety of motorcyclist has remained concern with the level of unprotected man-machine system and exposure, lack of body support, personal protective wears such as helmets, boots, jacket and gloves are required to serve as safety equipment for the motorcyclist [1].

Several model of motorcycle were imported to the country without recourse to the motorcyclist anthropometric dimensions or measurements. The consequence of this is the discomfort among the motorcyclist leading to musculoskeletal injuries and disorders. The work related cumulative trauma disorders of the motorcyclist may result in physiological illness. Due to prolong stress in a fixed position for long distance riding could lead to accident, body injury or death. Physical risk factors such as awkward posture, exertion repetition and work duration could also contributed to high level of musculoskeletal disorder in the shoulders, neck, arm etc [3].

Jaiyesimi et al., [4] investigated the work related musculoskeletal disorders and predisposing factors among 200 commercial motorcyclists in Ibadan north local government

area of Oyo State but could not cover large geographical area. Onawumi and Oyewale [1] studied on the survey of the motorcyclist and work related musculoskeletal disorders among 300 commercial motorcyclists but did not report or investigated the prevalence of musculoskeletal disorders or the risk factors. The research only focuses on the associated problem with respect to ergonomic design of different imported motorcycles.

Several studies of high prevalence in musculoskeletal disorders among different professionals in Abeokuta metropolis have been researched and reported by the author [3], [5, 6]. Due to incessant accident and complain of absence from work couple with pains by the commercial motorcyclist, this present research was aimed and designed to investigate the cumulative trauma disorders among the commercial motorcyclist leading to discomforts and related hazards and survey the model of motorcycle used in Abeokuta, Ogun State.

Methodology

The cross-sectional study was carried out between October 2021 and January 2022 to investigate the prevalence of musculoskeletal disorders (MSDs) among the motorcyclist leading to discomforts in Abeokuta areas, such as Fajol hotel junction, Gbonogun junction, Oloke junction, Olokuta junction, Panseke, Olomore area all in Ogun State. Snowball technique was used to reach out to the motorcyclist, because most of the cyclist decline interview with acclaimed stranger due to the security situation in the areas.

A self–administered questionnaire divided into three sections was used to conduct the interview base on the survey needed. The first section relates to socio-demographic information of the respondents, second section is the work-related characteristics of the motorcycle while the third section is the standardized Nordic musculoskeletal questionnaire (SMNQ) The question was developed for subjective approach correlating to twelve anatomical area of the body such as neck, shoulder, elbow, hands/wrists, upper back, low back, hip/thigh, knee, ankle/feet, eyes, ears and head based upon the areas where symptoms accumulated.

Statistical Data Analysis

Statistical Package for Social Sciences (SPSS) 23.0 version and Microsoft word excel (2010) was used for data analysis to estimate the descriptive statistic (frequencies and percentile), and elucidate the prevalence of work related musculoskeletal symptoms relating to demographic characteristics. Chi square test was also employed to assess the relationship between the prevalence of musculoskeletal disorders and demographic characteristic. Level of significance was set at $P<0.05$

Result

Study characteristics

Four hundred and fifty (450) self administered questionnaire were distributed to the motorcyclist. Four hundred and twelve were return with response rate of 91.6% with all male riders.

Table 1

Socio-demographic characteristics of the motorcyclist (n = 412)

	Variables	Frequency (n)	Percent (%)	p-value (p<0.05)
A	**Gender**			
	Male	412	100	0.000
	Age (years)			
B	21 – 25	189	45.9	
	26 – 30	68	16.5	

Continuation Table 1

	31 – 35	**85**	**20.6**	
	36 – 40	**57**	**13.8**	
	41 – 45	**13**	**3.2**	**0.000**
	Marital status			
C	Married	330	80/1	
	Single	82	19.9	0.000
	Education Level			
D	Primary School	36	8.7	
	Secondary School	266	64.6	
	* ND / **NCE	110	26.7	0.000

*ND – National Diploma

**NCE – National Certificate of Education

The motorcyclists in Abeokuta, Ogun State Nigeria peak through the age of 21 – 25 years (45.9%) as revealed in the Table 1 above.

Table 2

Characteristics of Work-Related

	Variable	Frequency (n)	Percent (%)	p-value (p<0.005)
	Year of Experience (years)			
A	0 – 5	327	79.4	
	6 – 10	85	20.6	0.000
	Working days per week			
B	4days	168	40.8	
	6days	85	20.6	
	7days	159	38.6	0.000
	Working hour per day			
C	>8hours	85	20.6	
	8hours	72	17.5	
	<12hours	255	61.9	0.000
	Tiredness			
D	Yes	412	100	
	No	0	0	0.000
	Frequency of tiredness			
E	Often	163	39.6	
	Sometimes	249	50.4	0.000
	Observe break			
F	Yes	252	61.2	
	No	160	38.8	0.000
	Length of break			
G	>1hour	163	39.6	
	<1hour	249	60.4	0.000
	Action taken when tired			
H	Self Medication	247	60.0	
	Taken herbs	165	40.0	0.000
	Smoking			
I	Yes	336	81.6	
	No	75	18.4	0.000
	Drinking Alcohol			
J	Yes	252	61.2	
	No	160	38.8	0.000

Majority of this group are youth who either dropout of secondary school or school certificate holders. The highest educational level of the motorcyclist was a secondary school certificate (64.6%) and most of them were married (80.1%).

Table 2 above shows the work-related characteristics of the motorcyclists. Majority (79.4%) of the motorcyclists had 0 – 5 yers of experiences in the riding and operation of the motorcycle. The results also revealed that 40.8% spent 4 days out 7days in a week to ride the motorcycle for commercial purposes working for more than 12 hours (61.9%) in a day respectively. Similarly, majority of the motorcyclist get tired while riding through the various environmental conditions such as dust, wind, noise, sooth etc on the road and 60.4% claimed sometimes feel tired while 39.6% often get tired. In view of this, tiredness, 61.2% reported observing rest of more than one hour (60.4%) every operational day.

Similarly, 81.6% and 61.2% of the motorcyclists smoke cigarette or like and engaged in the drinking of alcohol respectively during the break period. However, Table 2 above also shows the action taken when the motorcyclist get tired. Majority (60.0%) engaged in self medication while 40.0% uses herbs/concoctions to re-energize the lost strength.

Characteristic and prevalence of Musculoskeletal Disorders

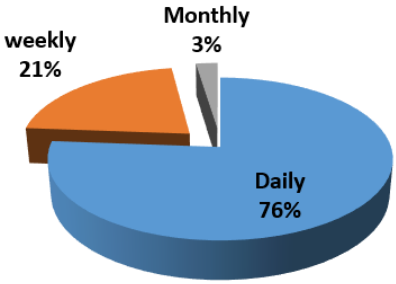

Figure 1. frequency of musculoskeletal Pains.

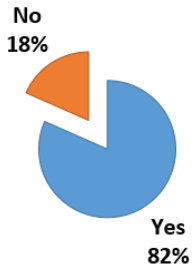

Figure 2. Prevalence of Musculoskeletal Disorders.

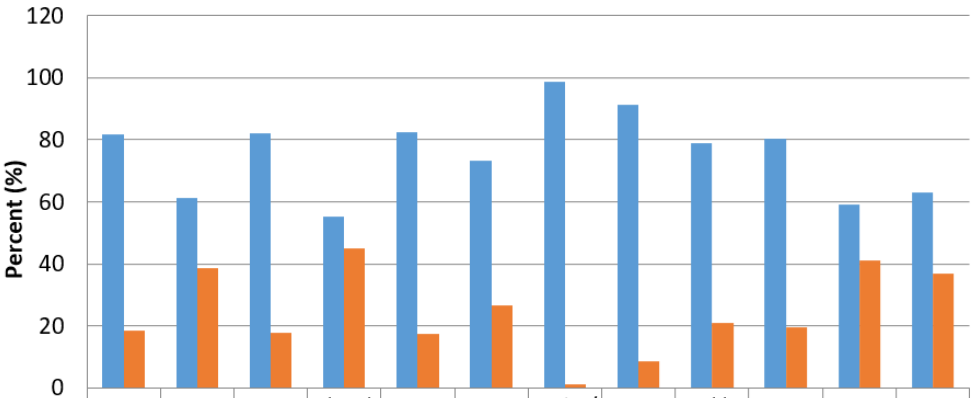

	Low Back	Leg	Upper Back	Shoulder	Neck	Knee	Wrist/ Hand	Thigh	Ankle /feet	Ears	Eyes	Head
Yes	81.6	61.2	82	55.1	82.5	73.3	98.8	91.3	78.9	80.3	59	63.1
No	18.4	38.8	18	44.9	17.5	26.7	1.2	8.7	21.1	19.7	41	36.9

Figure 3. Prevalence of Musculoskeletal pains.

The result of the study as shown in Figure 1 shows that most (76.2%) of the cyclist experiences pain everyday and 82% equally reportedly experienced pain in major body region (figure 2). Similarly, figure 3 also revealed the most commonly affected body regions among the motorcyclists were lower back (81.6%), leg (61.2%), upper back (82.0%), shoulder (55.1%),

neck (82.5%), knee (73.3%), wrist/hand (98.8%), thigh (91.3%), ankle/feet (78.9%), ears (80.3%), eyes (59.0%), and head (63.1%) respectively.

Discussion

The study demonstrated that more than 80% of the motorcyclists reported work-related musculoskeletal disorders (WRMSDs). This is about 255 higher than that 60% MSDs prevalence rate of commercial motorcyclist in Lagos Nigeria [7] and 10% lower compared with similar study of Jaiyesinmi et al., [4]. High level of WRMSDs among commercial motorcyclist may be attributed to the riding requiring excessive use of body regions. Consistent uses of all body parts are very important to maintain stability which involves maneuvering [8].

Most of the motorcyclist experience significant stress during and after riding for a long period of over 12hours. This stress was assessed on twelve body parts as shown in figure 3. The high prevalence of wrist/hand (98.8%) and thigh (91.3%) could be observed from the study. The other body regions, most affected was lower back, upper back, neck and knee. This study was comparable with [1, 4, 8].

Authors discovered that most of the studies in Nigeria found lower back to be most affected body region among cars, buses and trucks drivers [9, 10] and this is due to the long static and awkward position while driving and this is also very applicable to motorcyclist. Onawumi and Oyewale [1] reported that neck and head of the riders were upset which forced the rider to adjust to awkward position. Majority of the motorcyclist complained of lower back, wrist/hand and thigh while considerable number (55.1%) complained of shoulder related pains as against Onawumi and Oyewale [1] study. Prolong sitting and fixed posture could lead to muscular fatigue [11].

Ergonomic design of the motorcycle may also be attributed to discomfort of the rider. Majority of the motorcycle used in operation lack back support. Similarly, vibration exposure from the handbar could also lead to symptoms in the wrist/hand and shoulder [12]. The occurrence of WRMSDs among motorcyclists could lead to work inefficiency and low productivity. This is a major characteristics of RMSDs as highlighted by Centre for Disease Control (CDC) that “MSDs are associated with high cost to employers such as absenteeism, lost productivity and high increase health care, disability and workers compensation cost” [13].

Conclusion

The study shows that high prevalence of WRMSDs existed among the commercial motorcyclist in Abeokuta Nigeria. Socio-demographic and characteristics of work-related were identified as work related risk factors. Riding hours, posture, smoking and alcoholic drinking also played major factor associated with higher low back pains among the motorcyclists.

The stress and discomforts are seriously associated with the design failure of the motorcycle which is as a result of non-used of anthropometric dimension of the Nigerian motorcyclists. This stress and discomfort posed hazard to the rider due to the importation of the motorcycle to Nigeria without recourse to the adult population anthropometric dimension.

This study recommends that reduction in the hours spent in riding (working hours) could reduce the WRMSDs. Similarly, the anthropometric dimension of the adult Nigerians could also improve the ergonomic design of the motorcycle.

Limitation of the study

Most of the motorcyclist hinged on the security of the area and are not ready to attend to stranger whom they thought may use the data collected for rituals or other things. In view of this, authors resulted in the use of snowball techniques to reach out to their parks. Some of the motorcyclist (8.44%) claimed to be busy or in hasten and did not return the collected questionnaire with them.

References

1. Onawumi AS., Oyawale F.A. (2016). Ergonomic survey of commercial motorcyclist in Nigeria. Int J Eng Sci. 2016; 5 (2): pp. 23 - 28.
2. Karmegam K, Sapuan SM, Ismail MY, Ismail N, Shamsul Bahri MT, Seetha P. A. (2008). Study on motorcyclist's riding discomfort in Malaysia. Engineering e-Transaction, 4 (1): pp. 39 - 46.
3. Musa A.I. and Qutubuddin S.M. (2020). Ergonomics Study of the Incidence of Musculoskeletal Disorder among the School Teachers in Egba Division of Ogun State Nigeria. Journal of Science and Technology Research, Faculty of Engineering University of Benin Nigeria, Volume 2 (1) pp. 13 -2 0, ISSN 2680-5821 www.nipesjournals.org.ng.
4. Jaiyesinmi A.O., Areoye O.J., Olagbegi O.M., Bolarinde S.O., Uduonu E.C. (2018). Work-related musculoskeletal disorders and predisposing factors among commercial motorcyclists in Ibadan North local Government Area, Nigeria. Occupational Health Southern Africa, Volume 24, No 2 May/June 2018. www.occhealth.co.za
5. Musa A.I. (2020). Social Distancing and Musculoskeletal Disorder in Supermarket during COVID-19 Pandemic in Ogun State Southwest Nigeria. Journal of Science and Technology Research, Faculty of Engineering University of Benin Nigeria, Volume 2 (4) pp. 97 - 103, ISSN 2680-5821, www.nipesjournals.org.ng
6. Musa A.I., Yussouff A.A., Raji N.A., Ogedengbe T.S. and Rasheed S.O. (2017). Ergonomics Investigation of Musculoskeletal disorder among the Workforce of Waste Management Industry in Nigeria. Transaction of VSB-Technical University of Ostrava, Safety Engineering series, Volume 12 (2), DOI 10.1515/tvsbses-2017-0003 www.tses.vsb.cz
7. Akinbo S R, Odebiyi D.O, Osasan A.A. (2008). Characteristics of back pain among commercial drivers and motorcyclists in Lagos, Nigeria. West Afr J Med., 27(2): pp. 87 - 91.
8. Mohd Hafzi M.I, Rohayu S, Faradila P.N, Shaw V.W. (2011). Prevalence and risk factors of musculoskeletal disorders of motorcyclists. Malaysian Journal of Ergonomics. 2011; 1: pp. 1 - 10.
9. Akinpelu A.O, Oyewole O.O, Odole A.C, Olukoya R O. (2011). Prevalence of musculoskeletal pain and health seeking behaviour among occupational drivers in Ibadan, Nigeria. Afr J Biomed Res. 2011; 14, pp. 89 - 94.
10. Ojoawo AO, Onaade O, Adedoyin RA, Okonsi A .(2014). Assessment of work-related musculoskeletal pain among professional drivers in the service of a tertiary institution. Am J Health Res., 2 (5-1): pp. 56 - 60.
11. Pope, M., Magnusson M., Lundstrom R., Hulshof C., Verbeek J and M. Bovenzi M. (2002). Guidelines from whole-body vibration health surveillance. *Journal of Sound and Vibration*, vol. 253(1), pp. 131 - 167.
12. Haworth N and Rowden,P. (2006). Investigation of fatigue related motorcycle crashes – Literature review (RSD-0261). Report prepared for VicRoads by CARRS-Q.
13. The Centre for Disease Control and Prevention (CDC) (2017). Work-related musculoskeletal disorders & ergonomics. Workplace Health Promotion (Workplace Health Strategies); Available from: https://www.cdc.gov/workplacehealthpromotion/healthstrategies/musculoskeletaldisorders/ (accessed 17 Jul. 2021).

Journal of Engineering Science *Vol. XXIX, no. 1 (2022), pp. 112 - 120*
Fascicle *Architecture, Civil and Environmental Engineering* *ISSN 2587-3474*
Topic *Civil Engineering and Management* *eISSN 2587-3482*

https://doi.org/10.52326/jes.utm.2022.29(1).10
CZU 625.7:551.435(478)

LANDSLIDE PROTECTION OF ROADWAY NETWORK DURING THE CONSTRUCTION AND RECONSTRUCTION

Vladimir Polcanov, ORCID: 0000-0001-8389-2128,
Alina Polcanova, ORCID: 0000-0001-5826-8278,
Alexandru Cîrlan*, ORCID: 0000-0003-4009-2790

Technical University of Moldova, 168 Stefan cel Mare Blvd., Chisinau, Republic of Moldova
*Corresponding author: Alexandru Cîrlan, *alexandru.cirlan@cms.utm.md*

Received: 12. 17.2021
Accepted: 01. 28. 2022

Abstract. The article discusses an example of construction and operation of a high embankment of the road, which was constructed in the central part of Moldova. A detailed historic reference about the behavior of the embankment over 40 years of its operation is given. The reasons for the repeated deformations of the embankment have been identified. The analysis of the effectiveness of the undertaken landslide prevention works has been performed. In order to increase the effectiveness of landslide protection, the authors propose a procedure for multifactorial analysis of the interaction of complex natural systems and various engineering structures, which will allow designers to reasonably predict and make accurate design decisions in diverse geological settings.

Keywords: *effectiveness, embankment, highway, landslide deformations, landslide prevention works, rheology.*

Rezumat. Articolul discută un exemplu de construcție și exploatare a unui terasament înalt al drumului, care a fost construit în partea centrală a Moldovei. Se oferă o referință istorică detaliată despre comportamentul terasamentului pe parcursul a 40 de ani de funcționare. Au fost identificate motivele deformărilor repetate ale terasamentului. A fost efectuată analiza eficienței lucrărilor de prevenire a alunecărilor de teren întreprinse. Pentru a crește eficacitatea protecției alunecărilor de teren, autorii propun o procedură de analiză multifactorială a interacțiunii sistemelor naturale complexe și a diferitelor structuri inginerești, care să permită proiectanților să prezică în mod rezonabil și să ia decizii de proiectare precise în diverse setări geologice.

Cuvinte cheie: *eficacitate, terasament, autostradă, deformări alunecări de teren, lucrări de prevenire a alunecării, reologie.*

Introduction

The plans for the reconstruction of existing highways and construction of new highways, outlined by the Government of the Republic of Moldova, presume the encouragement of additional investments into the road industry. The effectiveness of their

use will be largely determined by the consideration of all hazardous geological processes that can have a negative impact on the road. Among the main of them are landslide developments [1 - 3].

Analysis of archive materials of IPDA ("*INSTITUTUL DE PROIECTĂRI DRUMURI AUTO*") and "*Intexnauca*" showed that during the construction and operation of the roads in Moldova, cases of the instability of roadside slopes, slopes of engineering structures, destruction of road topping, catchwater, retaining and enclosing structures have been observed on numerous occasions. This is due to the need to construct deep excavations and high embankments in tough terrain in Moldova.

At present time, about 170 landslides have been recorded on the motorways and railways of the republic. Despite the relatively small number of such locations, they occupy a significant area and often cover neighboring slopes. Most of the surveyed landslides are in an active development stage.

Due to the lack of accurate cost data, there is a significant range of values in the assessment of total damage. Roughly speaking, highways of the republic alone might cost 40 million US dollars.

The aforementioned point confirms the justifiability of recognizing the need to solve the landslide problem as one of the most important economic problems.

Justification for conducting the study

Upon choosing an object, setting the main goal and objectives of the study, a preliminary analysis of the landslides development on the highways and railways of Moldova was conducted. The results of the undertaken analysis are presented in [2].

Based on a detailed inspection of 80 locations, which are subject to landslide deformations, it was established that the anthropogenic factor was the cause of the landslide development in 25% of cases. Improper management of construction works, insufficient land development for construction, lack of effective anti-landslide protection, and low quality of performed work caused some of the landslides. An example is the case of partial destruction of the railroad section in the southern Moldova, between the towns of Cahul and Giurgiulesti in 2014. A kick-start of landslide processes in this area required an attraction of additional investments of more than $20 million.

The foregoing implies the need for paying closer attention to ensuring the safety of construction and operation of highways.

In this situation, look-ahead research, which is oriented to exclude the influence of the anthropogenic factor on the development of the landslide process, should be recognized as mandatory.

The quality of predevelopment research, which is the basis for the further feasibility study of an investment and construction project, is determined, inter alia, by the objectivity of the performed engineering and geological surveys [4]. Unfortunately, until now in the republic there are no regulatory documents in the field of design and construction, which take into account the diversity and specific regional features of the landslides evolvement. The studies conducted by the authors confirm that during the preparation of programs for engineering surveys, insufficient attention is paid to such fundamental issues as reducing the cost of surveys, cost-effectiveness analysis of works, acceleration of surveying, increasing the degree of their reliability.

Main objective of studies

The construction and reconstruction of highways planned for the near future will require the solution to problems related to ensuring the stability of natural slopes and slopes of engineering structures. Evidence shows that to ensure their long-term stability it will be necessary to develop a complex of landslide prevention works, which should take into account the rheological nature of deformation development [1, 2, 5].

Economic efficiency and economic expediency of the landslide control project will depend on how competently it will be developed. The cost of protective measures will undoubtedly have an impact on the total cost of road construction (reconstruction).

We chose to research a section of the Chisinau-Giurgiulesti highway, bypassing the town of Ialoveni. The main objective of the planned studies was to identify the reasons for recurrent deformations of the embankment and the effectiveness of the prescribed landslide prevention works.

Study techniques

The speed of detecting deformations of landslide massifs, recorded in the dynamics of their development, is universal information that allows revealing many aspects of the landslide process. In most cases, it is very difficult to obtain this information; therefore, experts can estimate the speed and amplitude of landslide processes only on the basis of visual observations. During these studies we used:

- Geodesic observational techniques with the use of modern electronic devices that allow obtaining sufficiently accurate observation results on the basis of a network of marks;
- Field geotechnical survey of natural slopes and road embankment slopes;
- Laboratory studies of the soils from the deformation location for determination of steady strength and rheological parameters: lightweight strength, viscosity grade, bond, cohesive properties and more;
- Graphic, analytical, and mechanical-mathematical simulations.

Survey results. Discussion

Following the main goal of the survey, the authors analyzed the extensive material which was obtained during the study of tech-work projects and detailed designs of landslide prevention works that were carried out on the considered section of the road [6 - 10].

Experts began to research the location in 1972. The program of surveys, which were carried out at that time, had a provision for the revealing the special aspects of geotechnical and hydrogeological conditions, as well as the physic-mechanical properties of soils for designing of the needed deformation prevention works [7].

Embankment construction works and the setup of strengthening and drainage structures were carried out from 1977 to 1980.

Unfortunately, deviations from the design decisions were observed during the construction phase: the embankment filling was performed with disturbances of process conditions. Confirmation of this fact comes from unacceptable fluctuations in the moisture-density of soils; the slopes were not strengthened, there were no trench drains, etc.

The road was in operation until August of 1984. It is worthwhile noting that during this period there were no regular observations over the condition of the embankment; for

this reason, the beginning of the process of slowly developing creep deformations in the mass of the embankment was not recorded.

On the 27th and 28th of August, 1984, the highway services established the existence of cracks in the concrete slabs of the right lane and displacement of the metal marginal bars. Serious movements occurred on September 4, 1984, when deformations of the lower part of the right slope began. The breakage wall was located below the berm; its height was 0.1 - 0.5m; deformed slope's width was 10 – 12m; its length - about 100,0m. Ground displacement (to the right) was up to 1.5m. The assumed thickness of the rocks, which were involved in the landslide dislocation, was estimated at 20 m; the volume of soil was estimated at 350-600 thousand m^3.

During the period of September 5 - 19 experts observed how the stage of the steady-condition creep develops into a progressing one. During the night of September 20, 1984, the embankment collapsed. The landslide was 140m wide; its length was 130m; the height of the breakage wall was 9.0m.

The landslide body had a block structure; the blocks were separated by deep (up to 6 meters) transversal cracks. The sliding tongue had a form of protrusion rampart up to 3.0m high. The surface outside the protrusion rampart was covered with a dense network of cracks.

In 1985, experts worked out a complex of works for restoration of the embankment [8], which included:

- dismantling the embankment (in the deformed area) to a depth of 9 meters;
- restoration of the embankment with slopes 1:2 and 1:3;
- setup of a tail slope;
- setup of a system of small sheet piles;
- setup of three-rowed retaining construction made of driven piles;
- setup of drainage and run-off systems.

The project was implemented in part.

In 1985 the road section was put into operation. However, as long ago as in August 1986 (after the earthquake), cracks with a width of up to 10 cm and a length of up to 25 meters were found on the slope and the shoulder of the road. The cracks periphery corresponded with the boundary of the right side of the landslide that had occurred earlier.

Arranged instrumental observations revealed the development of slow deformations of the embankment. The power of the tail slope was increased in order to stabilize them.

After the completion of works, the deformations of the embankments stopped. However, three years later, in the summer of 1994, the previously formed cracks opening and the formation of a significant deflection of the earthwork surface occurred. The next complex of landslide prevention works was issued in 1995 [9]. Unfortunately, planned works were not fully carried out this time either. As a consequence of this, the process of deformation development resumed.

Cracks with an opening width of up to 1.0 cm were formed for the space of 130 meters on the road surface, along its centerline and to the left of it by 0.5 - 1.0 m. On the right side, a pattern of a possible landslide was formed. It could be traced along the cracks with an opening width of 10 - 15 cm and a newly formed ledge, which had a height of 40 cm.

The right driving lane has descended vertically by 20 - 60 cm for the space of approximately 100.0 m. Horizontal displacements appeared, resulting in the deformation of the water gutters and their partial destruction.

Therefore, a complex of anti-landslide measures, including a one- and two-row structure made of Gambia piles, failed to guarantee the operation of the embankment and failed to prevent the development of deformations.

A new project was developed in 2009 [10]. Its development was preceded by detailed studies of the environmental conditions, field and laboratory trials, and numerous calculations. The causes and factors of the instability of the embankment were identified based on them.

The following was taken into account during the development of a new complex of measures:

- The embankment was constructed on an inclined surface of primary rocks. The incline of the natural slope along the centerline of the road is on average 4°; in the direction of dip line – 9 - 13°;
- The surveyed part of the embankment is located at the junction of two geomorphological elements: the floodplain of the brook (with a slight incline) and the slope of mean steepness;
- The embankment base on the slope is composed of Sarmatian clay, which is subject to creep deformations under conditions of the creep threshold decrease, which happens with an increase of moisture and a disruption of lightweight strength (as a result of the creep process itself);
- The embankment slope lies on a thick mass of water-saturated floodplain deposits, which are in an incomplete stage of consolidation.
- Lithological composition of soils, which form the embankment, is heterogeneous;
- A change in the moisture conditions during periods of maximum precipitation and snow melting leads to a decrease of the ground strength in the particular sections of the embankment, both along strike and at depth;
- Unassured drainage promotes surface-water infiltration into the mass of the embankment and, consequently, causes a reduction of the strength of rocks.
- Erosion advancement on the slopes and at the base of the embankment leads to a decrease in local stability;
- Side slopes in some sites do not meet the requirements for long-term stability;
- The waterlogged upper layers of the embankment are exposed to the dynamic influence of automotive transport, which reduces the strength and stress-related characteristics of the soils of the capping layer.

The fundamental reason for the occurrence of landslide processes was the development of volumetric rheological deformations in the body of the embankment.

The following additional works were performed in accordance with the revised mechanism for the development of landslide deformations:

- Capping layer soil cut and fill to a depth of 3.0 - 5.0 m;
- Works concerning assurance of impermeability and frost resistance of soils, which compose the road border and located immediately below road topping;
- Works concerning assurance of water disposal and surface water controls;
- Works concerning groundwater flow control (setup of groundwater cutoff);
- Change of slope gradients;
- Reinforcement of ramps through sowing grass, by planting vegetation with an advanced root system, which slows down the advancing of erosional-landslide processes.

The project was executed in 2010 (Figures 1 - 4).

Figure 1. Restoration work at a site of embankment bypassing the town of Ialoveni.
Source: Bogza S. from "Simbo-proiect S.R.L." 2009.10.06.

Figure 2. Arrangement of bored piles in the right slope of the embankment.
Source: Bogza S. from "Simbo-proiect S.R.L." 2009.10.06.

Figure 3. Section of embankment in December of 2019.
Source: Rascovoi A. from Technical University of Moldova.

Figure 4. Section of embankment in December of 2019.
Source: Rascovoi A. from Technical University of Moldova.

In December of 2019, the authors of this work carried out a visual inspection of the embankment section and performed works. It showed that there are no significant deformations in the mass of the embankment. However, in some spots, in the surfacing, there are longitudinal and transverse cracks opening up to 2 cm wide (Figure 5, 6). The origin of the cracks can be explained by the unfinished consolidation of the newly filled soils and, presumably, by the insufficient rigidness of the road material.

Figure 5. Longitudinal cracks in the road surface. December 2019.
Source: Rascovoi A. from Technical University of Moldova.

Figure 6. Transversal cracks in the road surface. December 2019.
Source: Rascovoi A. from Technical University of Moldova.

Conclusions and suggestions

An analysis of the condition of a high embankment, which was constructed on the bypass of Ialoveni town in tough terrain, showed that the stability of its slopes cannot be ensured without the application of a set of measures based on identifying the mechanism of the evolvement of landslide deformations.

Ensuring the stability of embankments is not always possible, it requires significant efforts and material expenses.

In order to increase the effectiveness of landslide protection, the authors propose to create a procedure for multifactorial analysis of the interaction of complex natural systems and various engineering structures, which will allow designers to reasonably predict and make accurate design decisions in diverse geological settings.

Development of practical recommendations will facilitate, among other things, the appropriate selection of optimal alternative for the road renovation for the 9th Pan-European corridor with reference to the maintenance of ecological equilibrium in the most vulnerable part of the central Codri. In the long term, this will ensure the stability of the subgrade on the

examined road with the use of minimal financial and material resources and maintaining a high degree of reliability of key decisions. Multi-purpose use of survey results will allow to improve environmental protection and to ensure the protection of not only linear infrastructure but also valuable commercial lands.

Acknowledgments. The authors would like to express sincere gratitude to the management and staff of IPDA ("INSTITUTUL DE PROIECTĂRI DRUMURI AUTO"), "Intexnauca S.A." and "Simbo-proiect S.R.L." for the opportunity to use archival materials during the work on this article.

References

1. Polcanov V.N. *Roli reologicheskih processov v razvitii opolznej na territorii Moldovy* [The role of rheological processes in the development of landslides on the territory of Moldova]. Chisinau: UTM: Tehnica – UTM, 2013.
2. Polcanov V.N., Polcanova A.V. Opyt izuchenija inzhenerno-geologicheskih uslovij ustojchivosti sklonov i otkosov iskusstvennyh sooruzhenij [The experience of studying geologico-enginering stability conditions of natural slopes and slopes of engineering structures]. – Chisinau: UTM: Tehnica – UTM, 2017.
3. Cîrlan A. *Studiul proprietăților reologice ale solurilor pentru evaluarea stării de tensiune-deformație a terenurilor de fundații* [Investigation of the rheological properties of soils for the assessment the base stress-strain state]: Ph.D. Thesis [online]. Chisinau (Republic of Moldova): Technical University of Moldova, 2019. [accesat 13.07.2021]. Disponibil: http://www.cnaa.md/files/theses/2019/54491/alexandru_cirlan_thesis.pdf
4. Bondarik G.I. *Inzhenerno-geologicheskie izyskanija* [Engineering and geological resarch]. – Moscow: ID KDU, 2008.
5. Bukatchuk P.D., Blyuk I.V., Pokatilov V.P. *Geologicheskaja karta MSSR. M-b 1:200000 (Objasnitelinaja zapiska)* [Geological map of the MSSR. Sc. 1:200000 (Explanatory note)]. – Chisinau, 1988.
6. Polcanov V., Funieru N. *Despre proiectarea și edificarea construcțiilor rutiere pe teren accidentat pe teritoriul Moldovei* [About designing and building road construction on rough terrain on the territory of Moldova] In: Inginerie civilă şi educație. 2019. pp. 97-100.
7. *Tehno-rabochij proekt rekonstrukcii avtomobilinoj dorogi Kishinev-Bolgrad v rajone s. Jaloveny (obiekt №767) [The technical-working project for reconstruction of Chisinau-Bolgrad highway in the area of Ialoveni (object No. 767)]*. Archive of IPDA. – Chisinau, 1973.
8. *Otchet ob inzhenerno-geologicheskih izyskanijah dlja meroprijatij po vosstanovleniju nasypi na avtomobilinoj doroge Kishinev-Bolgrad na uchastke obhoda p.g.t. Kutuzovo (obiekt №1222)* [Report of engineering-geological surveys for measures to restore the embankment on the Chisinau-Bolgrad highway at the bypass section of the urban-type settlement. Kutuzovo *(object No. 1222*]. Archive of IPDA. – Chisinau, 1985.
9. *Otchet ob inzhenerno-geologicheskih izyskanijah dlja protivo-opolznevyh meroprijatij na avtomobilinoj doroge Kishinev-Chimishlija-Vulkjeneshti-Dzhjurdzhjuleshti-granica s Rumyniej na uchastke obhoda p.g.t. Jaloveni (obiekt №3170)* [Report on engineering-geological surveys for anti-landslide measures on the highway Chisinau-Cimislia-Vulcanesti-Giurgiulesti-border with Romania at the bypass section of the urban-type settlement. Ialoveni (object *No.* 3170).]. Archive of IPDA. – Chisinau, 1995.
10. *Otchet ob inzhenerno-geologicheskih izyskanijah na obiekte "Reabilitacija avtomobilinoj dorogi R3 Kishinjeu-Hyncheshti, uchastok obhoda gJaloven'"* [Report on engineering and geological surveys at the object "Rehabilitation of the R3 Chisinau-Hincesti road, bypass section of Ialoveni"]. Archive of UNIVERSCONS" S.R.L. – Chisinau, 2009.

Journal of Engineering Science *Vol. XXIX, no. 1 (2022), pp. 121 - 129*
Fascicle *Architecture, Civil and Environmental Engineering* *ISSN 2587-3474*
Topic *Environmental Engineering* *eISSN 2587-3482*

https://doi.org/10.52326/jes.utm.2022.29(1).11
CZU 551.55:504.3(478)

REGARDING THE CHARACTERISTICS OF THE WIND IN NORTHERN REGION DISTRICTS OF THE REPUBLIC OF MOLDOVA

Octavian Mangos*, ORCID: 0000-0003-2934-6040,
Vasile Rachier, ORCID: 0000-0003-4590-7012,
Ion Sobor, ORCID: 0000-0002-5387-126X,
Vadim Cazac, ORCID: 0000-0002-2887-7520

**Technical University of Moldova, 168 Stefan cel Mare Blvd., Chisinau, Republic of Moldova*
Corresponding author: Octavian Mangos, *octavian.mangos@ie.utm.md*

Received: 01. 22. 2022
Accepted: 02. 21. 2022

Abstract. The study is focused on three districts in the northern region of the Republic of Moldova - Briceni, Edinet and Ocnita. The maps were calculated and presented in terms of average annual wind speed and wind power density at a height of 100 m above ground level, wind rose and Weibull wind speed distribution. In the calculations performed for the three analyzed districts it was found that the average annual wind speed is between 6.84 and 7.35 m / s, and the wind power density - between 450 and 593 W / m^2. The highest annual average speed equal to 7.35 m / s was identified in Ocnita district. At the same time, having the maps of the wind speed and the power density, the convenient locations for the construction of the wind farms can be selected. For each district involved in the study, a location with a pronounced wind potential was identified, recommended for the location of any wind farms.

Keywords: *wind speed; power density, wind atlas method, software package WAsP 9.1.*

Rezumat. Studiul se concentrează pe trei raioane din regiunea de nord a Republicii Moldova - Briceni, Edineț și Ocnița. Au fost calculate şi prezentate hărțile în ceea ce privește viteza medie anuală a vântului și densitatea puterii eoliene la înălțimea de 100 m deasupra nivelului solului, roza vântului și distribuția Weibull a vitezei vântului. În calculelor effectuate pentru cele trei raioane analizate s-a constatat că viteza medie anuală a vântului este cuprinsă între 6,84 și 7,35 m/s, iar densitatea de putere eoliană - între 450 și 593 W/m^2. Cea mai mare viteză medie anuală egală cu 7,35 m/s a fost identificată în raionul Ocnița. Totodată, având hărțile vitezei vântului și a densității de putere, se pot selecta locațiile convenabile pentru construirea parcurilor eoliene. Pentru fiecare raion implicat în studiul respectiv au fost identificate câte un amplasament cu potențial eolian pronunțat, recomandat pentru amplasarea eventualelor parcuri eoliene.

Cuvinte cheie: *viteza vântului; densitatea de putere; metoda atlasului vântului; pachetul software WAsP 9.1.*

Introduction

The need for studies on wind characteristics and wind potential was highlighted when the drafting of the legal framework for the capitalization of Renewable Energy Sources (RES) started. The Law on renewable energy no. 160 of 12.07.2007 sets (for the fi rst time in our country's history) the objectives of the state policy in the fi eld of renewable energy, which were then updated in the Law on the promotion of renewable energy sources no. 10 of 26.02.2016. Law no. 10 creates the necessary framework for the application of Directive 2009/28/EC of the European Parliament and
of the Council of 23 April 2009 on the promotion of the use of energy from renewable sources, establishes the mechanism to support investors that will promote the use of RES and which will come into force in March 25, 2018 [1]. The roadmap in the fi eld of RES capitalization - National Plan of Action in the Field of Energy from Renewable Sources (NPERS) adopted by Government Decision no. 1073 of 27 December 2013 highlights the activities and objectives needed to be achieved for the years 2013-2020. Thus, in the list of Support mechanisms for promoting energy from renewable sources - electricity, heating and cooling and energy from renewable sources in transport, paragraph 58 provides for the Development of a study on the wind and solar potential resulting in the expected Atlas of the wind potential and Atlas of the solar potential.

Having said that, this study is focused on three districts - Briceni, Edineț and Ocnița, the main cause being the interest of local investors in capitalizing on the wind potential to produce electricity. According to the National Agency for Energy Regulation (NAER) [2] in 2019, the wind capacity installed in the respective districts constituted 43.3% of the total wind capacity of the country. Furthermore, due to the cubic relationship between wind velocity and output energy, sites with small percentage differences in average wind speeds can have substantial differences in available energy. Therefore, accurate and thorough monitoring of wind resource at potential site is a critical factor in the siting of wind turbines.

Methodology

In 1987 the Department of Meteorology and Wind Energy at Riso National Laboratory in Denmark has implemented Wind Atlas Method (WAM) as a powerful tool for wind data analyzing, wind energy resources mapping, power production calculation of a wind turbine or a wind farm. Over the years, WAM has become a standard method for assessing wind resources and wind turbine siting and has been used in over 100 countries worldwide. The first work at global level dedicated to assessing wind energy potential, should be considered European Wind Atlas published in 1989 [3]. The value of this Wind Atlas is more precious by attaching a set of programs called Wind Atlas Analysis and Application Program (WAsP) [4, 6], which can be used to process wind raw data, drawing meteorological station wind atlas and wind power potential estimation of a certain site. In this work was used the Wind Atlas Method and licensed software package WAsP 9.1.

WAM offers the possibility to transform wind data recorded over the years, called historical data, to describe the wind characteristics at one point or in a region where no measurements were made [14]. The length of the radius of the point where wind data are available, either historic or recent, to the point where we can predict the wind should not exceed 100 km [10].

Wind data collected by weather stations (normally, at height of 10 m above the ground) or through special campaigns of measurements at heights greater than 10 m, are

representative only for points where anemometer and vane are mounted for measuring wind speed and direction. These data are influenced by the site characteristic (orography, terrain roughness, obstacles) around the measurement tower and cannot be used directly to characterize the wind in an another location with different characteristics from those in which the measurement tower is mounted. In order to use data from one site to calculate speed and wind power density into another site, measured data are converted into so-called wind atlas data for the specific meteorological station [9].

WAM consists of two distinct procedures: first - to analyze wind in the measurement point and the second - the application of climatology data to obtain wind speed maps and wind power density, energy production etc. in a point (region) where no measurements were performed. To obtain Wind Atlas data on the surroundings measurement tower are carried out studies like identifying roughness class of the terrain, obstacles (buildings, forests protective stripes etc.) existing at a distance not exceeding 50 heights of that obstacle and it porosity [12, 13].

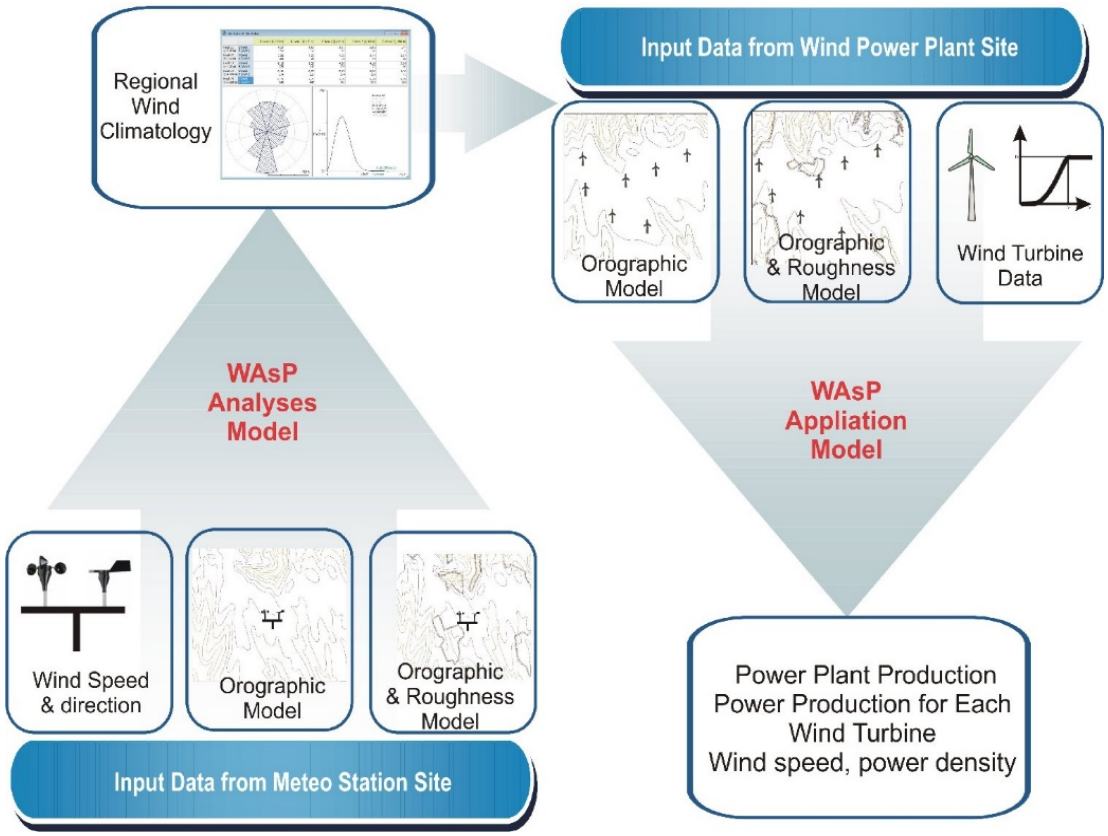

Figure 1. Wind Atlas methodology, done by authors.

Applying the analysis procedure of WAM, Figure 1 left, obtained wind atlas data, would have been recorded if the terrain roughness had been equal to 0 (water surface) and around measurement tower obstacles wouldn't exist. Wind atlas data are recalculated for 5 roughness classes, characterized by respective equivalent heights equal to 0,0; 0,03; 0,1; 0,4 and 1,5 m and 5 heights above the ground: 10, 25, 50, 100 and 200 m. With wind atlas data as input data, the reverse procedure is carried out, Figure 1 on the right, to yield the regional climatology of the wind in the region of interest.

At the applying phase of WAM, Figure 1 right, as the object of study can be: a wind turbine shown by the coordinates of the mounting point, a wind farm shown by the

coordinates of all turbines or a rectangular region with specified borders. As an input data are:

- Observed Wind Climate (OWC) at Balti meteorological station. OWC for all Moldova's 14 meteorological station are presented in [5];
- Terrain orography and roughness, obstacles in the immediate vicinity of the points of location of turbines;
- Turbine wind power characteristic P(u) and the height of rotation turbine axis [17, 18].

Depending on what we need: regional wind climatology of interest region at the specified height above the ground, wind energy resources maps in terms of mean wind speed and wind power density at the specified height above ground and average annual electricity production will be obtained. For each wind turbine: gross and net annual energy production, average speed at shaft rotation height, wind power density, energy losses due to the effects of turbulence caused by other turbine (wake losses) will be obtained.

Results

Wind maps. For three districts from north Moldova's region were calculated wind maps in terms of wind speed and wind power density. The results are presented in Figures 2 - 7.

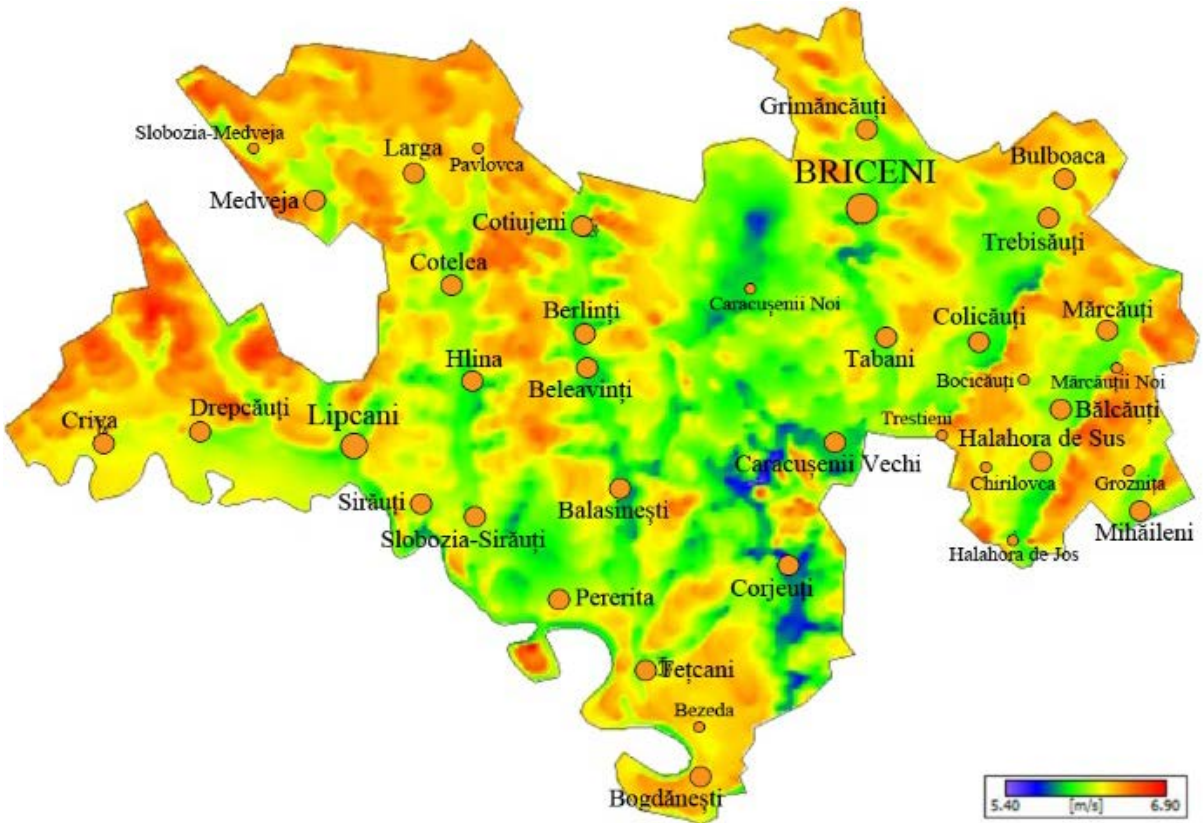

Figure 2. Briceni district: average annual wind speed - done by authors in WAsP 9.1 licensed software.

Having the maps of the wind speed and power density, we can do the next step: select a location for the construction of wind farms. For example, for the Briceni district, it was selected the hill located in southeast of the village of Balcauti. The advantage of this hill is the possibility of placing the wind turbines in a row perpendicular to the predominant wind direction.

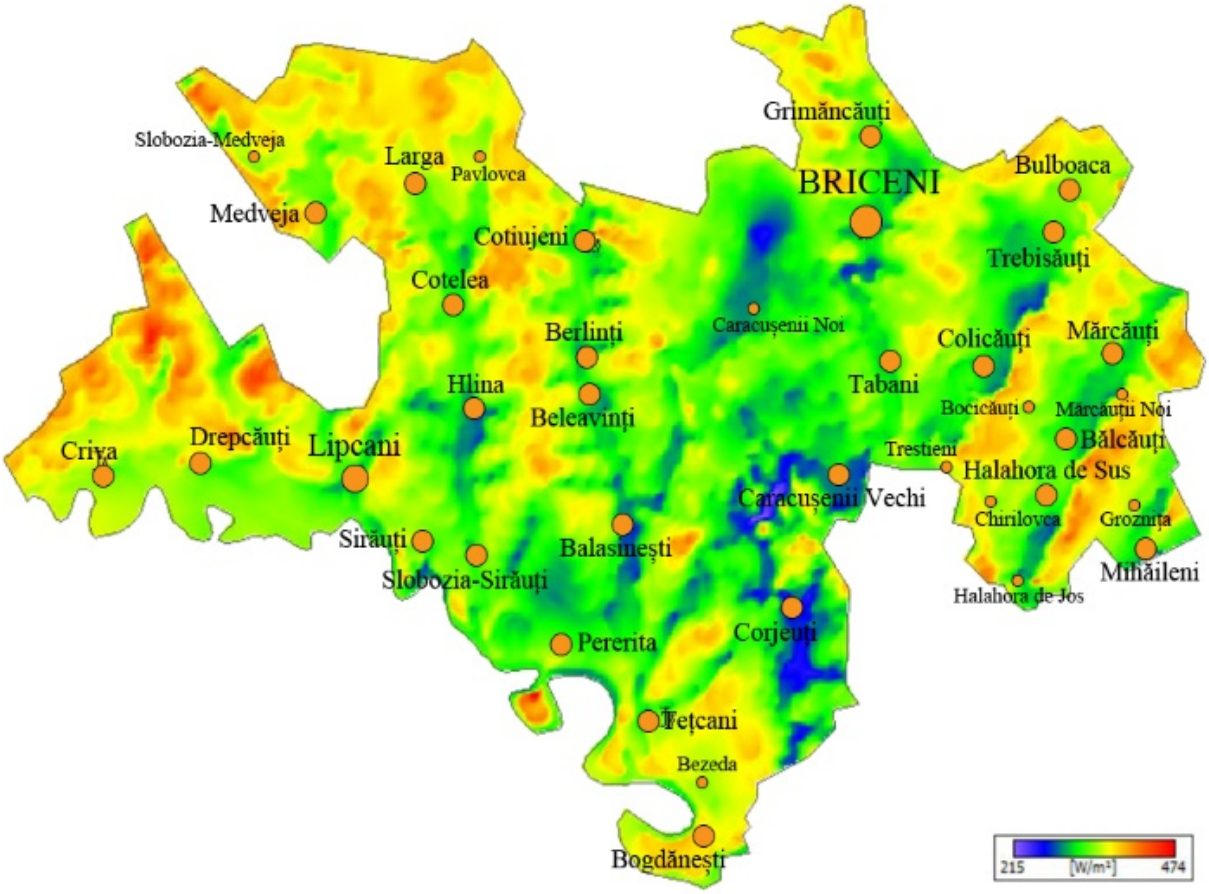

Figure 3. Briceni district: average annual wind power density - done by authors in WAsP 9.1 licensed software.

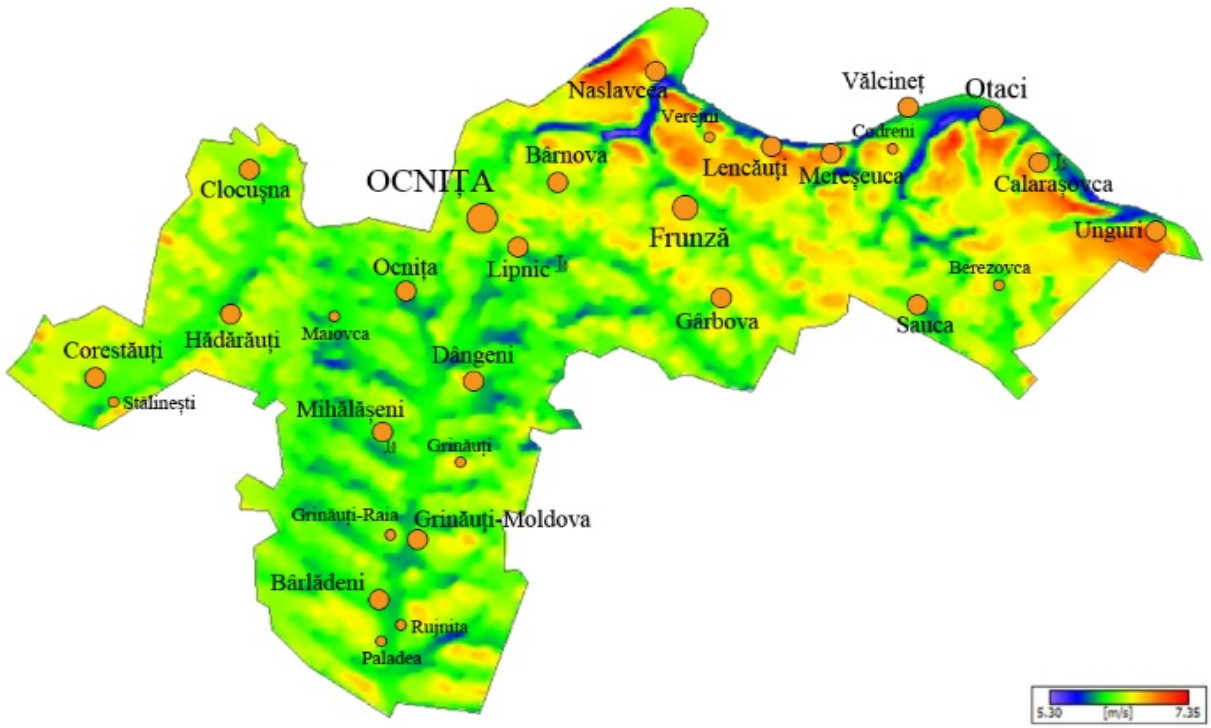

Figure 4. Ocnița district: average annual wind speed - done by authors in WAsP 9.1 licensed software.

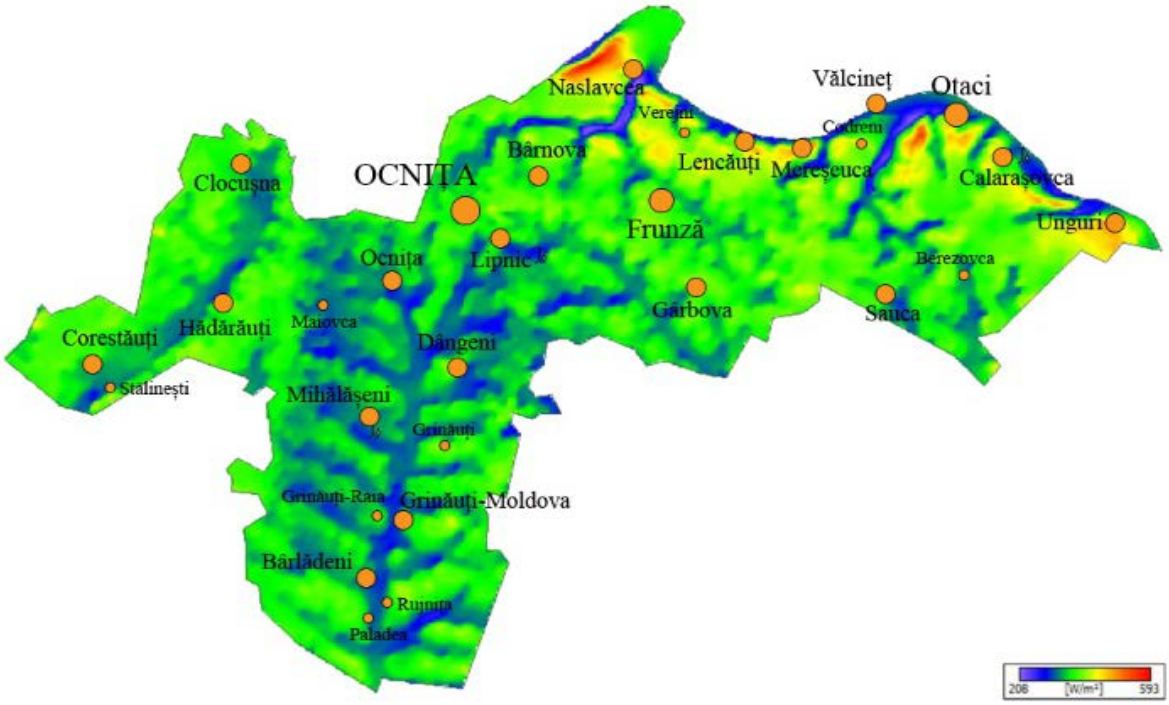

Figure 5. Ocnița district: average annual wind power density - done by authors in WAsP 9.1 licensed software.

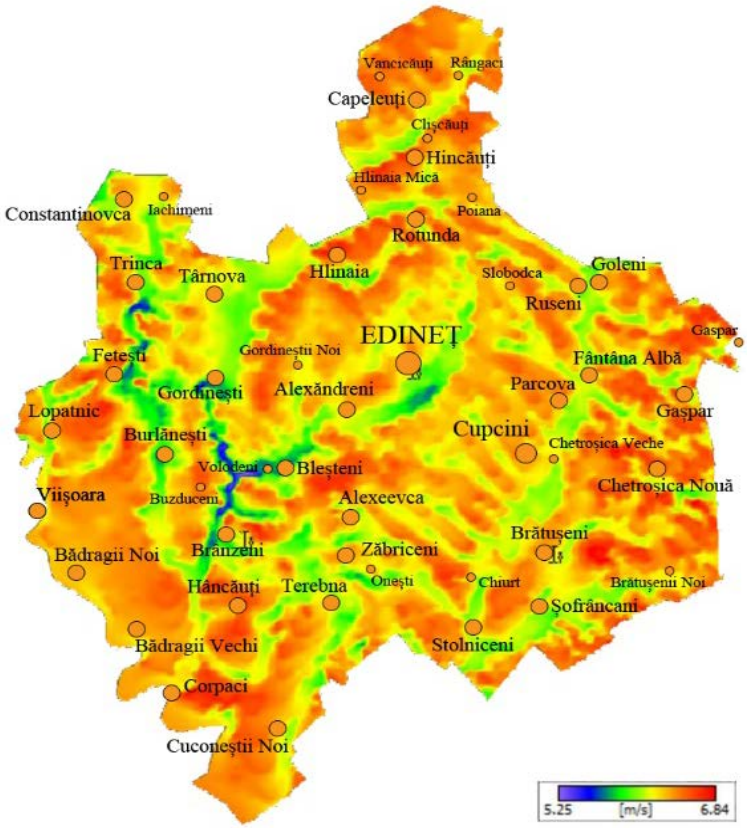

Figure 6. Edinet district: average annual wind speed - done by authors in WAsP 9.1 licensed software.

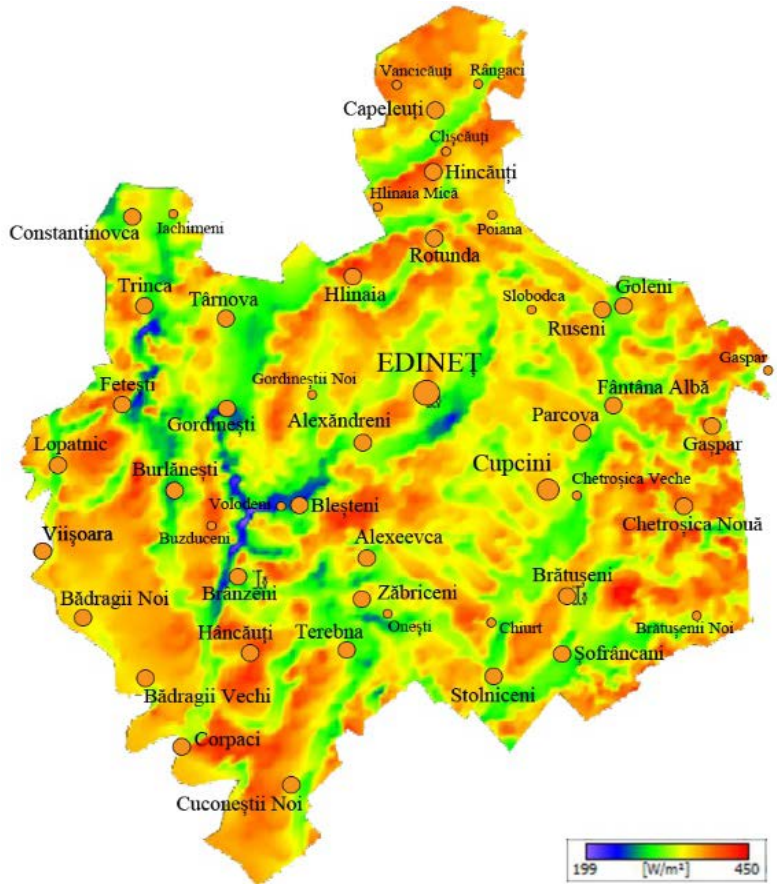

Figure 7. Edinet district: average annual wind power density - done by authors in WAsP 9.1 licensed software.

Applying the WAM, we also obtained wind rose & wind speed Weibull distribution, with the following results Figure 8:

1. Wind direction (wind rose) for 12 sectors.
2. Wind speed frequency distribution.
3. Weibull approximation of wind speed frequency distribution histogram.
4. The average wind speed in m/s and power density in W/m2.
5. Weibull approximation coefficients A and k.

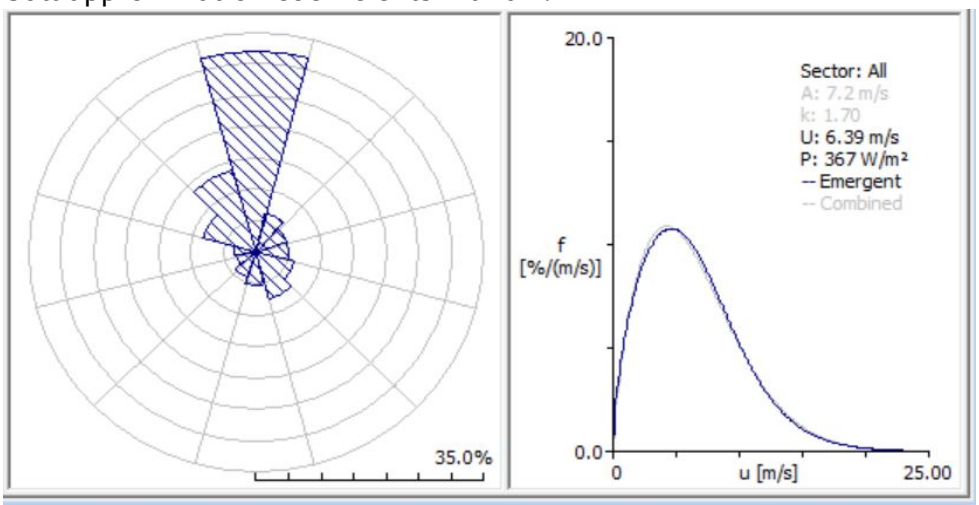

Figure 8a. Wind rose & wind speed Weibull distribution: Briceni district - done by authors in WAsP 9.1 licensed software.

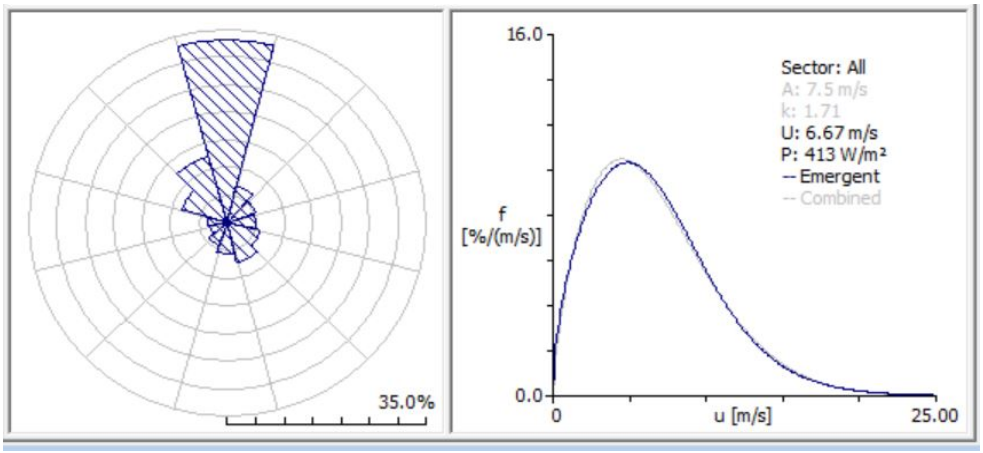

Figure 8b. Wind rose & wind speed Weibull distribution: Ocnița district - done by authors in WAsP 9.1 licensed software.

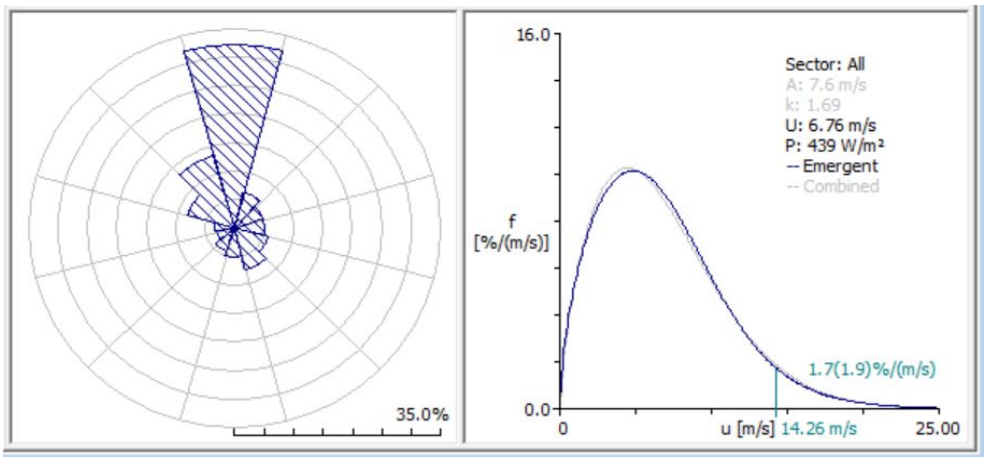

Figure 8c. Wind rose & wind speed Weibull distribution: Edinet district - done by authors in WAsP 9.1 licensed software.

For the analyzed districts, we have used historical wind data for a 10 years period from Balti weather station. The Balti weather station is situated near the Balti airport and is located about 2 km from the river Raut on its left bank, where the terrain is a relatively smooth meadow. To the south and southeast of the station, at distance of 4 - 10 km, the landscape is hilly, interspersed with valleys and ravines. The heights of the hills are 150 - 200 m. The width of the river valley in the station region varies between 4 - 5 km, and the river ranges from 3.5 to 5.5 m. Meteorological platform is on smooth area, covered with cover grassy and at about 70 m around it are located houses with solitary trees height of 4 - 5 m. At about 500 m in direction north is the route Balti - Floresti and the railway line. In the east of the station, about 100 m, extends the airport area and it is an open smooth field.

As a result of the calculations based on the obtained maps we performed the classification of the territory of each of the three districts according to the value of the power density and we determined the following:

- 48,62 % of the Briceni district surface has a power density between 350 - 400 W/m^2;
- 48,93 % of the Ocnita district surface has a power density between 350 - 400 W/m^2;
- 48,74 % of the Edinet district surface has a power density between 350 - 400 W/m^2.

According to the European Wind Atlas [3] and other publication, the areas, which has a power density, between 350 - 400 W/m^2, it is recommended to be used for possible wind farms.

Conclusions

1. In the three analyzed districts the average annual wind speed calculated at a height of 100 m above ground level is between 6,84 and 7,35 m/s and the wind power density - between 450 and 593 W/m^2. The highest average annual wind speed has been found in Ocnita district and is equal to 7,35 m/s.
2. For the development of wind farms, we recommend following sites:
   - Briceni district - the hill located southeast of the line connecting the villages of Halahora de Sus-Balcauți-Marcauți (See Figure 2);
   - Ocnița district - locations settled in the northeast at a distance of 5 - 8 km from the Dniester River (See figure 4);
   - Edinet district - in the northern and western areas, along the Prut river (See figure 6).
3. For all 3 districts about 48 % of the territory have a power density greater then 350 W/m^2, territory what can be used for possible wind farms.

Acknowledgments. This work was supported by the project no. 20.80009.7007.10 *„Studying the wind and solar energy potential of the Republic of Moldova and developing conversion systems for dispersed consumers”*.

References

1. LEGE Nr. 10 din 26-02-2016 privind promovarea utilizării energiei din surse regenerabile.
2. Report on the activity of the National Agency for Energy Regulation in 2019.
3. Ib Troen and E. L. Petersen. European Wind Atlas. RISO National Laboratory. Roskilde, 1989, 656 p. ISBN 87-550-1482-8.
4. Mortensen N. G., Landberg L., Troen Ib., Petersen E. L., Rathmann O. and Nielsen M. WAsP Utility Programs. Riso-I-2261(EN). Roskilde, 2004, 54 p.
5. Wind Energy Resources Atlas of the Republic of Moldova/Ion Sobor, Andrei Chiciuc, Vasile Racher; Univ. Tehn. a Moldovei, Agenția pentru Eficiență Energetică, AWS Truepower [et al.]. – Chișinău, 2017. – 176 p. ISBN 978-9975-87-275-1.
6. The Economics of Wind Energy. A report by European Wind Energy Association. March 2009, 155 p.
7. Erik Lundtang Petersen, The new generation of tools for prediction of wind power potential and site selection, Accesibil pe site-ul: http://orbit,dtu,dk/.
8. Weibull W. A statistical Distribution Function of Wide Applicability. Journal of Applied Mechanics, Transactions of the American Society of Mechanical Engineers. September, 1951, pp. 293-297.
9. Bowen A. J., and Mortensen N. G. WAsP prediction errors due to site orography. Riso-R-995(EN), Roskilde, 2004, 65 p. ISSN 0106-2840; ISBN 87-550-2320-7
10. Rathmann O., Mortensen N. G., Landberg L., and Antoniou I. Assessing the accuracy of WAsP in non-simple terrain. BWEA 18th Conference, 24-27 September, 1996, University of Exeter, UK, pp.1-6.
11. Bowen A. J., and. Mortensen Niels G Exploring the limits of WAsP: the Wind Atlas Analayses and Application Program. European Union Wind Energy Conference, 20-24 May 1996, pp.584-587.
12. Mortensen N. G., and Petersen E. L. Influence of topographical input data on the accuracy of wind flow modeling in complex terrain. European Wind Energy Conference & Exhibition 1997, Dublin Ireland, Octomber, 6-9 1997, pp.317-320.
13. Mortensen N. G., Bowen A. J., and Antoniou I. Improving WAsP predictions in (too) complex terrain. Proceedings of the European Wind Energy Conference, Athens (GR), 27 Feb - 2 Mar, 2006.
14. Sobor I., Chiciuc A., Azarov A., Rachier V. Variațiile diurne ale vitezei vântului în zona podișului central al Republicii Moldova, Buletinul AGIR, Volumul I, ianuarie - martie 2013, București, pag 139-144.
15. Alam Md. Mahbub et al. Wind speed and power characteristics at different heights for a wind data collection tower in Saudi Arabia. World Renewable Energy Congress, 8-13 May 2011, Linkoping, Sweden, pp. 4082-4089.
16. Redburna Rachel. Tall Tower Wind Iinvestigation of Northwest Missouri. MSc thesis. University of Missouri-Columbia, 2007.
17. Wizelius T. Developing wind power projects: theory and practice. London, 2009, 290 p. ISBN: 978-1-84407-262-0. Michael C. Brower (Ed), 2012. Wind Resource Assessment: A Practical Guide to Developing a Wind Project. John Wiley & Sons, 298 pp.
18. Manwell James F., McGowan Jon G, Rogers Anthony L. 2010. Wind energy explained: theory, design and application, 2nd Edition. John Wiley & Sons, 704 pp.

Journal of Engineering Science *Vol. XXIX, no. 1 (2022), pp. 130 - 141*
Fascicle *Architecture, Civil and Environmental Engineering* *ISSN 2587-3474*
Topic *Environmental Engineering* *eISSN 2587-3482*

https://doi.org/10.52326/jes.utm.2022.29(1).12
CZU 620.9:661.722

BIOMASS PRETREATMENT AS A KEY PROCESS IN BIOETHANOL PRODUCTIONS: A REVIEW

Toyese Oyegoke[1*], ORCID: 0000-0002-2026-6864,
Geoffrey T. Tongshuwar[2], ORCID: 0000-0002-8801-8525,
John E. Oguche[1], ORCID: 0000-0001-6319-7865

[1]*Ahmadu Bello University, Chemical Engineering Department, Samaru Campus, Zaria, Kaduna State, Nigeria*
[2]*Federal University, Biochemistry Department, Main Campus, Dutsinma, Dutsin-ma LGA, Katsina State, Nigeria*
*Corresponding author: Toyese Oyegoke, *OyegokeToyese@gmail.com*

Received: 11. 30. 2021
Accepted: 01. 14. 2022

Abstract. Solid wastes like lignocellulosic materials have proven to be of immense benefit to the production of bioethanol and have given a headway towards the deviation from the traditional use of fossil fuel which is has been a long-time primary source of fuel and energy globally. The transformation of lignocellulosic wastes into bioethanol is of importance to the environment. The recalcitrant nature of this substance, owing to the presence of lignin which serves as a deterrent, making it hard to access cellulose and hemicellulose, which are later converted to bioethanol, has raised much concern for researchers. Various strategies for feed preparation for overcoming this problem have been identified by researchers in the literature, including chemical, physical, and physiochemical approaches with enzymes. This review aims to bring together recent advances made by researchers in different pretreatment methods in optimizing the production of bioethanol. The advantages, disadvantages and the specific conditions for these pretreatment methods are also discussed in this review. Embedded in this review is also a report of the usage of some of these feed preparation strategies and the amount of bioethanol that was obtained by each process using different feedstock.

Keywords: *Bio-alcohols, biofuels, biorefinery, environment, wastes, cellulose, pollution.*

Rezumat. Deșeurile solide, cum ar fi materialele lignocelulozice, s-au dovedit a fi de un beneficiu imens pentru producția de bioetanol și au făcut progrese către abaterea de la utilizarea tradițională a combustibilului fosil, care a fost o sursă primară de combustibil și energie la nivel global. Transformarea deșeurilor lignocelulozice în bioetanol este importantă pentru mediu. Natura recalcitrantă a acestor substanțe, din cauza prezenței ligninei, care servește ca un factor de descurajare, îngreunând accesul la celuloză și hemiceluloză, care sunt ulterior transformate în bioetanol, a stârnit multă îngrijorare pentru cercetători. Cercetătorii din literatură au identificat diverse strategii de preparare a hranei pentru a depăși această problemă, inclusiv abordări chimice, fizice și fizico-chimice, enzimatice. Această revizuire își propune să reunească progresele recente realizate de

cercetători în diferite metode de pretratare pentru optimizarea producției de bioetanol. Avantajele, dezavantajele și condițiile specifice pentru aceste metode de pretratare sunt, de asemenea, discutate în această recenzie. În această revizuire este inclus și un raport despre utilizarea unora dintre aceste strategii de preparare a furajelor și cantitatea de bioetanol care a fost obținută prin fiecare proces folosind diferite materii prime.

Cuvinte cheie: *Bio-alcooli, biocombustibili, biorafinărie, mediu, deșeuri, celuloză, poluare*.

Introduction

The use of fossil fuels has proven to be unfriendly to the biosphere. The unfriendly nature has resulted into increased greenhouse gases in the atmosphere and an increase in the depletion of the ozone layer. Despite the depleting amount of fossil fuel, there is an increasing demand for fuel due to the increase in the number of industries and human activities dependent on energy [1]. Hence, there is a need to look for an alternative source of energy that is renewable and eco-friendly, which biofuels tend to offer. To save the world and the economy, a more eco-friendly source of fuel that is readily available at a cheaper rate needs to be provided. This subject has been the centre of energy research lately [2].

The use of biofuels as an alternative renewable and clean source of energy has attracted the attention of researchers all over the globe. Lignocellulosic biomass (examples of the biomass is in Figure 1 has proven to be promising. They include but are not limited to corn straw, sugarcane bagasse, cassava, rice straw. These parts of the plants are non-digestible by humans, which makes it better as there would be no competition for food. The use of this lignocellulosic feedstock also serves to recycle the waste, which is environmentally friendly [3 – 6]. Also, lignocellulosic materials are not available for bio-digestion due to the presence of residue (lignin) in lignocellulosic material, which limits fuel conversion and leads to low yield [7]. Hence there is a need for pretreatment of these materials to obtain a high yield of fuels.

Figure 1. Some Agro-wastes that could be used in bioethanol productions [8].

This paper focuses on reviewing the impact of the different pretreatment methods employed in the literature in bioethanol production using Nigeria biomass resources. This would aid in unveiling the most significant method that better promote the production of bioethanol in developing nations like Nigeria and to reveal areas where further studies are needed for the realization of biorefinery feasibility in developing nations.

Concept of Pretreatment

Lignocellulosic feedstocks are made up of a network of Cellulose, Hemicellulose and Lignin. Though promising, lignocellulosic feedstock offers a significant challenge due to recalcitrance. They are resistant to chemical and biological breakdowns making it hard for biofuel production. Due to this, pretreatment becomes very vital.

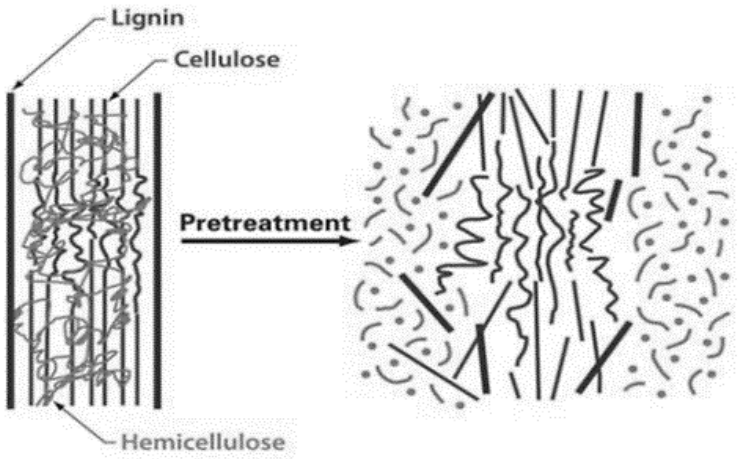

Figure 2. Effect of pretreatment on lignocellulosic biomass to liberate cellulose and hemicellulose [9].

Pretreatment is defined as the process that clears away both the physical and chemical barriers that make feedstock recalcitrant and make it susceptible to enzymatic hydrolysis [10 - 11].

The concept of pretreatment is aimed at making feedstocks susceptible to further treatment by making cellulose and hemicellulose more accessible. This could be achieved through various means. Pretreatment could break down solid feedstock or even reduce the degree of crystallization of cellulose.

Lignin is extracted owing to its phenolic nature, which thereby makes the feedstock more digestible [12]. Figure 2 shows the effect of pretreatment on lignocellulosic biomass to liberate cellulose and hemicellulose.

From Figure 2 above, it can be observed that pretreatment is a critical step. It is important to find pretreatment methods that can give a high yield of bioethanol and, at the same time, be economical and eco-friendly.

Biomass Pretreatment Significances to the Production of Bioethanol in a Biorefinery

The chemical composition of feedstock is such that if not pretreated, bioethanol production would not be efficient.

Pretreatment increases the efficiency and efficacy of bioethanol production. This is necessary because the cost of production of bioethanol is dependent on the cost-effective measure or method of pretreatment as it forms a very vital part of the production process.

Pretreatment breaks down the strong association within the cell wall by bringing about physical, chemical, and biological changes to it. Because different feedstocks have a varied abundance of Cellulose, Hemicellulose and Lignin, their outcome differs. A suitable pretreatment method is one that is cost-effective, require minimal energy to run, does not denature cellulose and hemicellulose and does not produce by-products that inhibit the activity of microorganisms that are responsible for hydrolysis and fermentation [12].

With the aim of creating a very suitable method of pretreatment, several methods have been developed, each with its pros and cons. They can be categorized into physical pretreatment, mechanical pretreatment, chemical pretreatment, biological pretreatment and combined physical and chemical pretreatment.

Physical Pretreatment Methods

Physical pretreatment is the first line of action in the pretreatment process (Julie et al., 2018), which usually prepares feedstock for further treatment. This kind of pretreatment is sometimes referred to as mechanical pretreatment, which has been recorded to be the most widely used form of pretreatment [13]. In addition, this method breaks the biomass into smaller particles amiable by increasing the surface area, dissociating tissue, and disrupting the cell wall, which thereby aids in speeding up the rate of enzymatic hydrolysis. It also decreases the crystallization of biomass and reduces the degree of polymerization. Examples of these methods are milling, ultrasonication, microwave, and mechanical extrusion [2].

Milling

This method aids to reduce both the particle size and crystallinity of feedstock. It can reduce the size of biomass up to 0.2 mm. This type of physical pretreatment offers a significant advantage being physical. It does not produce inhibitors like furfural and hydroxyl methyl furfural (HMF) and therefore gives a high yield of bioethanol. However, its high energy demand makes it an uneconomical process on an industrial scale [13].

There are five different milling methods. Examples of such are ball, colloidal, hammer, vibrio-energy, and two-roll milling (pictorial view of milling forms in Figure 3). The choice of the milling process to employ is strongly dependent on the nature of the feedstock. However, it has been reported that the colloidal milling suit perfectly for wet feedstock, while hammer milling will suit best for dry feedstock like wastepaper. Although, literature has indicated that ball milling can be applicable for both the dry and wet feedstock. Milling enhances enzymatic hydrolysis [11] as it reduces the size of particles. This makes it easier for cellulose enzymes as cellulose is exposed.

A survey of the literature indicated that many studies have considered the exploration of a wide range of biomass resources, some of which includes cassava peels [15 – 17], cassava starch [18 – 23], sugarcane bagasse [21], [24 – 28], bark, corncob, stalk, husk, sweet potato peels [24], cassava pulp [20], banana pseudostem [29], and other solid agricultural residues [23]. Moreover, the studies indicated that the use of this pretreatment (milling) in the production of bioethanol yields 52.00 % (from cassava flours), 97.40 % (from cassava peels), 5.85 % (from cassava starch), 26.74 % (sugarcane bagasse, bark, corncob, stalk, and husk), 23.80 % (cassava peels), 47.99 % (sweet potato peels), 82.40 % (cassava pulp), 16.00 % (cassava), 9.03 % (sugarcane bagasse),67.00 % (sugarcane), 31 % (sweet potato peel), 14.46 g/cm^3 (41.00%) (cassava peel), 0.31 g/g (31.00 %) (cassava), 84.00 % (banana pseudostem), and 35.00 % (cassava effluent and solid agricultural residue), based on the report from the literature.

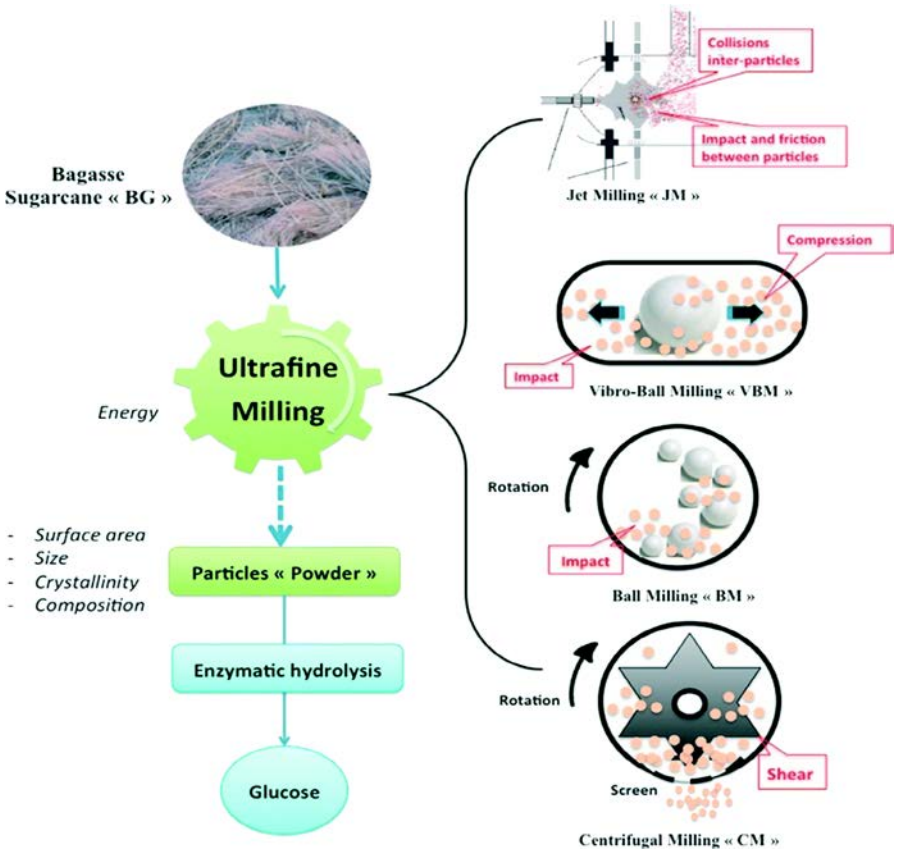

Figure 3. A pictorial display of the variety of milling biomass [14].

Ultra-sonication

Cavitation through high-frequency ultrasonic waves forms the working principle of this method. These approach forces lead to the separation of the complex network of the polysaccharide components of the feedstock, and a graphical illustration of the process is presented in Figure 4.

It also enhances the extraction of desired compounds like cellulose, hemicellulose, and lignin. This technique is carried out at 20 kHz and 200 kW for 10 minutes [13]. The works of Zhang et al. [30] employed the use of sweeping frequency ultrasonic pretreatment approach in the processing of okra into 16.7% (0.564 mg/mg) okra pectin content. Ultrasound-assisted microwave extraction (UAME) approach was similarly deployed by Sengar et al. [31] in the extraction of pectin from tomato processing waste, where 73.33% of extracted pectin yield was reported.

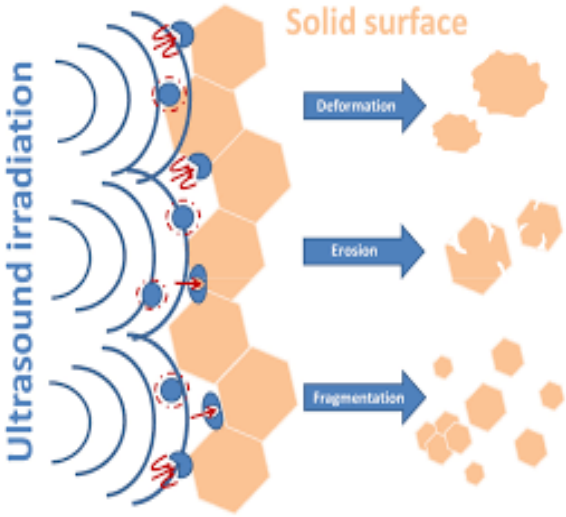

Figure 4. A demonstration of how the ultrasonic radiation impact the biomass in pretreating the materials [32].

Microwave

This method is commonly used due to its advantage. It has minimal energy requirement, short processing time, less inhibitor generation. This is carried out in closed containers as a high temperature is needed for optimal functioning. Penetration, reflection, and absorbance are associated with a microwave. It is from these attributes that the system for microwave pretreatment is built [2]. In microwave, the lignocellulosic structure is disrupted through di-electric polarization. The polarization causes a molecular collision, thereby generating heat energy that results in the disruption [33]. Examples of the studies that deployed the use of the microwave pretreatment method in the processing of calabash pulp juice [33], cassava [34], and cocoyam peel [35], where it was reported to have yielded 21.6 %, 20.49 %, 6g/100mL (9.40 %), and 50g/L (5.00 %), respectively.

Mechanical extrusion.

Extrusion is a process where feedstock is passed through a screw assembly called an extruder. The combined effect of high temperature and shear force caused by the blades in the barrel causes the disruption of the lignocellulosic structure [36]. Some of the advantages of this method include adaptability to modifications, the integrity of products being preserved, and a controllable environment. Moreover, there exist two types of extruders which are usually referred to as single and twin-screw extruders [2]. To enhance the activity of this process, chemicals like urea, Thiourea and sodium hydroxide can be added to the biomass [13], [37]. Other cases of studies that deployed the use of mechanical pretreatment/extrusion in the processing of sugarcane [38] and pineapple peels [39] to yield 9.20 cl/L (72.70 %) and 5.82 %v/v, respectively.

Chemical Pretreatment Methods

In practice, chemical pretreatment often comes next to physical pretreatment. The two main chemical pretreatments are acid and alkaline pretreatment. However, there are other methods like Ionic liquid and organic solvent pretreatment.

Alkali pretreatment

In this type of chemical pretreatment, alkali is added to the feedstock. This method causes swelling, which decreases the crystallinity and increases the specific area of the biomass. This further leads to the unfolding of lignin from polysaccharide moiety. Through this method, lignin is dissolved, and polysaccharides are exposed for further hydrolysis [12].

Compared to mechanical methods, the energy requirement of alkali pretreatment is low. However, it takes a lot of time to complete. It takes hours or days. The hydroxides of ammonium, sodium, calcium, and potassium are the commonly used base for alkali pretreatment. The setup for alkali pretreatment is a heating element, temperature controller, a tank, water jacket, CO_2 scrubber, manifold for water and air, pump, tray, and frame. A lime slurry is first prepared with a desired base and water. It is then sprayed of the feedstock and stored for hours or days [2]. The dissociation of lignin and the removal of acetyl groups, and ironic acid substitution in hemicellulose confer a great advantage to alkaline pretreatment. However, the difficulty in the recovery of the reagents used in this technique has proven to be disadvantageous and needs to be looked into. It is also observed that feedstocks with high levels of lignin are not favoured by this method [36].

A further survey of works reported in the literature on the deployment of alkali pretreatment method for the production of bioethanol from varying biomass like rice husk,

elephant grass, corn stover, rice straw, rice husk, groundnut shell, and a lot more [40 – 44]. Findings from the survey of the literature indicated that most of the studies that deploy alkaline pretreatment approach often use sodium hydroxide in the processing of the biomass into sugar and bioethanol, where it was reported to yield 6.25 % [Rice husk] [40], 78.00 % [Elephant grass stem] [41], 11.30 % [Corn stover] [42], 49.50 % [Rice straw] [43], 132.7 mg/mL [Cassaval peels] [45], 81 % [Sugarcan bagasse] [4], and 24.14 % [Groundnuts shell] [44].

Acid pretreatment

As the name implies, acids are used for the pretreatment of feedstock. A significant challenge to this method is the production of the inhibitory substance. Furfural, hydroxyl methyl furfural (HMF) and phenolic acid are produced in large amounts. However, measures have been developed to take care of that [36]. Acid pretreatment is of two types; they vary on the basis of duration and temperature. The first one has a short duration of 1 - 5 min but a high temperature of 180^{o}C. The second has a high timeframe of 20 - 30 min and a temperature as low as 120^{o}C [2]. Both organic and inorganic acids find use in this pretreatment. Inorganic acids like sulfuric, nitric, and hydrochloric acids are used in both their concentrated and diluted forms. However, concentrated acids are very corrosive and demand extra safety measures, which makes the process more expensive. The use of concentrated acid is reported to yield a high number of inhibitory compounds. Pretreatment with dilute acids is used on an industrial scale as it is suitably cost-effective with little or no number of inhibitory compounds. Organic acids like Oxalic acid, maleic acid is normally used in acid pretreatment. Maleic acid is reported to have more glucose and xylose yield [2].

A Survey of the literature on the pretreatment of biomass indicated studies had proven the viability of deploying acid treatment methods in the processing of sugarcane bagasse, rice husk, banana skin/peels, maize stalks, corncob, orange peels, cassava peels, cowpea shells, yam peels, and a lot more [5], [46 – 48]. The deployment of hydrochloric acid [for sawdust] [46], Sulphuric acid [for cassava peels] [45], sulphuric acid [for rice husk] (Mustafa et al., 2019), sulphuric acid [for rice stalk] [50], pretreatment yields 43.9%, 190.04 mg/mL, 25.35 %, and 5.06 % sugar yield, respectively.

Ionic liquids

Ionic liquids are liquids containing cations or anions. These liquids are known to be thermally stable, nontoxic, have high polarity, low melting point and less vapour pressure. The relationship between ionic liquid and feedstock is primarily affected by temperature, cations and anions and the duration of pretreatment [2]. Cations and anions both play significant roles in solubilizing cellulose and lignin. They do so by disrupting the intermolecular hydrogen bond between cellulose and the lignin network by competing for the same hydrogen bonds. While the cations are strictly organic in nature, the anions are both organic and inorganic. Imidazolium and pyridinium are examples of organic cations [36]. Another advantage of the ionic liquid is its recovery during the process. However, the use of this pretreatment is not compatible with cellulose activity [2].

Organic solvent

Organic solvents like acetone, methanol, ethylene glycol and ethanol are used in the pretreatment of feedstock. A catalyst aids this method of pretreatment. Some acids, bases and salts are added to the medium to either fasten delignification or regulate the temperature. In research conducted by Sidiras and Loanna [3], a cellulose concentration of

72% w/w and a lignin concentration of 59% w/w was obtained using acetone and sulfuric acid as catalyst.

This pretreatment type is widely used in extracting lignin from biomass. Lignin is a valuable substance of industrial use. The disruption of the bond between lignin and cellulose causes an increase in the surface area of cellulose. This makes it readily accessible to enzymes. As a result, a higher yield of bioethanol is produced. The recovery and reuse of solvents is an added advantage to this pretreatment. However, the chemicals are volatile and expensive. A high amount of energy is needed to recover and recycle the organic solvents, and they also are flammable [36]. The use of lime (organic catalyst) employed in the pretreatment of the sugarcane juice at temperature (35 C) and 5 hours yielded 19.30 % bioethanol [51]. Ethanoic acid and methanol pretreatment were employed in the processing of cassava peels [45] and cassava peels [52] into 51.50 mg/mL sugar and 331.79 mg/L glucose (including 45.3 mg/L rhamnoses and 46.52 mg/L xylose) yield.

Combined Chemical-mechanical Pretreatment Methods

This method combines both physical and chemical methods. It is also known as the physicochemical method. Examples of such kinds of this method include ammonia fibre explosion, steam explosion, and carbon dioxide explosion.

Steam explosion method

The steam explosion method is known for its little chemical use and low energy consumption. In this method, is exposed to high pressure saturated steam, after which pressure is reduced. This method results in an explosive decompression leading to the disruption of lignin and cellulose degradation. The steam is injected at a temperature of 160-260 0C and 0.69 and 4.83 MPa. The pressure is provided but for a few minutes. Carbon dioxide and sulfuric acid are used to decrease the time and formation of inhibitory substances and increase the efficiency of removing hemicellulose. Moisture content, particle size, temperature are factors that affect steam explosion. This technique is not very effective for softwood. [2]. One of the works that deployed the use of this approach includes Gayalai-Korpos et al. [53] whose studies employed the approach to pretreat sweet sorghum bagasse from which 58% cellulose were obtained resulting to a rise in the bioethanol yield.

Ammonia fibre explosion (AFEX)

Ammonia fibre expansion (AFEX) is known for being a thermochemical pretreatment that utilizes volatile ammonia as the main reactant for cellulosic biomass pretreatment [54]. The feedstock is treated with liquid ammonia at high temperatures and pressure. The pressure is then reduced. This process is similar to steam explosion. Owing to the volatile nature of ammonia, it is easily recovered and recycled. The process is usually carried out at a temperature of 90^{o}C for about 30 min. Some of the works that deployed the use of the ammonia fibre explosion in the processing of biomass into bioethanol fuels include the report of the Bals et al. [55] that transforms switchgrass to bioethanol. Similarly, Feher et al. [56] deployed the use of aqueos ammonia pretreatment approach in their study to pretreat corn fibre which later yielded 79% bioethanol via the process.

Carbon dioxide explosion

This method is similar to steam and ammonia explosion and shares similar principles. High-pressure CO_2 reacts to carbonic acid, thereby improving the hydrolysis rate. The yield

gotten from this process is lower than that of steam and ammonia explosion [2]. It was further reported that CO_2 reacts to carbonic acid, thereby improving the hydrolysis rate. The yield is gotten from this process. Examples of studies that employed the use of this approach in their studies include Kim and Hong (2001), which employs the use of aspen and southern yellow pine; Puri and Mamers [58] employs the processing of wheat straw, bagasse, and Eucalyptus regnans woodchips; and Toscan et al. [59] employ the processing of wheat straw, bagasse, and Eucalyptus regnans woodchips; and many other feedstocks in the production of bioethanol.

Conclusions

The shift from fossil fuel to renewable sources of energy like biofuels is not without its challenges. The competition for food between the industries and humans has led to the use of solid waste and other cellulosic feedstocks. This approach helps recycle waste but is not sufficient in producing biofuel due to recalcitrance.

Pretreatment of feedstock is a way of optimizing the production of bioethanol from the feedstock. Different forms of pretreatment exist. They range from physical to chemical with varying strength. The most effective pretreatment type is the one that is cost-effective and gives a high yield of bioethanol.

More work needs to be done in order to optimize the production of bioethanol so that it can compete in production cost with its fossil fuel counterpart. We recommend that researchers consistently report their pretreatment type with the conditions used. And further studies are encouraged to consider the techno-economic evaluation and SWOT (Strength, Weakness, Opportunity, and Threats) analysis of the various biomass pretreatment methods reviewed in this report.

Acknowledgements. The authors appreciate the support of the Pencil Research Team and other resource persons that must have contributed to the completion of the study.

Conflict of Interest

The authors declare no conflict of interest.

References

1. Adeyemo O., Ja'afaru M., Abudulkadir S. and Salihu A. "Saccharification and Fermentation of Cellulolytic Agricultural Biomass to Bioethanol using Locally Isolated Aspergillus niger S48 and Kluyveromyces sp. Y2, respectively," Periodica Polytechnica Chemical Engineering, vol. 65, no. 4, pp. 505–516, Aug. 2021, doi: 10.3311/PPCH.17900.
2. Muhammad A. N., Iqbal I., Riaz F., Karadag A. and Tabatabaei M. "Different Pretreatment Methods of Lignocellulosic Biomass for Use in Biofuel Production," in Biomass for Bioenergy - Recent Trends and Future Challenges, A. E.-F. Abomohra, Ed. IntechOpen, 2019. doi: 10.5772/INTECHOPEN.84995.
3. Sidiras D. K., and Loanna S. S. "Organosolv Pretreatment as a Major Step of Lignocellulosic Biomass Refining," 2015. Accessed: Oct. 23, 2021. [Online]. Available: http://dc.engconfintl.org/biorefinery_I/18
4. Shaibani N., Yaghmaei S., Andalibi M. R. and Ghazvini S. "Ethanol production from sugarcane bagasse by means of on-site produced and commercial enzymes; a comparative study," Periodica Polytechnica Chemical Engineering, vol. 56, no. 2, pp. 91–96, Dec. 2012, doi: 10.3311/PP.CH.2012-2.07.
5. Fehér C., Barta Z., and Réczey K. "Process considerations of a biorefinery producing value-added products from corn fibre," Periodica Polytechnica Chemical Engineering, vol. 56, no. 1, pp. 9–19, Jun. 2012, doi: 10.3311/PP.CH.2012-1.02.
6. Kálmán G., and Réczey K. "Possible ways of bio-refining and utilizing the residual lignocelluloses of corn growing and processing," Periodica Polytechnica Chemical Engineering, vol. 51, no. 2, pp. 29–36, Jun. 2007, doi: 10.3311/PP.CH.2007-2.05.

7. Battula S. K., Gantala S. S. N., Besetty T., Narayana S. K. V., and Gopinadh R. "Industrial production of lactic acid and its applications," Internaational Journal of Biotech Research, vol. 1, no. 1, pp. 42–54, 2018, Accessed: Oct. 23, 2021. [Online]. Available: https://www.researchgate.net/publication/330292057_Industrial_production_of_lactic_acid_and_its_applications
8. Nathan G. "Agro-industry seed 'waste' is promising source of oils and ingredients," NUTRA, Dec. 01, 2014. https://www.nutraingredients.com/Article/2014/12/01/Agro-industry-seed-waste-is-promising-source-of-oils-and-ingredients (accessed Nov. 09, 2021).
9. Brock S., Kuenz A., and Prüße U. "Impact of Hydrolysis Methods on the Utilization of Agricultural Residues as Nutrient Source for D-lactic Acid Production by Sporolactobacillus inulinus," Fermentation , vol. 5, no. 1, p. 12, Jan. 2019, doi: 10.3390/FERMENTATION5010012.
10. Jönsson L. J., and Martín C. "Pretreatment of lignocellulose: Formation of inhibitory by-products and strategies for minimizing their effects," Bioresource Technology, vol. 199, pp. 103–112, Jan. 2016, doi: 10.1016/J.BIORTECH.2015.10.009.
11. Tongshuwar G. T., and Oyegoke T. "A Brief Survey of Biomass Hydrolysis As A Vital Process in Bio-refinery," FUDMA Journal of Sciences, vol. 5, no. 3, pp. 407–412, Nov. 2021, doi: 10.33003/FJS-2021-0503-724.
12. Kucharska K., Rybarczyk P., Hołowacz I., Łukajtis R., Glinka M., and Kamiński M. "Pretreatment of Lignocellulosic Materials as Substrates for Fermentation Processes,"Molecules, vol. 23, no. 11, p. 2937, Nov. 2018, doi: 10.3390/MOLECULES23112937.
13. Amin F. R,. et al., "Pretreatment methods of lignocellulosic biomass for anaerobic digestion," AMB Express , vol. 7, no. 1, pp. 1–12, Mar. 2017, doi: 10.1186/S13568-017-0375-4.
14. Rahmati S., et al. "Pretreatment and fermentation of lignocellulosic biomass: reaction mechanisms and process engineering," Reaction Chemistry & Engineering, vol. 5, no. 11, pp. 2017–2047, Oct. 2020, doi: 10.1039/D0RE00241K.
15. Monday Osagie A. "Statistical Investigation on the Hydrolysis and Fermentation Processes of Cassava Peels in the Production of Bioethanol," International Journal of Statistical Distributions and Applications, vol. 3, no. 3, pp. 47–55, 2017, doi: 10.11648/j.ijsd.20170303.14.
16. Ebabhi A. M., Adekunle A. A. and Adeogun O. O. "Potential of some tuber peels in bioethanol production using Candida tropicalis," Nigerian Journal of Basic and Applied Sciences, vol. 26, no. 2, pp. 17–22, Mar. 2019, doi: 10.4314/njbas.v26i2.3.
17. Obianwa C., Edak A. U., and Godwin I. "Bioethanol production from cassava peels using different microbial inoculants," African Journal of Biotechnology, vol. 15, no. 30, pp. 1608–1612, Jul. 2016, doi: 10.5897/ajb2016.15391.
18. Ademiluyi F. T., and Mepba H. D. "Yield and Properties of Ethanol Biofuel Produced from Different Whole Cassava Flours," ISRN Biotechnology, vol. 2013, pp. 1–6, Jan. 2013, doi: 10.5402/2013/916481.
19. Ajibola F. O., Edema, and Oyewole. "Enzymatic Production of Ethanol from Cassava Starch Using Two Strains of Saccharomyces cerevisiae," Nigerian Food Journal Official Journal of Nigerian Institute of Food Science and Techonology www.nifst.org NIFOJ, vol. 30, no. 2, pp. 114–121, 2012, [Online]. Available: www.nifst.org
20. Ndubuisi I. A., Nweze J. E., Onoyima N. J., Yoshinori M., and Ogbonna J. C. "Ethanol Production from Cassava Pulp by a Newly Isolated Thermotolerant LC375240," Energy and Power Engineering, vol. 10, no. 10, pp. 457–474, 2018, doi: 10.4236/epe.2018.1010029.
21. Isah Y., Kabiru H. D., Danlami M. A., and Kolapo S. F. "Comparative Analysis of Bioethanol Produced From Cassava Peels and Sugarcane Bagasse by Hydrolysis Using Saccharomyces Cerevisiae," J. Chem Soc. Nigeria, vol. 44, no. 2, pp. 233–238, 2019.
22. Ogbonna C. N., and Okoli E. C. "Evaluation of the Potentials of Some Cassava Varieties in Nigeria for Bio-Ethanol Production," Bio-Research, , vol. 8, no. 2, pp. 674–678, 2010.
23. Izah S. C., and Ohimain E. I. "Bioethanol Production from Cassava Mill Effluents Supplemented with Solid Agricultural Residues Using Bakers' Yeast (Saccharomyces cerevisiae)," Journal of Environmental Treatment Techniques, vol. 3, no. 1, pp. 47–54, 2015, [Online]. Available: http://www.jett.dormaj.com
24. Braide W., Kanu I., Oranusi U., and Adeleye S. "Production of bioethanol from agricultural waste," Journal of Fundamental and Applied Sciences, vol. 8, no. 2, p. 372, May 2016, doi: 10.4314/jfas.v8i2.14.
25. Misau I. M., Bugaje I. M., Mohammed J., Mohammed I. A., and Diyau'deen .B.H. "Production Of Bio-Ethanol From Sugarcane: A Pilot Scale Study In Nigeria," International Journal of Engineering Research and Applications (IJERA), vol. 2, no. 4, pp. 1142–1151, 2012, [Online]. Available: www.ijera.com

26. Oyegoke T., and Dabai F. "Techno-economic feasibility study of bioethanol production from a combined cellulose and sugar feedstock in Nigeria: 2-economic analysis," Nigerian Journal of Technology, vol. 37, no. 4, pp. 921–926, Nov. 2018, doi: 10.4314/njt.v37i4.9.
27. Oyegoke T., and Dabai F. "Techno-economic feasibility study of bioethanol production from a combined cellulose and sugar feedstock in Nigeria: 1-modeling, simulation and cost evaluation," Nigerian Journal of Technology, vol. 37, no. 4, pp. 913–920, Nov. 2018, doi: 10.4314/njt.v37i4.8.
28. Oyegoke T., Dabai F., Abubakar Muhammed J., and Jibiril B. El-Yakubu. "Process Modelling and Economic Analysis for Cellulosic Bioethanol Production in Nigeria," in 1st National Conference On Chemical Technology (NCCT 2017) , 2017, pp. 125–128. [Online]. Available: http://www.narict.gov.ng/ncct/
29. Ingale S., Joshi S. J., and Gupte A. "Production of bioethanol using agricultural waste: Banana pseudo stem," Brazilian Journal of Microbiology, vol. 45, no. 3, pp. 885–892, 2014, [Online]. Available: www.sbmicrobiologia.org.br
30. Zhang L., et al., "Effect of ultrasonic pretreatment monitored by real-time online technologies on dried preparation time and yield during extraction process of okra pectin," Journal of the Science of Food and Agriculture, vol. 101, no. 10, pp. 4361–4372, Aug. 2021, doi: 10.1002/JSFA.11076.
31. Sengar S., Rawson A., Muthiah M., and Kalakandan S. K. "Comparison of different ultrasound assisted extraction techniques for pectin from tomato processing waste," Ultrasonics Sonochemistry, vol. 61, no. 104812, pp. 1–10, Mar. 2020, doi: 10.1016/J.ULTSONCH.2019.104812.
32. Kuna E., Ronan B., Valange S., Chatel G., and Juan C. C. "Sonocatalysis: A Potential Sustainable Pathway for the Valorization of Lignocellulosic Biomass and Derivatives," Top Curr Chem (Z), vol. 375, no. 41, pp. 1–20, 2017, doi: 10.1007/s41061-017-0122-y.
33. Aguilar-Reynosa A., Romaní A., R. Ma. Rodríguez-Jasso, Aguilar C. N., Garrote G., and Ruiz H. A. "Microwave heating processing as alternative of pretreatment in second-generation biorefinery: An overview," Energy Conversion and Management, vol. 136, pp. 50–65, Mar. 2017, doi: 10.1016/J.ENCONMAN.2017.01.004.
34. Nwogwugwu N. U., Abu G. O., Akaranta O., and Chinakwe E. C. "Application of Response Surface Methodology for Optimizing the Production of Bioethanol from Calabash (Crescentia cujete) Substrate Using Saccharomyces cerevisiae," Journal of Advances in Microbiology, pp. 1–12, Jul. 2019, doi: 10.9734/jamb/2019/v17i230139.
35. Etudaiye H., Ukpabi U., Egesi E., and Ikpeama A. "Evaluation of Flour and Starch Qualities from Three Cassava Varieties for Ethanol Production Using a Novoenzyme and a Strain of Dried Saccharomyces cerevisiae (Yeast)," Annals of Advanced Agricultural Sciences, vol. 4, no. 1, pp. 1–7, Feb. 2020, doi: 10.22606/as.2020.41001.
36. Adegunloye D., and Udenze D. "Effect of Fermentation on Production of Bioethanol from Peels of Cocoyam Using Aspergillus niger and Saccharomyces cerevisiae," Journal of Advances in Microbiology, vol. 4, no. 2, pp. 1–8, Jan. 2017, doi: 10.9734/jamb/2017/34032.
37. Baruah J., et al. "Recent Trends in the Pretreatment of Lignocellulosic Biomass for Value-Added Products," Frontiers in Energy Research, vol. 6, no. Dec, p. 152, Dec. 2018, doi: 10.3389/FENRG.2018.00141.
38. Kumar R., Tabatabaei M., and Karimi K. "Sárvári Horváth I. Recent updates on lignocellulosic biomass derived ethanol-A review," Journal homepage: www.biofueljournal.com Kumar et al. / Biofuel Research Journal, vol. 9, pp. 347–356, 2016, doi: 10.18331/BRJ2016.3.1.4.
39. Nwufo O. C., Nwaiwu C. F., Igbokwe J. O., and Nwafor O. M. I. "Production and characterisation of bio-ethanol from various Nigerian feedstocks," International Journal of Ambient Energy, vol. 37, no. 5, pp. 469–473, Sep. 2015, doi: 10.1080/01430750.2014.986290.
40. Oiwoh O., Ayodele B. V., Amenaghawon N. A., and Okieimen C. O. "Optimization of bioethanol production from simultaneous saccharification and fermentation of pineapple peels using Saccharomyces cerevisiae," Journal of Applied Sciences and Environmental Management, vol. 22, no. 1, pp. 54–59, Feb. 2018, doi: 10.4314/jasem.v22i1.10.
41. Ahmad F. U., Bukar A., and Usman B. "Production of bioethanol from rice husk using Aspergillus niger and Trichoderma harzianum," Bayero Journal of Pure and Applied Sciences, vol. 10, no. 1, pp. 280–294, Jan. 2018, doi: 10.4314/bajopas.v10i1.56s.
42. Aiyejagbara M., et al., "Production of Bioethanol from Elephant Grass (Pennisetum purpureum) Stem," International Journal of Innovative Mathematics, Statistics & Energy Policies, vol. 4, no. 1, pp. 1–9, 2016, [Online]. Available: www.seahipaj.org

43. Evuensiri Onoghwarite O., N. Victor Ifeanyichukwu Obiora, E. Akachukwu Ben, and N.-O. Ekpe Moses, "Bioethanol production from corn stover using Saccharomyces cerevisiae," International Journal of Scientific & Engineering Research, vol. 7, no. 8, pp. 290–293, 2016, [Online]. Available: http://www.ijser.org
44. Tsunatu D. Y., Atiku K. G., Samuel T. T., Hamidu B. I., and Dahutu D. I. "Production of bioethanol from rice straw using yeast extract peptone dextrose," Nigerian Journal of Technology (NIJOTECH), vol. 36, no. 1, pp. 296–301, 2017, doi: 10.4314/njt.v36i1.36.
45. Nyachaka C. J, Yawas D. S, and Pam G .Y. "Production And Performance Evaluation Of Bioethanol Fuel From Groundnuts Shell Waste," American Journal of Engineering Research (AJER), vol. 02, pp. 303–312, 2013, [Online]. Available: www.ajer.org
46. Ovueni U. J., Jeje A. O., and Sadoh O. Y. "Effect of Acid and Alkali Pretreatments on the Structural and Compositional Properties of Cassava Peels," International Journal of Scientific & Engineering Research, vol. 11, no. 5, pp. 116–121, 2020, Accessed: Nov. 06, 2021. [Online]. Available: https://www.ijser.org/researchpaper/Effect-of-Acid-and-Alkali-Pretreatments-on-the-Structural-and-Compositional-Properties-of-Cassava-Peels.pdf
47. Yahaya U., Adamu U. A., Adamu I., Abdul'Aziz R. A., Sadiq I. M., and. Kurawa I. A. "Effects of Dilute Hydrochloric Acid Pretreatment Oneucalyptus Camaldulensis Sawdust for Bioethanol Production," International Journal of Research Studies in Science, Engineering and Technology, vol. 5, no. 10, p. 22, 2018, Accessed: Nov. 06, 2021. [Online]. Available: http://ijrsset.org/pdfs/v5-i10/4.pdf
48. Ummalyma S. B., et al. "Sono-Assisted Alkali and Dilute Acid Pretreatment of Phragmites karka (Tall Reed Grass) to Enhance Enzymatic Digestibility for Bioethanol Conversion," Frontiers in Energy Research, vol. 8, p. 340, Apr. 2021, doi: 10.3389/FENRG.2020.594452/BIBTEX.
49. Awoyale A., and Lokhat D. "Experimental determination of the effects of pretreatment on selected Nigerian lignocellulosic biomass in bioethanol production," Scientific Reports 2021 11:1, vol. 11, no. 1, pp. 1–16, Jan. 2021, doi: 10.1038/s41598-020-78105-8.
50. Mustafa H. M., Bashir A., and Dahiru S. M. "Production of Bioethanol from Sulfuric Acid Pretreated Rice Husk using Co-culture of Saccharomyces Cerevisiae and Aspergillus Niger," Science World Journal, vol. 14, no. 4, pp. 107–110, 2019, doi: 10.1007/s12155-010-9088-0.
51. Charanchi A. S., Ado S. A., and Hussaini I. M. "Studies on Bioethanol Production from Rice Stalk using Co-cultures of Aspergillus niger and Saccharomyces cerevisiae," UJMR, vol. 3, no. 2, pp. 88–95, 2018, [Online]. Available: www.ujmr.umyu.edu.ng
52. Suleiman B., Abdulkareem S. A., Afolabi E. A., Musa U., Mohammed I. A., and Eyikanmi T. A. "Optimization of bioethanol production from Nigerian sugarcane juice using factorial design," Advances in Energy Research, vol. 4, no. 1, pp. 69–86, Mar. 2016, doi: 10.12989/eri.2016.4.1.069.
53. Olanbiwoninu A. and Odunfa S. A. "Production of Fermentable Sugars from Organosolv Pretreated Cassava Peels," Advances in Microbiology, vol. 05, no. 02, pp. 117–122, Feb. 2015, doi: 10.4236/AIM.2015.52012.
54. Gyalai-Korpos M., Fülöp T., Sipos B., and Réczey K. "Processing sweet sorghum into bioethanol - an integrated approach," Periodica Polytechnica Chemical Engineering, vol. 56, no. 1, pp. 21–29, Jun. 2012, doi: 10.3311/PP.CH.2012-1.03.
55. Chundawat S. P. S., et al. "Ammonia Fiber Expansion (AFEX) Pretreatment of Lignocellulosic Biomass," JoVE (Journal of Visualized Experiments), vol. 2020, no. 158, p. e57488, Apr. 2020, doi: 10.3791/57488.
56. Bals B., Rogers C., Jin M., Balan V., and Dale B. "Evaluation of ammonia fibre expansion (AFEX) pretreatment for enzymatic hydrolysis of switchgrass harvested in different seasons and locations," Biotechnology for Biofuels, vol. 3, no. 1, pp. 1–11, 2010, doi: 10.1186/1754-6834-3-1.
57. Fehér A., Bedő S., and Fehér C. "Comparison of Enzymatic and Acidic Fractionation of Corn Fiber for Glucose-rich Hydrolysate and Bioethanol Production by Candida boidinii," Periodica Polytechnica Chemical Engineering, vol. 65, no. 3, pp. 320–330, May 2021, doi: 10.3311/PPCH.17431.
58. Kim K. H., and Hong J. "Supercritical CO2 pretreatment of lignocellulose enhances enzymatic cellulose hydrolysis," Bioresource Technology, vol. 77, no. 2, pp. 139–144, Apr. 2001, doi: 10.1016/S0960-8524(00)00147-4.
59. Puri V. P., and Mamers H. "Explosive pretreatment of lignocellulosic residues with high-pressure carbon dioxide for the production of fermentation substrates," Biotechnology and Bioengineering, vol. 25, no. 12, pp. 3149–3161, 1983, doi: 10.1002/BIT.260251226.
60. Toscan A., et al. "High-pressure carbon dioxide/water pre-treatment of sugarcane bagasse and elephant grass: Assessment of the effect of biomass composition on process efficiency," Bioresource Technology, vol. 224, pp. 639–647, Jan. 2017, doi: 10.1016/J.BIORTECH.2016.11.101.

Journal of Engineering Science *Vol. XXIX, no. 1 (2022), pp. 142 - 150*
Fascicle *Food Engineering* *ISSN 2587-3474*
Topic *Food Technologies and Food Processes* *eISSN 2587-3482*

https://doi.org/10.52326/jes.utm.2022.29(1).13
CZU 637.146.34:667.275.5

COLOR STABILITY OF YOGURT WITH NATURAL YELLOW FOOD DYE FROM SAFFLOWER (*CARTHAMUS TINCTORIUS L*)

Liliana Popescu, ORCID ID: 0000-0003-3381-7511,
Aliona Ghendov-Moșanu, ORCID ID: 0000-0001-5214-3562,
Alexei Baerle, ORCID ID: 0000-0001-6392-9579,
Alexandra Savcenco*, ORCID ID: 0000-0002-1962-3959,
Pavel Tatarov, ORCID ID: 0000-0001-9923-8200

Technical University of Moldova, 168 Stefan cel Mare Blvd., Chisinau, Republic of Moldova
*Corresponding author: Alexandra Savcenco, *alexandra.savcenco@tpa.utm.md*

Received: 11. 28. 2021
Accepted: 01. 18. 2022

Abstract. The article elucidates the possibility of using the yellow dye, obtained from saffron petals (*Carthamus Tinctorius L.)* in the food industry. This powdered dye, added to yoghurt in concentrations of 0.3 - 0.4%, in addition to its yellow color, gives the yoghurt samples a light aroma of saffron flowers and demonstrates high stability during storage at 4° C. for 28 days. The values of the chromatic coordinates, L *, a *, b *, of the yogurt samples did not undergo considerable changes during the storage stage, the color difference ΔE being ⩽ 0.79, which indicates a high stability of the dye in yogurt. samples. The chromatic analysis data correlate with the results obtained by the reverse phase HPLC method, which identified the presence of four intact yellow chalcones in the yoghurt. The results of this study will encourage the cultivation of saffron, the extraction of natural dyes and their use in the food industry.

Keywords: *chromaticity coordinates, color analysis, food additive, natural food.*

Rezumat. Articolul elucidează posibilitatea de utilizare a colorantul galben, obținut din petale de șofrănel (*Carthamus Tinctorius* L.) in industria alimentara. Acest colorant, adăugat în formă de pudră la iaurt în concentrații de 0,3 - 0,4%, pe lângă culoarea galbenă, conferă probelor de iaurt o aromă ușoară de flori de șofrănel și demonstrează stabilitate ridicată în timpul păstrării la 4°C timp de 28 de zile. Valorile coordonatelor cromatice, L*, a*, b*, ale probelor de iaurt nu au suferit modificări considerabile în timpul etapei de păstrare, diferența de culoare ΔE fiind ⩽ 0,79, ceea ce indică o stabilitate ridicată a colorantului în iaurt. mostre. Datele analizei cromatice sunt corelate cu rezultatele obținute prin metoda HPLC în fază inversă, care a identificat prezența a patru calcone galbene intacte în iaurt. Rezultatele acestui studiu vor încuraja cultivarea șofrănelului, extragerea coloranților naturali și utilizarea lor în industria alimentară.

Cuvinte cheie: *coordonate cromatice, analiza culorii, aditiv alimentar, alimente naturale.*

Introduction

We are currently witnessing an increase in consumer demands for natural foods, as people aspire to a healthier lifestyle. Natural food colorings play a special role in this trend.

Quantum transitions (absorption) corresponding to the wavelengths of visible light are due to the presence of a system of conjugated double bonds (CDB) in molecules. However, the cause of dyes instability is that CDB systems are unstable to the action of active oxidizing agents and free-radicals. That is why, natural dyes have biological activity (and chemical instability): the ability to neutralize free radicals which causes oxidative stress and even mutations.

Modern science finds thousands of natural dyes with potential biological activity in flowers and fruits of higher plants. Mostly red dyes, anthocyanins, are very well known to the consumer, which cannot be said about chalcones – majorly yellow and less often – red compounds [1]. Chalcones are phenolic dyes with an unclosed benzopyran skeleton. These compounds are characteristic for the *Asteraceae* family. Safflower (*Carthamus Tinctorius, Asteraceae*) is often confused even in scientific literature with Saffron (*Crocus Sativus, Iridaceae*), because partial similarly names and visual aspect of dye-containing raw material. Safflower petals contain, according to various sources, 5 - 11 different yellow chalcones, the most famous of which are: Hydroxisafflower Yellow A (HSYA), Anhidrosafflower Yellow B (AHSYB) and Precarthamin [2]. Being the basic phenols of the Safflower petals, these compounds, in addition to its coloring properties, exhibits a wide range of biological functions, including anticoagulant, vasodilation and antioxidant activities [3].

Color is an important factor in the quality of fruit yogurt, influencing the acceptability of the product to the consumer [4]. It is one of the first characteristics perceived and is used by consumers to appreciate the quality of food [5, 6]. Unfortunately, the attractive color of fruit yogurt is not preserved during storage [6]. The food industry uses food coloring to improve the color and acceptance of fruit yogurts [7].

The goal of the study was to evaluate color stability of yogurt during storage by determining the chromaticity coordinates, measured using the CIE color space L* a* b*. Our results could be useful for the development of an effective strategy for the manufacturing of dairy products with high color stability.

Materials and methods

Plant material. Yellow florets of Safflower, grown in Republic of Moldova, were used. Petals were dried in the dark, at max 40°C in the dark to relative humidity less than 2%.

Yellow Food Dye from Safflower. YFDS was prepared by modifying of previously patented method [8]. Dried Safflower petals (40g) were extracted with 400g of a Na_2CO_3 2% (w) cold solution. The resulting dark-brown opaque extract was treated with 1g microcrystalline cellulose Flocel-102 (India) and 2g of activated carbon („Balkan Pharmaceuticals", Moldova) and centrifuged for 10 minutes at 6000 rpm, resulting brown (very concentrated yellow) solution. Citric acid crystals were added to this solution until pH=4.5. Resulted dark-brown solution was concentrated in a rotary evaporator. Then, three volumes of food grade Ethyl Alcohol, 96% (v), were added and mixed intensively, resulting formation of the brown viscous phase. This phase was dried at 70-75°C under vacuum of 80-100mbar and mechanically powdered. The yield of dry YFDS powder was of 13g.

Yogurt preparation. Yogurt was obtained using milk with a fat content of 2.6%, skimmed milk powder and natural yellow coloring from Safflower petals (0.1; 0.2; 0.3 and

0.4% (w/w)). The standardized milk was filtered, pasteurized at a temperature of 90-94°C for 2 - 8 min, cooled to a temperature of 40 - 42°C, seeded with yogurt starter cultures and packed in glass jars. The packaged yogurt samples were kept at a temperature of 39 -42°C until the formation of the curd with a pH of 4.50-4.55, then were cooled in the refrigerator to a temperature of 2-6°C and stored there for 28 days.

Sensory analysis of yogurt was done by scoring in accordance with SM ISO 22935-3:2015 [9].

Syneresis Index. The syneresis rates of the yoghurts were determined by a centrifugal acceleration test. 10 grams of yogurt sample were placed in a test tube and centrifuged at 1200×g for 10 minutes at room temperature. The amount of serum separated from the samples was measured to estimate the syneresis index, which was expressed in % (w/w) [10].

Viscosity was determined with Brookfield DV-III Ultra rotational viscometer at the storage temperature of yogurt samples according to the method [10] with some modifications. The yogurt samples were lightly mixed 30 times for homogenization. Viscosity was determined at the shear rate (75 min^{-1}).

The pH was measured with a digital pH-meter (Mettler Toledo, SUA) at 20°C.

Fat content was measured by the Gerber methods [11].

Dry matter content was measured by the SM ISO 6731:2014 [12].

HPLC analysis. Photodiode Array (PDA) integrated HPLC instrument "Provenience-i LC-2030C 3D-Plus (by "Shimadzu"), equipped with reversed-phase C_{18}-column "Phenomenex" (4.6×150mm×4μm) was used. A gradient elution technique was realized with two mobile phases: Water, containing Acetic Acid 1.0% (v) (Phase A) and Acetonitrile, containing Acetic Acid 1.0% (v) (Phase B). Default flow: Phase B 5% at the constant rate of 0.5 mL/min. Constant oven and detection cell temperatures were of 25°C. Elution gradient program: 0-2 min – default flow; 2-18 min – Phase B 5%-40%; 18-20 min – Phase B 40%-90%; 20-24 min – Phase B 90%; 24-25 min - Phase B 90%-5%; 25-40 min – default flow.

Color analysis. The CIE-Lab parameters, L* (brightness), a* (green versus red coordinate) and b* (blue versus yellow coordinate), were measured on a white calibration block using a Chroma Meter CR-400/410 colorimeter (Konica Minolta, Tokyo, Japan) according to the method of Loypimai P. et al. [13]. The instrument was calibrated with a standard white and black reference tiles. A sample of yogurt was homogenized and placed in a 2 cm thick glass cuvette. Each sample was analyzed at five distinct points.

Color analysis of the two types of yogurt were conducted based on the variations of L*, a*, b*, and the color differences (ΔE) were determined. The determination of ΔE was performed using the following Equation (1):

$$\Delta E = \sqrt{(L_i^* - L_o^*)^2 + (a_i^* - a_o^*)^2 + (b_i^* - b_o^*)^2}, \quad (1)$$

where: L_o^*, a_o^* and b_o^* are the values of the samples at zero time and : L_i^*, a_i^* and b_i^* are the values of each sample with time. ΔE comparisons were made based on two different factors: in relation to the color obtained at t = 0 days with respect to the control sample; and based on its own color at t = 0 days [14].

Statistical Analysis. Confidence interval was appreciated for 95% confidence level.

Results and Discussion

Sensory and physico-chemical property of yogurt

The YFDS was added to the yogurts during the production to form the concentrations of 0.1; 0.2; 0.3 and 0.4% (w/w). The sensory analysis of the yogurt was made on the basis of the 5-point scale by the commission of 10 trained evaluators.

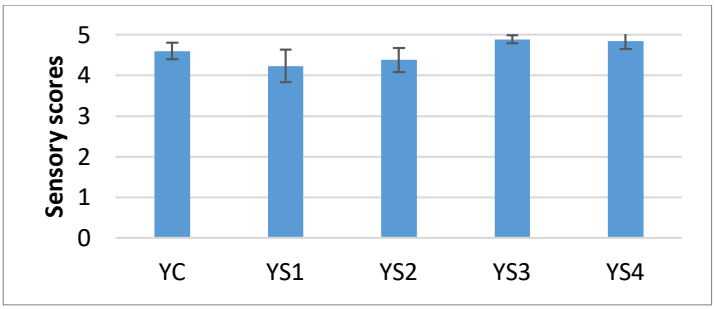

Figure 1. Sensory evaluation of yogurt with YFDS.
YC: classic yogurt (control sample); YS1-YS4: yogurts with YFDS, 0.1%-0.4% (w/w), respectively.

Following the sensory analysis, it was found that all yogurt samples had a firm curd, without removal of whey. As the amount of Safflower dye increases, so does the intensity of the yellow color of the yogurt samples. The introduction of Safflower dye in proportions of 0.3 and 0.4% in addition to the yellow color gives the samples of yogurt and a light aroma of Safflower flowers. Finally, it can be concluded that the addition of Safflower dye has an attractive yellow color and can simulate the color of apricots and other fruits in yogurt.

Similar results were obtained when using safflower petal extract in ice cream samples [15].

The physicochemical composition of the yogurts is shown in Table 1.

Table 1

Physico-chemical properties of yogurt samples

Yogurt Code*	YC	YS1	YS2	YS3	YS4
YFDS	**none**	**0.1%**	**0.2%**	**0.3%**	**0.4%**
Dry substance, %	11.7 ± 0.1	11.8 ± 0.1	11.9 ± 0.2	12.0 ± 0.2	12.1 ± 0.2
Fats, %	3.00 ± 0.11	2.97 ± 0.10	2.96 ± 0.09	2.96 ± 0.09	2.96 ± 0.09
pH	4.40 ± 0.03	4.41 ± 0.03	4.46 ± 0.03	4.48 ± 0.03	4.44 ± 0.03
Viscosity, Pa·s	3.31 ± 0.17	3.90 ± 0.20	3.84 ± 0.19	3.93 ± 0.20	3.97 ± 0.18
Syneresis index, %	70.86 ± 0.71	66.31 ± 0.67	62.84 ± 0.63	60.78 ± 0.61	61.65 ± 0.62

*YC: classic yogurt (control sample); YS1 – YS4: yogurts with YFDS, 0.1-0.4% (w/w), respectively.

The dry matter content was found to be slightly higher in the samples of Safflower dye yogurt than in the control. A similar trend was observed for the viscosity of yogurt. It was found that the fat content decreases with increasing dye concentration. Yogurt samples with the addition of Safflower dye have a pH value similar to the dye-free yogurt sample. Therefore, the addition of dye obtained from Safflower petals induces the yellow color of yogurt without influencing its physico-chemical properties.

The evolution of the yogurt color depending on the amount of dye

The color of fruit yogurt has a remarkable influence on consumer acceptance and is also an indicator of changes in the concentration of pigments that occur during storage [6].

The values of the chromaticity coordinates, L *, a *, b *, of the yoghurts with the addition of natural dye from Safflower petals are presented in Table 2. As a control sample, the classic yogurt without additives was used.

Table 2

CIE-Lab parameters of classic yogurt (control sample) and yogurts with YFDS

Chromaticity coordinates	Yogurt*				
	YC	YS1	YS2	YS3	YS4
L*	75.08	75.31	74.79	74.40	74.62
a*	-2.90	-4.18	-4.71	-5.20	-5.21
b*	9.06	13.29	15.53	17.96	18.41
ΔE (YS (dyed) vs YC (control)	-	4.43	6.72	9.22	9.64

*YC: classic yogurt (control sample); YS1 – YS4: yogurts with YFDS, 0.1-0.4% (w/w), respectively.

The color differences between classic yogurt and YFDS-added yogurt were determined by ΔE. When 0<ΔE<1, the assessors does not perceive the color difference, 1<ΔE<2 only the experienced assessors can observe the color difference, finally, if 2<ΔE<3.5, the color differences are observed even the inexperienced assessors [16].

According to the data presented in Table 2, ΔE increases in proportion to the increase in the concentration of Safflower dye in yogurt, from 4.43 to 9.64. ΔE correlates with the results of sensory analysis, through which with the naked eye a slight increase in the intensity of the shade of yellow is detected along with the increase in the concentration of safflower dye.

Color stability during storage of yogurt

Stability of yogurt color with the addition of natural dye Safflower YS3 and YS4 was determined during 28 days of storage (Table 3). As a control sample, the yogurt with the addition of synthetic dye E 102 of yellow color similar to that of Safflower dye was used, so that the color of the yogurt with E 102 is very close to that of the yogurt YS4, ΔE being 0.86. Dye E 102 is used in the manufacture of dairy products at the industrial level, demonstrating a high stability during storage of finished products.

Table 3

Behavior of chromaticity coordinates of the yogurts with the addition of natural dye Safflower as a function of storage time

Parameters	Storage time, days	Yogurt*		
		YS3	YS4	YT
L*	0	74.40	74.62	75.18
	3	74.42	74.51	75.17
	7	74.35	74.46	75.12
	14	74.54	74.29	75.23
	21	74.58	74.03	75.29
	28	74.62	73.97	75.48
a*	0	-5.20	-5.21	-5.85
	3	-5.15	-5.30	-5.84
	7	-5.00	-5.35	-5.84
	14	-5.08	-5.34	-5.85
	21	-5.10	-5.32	-5.89
	28	-5.12	-5.32	-5.90

Continuation Table 3

b*	0	17.96	18.41	18.29
	3	18.34	18.62	18.21
	7	18.70	18.91	18.11
	14	18.32	18.90	18.30
	21	18.25	18.89	18.46
	28	18.05	18.86	18.65
h°	0	106.15	105.80	107.74
	3	105.69	105.89	107.78
	7	104.97	105.80	107.87
	14	105.50	105.78	107.73
	21	105.61	105.73	107.70
	28	105.84	105.75	107.55
C*	0	18.70	19.13	19.20
	3	19.05	19.36	19.12
	7	19.36	19.65	19.03
	14	19.01	19.64	19.21
	21	18.95	19.62	19.38
	28	18.76	19.60	19.56

*YT: yogurt with synthetic dye E 102; YS3, YS4: yogurts with YFDS, 0.3 and 0.4% (w/w), respectively.

As can be seen in Table 3, the L* parameter showed average values between 73.97 and 75.48 units during the 28 days of storage, indicating that the samples had a high brightness, similar to the value t=0 days. Regarding the coordinate a*, the average values were between -5.90 and -5.00 units. The values of the chromatic coordinates a* indicate a negative value that represents the green area. In the case of the b* chromaticity coordinate, the average values were between 17.96 and 18.91 and all are located on the positive side of the axis, which represents the yellow area. The samples showed uniformity in the three chromatic coordinates L*, a*, b* throughout the storage period for both the control yogurt and the yogurt with natural coloring from Safflower petals.

The color shade (h°) remained almost constant during the storage of yogurts with coloring from Safflower petals, which indicates that the color of the yogurt does not change during storage. Most likely there is no degradation of chalconic dyes in the composition of YFDS and in the lipid-protein matrix of the yogurt.

During storage, neither significant differences in chromium (C*) were observed for all yogurt samples, indicating that the color of the yogurt remains as intense over time.

In general, the chromatic coordinates of the samples of yoghurt with coloring of Safflower petals did not undergo considerable changes during the storage stage.

Photodiode Array detection demonstrate presence of four yellow chalcones in Yogurt: Hydroxysafflower Yellow A, Precarthamin, Unidentified (but with UV-Vis pattern, characteristic for yellow chalcones of Safflower), and Anhydrosafflower Yellow B (Figure 2).

Chromatographical data, obtained by calculation of relative peak areas of chalcones in the samples of YFDS and YFDS-colored Yogurts, demonstrate no significant changes in the chalcones ratio during storage period (Table 4).

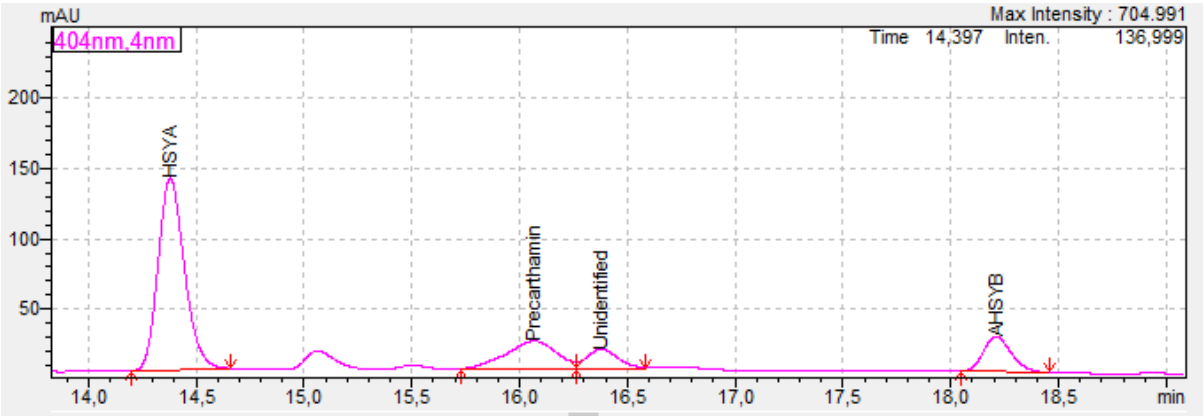

Figure 2. HPLC profile of chalcones in YFDS-colored yoghurts after 14 days of storage.

Table 4

Relative content of yellow chalcones in Yogurt after 14 days of storage

Yellow chalcones in Yogurt	R_T, min	λ_{max}, nm	Relative peak Area, %
Hydroxysafflower Yellow A	14.4	339, 402	62
Precarthamin	16.1	327 sh, 407	18
Unidentified	16.4	406	8
Anhydrosafflower Yellow B	18.2	335 sh, 409	12

Chemical degradation of chalconic components in YFDS could result in significant changes in brightness during yogurt storage, but HPLC data confirm that yellow substances remain chemically intact during yogurt storage.

Color differences during the storage period were determined by ΔE. Figure 3 shows the color differences (ΔE) obtained during the 28 day storage for synthetic dye and Safflower dye yogurts.

The color difference ΔE for samples with natural dye from Safflower petals throughout the storage period was ⩽ 0.79, which is an extremely satisfactory result, as ΔE ⩽ 3.0 cannot be detected with the naked eye [17].

The above facts indicate that the natural colorant of Safflower petals was stable throughout the storage period at refrigeration temperatures, with no significant changes in any of the three color coordinates.

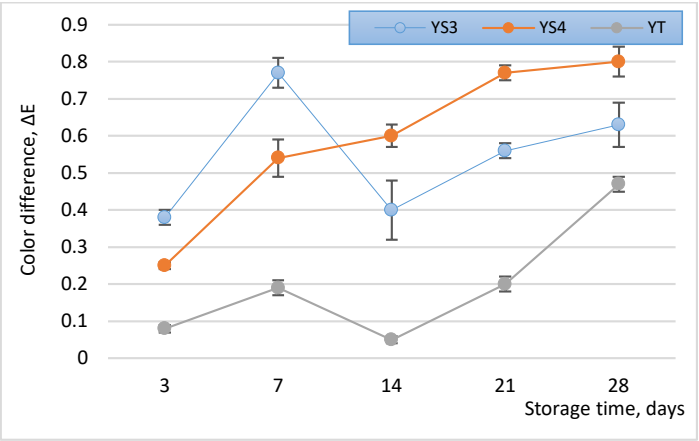

Figure 3. Color difference (ΔE) of the yogurt with YFDS of storage time. ΔE comparisons were made based on its own color at t=0 days.

YT: yogurt with synthetic dye Tartrazine (E 102); YS3, YS4: yogurts with YFDS, 0.3 and 0.4% (w/w), respectively.

The high stability of the natural coloring of Safflower petals in the protein-lipid matrix of yogurts taken in this study contrasts with [18], in which were pointed out that colors from natural sources tend to lose their coloring power or disappear over time in storage studies.

Conclusions

The possibility of using Yellow Food Dye from Safflower to form the natural yellow color in yogurts has been demonstrated. Principal yellow chalcones of Safflower (HSYA, Precarthamin and AHSYB) ratio, does not suffering significant changes in the composition of Yogurt during storage period. Yogurt production allows YFDS to be packaged in the lipid-protein matrix of the dairy product. The color parameters remain stable during the 28 days of storage. The results of this study contribute to encouraging the use of Safflower dyes in natural foods. This study confirms, that Safflower petals (usually wastes, resulting of the Safflower growing) are valuable source for the production of harmless yellow food dyes for the dairy industry of Moldova and Romania.

Acknowledgments. The research was funded by State Project no. 20.80009.5107.09 "*Improving of food quality and safety through biotechnology and food engineering*", running at Technical University of Moldova.

References

1. Baerle A., Savcenco A., Tatarov P., Fetea F., Ivanova R., Radu O. Stability limits of a red Carthamin–cellulose complex as a potential food colourant. Food & Funcions, 2021 (2), pp. 8037-8043. https:// doi.org/10.1039/D1FO01376A
2. Zhang L., Tian K., Tang Z.-H., Chen X.-J., Bian Z.-X., Wang YI-T., Lu J.-J. Phytochemistry and Pharmacology of Carthamus tinctorius L. The American Journal of Chinese Medicine, 2016, 44 (2), pp. 197-226. Doi: 10.1142/ S0192415X16500130
3. Fangma Y., Zhou H., Shao C., Yu L., Yang J., Wan H., He Y. Hydroxysafflor Yellow A and Anhydrosafflor Yellow B Protect Against Cerebral Ischemia/Reperfusion Injury by Attenuating Oxidative Stress and Apoptosis via the Silent Informa. Front Pharmacol, 2021 (12). https://doi.org/10.3389/fphar.2021.739864
4. Lin W-S., Hua He P., Chau C-F., Liou B-K., Li S., Pan M-H. The feasibility study of natural pigments as food colorants andseasonings pigments safety on dried tofu coloring. Food Science and Human Wellness, 2018, 7 (3), pp. 220–228. Doi: 10.1016/j.fshw.2018.09.002
5. Giusti M. M., Wrolstad R. E. Acylated anthocyanins from ediblesources and their application in food system. Biochemical Engineering Journal, 2003, 14(3), pp. 217–225. Disponibil: doi:10.1016/S1369-703X(02)00221-8
6. Scibisz I., Ziarno M., Mitek M. Color stability of fruit yogurt during storage. Journal of Food Science and Technology, 2019, 56 (4), pp. 1997-2009. Doi:10.1007/s13197-019-03668-y
7. Luzardo-Ocampo I. Ramírez-Jiménez A. K., Yañez J., Mojica L., Luna-Vital D. A. Technological applications of natural colorants in food systems: A Review. Foods, 2021, 10, 634, 34p. https:// doi.org/10.3390/foods10030634
8. Savcenco A., Baerle A., Tatarov P., Ivanova R. Process for producing dyes from Safflower petals. Patent of Moldova, MD-1453, issued 31.03.2021.
9. SM ISO 22935-3:2015. Milk and milk products. Sensory analysis. Part 3: Guidance on the method of assessing conformity with product specifications for the determination of sensory properties by point counting. - in Romanian.
10. Dönmez Ö., Mogol B. A., Gökmen V. Syneresis and rheological behaviors of set yogurt containing green tea and green coffee powders. Journal of Dairy Science, 2017, 100 (2), pp. 901-907. https:// doi.org/10.3168/jds.2016-11262
11. SM ISO 11870:2014. Milk and dairy products. Determination of fat content. General guidelines for the use of butyrometer methods. - in Romanian.
12. SM ISO 6731:2014 Milk, cream and evaporated milk - determination of total solids content (reference method) - in Romanian.

13. Loypimai P., Moongngarm A., Chottanom P. Thermal and pH degradation kinetics of anthocyanins in natural food colorant prepared from black rice bran. Journal of Food Science and Technology, 2016, 53 (1), pp. 461-470. Doi: 10.1007/s13197-015-2002-1
14. Mezquita P.C., Barragán-Huerta B.E., Ramírez J.P., Hinojosa C.O. Stability of astaxanthin in yogurt used to simulate apricot color, under refrigeration. Food Science Technology, Campinas, 2014, 34 (3), pp. 559-565. Doi: 10.1590/1678-457x.6386
15. Machewad G.M., Ghatge P., Chappalwar V., Jadhav B., Chappalwar A. Studies on extraction of Safflower pigments and its utilization in ice cream. Journal of Food Processing and Technology, 2012, 3 (8), 3p. Doi: 10.4172/2157-7110.1000172
16. Mokrzycki W., Tatol M. Colour difference ΔE-A survey. Machine Graphics and Vision, 2011, 20 (4), pp. 383-411.
17. Hong S.I., Han J.H., Krochta J.M. Optical and surface properties of whey protein isolate coatings on plastic films as influenced by substrate, protein concentration, and plasticizer type. Journal of Applied Polymer Science, 2004, 92 (1), pp. 335-343. Doi:10.1002/app.20007
18. Krammerer D., Schillmoller S., Maier O., Schieber A., Reinhold C. Colour stability of canned strawberries using black carrot and elderberry juice concentrates as natural colorants. European Food Research and Technology, 2007, 224 (6) pp. 667-679. Doi: 10.1007/s00217-006-0356-3

Journal of Engineering Science *Vol. XXIX, no. 1 (2022), pp. 151 - 163*
Fascicle *Food Engineering* *ISSN 2587-3474*
Topic *Food Industry and Management* *eISSN 2587-3482*

https://doi.org/10.52326/jes.utm.2022.29(1).14
CZU 661.746.3:663.26(478)

POSSIBILITY AND NECESSITY OF TARTARIC ACID PRODUCTION IN THE REPUBLIC OF MOLDOVA

Vladislav Reşitca[1], ORCID: 0000-0002-6063-1731,
Anatol Balanută[1]*, ORCID: 0000-0002-4153-1065,
Iurie Scutaru[1], ORCID: 0000-0002-9199-5183,
Ecaterina Covaci[1], ORCID: 0000-0002-8108-4810,
Aliona Sclifos[1], ORCID: 0000-0002-6070-0936,
Antoanela Patraș[2], ORCID: 0000-0002-4054-4884,
Ana-Maria Borta[1], ORCID: 0000-0001-5623-3063

[1]*Technical University of Moldova, 168 Stefan cel Mare Blvd., Chisinau, MD-2045, Republic of Moldova*
[2]"Ion Ionescu de la Brad" Iasi University of Life Sciences, 3 Mihail Sadoveanu Alley, 700490, Romania
*Corresponding author: Anatol Balanuţă, *anatol.balanuta@enl.utm.md*

Received: 12.16.2021
Accepted: 01.24.2022

Abstract. The wine industry has been and remains a source of natural- tartaric acid. The tartaric acid can be obtained from such wastes as grape marcs, yeast, vinasse and wine stone. But the use of these wastes was limited in the Republic of Moldova by the production of tartaric acid lime (calcium tartrate) and wine stone, which were shipped to Ukraine and Armenia where the finished product is obtained. Currently, tartaric acid is used in considerable quantities in the winemaking and food industry, being a quite expensive imported product. The Department of Oenology and Chemistry has developed a complete technological scheme for the use of wine wastes to obtain the finished product – tartaric acid. The realization of the proposed tartaric acid production in the Republic of Moldova is important for the country's economy and it does not require large investments. Wineries can also help to organize tartaric acid production by providing calcium tartrate, wine stone, pressed or dried yeast, and other ingredients.

Keywords: *tartaric acid, calcium tartrate, winemaking, circular bioeconomy, vinasse, wine stone.*

Rezumat. Industria vinului a fost și rămâne o sursă de acid tartric natural. Acidul tartric poate fi obținut din deșeuri precum tescovina de struguri, drojdia de vin, vinasa și semințele de struguri. Dar utilizarea acestor deșeuri a fost limitată în Republica Moldova la producția de tartrat de calciu și piatră de vin, care erau expediate în Ucraina și Armenia, unde se obținea produsul finit. In prezent acidul tartric este folosit in cantități considerabile in vinificație și industria alimentara, fiind un produs de import scump. Departamentul de Oenologie și Chimie a elaborat o schemă tehnologică completă de utilizare a deșeurilor de vin pentru obținerea produsului finit – acid tartric. Realizarea producției propuse de acid tartric în Republica Moldova este importantă pentru economia țării și nu necesită investiții mari. Cramele pot

recurge, de asemenea, la organizarea producției de acid tartric, oferind tartrat de calciu, piatră de vin, drojdie presată sau uscată și alte ingrediente.

Cuvinte cheie: *acid tartric, tartrat de calciu, bioeconomie circulară, vinasă, piatră de vin.*

Introduction

The wine industry has been and remains a source of tartaric acid in wine wastes. The use of wine wastes in Moldova was limited to the production of tartaric acid lime (calcium tartrate), wine stone and dried yeast. So, tartaric acid remains to be a quite expensive imported product. Considering that only 30 - 40% of wine wastes currently are reused globally, the recycling strategy must be reassessed. When properly managed, secondary wine products may be used to generate value-added goods. The physicochemical characteristics of wine wastes indicate that they contain a wide variety of extractable substances used by food, pharmaceutical, and other industries. The usage of wine industry generated by-products would result in fewer wastes and develop rich bioactive component extracts with various uses [1]. The environmental impact should be taken into account, when processing wastes into tartaric acid.

The goal of this research was to develop a complete technological scheme for the use of wine waste to obtain the finished product - tartaric acid. The article includes an in-depth study of current developments in the field, both internationally and nationally.

The implementation of the proposed production of tartaric acid in the Republic of Moldova has an essential significance for the country's economy. It does not require large investments. Wineries can also participate in organizing the production of tartaric acid by supplying calcium tartrate, wine stone, pressed or dried yeast.

1. Tartaric acid

Tartaric acid is an organic acid, mainly found in grapes but also in a wide variety of fruits. L(+)-tartaric acid is the most common type of acid found in nature, while D(-)-tartaric acid sources are limited [2]. The main sources of tartaric acid on the market are: recovery from winery waste, chemical synthesis (from maleic anhydride) or of microbiological origin [3].

L(+)-tartaric acid is traditionally formed as a solid crystals in the wine fermentation process, and this mode of manufacturing is heavily influenced by grape maturity and environmental factors. Chemical synthesis of L(+)-tartaric acid using maleic acid is possible, but this results in a significantly less soluble racemic DL-form that is not acceptable for inclusion in foods. The D(-)-tartaric acid presence makes it hazardous to human health. High production cost also limits the commercial utilization of the chemical process. For the manufacture of both tartaric acid forms, microbial methods are currently considered to be more simple and cost-effective [2].

Utilizing tartaric acid is more expensive than citric and malic acids, and in comparison to most other organic acids, it has the least antimicrobial properties. Furthermore, when it is dissolved in hard water, an unwanted insoluble precipitate of calcium tartrate might occur [4].

As a winemaking additive, principle of action is based on part of the tartaric acid added to the wine will lead to the precipitation of potassium bitartrate and thus a drop in the pH of the wine. Possible side effects are increased tartaric instability in wine, and at high doses, can impart a bitter flavor and give wine astringency. Verification of the effectiveness of the treatment is done by measuring total acidity and pH of wine. Cost of this additives varies from 5 to 6 €/kg i.e., between 0.5 and 0.6 €·hL^{-1} of treated wine (dose 100 g·hL^{-1}) [5].

L(+)-tartaric acid is consumed in different industries, including food, pharmaceutical, chemical, and polyester production. In the pharmaceutical industry, D(-)-tartaric acid is also important [2]. Tartaric acid is preferred in cranberry or grape-based foods, such as wines, jellies, and confectioneries [4].

Main winemaking application, according to the International Code of Oenological Practices is acidification of musts and wines i.e., increasing the titrating acidity and real acidity (decreasing the pH). Tartaric acid addition develops balanced wines from the point of view of taste sensations, promotes good biological development and smooth maturation of the wine and fixes a lack of natural acidity [5].

In recent years, green extraction technologies for obtaining high-value bioactive chemicals from raw natural materials and wastes have gotten a lot of interest. A natural deep eutectic solvent was explored - L(þ)-tartaric acid, as a possible solvent for extracting phenolic compounds [21, 22].

Polytartaric acid, a novel polymer having several pendant negatively charged carboxylate groups, was investigated as a potential coating material for magnetic nanoparticles. Polytartaric acid is produced by simply heating tartaric acid as a sustainable natural product under controlled conditions without the need for a solvent or a catalyst [8]. The utilization of wine by-products as a substrate for the production of polymer building blocks and as polymer reinforcing fillers is investigated [9].

Esters/ethers produced from tartaric acid, were obtained, thoroughly described, and evaluated as PVC plasticizers. They found to be completely compatible with PVC, have an acceptable plasticizing effect, have a minimal migration potential, and have no effect on the polymers' thermal stability. Traditional phthalate plasticizers may be replaced by these biobased compounds [10].

The magnesium oxychloride cement (MOC) production aids in the CO emissions reduction and recycling of potash industrial waste. Biobased chitosan (CS) and tartaric acid (TA) were used as organic chelating components to enhance the MOC's compressive strength and water resistance, as they give more active sites for Mg ions in the cement [11].

1.1 Composition of winemaking by-products

Winery wastes can differ in composition, depending on harvesting period and conditions. Table 1 shows the content of tartaric compounds in the main wine wastes.

Table 1

Content of tartaric compounds (recalculated in tartaric acid) in the main wine wastes

Wine wastes	Tartaric compounds
Winemaking marcs:	
- white wine, g/kg	0.5-2.0
- red wine, g/kg	0.7-2.5
- fortified wine, g/kg	12-30
Pressed yeast, g/kg	10-60
Dried yeast, g/kg	Min 25
Wine stone, g/kg	Min 520
Vinasse, g/dm^3	2.9

Grape stalks (leaves and shoots), grape seeds, wine lees, and grape marc (pomace) are solid residues produced by the winemaking industry, and their chemical composition varies depending on the source.

Grape marc (pomace) is a solid product produced during the primary grape juice production process, that comprises both water-soluble and water-insoluble components. It contains a significant amount of protein, pectin and cellulose, and has a moisture level of 40-81 %. Monosaccharides, polysaccharides, and oligosaccharides are water-soluble compounds, but polysaccharides incorporated in cell walls are water-insoluble [12].

In the Table 2 the main characteristics of the tartaric raw materials are presented.

Table 2

Characteristic of tartaric raw materials [13]

Raw material	Humidity, %, max	Tartaric acid content, %, min	Insoluble impurities content, %, max	Medium
Liquid yeast sediment:				
dry	97	2.5	1.0	acidic
fortified	97	3.5	1.0	acidic
Dry yeast sediments:				
I grade	5.0	25.0	50	acidic
II grade	5.0	20.0	55	acidic
Calcium tartrate:				
I grade	3.0	45.0	8	neutral
II grade	3.0	40.0	15	pH 6.5-7.0
Wine stone:				
I grade	2.0	65.0	3.0	acidic
II grade	3.0	55.0	10.0	acidic
Lime sediment:				
I grade	3.0	40.0	10.0	neutral
II grade	3.0	30.0	10.0	neutral

Wine lees form at the end of the fermentation in the winemaking process. They contain inorganic components, organic acids, and phenolic compounds. Solid part of wine lees is represented by cellulose, hemicellulose, lignin, seeds, grains, organic and inorganic salts.

Vinasse, which is made up of leftover fermentation broth, is the liquid fraction of wine lees. It is the primary source of polyphenol chemicals and includes around 58 % water by weight, with a pH of 3.5 [12]. Vinasse should be used immediately after the distillation of wine and its clarification.

The yeast, obtained by pressing the rotating drum filter, can be immediately transported to the tartaric acid production plant or can be pre-dried. After extraction, pressed yeast can be washed with water and then used as a food additive for animals or as compost.

2. Previous experience in the field

According to a 2006-year survey of European wineries on waste disposal:

Grape stalks were mainly land-spread in Italy, Spain, and France, and mostly disposed of (in landfills) in Greece. The pomace was distilled in Italy, France, and Spain. In Spain still, 50% was land-spread, and in Greece, 67% of pomace ended up in landfills. Wine lees were mostly used for distillation in all mentioned countries. In Spain, filter cakes were used for

tartaric acid production, in France for land-spreading, and composted in Italy. In Greece, they were discarded.

In the US, Canada, and Australia, winemaking wastes are preferred to be composted. South Africa also composts the majority of wineries' wastes, but some refineries produce cream of tartar, calcium tartrate, and grape wine spirit. Most of the winemaking countries are also producing grapeseed oil [14].

2.1 Situation in the Republic of Moldova

In 2021, the questionnaire was held, in which participated wineries, that cumulatively generate approximately 25-30% of the total by-products in the sector. In the set of questions on the main challenges of transition and implementation of the circular business model within the enterprise, the following ranking was obtained:

- Lack of technological and technical solutions for the recovery of wine by-products - 64%
- Lack of adequate and clear information on circular economy opportunities - 43%
- Lack of employment and financial risks obtained equal scores - 14% each
- Other transition and implementation issues were not identified, 0%

57% of wine companies do not capitalize on wine by-products, and 43% do so. Among that 43% of enterprises, more than 66% process small quantities (less than 50%) of the total amount of by-products generated [15].

China imports from Moldova grape seeds, oil and tartaric acid, because the EU has banned the import of tartaric acid synthesized from petroleum products. Now China starts producing natural tartaric acid. The EU market is only 60% satisfied with this product. The current shortage of tartaric acid at 40% creates good opportunities for our country. Also, a Spanish investor "Agrovin" placed his production in Gagauzia and buys wine yeast from Moldova. Ethanol and tartaric acid are extracted from them, so almost everything is recycled [16].

Nevertheless, out of the total volume, only a small part of the by-products of winemaking is processed. At some enterprises, wine-making waste is stored outside the settlements. They heat up, the surface is covered with billions of spores that spread to farmland. This leads to the fact that it is necessary to increase the load of phytoncides and pesticides [16].

2.2 Amount of wasted resources (winemaking waste)

In developed wine-making countries, wine-making waste is processed to obtain from them other necessary products. For a long time, this topic was not of interest to manufacturers in Moldova, apart from isolated cases. But the European Union allocated money for the implementation of a cross-border project, in which Moldova and Ukraine are involved, in order to create clusters for the processing of secondary wine products.

According to the ONVV, for 2010-2017 in our country, an average of 250 thousand tons of grapes were processed. Of these, 18 million decaliters of wine and 3.5 million decaliters of wine materials for distillate worth $200 million were produced.

Also, from this amount of wine and cognac production, secondary products were obtained: 80 thousand tons of pomace, 40 thousand tons of stillage, 25 thousand tons of seeds, 20 thousand tons of yeast and 10 thousand tons of ridges [16].

For 1000 decaliters of wine materials, the following amount of yeast sediments is formed: liquid yeast at the first removal of wine - 50 decaliters; precipitation during the subsequent removal of wine - 15 dal; squeezed out (pressed) yeast sediments - 200 kg [17].

3. Demand for tartaric acid on the market

In 2013, Europe was the largest regional market, accounting for 39.4 % of market volume. This market is predicted to develop due to high tartaric acid demand in winemaking countries [17, 18]. Because of its antioxidant effects, tartaric acid is increasingly being used in functional foods and energy drinks [18].

Antibiotics and cardiotonics both include tartaric acid as an excipient. Its rising use as a component of gypsum in the construction industry, in soil fertilizers and metal cleaning is likely to contribute to the market growth [19]. In the coming future, the market is projected to benefit from tartaric acid's adoption in niche applications [20].

The COVID-19 pandemic has impacted nearly every industry in every location, with the majority of manufacturing enterprises either shutting down or functioning with minimal production and staff. Despite this, there's still a demand for food. Food and beverage sales were observed to be high, prompting producers to adapt their sales tactics and transfer to online platforms [21].

Increased pricing has resulted from decreased availability in Europe and North America, which is projected to provide problems to market players [19]. The negative impact of the COVID - 19 pandemic is expected to inhibit the natural tartaric acid market's growth [20].

The worldwide tartaric acid market is predicted to develop at a sustainable rate during 2020 - 2030. The global tartaric acid industry is being fueled by rising wine and processed food consumption. The tartaric acid market is expected to rise 1.5 times in volume by the end of 2030, owing to the growing wine sector [21].

4. Methods for tartaric acid production

Wine lees have been mainly used as a raw material for the extraction of tartaric acid and ethanol since they cannot be used as animal feed due to high polyphenol content [22]. The reported yield for tartaric acid production is 100 – 150 kg per ton of wine lees. Among winery wastes, recovery of tartaric acid has been well established for wine lees and grape marc [23].

4.1 Basic methods

L(+) tartaric acid can be extracted from tartar, wine lees, and grape pomace, according to industry information. Tartaric acid usually represented by monopotassium tartrate (80–90 % in tartar) and calcium tartrate in these products.

These secondary raw materials are firstly neutralized by CaOH or $CaCO_2$, followed by concentration and centrifugation, resulting in calcium tartrate. In a decomposing tank, it is then treated with sulfuric acid to generate tartaric acid, which is refined through concentration and crystallization (Figure 1) [10, 12]

Determined optimum values for tartaric acid extraction from solid wastes are: pH (2.0), temperature (45°C), contact time (30 min), and solid to solvent (ethanol) ratio (1:6 w/v) for red and white tartar wastes respectively [24].

After filtration and purification (especially demetallization), the tartaric acid is concentrated by vacuum evaporation; then tartaric acid is transformed in solid form by crystallization, washing and drying. The resulting gypsum, as well, can be used as a building material [3, 4].

In cognac production, as a result of the extraction of tartaric acid from vinasse by precipitation with milk of lime, tartar (salts of tartaric acid) is formed. The remainder of the

stillage after removing tartaric acid from it (and when bringing the active acidity to an optimal level) can be used as fertilizer for some types of soils without contaminating them [27].

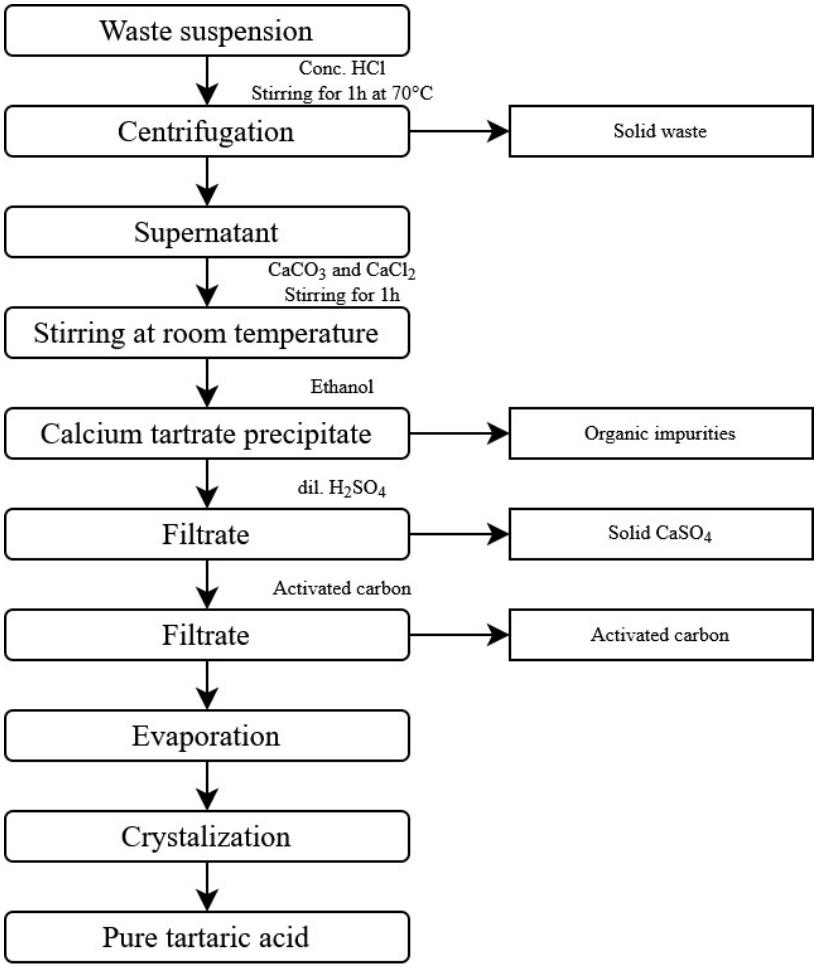

Figure 1. Recovery of tartaric acid from red and white tartar wastes [28].

For such materials, as dregs and marc, calcium tartrate is extracted in an ensuing manner: they are first mixed with water and then ethanol is removed in fractioning columns. Calcium tartrate is formed when wine marc is neutralized with calcium salts and remains suspended in the form of crystals then the wine marc is centrifuged through a series of cyclone separators. Due to the abrasive effect of the tartrate crystals on the pumps and cyclones, frequent stops for maintenance and repair are also required, resulting in significant downtime expenses [14].

Patent EP1288288 provides a solution to this problem.

Vibration makes tartrate crystals precipitate easier since it significantly reduces the friction between the tartrate crystals and the liquid medium. Calcium tartrate gathers at the outflow conduit in this procedure. Crystals have high purity and the possible tartrate recovery rate is nearly 100%. The plant is thought to be easy to build, cost-effective, quiet, and has an unlimited lifespan [29]. An alternative method of tartaric acid recovery exists. Firstly, the wine waste materials are treated with KOH solution (80°C and pH 8) and possible contaminants are eliminated with activated carbon. Then, potassium tartrate precipitation is done by the addition of saturated tartaric acid solution. Sulfuric acid (pH 2) is added to the obtained precipitate to redissolve it at 70°C. Removal of interfering K+ and SO_2– ions is performed by ion exchange resins. After removing the impurities, the solution is concentrated by evaporation, following crystallization at 4°C [34, 35].

Those conventional recovery methods let to obtain a high yield. Nevertheless, the process has its disadvantages: complexity, cost, laboriousness, and environmental impact caused by higher quantities of produced calcium sulfate deposit [23]. Solvent extraction yield is up to 90%. Adsorption method is easy to operate, but has low capacity and adsorbents have short lifetime. Adsorption methods let to achieve the 75 – 99% yield [32].

4.2 Environment friendly methods

4.2.1 Electro-membrane method for tartaric acid recovery

To enhance process efficiency and reduce production costs, it is essential to reform the technological aspects of organic acids recovery. Electro-membrane processes let to separate organic acids from mixed solution, avoiding usage of any solvent, so the main purifying elements are ion-exchange membranes. This method also provides elevated product purity and yield.

The main known electro-membrane process for the recovery of the tartaric acid is electrodialysis. The operation parameters for electrodialysis for tartaric acid recovery are: temperature (25 – 40°C) and feed solution (10 kg m^{-3} tartaric acid and 60 kg m^{-3} glucose). As a result, final acid concentration achieved is 170–300 kg·m^{-3} with energy consumption of 5.103–12.103 kJ·kg^{-1} [32].

There are also studies on electrochemical reduction of oxalic and glyoxylic acids for development of a feasible green and sustainable synthesis of tartaric acid in aqueous and/or acetonitrile solvent utilizing silver and lead electrodes [33].

In a GB756854 patent, a process of extracting potassium hydrogen tartrate from wine lees was proposed. According to technology, tartrate ions are removed from the wine lees solution by passing it through anion-exchange material in the hydroxyl form and its elution with KOH or NaOH or H_2SO_4. Then, adsorbent effluents are electrolyzed in separate cells. The tartaric acid separation takes place in the anode compartment from the anion exchange material effluent. Similarly, in another cell, KOH is separated in the cathode compartment from the cation exchange material effluent. The reaction of tartaric acid and KOH results in obtaining the tartar cream. The advantages of this solution are recovering tartar cream from byproducts and limited usage of chemicals in the process [14].

For rich in potassium hydrogen tartrate (KHT) vinasses, anionic- (AEM) and cationic-exchange membranes (CEM), as well as bipolar ones (BPM), can be used to concentrate KHT in the pre-distilled solution. Firstly, standard membrane electrodialysis (CEM-AEM-CEM configuration), followed by bipolar membrane one (using (anode)-CEM-BPM-AEM-CEM-(cathode) configuration). The high efficiency and purity of the product were shown applying a combination of membranes during electrodialysis [34].

The high selectivity of membranes allows producing tartaric acid with relatively high purity, without discards of solid wastes, compared to the traditional process. At the same time, if strong acid resin filling is used, this method provides a high production rate and relatively low energy consumption [35].

The conductive spacer can be very efficacious in assisting the transport of the hydrogen ions in the product compartment. It is supposed, that this technology can be integrated effortlessly into the production of tartaric acid by bipolar membrane electrodialysis. The application of the conductive spacer can also cause some unanticipated issues, such as the decreasing production rate and current efficiency, caused by “hydrogen ion short circuit” [36].

4.2.2 Ultrasound-assisted extraction

Tartaric acid can be extracted from wine lees also by ultrasound-assisted extraction (in combination with H_2SO_4). The optimal conditions for the process were determined. Raw materials' solid to liquid ratio should be of 1:3, using the H_2SO_4 solution of concentration 0.06 mol·L^{-1}. Ultrasound treatment duration should be 6 minutes, with magnetron power of 500W. The total extraction time reaches 15 - 20 min, holding the 75 – 80°C temperature. Retaining mentioned conditions, the final tartaric acid yield may reach 74 g·kg^{-1} [37].

4.2.3 Ion-exchange resins

This method for treating a liquid discharge from the wine-alcohol industry includes contacting the discharge with an anionic exchange resin and obtaining a cationic solution containing potassium cations and chloride anions, which is concentrated to produce a potassium-enriched solution suitable for fertilization. It further includes renewing the anionic exchange resin with a sodium chloride solution to create an anionic tartrate solution from which a tartaric acid-enriched solution or a calcium tartrate precipitate can be formed. Any liquid waste originating from the wine-alcohol sector, both from the winemaking industry and from the vinification by-product exploiting industry, characterized by tartrate anions and potassium cations, can be used in this technique. It is preferred that liquid discharge to be the vinasse [38].

Kontogiannopoulos et al. (2016) invented a cost-effective approach for recovering tartaric acid from wine lees employing a cationic exchanger to make the process more environment-friendly. The determined optimal method for the extraction is maintaining the pH of 3.0, the addition of 10 ml·g^{-1} of water in the dry material, and the addition of a cation exchanger of 3.5 g·g^{-1} to dry lees. Cation exchange resin usage under ambient temperature allows avoiding the calcium sulfate waste generation, attributable to the standard process. Following the described method may result in a tartaric acid yield of 74.9% and 98.8% efficiency of potassium elimination [39].

4.2.4 Crystallization

Salgado et al. propose a different tartaric acid recovery scheme. To achieve a rich in tartaric acid solution, the liquid raw material gets concentrated (up to 1/3 of the starting volume) in rotavapor (50◦C). Thereafter, tartaric acid precipitation with ethanol (1:1 v/v) takes place, and crystallization is performed at −20◦C for 24 h. After warming up to 4◦C, crystals are isolated by centrifugation and washed [31].

4.2.5 Nanofiltration

Some studies propose that nanofiltration with a membrane pore size of around 1 kDa can provide excellent separation filtration. In this case, the filtrate will contain a quite high concentration of tartaric acid, which could be later refined by evaporation and crystallization. The remaining concentrate will be a substance, rich in polyphenols, which can be further used as a source of antioxidants [40].

4.3 Local developments

There were several Moldovan patents issued in last 20 years, showing that the tartaric acid extraction from winemaking wastes already was in the field of scientific interest, but, unfortunately, did not find their application on a large scale.

The first mentioned invention is for a method of tartaric acid production from winemaking waste-provided calcium tartrate. The technological process includes mixing calcium tartrate with water at 85 - 90°C and dissolving it in 5.0 - 8.5% H_3PO_4 solution. Next, neutralizing the excess acid with $CaCO_3$ and filtering the resulting precipitate. The remaining solution should be treated with calcium hexacyanoferrate(II), with further removal of the precipitate, and eliminating impurities using activated charcoal. The final product is obtained by crystallization [41].

The second invention is in the field of organic compound purification, specifically tartaric acid purification. The invention is summarized as tartaric acid dissolution in water, treatment with 5% activated charcoal, filtration, and xylene addition. Azeotropic distillation is used for separation, followed by crystal washing (with ether or acetone) and drying at 60-80°C. The implementation of the tartaric acid crystallization process from an azeotropic mixture allows for faster crystallization and separation of the finished product, as well as higher yields (95 - 96%) [42].

The next invention is in the field of wine industry waste processing and utilization for tartaric acid production. The procedure involves dissolving tartrates with pure water and proof-filtering the solution. This is followed by the ion-exchange extraction of tartaric acid, using Amberlite LA-2 as an anionite. Finished by crystallization of the tartaric acid, utilizing butyl acetate as a polar solvent. The invention effects by boosting the efficiency of the tartaric acid production process, increases the purity of the resulting tartaric acid, with reduced usage of chemical solvents [43].

Duca (2011) proposed a technological process of obtaining tartaric acid in the pilot plant. Calcium tartrate with a concentration of 52% tartaric acid was analyzed as the starting material. Thus, the potential of the installation is as follows: processing 850 kg of calcium tartrate, obtaining 450 kg of tartaric acid. The basic steps for obtaining tartaric acid are the following: dissolution of the raw material in the reactor; filtration of the mixture under pressure; purification of the filtered solution with activated carbon and mineral sorbent; reactive extraction of tartaric acid in the plate extractor; re-extraction of tartaric acid in the plate extractor; crystallization in an azeotropic medium in crystallizer-evaporator; filtering crystals and washing them; drying the crystals in the vacuum drying plant and capturing the solvent in the refrigerant [13].

4.4 Proposed recovery scheme

A conventional method for tartaric lime obtaining is proposed. Drinking water at room temperature is mixed with the solid-type tartaric raw material. Of course, the efficiency of extracting tartrates will be more efficient at 60-70°C, but in this case, energy consumption is rising. The diffusion juice of raw material is mixed with $CaCO_3$ introduced to the mixing chamber. In the case of a liquid by-product (vinasse), the washing step is unnecessary, and $CaCO_3$ is added right away.

As a result of treatment:

$$H_2C_4H_4O_6 + CaCO_3 \rightarrow CaC_4H_4O_6 \downarrow + H_2O + CO_2$$
$$KHC_4H_4O_6 + CaCO_3 \rightarrow CaC_4H_4O_6 \downarrow + KOH + CO_2$$
$$K_2C_4H_4O_6 + CaCl_2 \rightarrow CaC_4H_4O_6 \downarrow + 2KCl$$

For the accumulation of calcium tartrate, treatment can be carried out several times in the same vessel. Then, the tartaric lime is washed with water, dried and transferred to the

tartaric acid production plant. The washed pomace can be used for further seed separation or as an addition to animal feed, compost, etc.

For the purification of tartaric acid, the staff of the Department of Oenology and Chemistry suggests using electrodialysis to separate cations, especially Ca^{2+}, and to concentrate the tartaric acid solution until the final evaporation (Figure 2).

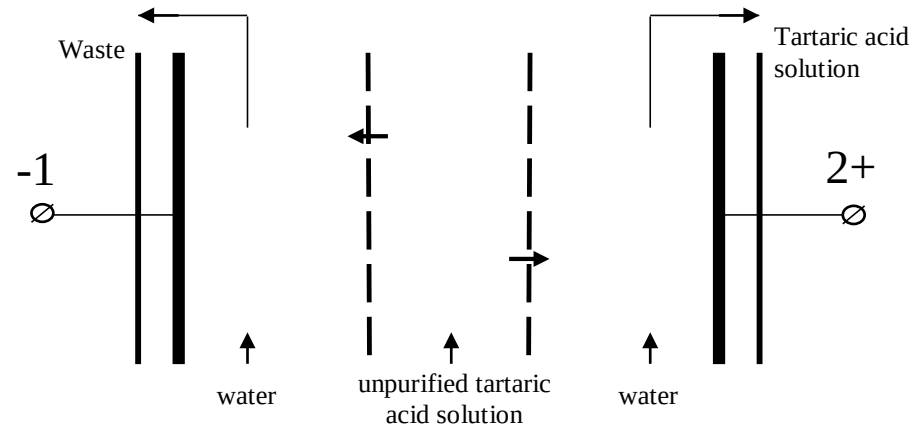

Note: 1, 2 – anode (+) and cathode (-) electrodes
M - selectively permeable membrane with (-) and (+) charge

Figure 2. Diagram of purification and concentration of tartaric acid solution by electrodialysis.

Electrodialysis can be used to separate and concentrate tartaric acid from diffusion juice. Under the action of electric current, cations will be separated from the semi-permeable membrane with positive charge, while the anions of tartaric acid from the semi-permeable membrane with negative charge. The use of electrodialysis, except the purification of tartaric acid, will reduce energy costs when concentrating the tartaric acid solution by evaporation [13].

The implementation of proposals for the production of tartaric acid can be carried out at one of the wineries, which is currently not engaged in grape processing activities. This implementation brings not only economic support, but also has social and environmental value.

Conclusions

- The main wine wastes from which tartaric acid can be produced are pomace, yeast, wine stone and vinasse.
- The production of tartaric acid from wine waste is possible and necessary without large investments, and will lead to the solution of economic, social and ecological issues.
- To solve ecological issues when using wine wastes in technological processes, it is necessary to exclude the use of aggressive and expensive reagents.
- For every one million dal of wine produced, 50 - 80 tons of tartaric acid can be obtained from the processing of wine wastes.
- The implementation of electrodialysis is recommended for the purification and concentration of tartaric acid solutions.

Acknowledgments. Research was funded by Project no. 2 SOFT/1.2/83 "*Intelligent valorization of agro-food industrial wastes (INTELWASTES)"*, running at the Technical University of Moldova, Department of Oenology and Chemistry, Micro-winery Center.

References

1. Musteață G., Balanuță A., Filimon R., Băetu M. Capitalization of secondary wine products-an opportunity for the wine sector of republic of Moldova and Romania. In: *Journal of Social Sciences*, 2021, 4(2), pp. 117–127.
2. Xuan J., Feng Y. Enantiomeric Tartaric Acid Production Using cis-Epoxysuccinate Hydrolase: History and Perspectives. In: *Molecules*, 2019, 24(5), p. 903.
3. Younes M., Aquilina G., Castle L., Engel K., Fowler P., Frutos Fernandez M., FÜRST P., Gürtler R., Gundert-Remy U., Husøy T. Re-evaluation of L(+)-tartaric acid (E 334), sodium tartrates (E 335), potassium tartrates (E 336), potassium sodium tartrate (E 337) and calcium tartrate (E 354) as food additives. In: *EFSA Journal*, 2020, 18(3), p. e06030.
4. Gurtler J., Mai T. Preservatives. Traditional Preservatives – Organic Acids. In: Batt, C. – Patel, P., ed *Encyclopedia of Food Microbiology: Second Edition*. Academic Press, 2014, pp. 119–130.
5. IFV - intrants bio [online]. 2021. [accessed: 27.12.2021]. Available: http://www.vignevin.com/pratiques-oeno/index.php?etape=1&operation=7&onglet=Origine
6. Koutsoukos S., Tsiaka Th., Tzani A., Zoumpoulakis P., Detsi A. Choline chloride and tartaric acid, a Natural Deep Eutectic Solvent for the efficient extraction of phenolic and carotenoid compounds. In: *Journal of Cleaner Production*, 2019, 241, pp. 118-384.
7. Makris D., Passalidi V., Kallithraka S., Mourtzinos I. Optimization of polyphenol extraction from red grape pomace using aqueous glycerol/tartaric acid mixtures and response surface methodology. In: *Preparative Biochemistry & Biotechnology*, 2016, 46(2), pp. 176–182.
8. Nan A., Filip Xe., Dan M., Marincaş O. Clean production of new functional coatings of magnetic nanoparticles from sustainable resources. In: *Journal of Cleaner Production*, 2019, 210, pp. 687–696.
9. Nanni A., Parisi M., Colonna M. Wine By-Products as Raw Materials for the Production of Biopolymers and of Natural Reinforcing Fillers: A Critical Review. In: *Polymers* 2021, 13(3), p. 381.
10. Howell B., Sun W. Biobased Plasticizers from Tartaric Acid, an Abundantly Available, Renewable Material. In: *Industrial & Engineering Chemistry Research*, 2018, 57(45), pp. 15234–15242.
11. Han Y., Ye Qi., Xu Y., Li J., Shi Sh. Bioinspired Organic-Inorganic Hybrid Magnesium Oxychloride Cement via Chitosan and Tartaric Acid. In: *ACS Sustainable Chemistry and Engineering*, 2020, 8(51), pp. 18841–18852.
12. Bharathiraja B., Iyyappan J., Jayamuthunagai J., Kumar R., Sirohi R., Gnansounou E., Pandey A. Critical review on bioconversion of winery wastes into value-added products In: *Industrial Crops and Products*, 2020, 158, p. 112954.
13. Duca G. *Produse vinicole secundare* [Secondary wine products]. Chișinău: Știința, 2011.
14. Galanakis C. *Handbook of grape processing by-products*. Elsevier, 2017.
15. Bugaian L., Arpentin G., Diaconu C. Perception of the circular economy by the wine sector of the Republic of Moldova. In: *Competitiveness and sustainable development in the context of European integration*, Chişinău, 2021. pp. 95–101.
16. Taran A. The hidden reserves of the wine industry [online]. 2018. [accessed: 08.01.2022]. Available: https://wine-and-spirits.md/tajnye-rezervy-vinnoj-industrii/
17. Sviridov D. Development of technology for the use of secondary resources of the viticulture and wine industry in order to increase the biological value of food products: Ph.D. Thesis. Moscow, 2017 [in Russian].
18. Grand View Research. Tartaric Acid Market Size Worth $425.0 Million by 2020 [online]. 2015. [accessed: 20.12.2021]. Available: https://www.grandviewresearch.com/press-release/global-tartaric-acid-market
19. Grand View Research. Global Tartaric Acid Market Size, Share & Trends Report, 2020 [online]. 2015. [accessed: 20.12.2021]. Available: https://www.grandviewresearch.com/industry-analysis/tartaric-acid-market
20. Mordor Intelligence. Tartaric Acid Market | 2021 - 26 | Industry Share, Size, Growth [online]. 2021. [accessed: 20.12.2021]. Available: https://www.mordorintelligence.com/industry-reports/tartaric-acid-market
21. Persistence Market Research. Global Tartaric Acid Market: Industry Analysis & Forecast [online]. 2020. [accessed: 20.12.2021]. Available: https://www.persistencemarketresearch.com/market-research/tartaric-acid-market.asp
22. Kokkinomagoulos E., Kandylis P. Sustainable Exploitation of By-Products of Vitivinicultural Origin in Winemaking. In: *Proceedings*, 2020, 67(1), p. 5.
23. Ahmad B., Yadav V., Yadav A., Rahman M., Yuan W., Li Zh., Wang Xi. Integrated biorefinery approach to valorize winery waste: A review from waste to energy perspectives. In: *Science of The Total Environment*, 2020, 719, p. 137315.
24. Aryal M., Liakopoulou-Kyriakides M. Optimization studies for tartaric acid, phenolics, sugars, and antioxidant activity from industrial red and white tartar wastes. In: *Engineering Research Express*, 2020, 2(2), p. 025042.

25. Popa Gh., Parasca P. Improvement of Technology for Obtaining Tartaric Lime from Yeast Sediments. In: *Sadovodstvo, vinograd i vinodeliye Moldavii*, 1985, 9, pp. 39–41 [in Russian].
26. Razuvayev N., Nechayeva P., Belyayev V. Technology of Complex Processing of Grape Pomace and Yeast Sediments in the Stream. In: *Voprosy vinogradarstva i vinodeliya*, 1971, pp. 434–437 [in Russian].
27. Găină B. Winemaking: Waste into income? [online]. 2005. [accessed: 06.01.2022]. Available: http://www.vinmoldova.md/reviews/vinodelie-othody-v-dohody/ [in Russian].
28. Moschona A., Ziagova M., Aryal M., Iliadou A., Liakopoulou-Kyriakides M., Kyriakidis D. Recovery of Tartaric Acid and Added-Value Phenolics from Wine Wastes Towards an Integrated Treatment and Commercial Valorisation. In: *5th International Conference on Environment Science and Engineering*, 2015, pp. 116–120.
29. BALICE DISTILLATI S.R.L., IT. Process and plant for calcium tartrate extraction from wine-making by-products. Patent no. EP1288288B1. Inventor: Gennaro BALICE. Int. cl.: C12F3/00; C12H1/06. Publ.: EPO, 2005-12-14.
30. Yalcin D., Ozcalik O., Altiok E., Bayraktar O. Characterization and recovery of tartaric acid from wastes of wine and grape juice industries. In: *J Therm Anal Calorim*, 2008, 94(3), pp. 767–771.
31. Salgado J., Rodríguez N., Cortés S., Domínguez J. Improving downstream processes to recover tartaric acid, tartrate and nutrients from vinasses and formulation of inexpensive fermentative broths for xylitol production. In: *Journal of the science of food and agriculture*, 2010, 90(13), pp. 2168–2177.
32. Handojo L., Wardani A., Regina D., Bella C., Kresnowati M., Wenten I. Electro-membrane processes for organic acid recovery. In: *RSC Advances*, 2019, 9(14), pp.7854-7869.
33. Garcia A., Sánchez-Martínez C., Bakker I., Goetheer E. Sustainable Electrochemical Production of Tartaric Acid. In: *ACS Sustainable Chemistry and Engineering*, 2020, 8(28), pp. 10454–10460.
34. Vecino X., Reig M., Gibert O., Valderrama C., Cortina J. Integration of Monopolar and Bipolar Electrodialysis Processes for Tartaric Acid Recovery from Residues of the Winery Industry. In: *ACS Sustainable Chemistry & Engineering*, 2020, 8(35), pp. 13387–13399.
35. Zhang K., Wang M., Wang D., Gao C. The energy-saving production of tartaric acid using ion exchange resin-filling bipolar membrane electrodialysis. In: *Journal of Membrane Science*, 2009, 341(1-2), pp. 246–251.
36. Zhang K., Wang M., Gao C. Ion conductive spacers for the energy-saving production of the tartaric acid in bipolar membrane electrodialysis. In: *Journal of Membrane Science*, 2012, 387–388(1), pp. 48–53.
37. QU H. Optimization of Ultrasound-Assisted Extraction of Tartaric Acid from Wine Lees. In: *Food Science*, 2014.
38. Pedros Llevata Francisco ES. *Method for treating wine-alcohol industry liquid discharges*. Patent no. EP1832649A1. Inventor: Pedros Llevata Francisco. Int. cl.: C07C51/02; C07C59/255; C12F3/00; C12F3/06. Publ.: EPO, 2007-09-12.
39. Kontogiannopoulos K., Patsios S., Karabelas A. Tartaric acid recovery from winery lees using cation exchange resin: Optimization by Response Surface Methodology. In: *Separation and Purification Technology*, 2016, 165. pp. 32–41.
40. Kontogiannopoulos K., Patsios S., Mitrouli S., Karabelas A. Tartaric acid and polyphenols recovery from winery waste lees using membrane separation processes. In: Journal of Chemical Technology & Biotechnology, 2017, 92(12), pp. 2934–2943.
41. PUBLIC INSTITUTION "SCIENTIFIC-PRACTICAL INSTITUTE OF HORTICULTURE AND FOOD TECHNOLOGIES", MD. Procedeu de obţinere a acidului tartric din tartratul de calciu obţinut din deşeuri vinicole [Process for obtaining tartaric acid from calcium tartrate obtained from wine waste]. Patent no. 4504. Inventor: Tudor Bounegru. Int. cl.: C07C 59/255; C07C 51/02. Publ.: BOPI, 2018-03-31.
42. STATE UNIVERSITY OF MOLDOVA, MD. Procedeu de purificare a acidului tartric [Tartaric acid purification process]. Patent no. 2428. Inventor: Aliona Mereuţă, Corneliu Oniscu, Tamara Ceban, Gheorghe Duca. Int. cl.: C07C 51/42. Publ.: BOPI, 2004-11-30.
43. STATE UNIVERSITY OF MOLDOVA, MD. Procedeu de obţinere directă a acidului tartric din produsele vinicole secundare [Process for the direct production of tartaric acid from by-products]. Patent no. 2407. Inventor: Aliona Mereuţă, Corneliu Oniscu, Victor Covaliov, Gheorghe Duca, Liviu Vacarciuc. Int. cl.: C07C 51/42; C07C 51/43. Publ.: BOPI, 2004-03-31.

Journal of Engineering Science *Vol. XXIX, no. 1 (2022), pp. 164 - 175*
Fascicle *Food Engineering* *ISSN 2587-3474*
Topic *Biotechnologies, Food Chemistry and Food Safety* *eISSN 2587-3482*

https://doi.org/10.52326/jes.utm.2022.29(1).15
CZU 634.743(478)

ANTIMICROBIAL PROPERTIES OF SEA BUCKTHORN GROWN IN THE REPUBLIC OF MOLDOVA

Elisaveta Sandulachi[1], ORCID: 0000-0003-3017-9008,
Artur Macari[1], ORCID: 0000-0003-4163-3771,
Daniela Cojocari[2*], ORCID: 0000-0003-0445-2883,
Greta Balan[2], ORCID: 0000-0003-3704-3584,
Sergiu Popa[3], ORCID: 0000-0002-1146-9504,
Nadejda Turculet[1*], ORCID: 0000-0002-1563-7210,
Aliona Ghendov-Mosanu[1], ORCID: 0000-0001-5214-3562,
Rodica Sturza[1], ORCID: 0000-0002-9552-1671

[1]*Technical University of Moldova, 168 Stefan cel Mare Blvd., Chisinau, Republic of Moldova*
[2]*"Nicolae Testemitanu" State University of Medicine and Pharmacy of the Republic of Moldova, 165 Stefan cel Mare Blvd., Chisinau, Republic of Moldova*
[3] *State Agrarian University of Moldova, Chisinau, 42 Mircesti Street, Republic of Moldova.*
*Corresponding authors: Daniela Cojocari, *daniela.cojocari@usmf.md*
Nadejda Turculet, *nadejda.turculet@saiem.utm.md*

Received: 01.14. 2022
Accepted: 12. 28. 2022

Abstract. This study deals with the antibacterial activity of Sea buckthorn (SB) (*Hippophae rhamnoides* L.) grown in the Republic of Moldova. Eight sea buckthorn species were investigated: R1, R2, R4, R5, C6, AGG, AGA, Pomona, 2020 harvest, from Dubasari district, Pohrebea village of the Republic of Moldova. The sea buckthorn fruit was harvested during the complete sweeping phase. The antibacterial efficacy of Sea buckthorn on different microbial cultures (*Staphylococcus aureus*, *Bacillus subtilis*, *Salmonella Typhimurium*, *Escherichia coli, Candida albicans*) causing infections/diseases was investigated by agar disc diffusion method. The inhibition zones ranged from 12 to 30 mm: *Staphylococcus aureus* ATCC 25923 (21-30 mm); *Bacillus subtilis* ATCC6633 (19-29 mm); *Salmonella Typhimurium* ATCC 14028 (13-18 mm); *Escherichia coli* ATCC 25922 (12-18 mm). In the case of *Candida albicans* ATCC 10231, this fungal pathogen was resistant to SB. It was found that antimicrobial efficacy of SB depends on the species, concentration, and form of use (fruit puree, extracts with different solvents and powder). Results suggested that SB might be a valuable ingredient for the development of safe products for consumption.

Keywords: *Hippophae rhamnoides L., Gram-positive bacteria, gram-negative bacteria, inhibition zone, food safety.*

Introduction

Sea buckthorn (*Hippophaë rhamnoides* L.) (SB) is well known as a multifunctional plant, which is widely grown in Asia, Europe, and Canada. In recent years, great attention has been paid to the cultivation of this crop in the Republic of Moldova, to be used in various industries. Both fruits and sea buckthorn leaves, having a relevant composition in biologically active substances, are good for health [1]. Sea buckthorn has a great potential for use in maintaining the local landscapes, in the food industry (manufacture of juices, drinks, jams, powders, candies, natural dyes, etc.), in the pharmaceutical and cosmetics industry [2 - 3]. Sea buckthorn products are delicious, have an attractive appearance, a relevant content of antioxidants, vitamins, minerals and are beneficial to consumer health [4 - 5].

Currently, great attention is being paid to the use of berries, as therapeutic remedies and with a high content of polyphenols, used as natural antioxidants and as nutraceutical supplements, with antimicrobial, anticancer, antiallergic and other properties [6 - 8]. Sea buckthorn fruits have all these miraculous properties and can be used successfully in a healthy diet. In this direction, various research studies are carried out, SB being in the top of investigated berries. There are many studies [9 - 11], which report the relevance of SB for consumption. The authors note SB as a relevant source of dietary antioxidants belonging mainly to the class of phenolic compounds. The antioxidant and antimicrobial activity of berries depends largely on their chemical composition.

In the published bibliographic sources, the chemical composition of SB is quite varied, depending on several factors: variety, methods and time of cultivation, climatic conditions, etc. The authors of the sources [12 - 13] reported a content of vitamin C in SB in the range of 0.98 - 5.14 mg/g and a large number of phenolic substances, the largest share belonging to phenolic glycosides. The authors of two other studies [14 - 15] report that the vitamin C content in SB varies in the range of 0.59 to 4.07 mg/g and in the berries is predominant isorhamnetin and quercetin glycosides. Carotenoids are present mainly in form of β-carotene [16 - 17], vitamin E in form of α-tocopherol [18 - 19] and niacin is the most abundant of the B vitamins. Sea buckthorn has antibacterial properties, due to the high content of polyphenols in its composition. The authors of the studies [20-25] reported the inhibitory effect on the growth of gram-positive (*Streptococcus pneumoniae* and *Staphylococcus aureus*) and gram-negative (*Escherichia coli*, *Salmonella typhi* and *Shigella dysenteriae*) pathogenic bacteria.

Hippophae rhamnoides L. has a relevant chemical composition that possesses antioxidant and antimicrobial properties. The chemical composition of SB is found in many research studies [26 - 31]. The berries are rich in both hydrophilic and lipophilic phytochemicals, including ascorbic acid, tocopherols, carotenoids, essential fatty acids. and various phenolic compounds [32 - 34]. In recent years, more and more research is being done to determine the antioxidant properties of SB [35 - 39]. The study authors [34], [40 - 41] in their research found that flavonoids were a class of major bioactive components in SB fruits, leaves and seeds, which have been shown to have anti-inflammatory, immunomodulatory, antioxidant properties, cardiovascular, anti-cancer, etc.

Dienaitė et al. [42] reported that SB pulp is a relevant source of biologically active substances with antioxidant properties, which inhibit the development of cancer cells. The authors mention that the main role in this regard belongs to galloylated flavonols and tanshinlactone derivatives. Phenolic compounds in plants they exhibit anti-inflammatory activity *in vitro* and *in vivo*, their mechanism of action is the inhibition of enzymes, by binding with hydrosulphide groups and inactivating bacterial proteins [43 - 44].

The authors of the studies [36, 45] have correlated the antimicrobial properties with the content of phenolic compounds in sea buckthorn.

The antimicrobial activity of sea buckthorn fruits and leaves is also found in the study conducted by Qadir et al. [46], showing the inhibitory effect of berries on *Staphylococcus aureus* (MRSA), using the standard method of disc diffusion. Another study [47] found that aqueous and hydroalcoholic sea buckthorn leaf extracts inhibited the growth of *Bacillus cereus*, *Pseudomonas aeruginosa*, *Staphylococcus aureus*, and *Enterococcus faecalis*.

There is currently a tendency to replace synthetic preservatives with natural ones, using berries in any form in food manufacturing. Many researchers in his work have shown positive results showing that sea buckthorn can be used for medicinal and preservation purposes. The antioxidant and antimicrobial effects of berries imply its natural conservation potential [20, 48 - 54]. The results presented by the authors showed that fruits, extracts and powders of sea buckthorn can serve as relevant ingredients to obtain quality products, stable in storage and safe for consumption. Sea buckthorn samples showed microbial activity against Gram-positive bacteria: *Staphylococcus aureus* ATCC 6538P, *Bacillus cereus* ATCC 11778 and Gram-negative bacteria: *Pseudomonas aeruginosa* ATCC 27853 [22].

The antibacterial activity of SB has a fairly wide spectrum and can be evaluated by different methods. Tables 1, 2 and 3 include some international research results published in recent years.

Table 1

Minimum inhibitory concentration (mean) of sea buckthorn and positive control on different bacteria

Sea buckthorn	Bacteria								Source
	Bacillus subtilis	*Bacillus cereus*	*Bacillus coagulans*	*Staphylococcus aureus*	*Escherichi coli*	*Listeria monocytogenes* EGDe	*Listeria monocytogenes* sp.	*Yersinia enterocolitica*	
Minimum inhibitory concentration, (mg/mL)									
Seed	1.52	24.39	6.10	12.20	6.10				
Pulp	0.19	3.05	0.10	12.20	12.20				
Leaf	3.05	48.78	1.52	12.20	12.20				[23]
Tetracycline hydrochloride	0.76	0.76	3.05	1.52	0.76				
Methanol extract	0.3	0.2	0.3				0.3	0.35	[24]
Seeds aqueous extract							0.75	1.00	[49]
Leaves extract							0.125		[37]
Hydroalcoholic concentrates C_1						2.6			[50]
C_2						5.2			
Hydroalcoholic extract H_1							2.6		[50]

Table 2

Antibacterial and antifungal activity of sea buckthorn

Bacteria	Diameter of inhibition zone, (mm)	Source	Bacteria	Diameter of inhibition zone, (mm)	Source
Klebsiella pneumoniae	8.0 ± 0.4	[55]	*Shigella dysenteriae*	20.67-15.23	[20]
Salmonella enterica	11.0 ± 0.3		*Agrobacterium tumefaciens*	*12±0.4 **13±0.2	[57]
Pseudomonas aeruginosa	20.0 ± 0.2		*Arcobacter butzleri*	18.0 ± 2.0	[58]
Acinetobacter baumannii	16.0 ± 0.1		*Arcobacter cryaerophilus*	28.0± 0.0	
Proteus mirabilis	20.0 ± 0.2		*Staphylococcus aureus*	10–14	[20]
Bacillus subtilis	*11.0±0.6 **12.0±0.5	[57]	*Proteus mirabilis*	20.0 ± 0.2	[55]
Bacillus thuringiensis	*13.0±0.5 **14.0±0.6		*Enterococcus faecalis*	18.0 ± 0.3	
Mucor indicus	**14±0.2		*Tilletia indica*	**11±0.4	[57]

*Fresh crude leaf extract. **Concentrated crude leaf extract

The results in Table 2 show different antimicrobial and antifungal influences of sea buckthorn depending on the genus of pathogenic bacteria.

Table 3

Inhibitory activities of sea buckthorn extracts on arcobacters [58]

Extract	*Arcobacter butzleri* CCUG 30484	*Arcobacter butzieri* UPa 2015/6	*Arcobacter cryaerophilus* CCM 3934	*Arcobacter cryaerophilus* UPa 2015/16
	Diameter of inhibition zone (mm)			
EtOH extract	28.5 ± 2.4	24.5 ± 2.1	23.0 ± 1.0	25.5 ± 0.7
Extract in PBS*	18.0 ± 2.0	20.5 ± 0.7	28.0 ± 0.0	20.3 ± 1.5
EtOH 96% (v/v)	16.0 ± 0.1	15.3 ± 0.1	15.3 ± 0.1	15.5 ± 0.1

*PBS- phosphate buffered saline.

The data in Table 3 show that the sea buckthorn extracts had an inhibitory activity on *Arcobacter* bacteria and may be recommended as an antimicrobial agent.

Materials and methods

Eight sea buckthorn species were investigated: R1, R2, R4, R5, C6, AGG, AGA, Pomorancevaia, 2020 harvest, from Dubasari district, Pohrebea village of the Republic of Moldova. The sea buckthorn fruit was harvested during the complete sweeping phase. Sea buckthorn samples were frozen at -25°C. For testing antimicrobial properties, berries kept frozen for 6 months were used.

The antimicrobial activity of SB was evaluated by the agar diffusion method. In this study we used inhibition zone test, also called Kirby-Bauer Test [59]. It is a qualitative method used to measure and compare the inhibitory activity levels of the tested substances (different fractions of eight sea buckthorn species: pulp, extracts, powder). The diameter of the

inhibition zone which marks the absence of microbial growth was measured with the shubler ruler. Bacterial cultures namely: *Staphylococcus aureus* ATCC 25923, *Bacillus subtilis* ATCC 6633, *Salmonella Typhimurium* ATCC 14028, *Escherichia coli* ATCC 25922, *Candida albicans* ATCC 10231 were obtained from the Microbiology and Immunology Department, "Nicolae Testemitanu" State University of Medicine and Pharmacy.

All calculations were done using Microsoft Office Excel 2007 (Microsoft, USA). Data obtained in this study are presented as mean values ± the standard error of the mean calculated from 3 parallel experiments.

Results and Discussions

The antimicrobial activity of the eight SB species was evaluated by the agar diffusion method. Areas of inhibition of the development of the tested microorganisms were estimated. The results obtained are included in Table 4.

Table 4

Antimicrobial activity of sea buckthorn species grown in the Republic of Moldova

Sea buckthorn species	Diameter of inhibition zone (mm)				
	Staphylococcus aureus ATCC 25923	*Bacillus subtilis* ATCC 6633	*Salmonella typhimurium* ATCC 14028	*Escherichia coli* ATCC 25922	*Candida albicans* ATCC 10231
R1	22.0 ± 0.1	19.0 ± 0.1	R	12.0 ± 0.2	R
R2	24.0 ±0.1	22.0 ± 0.2	13.0 ± 0.1	13.0 ± 0.1	R
R4	26.0 ±0.1	24.0± 0.1	15.0 ± 0.1	15.0 ± 0.1	R
R5	26.0 ±0.1	25.0 ± 0.1	14.0 ± 0.2	15.0 ± 0.1	R
C6	24.0 ± 0.2	26.0 ± 0.1	14.0 ± 0.1	17.0 ± 0.1	R
AGG	29.0 ± 0.2	28.0 ± 0.1	18.0 ± 0.1	18.0 ± 0.1	R
AGA	30.0 ± 0.1	29.0 ± 0.1	18.0 ± 0.1	18.0 ± 0.1	R
Pomorancevaia	21.0 ± 0.2	22.0 ± 0.1	R	12.0 ± 0.1	R

R- resistant

Obtaining different zones of inhibition for the same microorganism can be explained by the different chemical composition of the tested sea buckthorn species (content of antioxidants, organic acids, etc.). The results obtained by us correlate with the results reported by other authors. Kumar et al. [20], by the agar diffusion method, found that an area of inhibition for *Escherichia coli* and *Staphylococcus aureus* was respectively, 10.2 mm and 12.3 mm. In this paper the authors also present the evaluation of the inhibitory effect of SB with the help of the percentage reduction test. A result of 96.0% and 93.0% is reported for *Staphylococcus aureus* and *Escherichia coli*, respectively. Another study by Arora et al. [37] reported a high total phenolic content (278.80 mg GAE/g extract, methanolic extract from SB leaves) with a minimum inhibitory concentration (MIC) value of 125 µg/mL against *Listeria monocytogenes*. Scalbert A. [60] described the mechanism of inactivation and destruction of microorganisms. The researcher mentioned that the microbicidal activity of SB extracts is probably due to their ability to form complexes with extracellular proteins of bacteria, covalent bond formation, hydrophobic effects, and inactivating transport enzymes. A study by Chouhan et al. [61] reveals that the antimicrobial effect of sea buckthorn is due to the phenolic compounds that are present in the berries. The authors reported that SB had an

antimicrobial effect against *Escherichia coli*, *Salmonella typhi*, *Shigella dysenteriae*, *Streptococcus pneumoniae* and *Staphylococcus aureus* [62].

Reporting different results of sea buckthorn microbial activity can be justified by the difference between the chemical composition of the sea buckthorn varieties and the sea buckthorn samples tested. For example, in the study by Zheng et al. [63] shows the difference between the organic acid content present in different sea buckthorn species. The authors found that the content of malic acid and quinic acid (main acids) was higher in the Pertsik variety and in Vitaminaya, respectively. The highest share of ascorbic acid was in the Oranzhevaya variety and the lowest in Vitaminaya. The antimicrobial activity of sea buckthorn also depends on the climatic conditions, the region in which the berries are grown. Confirmation of this can be found in published scientific papers. For example, the study authors [64] reported that SB in northern Finland had a higher content of quinic acid, glucose, L-quebrachitol and ascorbic acid than SB in Canada. The data [65] are also significant, includes the fatty acid composition of sea buckthorn lipids of different origins.

The antimicrobial activity of sea buckthorn is directly proportional to the antioxidant activity. These properties of berries depend on the degree of ripening of the fruit and the period of harvest. The results of the study [17] this aspect. The authors found that, for different periods of growth, the antioxidant activity of SB fruits proved to be different. The varieties of late and medium maturation had the highest antioxidant activity than in other periods. The authors argue this with the different content of vitamin C in the fruit. The authors of another study [48] reported the presence in SB of acids: neochlorogenic, chlorogenic, *trans-p*-caffeic, *trans-p*-coumaric, *trans-p*-synaptic, *trans-p*-ferulic and rosmarinic acid. So the presence of other acids in sea buckthorn characterizes the antimicrobial properties of the fruit.

Figure 1 shows the images of the inhibition zones of different sea buckthorn species on the tested microorganisms.

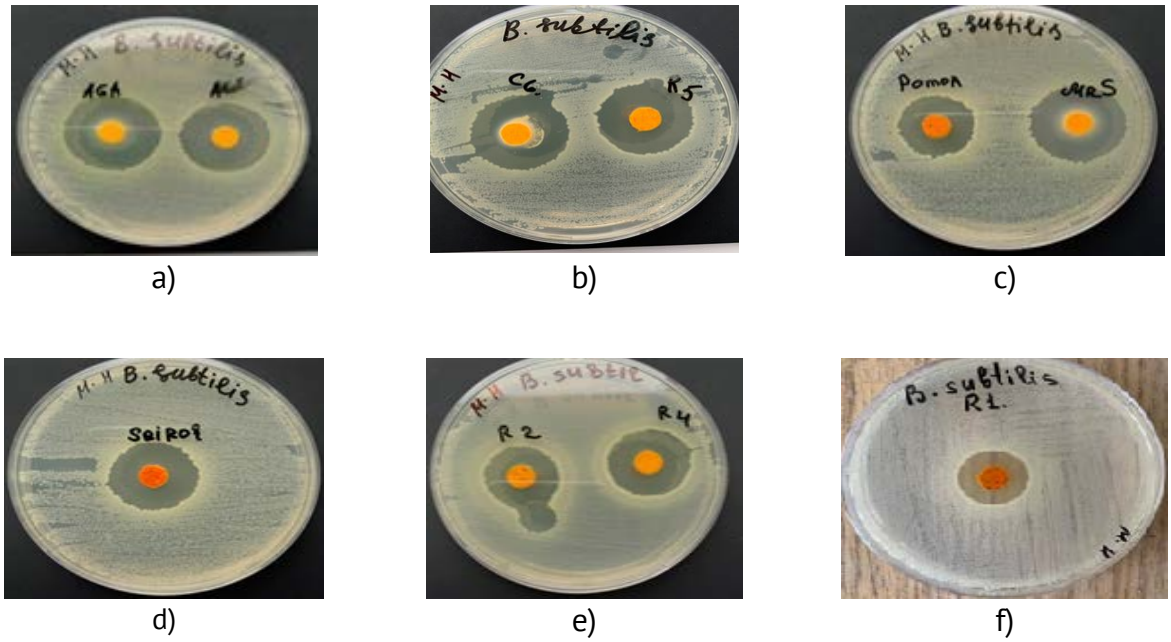

a) b) c)

d) e) f)

Figure 1. Antimicrobial activity of different species of sea buckthorn grown in the Republic of Moldova on pathogenic bacteria - *Bacillus subtilis* ATCC 6633: a) AGA and AGG; b) C6 and R5; c) Pomorancevaia and Mr. Sandu; d) Seirol; e) R2 and R4; f) R1.

The results from Table 5 demonstrate the antimicrobial activity of powder and hydroethanolic extract from sea buckthorn fruits.

Table 5

The diameter of the growth inhibition zone of different species of pathogenic microorganisms under the action of sea buckthorn

Sea buckthorn	Diameter of inhibition zone (mm)						
	Staphylococcus aureus ATCC 25923	*Bacillus subtilis* ATCC 6633	*Salmonella typhimurium* ATCC 14028	*Escherichia coli* ATCC 25922	*Listeria monocytogenes* ATCC 19118	*Listeria monocytogenes* EGDe	*Candida albicans* ATCC 10231
Powder	22 - 30	19 - 29	13 - 19	12 - 18	16.07 - 16.59	30 - 32	R
Hydroethanolic extract	-	-	-	-	22.25 - 22.75	30 - 32	-

R- resistant.

As a result of the tests performed, it was found that SB powder was a pronounced antimicrobial activity against *Staphylococcus aureus* and *Bacillus subtilis*, the zone diameter of inhibition varied respectively, between 22-30 mm and 19-29 mm. Powder showed lower antimicrobial activity for *Salmonella typhimurium* – 13-19 mm, *Escherichia coli* – 12-18 mm and *Listeria monocytogenes* (Table 5). *Candida albicans* has shown resistance to sea buckthorn powder. Bibliographic sources attest that the sensitivity of pathogenic microorganisms to sea buckthorn powders is probably due to the structure of the cell wall and outer membrane [66]. Gram-positive bacteria are differed by significant differences in the outer layers, do not have an outer membrane and a periplasmic space [67]. In Gram-negative bacteria, the permeability of the cell wall is reduced due to the high level of phospholipids in the cell wall. Probably, the resistance of Gram-negative bacteria to sea buckthorn powder is related to the hydrophilic surface of their outer membrane, which consists of lipopolysaccharide molecules, presenting a barrier for the penetration of numerous compounds that have antimicrobial activity [68].

Figure 2 shows the influence of antimicrobial activity of sea buckthorn (hydroalcoholic extract, fruit and powder) at different concentrations of test substances on the growth of *Listeria monocytogenes* ATCC 19118.

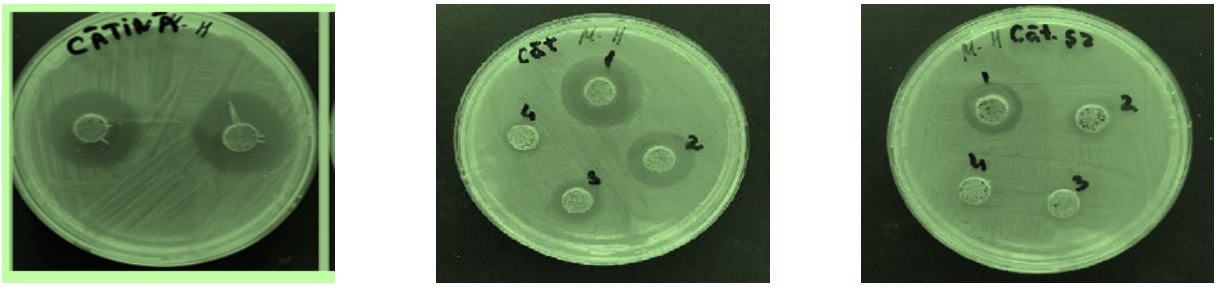

Sea buckthorn hydroalcoholic extract | Sea buckthorn fruit | Sea buckthorn powder

Figure 2. Inhibition Zone for *Listeria monocytogenes* ATCC 19118 using sea buckthorn. Concentration of test substances: 1 - 250 mg/mL; 2 -125 mg/mL; 3 - 62.5 mg/mL; 4 - 31.25 mg/mL.

Sea buckthorn has been shown to have antimicrobial properties on *Listeria monocytogenes*. These properties are probably due to the chemical composition of the berries, especially organic acids (citric, ascorbic, malic, succinic, lactic, acetic, etc.), tannins, flavonoids, and vitamins. The antimicrobial properties of certain classes of polyphenols and carotenoids are a means of developing new natural food preservatives due to increasing consumer pressure for food without the addition or with minimal use of harmful synthetic additives. However, this activity will always depend on the species of bacteria.

The antimicrobial mechanisms of polyphenols are based on their effects on cytoplasmic membrane destabilization, cell membrane permeability, extracellular microbial enzyme inhibition, direct action on microbial metabolism or deprivation of microbial growth substrates, especially essential minerals [69].

Furthermore, research of berries found that elagitanins showed varying degrees of antimicrobial activity in the growth of selected Gram-negative intestinal bacteria (*Salmonella*, *Staphylococcus*, *Helicobacter*, *Escherichia coli*, *Clostridium*, *Campylobacter*, and *Bacillus* strains), but are not active against beneficial probiotic lactic acid (Gram-positive bacteria). Galotanins have shown antibacterial activity against food bacteria, and Gram-positive bacteria have generally been more sensitive than Gram-negative bacteria. The activity of galotanins is attributed to their strong affinity for iron and is also linked to the inactivation of membrane-bound protein.

Carotenoids have antioxidant and antimicrobial activity against pathogenic bacteria such as colorless *Salmonella*, *Escherichia coli*, *Staphylococcus aureus* and *Listeria monocytogenes*, as well as toxigenic fungi such as *Aspergillus flavus*, *Aspergillus parasiticus*, *Aspergillus carbonarius* and *Aspergillus ochraceus*. Several studies investigating the action of carotenoids and essential oils against food spoilage organisms and food pathogens believe that they are more active against Gram-positive than Gram-negative bacteria, as evidenced in this research [70]. Gram-negative organisms are thought to be less susceptible to antibacterial action because they have an outer membrane that surrounds the cell wall, which restricts the diffusion of hydrophobic compounds through the lipopolysaccharide coating.

Conclusions

The paper tested the antimicrobial action of 8 varieties of sea buckthorn original from the Republic of Moldova on Gram-positive pathogenic bacteria (*Listeria monocytogenes*, *Staphylococcus aureus*, *Bacillus subtilis*) and Gram-negative (*Escherichia coli*, *Salmonella typhimurium*). The antifungal action on *Candida albicans* was also tested.

Various inhibition zones for the same microorganism were obtained for different varieties of SB. This can be explained by the different chemical composition of the SB species tested (content of antioxidants, organic acids, etc.). The antimicrobial activity of SB is directly proportional to the antioxidant activity. The microbicidal activity of SB extracts is due to their ability to form complexes with bacterial extracellular proteins, covalent bonds, hydrophobic effects and inactivating transport enzymes.

Following the tests, it was found that SB powder had a pronounced antimicrobial activity against *Staphylococcus aureus* and *Bacillus subtilis*, the diameter of the inhibition zone varied, respectively, between 22-30 mm and 19-29 mm. The powder showed lower antimicrobial activity for *Salmonella typhimurium* - 13-19 mm, *Escherichia coli* - 12-18 mm.

SB exhibits antimicrobial properties on *Listeria monocytogenes*, which are dependent on the SB species. *Candida albicans* has shown resistance to sea buckthorn powder.

The results of this research show that SB powder or extract, grown in the Republic of Moldova could be used as natural preservatives for food, thus expanding the category of food without or with a minimum of synthetic additives. Obviously, further studies are needed to evaluate the matrix effect of these foods on the antimicrobial activity of SB.

Acknowledgments. The authors would like to thank the Moldova State Project no. 20.80009.5107.09, *"Improvement of food quality and safety by biotechnology and food engineering"*, running at Technical University of Moldova.

References

1. Ma X., Yang W., Kallio H., Yang B. Health promoting properties and sensory characteristics of phytochemicals in berries and leaves of sea buckthorn (*Hippophaë rhamnoides*). In: *Critical Reviews in Food Science and Nutrition*, 2021, 35*,* pp. 1-19.
2. Lukša J., Vepštaitė-Monstavičė I., Apšegaitė V. et al. Fungal Microbiota of Sea Buckthorn Berries at Two Ripening Stages and Volatile Profiling of Potential Biocontrol Yeasts In: *Microorganisms*, 2020, 8(3), p. 456.
3. Guliyev V.B., Gul M., Yildirim A. *Hippophae rhamnoides* L.: Chromatographic methods to determine chemical composition, use in traditional medicine and pharmacological effects. In: *Journal of Chromatography B,* 2004, 812, pp. 291-307.
4. Ruan C-J., Rumpunen K., Nybom H. Advances in improvement of quality and resistance in a multipurpose crop: sea buckthorn. In: *Critical Reviews in Biotechnology*, 2013, 33, pp.126-144.
5. Bouras K., Kopsidas K., Bariotakis M., Kitsiou P. et al. Effects of Dietary Supplementation with Sea Buckthorn (Hip*pophae rhamnoides* L.) Seed Oil on an Experimental Model of Hypertensive Retinopathy in Wistar Rats. In: Biomedicine Hub, 2017, 2(1), pp. 1-12.
6. Arts I. C.W., Hollman P.C.H. Polyphenols and disease risk in epidemiologic studies. In: *The American Journal of Clinical Nutrition,* 2005, 81, pp. 317S–325S.
7. Williamson G., Manach C. Bioavailability and bioefficacy of polyphenols in humans. II. Review of 93 intervention studies. In: *The American Journal of Clinical Nutrition,* 2005, 81, pp. 243S–255S.
8. Puganen A., Kallio H.P., Schaich K.M., Suomela J-P., Yang B. Red/Green Currant and Sea Buckthorn Berry Press Residues as Potential Sources of Antioxidants for Food Use. In: *Journal of Agricultural and Food Chemistry*, 2018, 66 (13), pp. 3426-3434.
9. Bal L.M., Meda V., Naik S.N., Satya S. Sea buckthorn berries: A potential source of valuable nutrients for nutraceuticals and cosmeceuticals. In: *Food Research International,* 2011, 44, pp. 1718-1727.
10. Dong R., Su J., Nian H., Shen H., Zhai X. et al. Chemical fingerprint and quantitative analysis of flavonoids for quality control of Sea Buckthorn leaves by HPLC and UHPLC-ESI-QTOF-MS. In: *Journal of Functional Foods,* 2017, 37, pp. 513-522.
11. Tian Y., Liimatainen J., Alanne A., Lindstedt A. et al. Phenolic compounds extracted by acidic aqueous ethanol from berries and leaves of different berry plats. In: *Food Chemistry,* 2017, 220, pp. 266-281.
12. Hussain M., ALI S., Awan S., Hussain M., Hussain I. Analysis of minerals and vitamins in sea buckthorn (*Hippophae rhamnoids*) pulp collected from Ghizer and Skardu districts of Gilgit-Baltistan. In: *International Journal of Biosciences*, 2014, 4, pp. 144—152.
13. Sytařová I., Orsavová J., Snopek L., Mlček J. et al. Contribution of phenolic compounds, ascorbic acid and vitamin E to antioxidant activity of currant (Ribes L.) and gooseberry (Ribes uva-crispa L.) fruits. In: *Food chemistry*, 2019, 284, pp. 323-333.
14. Ma X., Yang W., Laaksonen O., Nylander M., Kallio H., Yang B. Role of Flavonols and Proanthocyanidins in the Sensory Quality of Sea Buckthorn (*Hippophaë rhamnoides* L.) Berries. In: *Journal of Agricultural and Food Chemistry,* 2017, 65, pp. 9871–9879.
15. Teleszko M., Wojdylo A., Rudzinska M., Oszmianski J., Golis T. Analysis of Lipophilic and Hydrophilic Bioactive Compounds Content in Sea Buckthorn (*Hippophae Rhamnoides* L.) Berries. In: *Journal of Agricultural and Food Chemistry,* 2015, 63 (16), pp. 4120–4129.
16. Andersson S.C., Rumpunen K., Johansson E., Olsson M. E. Tocopherols and Tocotrienols in Sea Buckthorn (*Hippophae Rhamnoides* L.) Berries during Ripening. In: *Journal of Agricultural and Food Chemistry*, 2008, 56 (15), pp. 6701–6706.
17. Sytařová I., Orsavová J., Snopek L., Mlček J. et al. Impact of phenolic compounds and vitamins C and E on antioxidant activity of sea buckthorn (*Hippophaë rhamnoides* L.) berries and leaves of diverse ripening times. In: *Food Chemistry*, 2020, 310, 125784.

18. Eccleston C., Baoru Y., Tahvonen R., Kallio H. et al. Effects of an antioxidant-rich juice (sea buckthorn) on risk factors for coronary heart disease in humans. In: *The Journal of Nutritional Biochemistry*, 2002, 13 (6), pp. 346-354.
19. Kallio H., Yang B., Peippo P., Tahvonen R., Pan R. Triacylglycerols, Glycerophospholipids, Tocopherols, and Tocotrienols in Berries and Seeds of Two Subspecies (ssp. *sinensis* and *mongolica*) of Sea Buckthorn (*Hippophae rhamnoides*). In: *Journal of Agricultural and Food Chemistry,* 2002, 50, pp. 3004—3009.
20. Kumar M.S.Y., Tirpude R.J., Maheshwari D.T. et al. Antioxidant and antimicrobial properties of phenolic rich fraction of Seabuckthorn (*Hippophae rhamnoides* L.) leaves *in vitro*. In: *Food Chemistry*, 2013, 141 (4), 3443-3450.
21. Różalska B., Sadowska B., Żuchowski J., Więckowska-Szakiel M., Budzyńska A. et al. Phenolic and Nonpolar Fractions of *Elaeagnus rhamnoides* (L.) A. Nelson Extracts as Virulence Modulators-In Vitro Study on Bacteria, Fungi, and Epithelial Cells. In: *Molecules*, 2018, 23 (7), 1498.
22. Criste A., Urcan A.C., Bunea A. et al. Phytochemical Composition and Biological Activity of Berries and Leaves from Four Romanian Sea Buckthorn (*Hippophae Rhamnoides* L.) Varieties. *Molecules*, 2020, 25(5), 1170.
23. Yue X.-F., Shang X., Zhang Z-J., Zhang Y.N. Phytochemical composition and antibacterial activity of the essential oils from different parts of sea buckthorn (*Hippophae rhamnoides L.*). In: *Journal of Food and Drug Analysis*, 2017, 25, pp. 327-332.
24. Negi P.S., Chauhan A.S., Sadia G.A., Rohinishree Y.S., Ramteke R.S. Antioxidant and antibacterial activities of various seabuckthorn (*Hippophae rhamnoides L.*) seed extracts. In: *Food Chemistry*, 2005, 92, pp. 119-124.
25. Jeong J.H., Lee J.W., Kim K.S. et al. Antioxidant and antimicrobial activities of extracts from a medicinal plant, sea buckthorn. In: *Journal of the Korean Society for Applied Biological Chemistry*, 2010, 53, pp. 33–38.
26. Yang W., Laaksonen O., Kallio H., Yang B. Proanthocyanidins in Sea Buckthorn (*Hippophaë Rhamnoides* L.) Berries of Different Origins with Special Reference to the Influence of Genetic Background and Growth Location. In: *Journal of Agricultural and Food Chemistry*, 2016, 64 (6), pp. 1274–1282.
27. Arimboor R., Kumar K.S., Arumughan C. Simultaneous Estimation of Phenolic Acids in Sea Buckthorn (*Hippophae Rhamnoides*) Using RP-HPLC with DAD. In: *Journal of Pharmaceutical and Biomedical Analysis*, 2008, 47 (1), pp. 31–38.
28. Tiitinen K.M., Hakala M.A., Kallio H.P. Quality Components of Sea Buckthorn (*Hippophaë Rhamnoides*) Varieties. In: *Journal of Agricultural and Food Chemistry*, 2005, 53 (5), pp. 1692–1699.
29. Pop R. M., Weesepoel Y., Socaciu C., Pintea A., et al. Carotenoid Composition of Berries and Leaves from Six Romanian Sea Buckthorn (*Hippophae Rhamnoides L.*) Varieties. In: *Food Chemistry*, 2014, 147, pp. 1–9.
30. Yang B., Kallio H. Composition and Physiological Effects of Sea Buckthorn (*Hippophaë*) Lipids. *Trends in Food Science & Technology*, 2002, 13 (5), pp. 160–167.
31. Ficze G., Mátravölgyi G., Furulyás D., Rentsendavaa C. Analysis of bioactive compounds of three sea buckthorn cultivars (*Hippophaë rhamnoides* L. 'Askola', 'Leikora', and 'Orangeveja') with HPLC and spectrophotometric methods. In: *European Journal of Horticultural Science*, 2019, 84 (1), pp. 31-38.
32. Aaby Martinsen B.K., Borge G.I.A., Røen D. Bioactive compounds and color of sea buckthorn (*Hippophae rhamnoides* L.) purees as affected by heat treatment and high-pressure homogenization. In: *International Journal of Food Properties*, 2020, 23 (1), pp. 651-664.
33. Patel C.A., Divakar K., Santani D., Solanki H.K., Thakkar J.H. Remedial prospective of Hippophae rhamnoides L. (Sea buckthorn). In: *ISRN Pharmacology*, 2012, 2012, 436857.
34. Ren R., Li N., SU C., Wang Y. et al. The bioactive components as well as the nutritional and health effects of sea buckthorn. In: *RSC Advances*, 2020, 10, 44654.
35. Mamedov N.A., Urbanowski M., Craker L.E. Study of antimicrobial activity of sea buckthorn oil (*Hippophae rhamnoides* L.) against *Helicobacter pylori*. In: *Acta Horticulturae*, 2015, 1098, pp. 91-94.
36. Michel T., Destandau E., Le Floch G., Lucchesi M.E., Elfakir C. Antimicrobial, antioxidant and phytochemical investigations of sea buckthorn (*Hippophaë rhamnoides* L.) leaf, stem, root and seed. In: *Food Chemistry,* 2012, 131, pp. 754–760.
37. Arora R., Mundra S., Yadav A., Stobdan T. Antimicrobial activity of seed, pomace and leaf extracts of sea buckthorn (*Hippophae rhamnoides* L.) against foodborne and food spoilage pathogens. In: *African Journal of Biotechnology,* 2012, 11, pp. 10424–10430.
38. Gao X., Ohlander M., Jeppsson N., Bjork L., Trajkovski V. 2000: Changes in antioxidant effects and their relationship to phytonutrients in fruits of sea buckthorn (*Hippophae rhamnoides L.*) during maturation. In: *Journal of Agricultural and Food Chemistry,* 2000, 48, pp. 1485-1490
39. Ramasamy T., Varshneya C., Katoch V.C. Immunoprotective effect of seabuckthorn (*Hippophae rhamnoides*) and glucomannan on T-2 toxin-induced immunodepression in poultry. In: *Veterinary Medicine International*, 2010, Article ID: 149373.

40. Jayashankar B., Mishra K.P., Ganju L., Singh S.B. Supercritical extract of Seabuckthorn Leaves (SCE200ET) inhibited endotoxemia by reducing inflammatory cytokines and nitric oxide synthase 2 expression. In: *International Immunopharmacology*, 2014, 20(1), pp. 89-94.
41. Basu M., Prasad R., Jayamurthy P. et al. Anti-atherogenic effects of seabuckthorn (*Hippophaea rhamnoides*) seed oil. In: *Phytomedicine*, 2007, 14(11), 770-777.
42. Dienaite L., Pukalskas A., Pukalskiene M. et al. Phytochemical Composition, Antioxidant and Antiproliferative Activities of Defatted Sea Buckthorn (*Hippophaë rhamnoides* L.) Berry Pomace Fractions Consecutively Recovered by Pressurized Ethanol and Water. In: *Antioxidants*, 2020, 9, 274.
43. Willett W.C. Balancing life-style and genomics research for disease prevention. In: *Science*, 2002, 296 (5568), pp. 695-698.
44. Slynko N.M., Kuibida L.V., Tatarova L.E. et al. Essential Oils from Different Parts of the Sea Buckthorn *Hippophae rhamnoides* L. In: *Advances in Bioscience and Biotechnology*, 2019, 10 (8). doi:10.4236/abb.2019.108018
45. Thomas M., Emilie D., Gaetan L.F., Marie E.L., Claire. E. Antimicrobial, antioxidant and phytochemical investigations of sea buckthorn (*Hippophae rhamnoides* L.) leaf, stem, root and seed. In: *Food Chemistry*, 2012, 131, pp. 754-760.
46. Qadir M.I., Abbas K., Younus A., Shaikh R.S. Report - Antibacterial activity of sea buckthorn (*Hippophae rhamnoides* L.) against methicillin resistant *Staphylococcus aureus* (MRSA). *Pakistan Journal of Pharmaceutical Sciences*, 2016, 29 (5), pp. 1711-1713.
47. Nitin K., Upadhyay M.S., Yogendra K., ASHEESH, G. Antioxidant, cytoprotective and antibacterial effects of sea buckthorn (*Hippophae rhamnoides* L.) leaves. In: *Food and Chemical Toxicology*, 2010, 48, pp. 3443-3448.
48. Gayibova S., Ivanisova E., Arvay J. et al. In vitro screening of antioxidant and antimicrobial activities of medicinal plants growing in Slovakia. In: *Journal of Microbiology, Biotechnology and Food Sciences*, 2019, 8 (6), pp. 1281-1289.
49. Chauhan A.S., Negi P.S., Ranteke R.S. Antioxidant and antibacterial activities of aqueous extract of sea buckthorn (Hippophae rhamnoides) seeds. In: *Fitoterapia*, 2007, 78, pp. 590–592.
50. Sandulachi E., Cojocari D., Balan G., Popescu L., Ghendov-Moşanu A., Sturza R. (2020) Antimicrobial Effects of Berries on Listeria monocytogenes. In: *Journal of Food and Nutrition Sciences*, 2020, 11, pp. 873-886.
51. Ghendov-Moşanu A., Cojocari D., Balan G., Sturza R. Antimicrobial activity of rose hip and hawthorn powders on pathogenic bacteria. In: *Journal of Engineering Science*, 2018, 4, 100-107, DOI:10.5281/zenodo.257676452.
52. Sturza R., Sandulachi E., Cojocari D., Balan G., Popescu L., Ghendov-Moşanu A. Antimicrobial Properties of Berry Powders in Cream Cheese. In: *Journal of Engineering Science*, 2019, 3, pp. 125-136.
53. Sandulachi E., Bulgaru V., Ghendov-Mosanu A., Sturza R. Controlling the Risk of Bacillus in Food Using Berries. In: *Food and Nutrition Sciences*, 2021, 12(6). https://doi.org/10.4236/fns.2021.126042
54. Cojocari D., Sturza R., Sandulachi E., Macari A., Balan G., Ghendov-Moşanu A. Inhibiting of accidental pathogenic microbiota in meat products with berry powders. In: *Journal of Engineering Science*. 2019, 1, pp. 114-122.
55. Lele V., Monstaviciute E., Varinauskaite I. et al. Sea Buckthorn (*Hippophae rhamnoides* L.) and Quince (*Cydonia oblonga* L.) Juices and Their By-Products as Ingredients Showing Antimicrobial and Antioxidant Properties for Chewing Candy. In: *Nutraceutical Journal of Food Quality*, 2018, Article ID 3474202.
56. Upadhyay N.K., Kumar M.S.Y., Gupta A. Antioxidant, cytoprotective and antibacterial effects of Sea buckthorn (*Hippophae rhamnoides* L.) leaves. In: *Food and Chemical Toxicology*, 2010, 48(12), pp. 3443-3448.
57. Gupta S.M., Gupta A.K., Ahmed Z., Kumar A. Antibacterial and Antifungal Activity in Leaf, Seed Extract and Seed Oil of Seabuckthorn (*Hippophae salicifolia D. Don*) Plant. In: *Journal of Plant Pathology & Microbiology*, 2011, 2, 105.
58. Kučerová S., Šilha D., Vytřasová J., Švecová B. Survival of Arcobacter butzleri and Arcobacter cryaerophilus strains in the presence of sea buckthorn extracts. In: *Journal of Food and Nutrition Research*, 2017, 56 (1), pp. 10–17.
59. Hudzicki J. Kirby-Bauer Disk Diffusion Susceptibility Test Protocol. American Society for Microbiology, Washington DC, 2016, 23.
60. Scalbert A. Antimicrobial properties of tannins. In: *Phytochemistry*, 1991, 30 (12), pp. 3875-3883.
61. Chouhan S., Sharma K., Guleria S. Antimicrobial Activity of Some Essential Oils - Present Status and Future Perspectives. In: *Medicines,* 2017, 4(3), 58.
62. Puupponen-Pimia R., Nohynek L., Meie R.C., Kahkonen M., Heinonen M., Hopia A. Antimicrobial properties of phenolic compounds from berries. In: *Journal of Applied Microbiology*, 2001, 90, pp. 494-507.

63. Zheng J., Yang B., Trépanier M., Kallio H. Effects of Genotype, Latitude, and Weather Conditions on the Composition of Sugars, Sugar Alcohols, Fruit Acids, and Ascorbic Acid in Sea Buckthorn (*Hippophaë rhamnoides* ssp. *mongolica*) Berry Juice. In: *Journal of Agricultural and Food Chemistry,* 2012, 60, 12, 3180−3189.
64. Kortesniemi M., Sinkkonen J., Yang B., Kallio H. NMR metabolomics demonstrates phenotypic plasticity of sea buckthorn (Hippophaë rhamnoides) berries with respect to growth conditions in Finland and Canada. In: *Food Chemistry*, 2017, 219, pp. 139-147.
65. Yang B.R., Kallio H.P. Fatty acid composition of lipids in sea buckthorn (Hippophae rhamnoides L.) berries of different origins. In: *Journal of Agricultural and Food Chemistry*, 2001, 49, pp. 1939-1947.
66. Cowan M. Plants products as antimicrobial agents. Clinical Microbiology Reviews, 1999, 12, 564-582.
67. Lopez P., Sanchez C., Batlle Nerin C. Solid- and vapor-phase antimicrobial activities of six essential oils. Susceptibility of selected food borne bacterial and fungal strains. In: *Journal Agricultural Food Chemistry*, 2005, 53, 6939-6946.68.
68. Nikaido H. Outer membrane. In: *Escherichia coli and Salmonella typhimiruim: Cellular and Molecular Biology*. Ed. by: Neidhardt FC. Washington: American Society for Microbiology Press; 1996, 29-47.
69. Skenderidis P., Leontopoulos S., Petrotos K., Mitsagga C., Giavasis I. The In Vitro and In Vivo Synergistic Antimicrobial Activity Assessment of Vacuum Microwave Assisted Aqueous Extracts from Pomegranate and Avocado Fruit Peels and Avocado Seeds Based on a Mixtures Design Model. In: *Plants*, 2021, 10 (9), 1757.
70. Ben Hsouna A., Ben Halima N., Smaoui S. et al. Citrus lemon essential oil: chemical composition, antioxidant and antimicrobial activities with its preservative effect against Listeria monocytogenes inoculated in minced beef meat. In: *Lipids in Health and Disease*, 2017, 16, 146.